Assessing trophodynamics of a Newfoundland rhodolith (*Lithothamnion glaciale*) bed using lipid, fatty acid, and stable isotope analyses

by

© Sean M. Hacker Teper

A thesis submitted to the School of Graduate Studies

in partial fulfilment of the requirements for the degree of

Master of Science, Marine Biology

Department of Ocean Sciences

Faculty of Science

Memorial University of Newfoundland

St. John's, Newfoundland and Labrador, Canada

January, 2022

Abstract

Rhodoliths (free-living, non-geniculate red coralline algae growing as balls, branched twigs, or rosettes) often form dense aggregations, termed rhodolith beds, at depths of up to 150 m in tropical to polar seas. The important contribution of rhodolith beds to marine biodiversity and global calcium carbonate production has, in part, triggered the recent increase in number of studies of factors and processes regulating their structure and function with, however, little attention to feeding relationships. The present thesis investigated trophodynamics of a rhodolith (*Lithothamnion glaciale*) bed in St. Philip's, Newfoundland (Canada) with a combination of lipid, fatty acid, and stable isotope analyses. I quantified lipid composition, energy transfer, essential nutrients, and seasonal and spatial variability among six dominant echinoderm, bivalve, gastropod, and polychaete species, two algal species, seawater, and sediment beneath individual rhodoliths. Results suggest strong benthic-pelagic coupling in that rhodolith bed organisms utilize phytoplankton, especially diatoms, as a main food source during blooms. I identified three distinct trophic levels among associated macrofauna and flora (producers, suspension/filter feeders and grazers, and predators), while discovering a potential resource partitioning relationship among organisms in which first- and second-order consumers share a common resource (diatoms or kelp). Diets shifted in response to seasonal food availability and life history requirements, but were unaffected by riverine input proximity. Based on my findings, I conceptualized a partial food web detailing the interpreted linkages among food sources and organisms in the studied rhodolith bed. This proposed food web delineates relationships among organisms and essential nutrients in cold water systems, while demonstrating the interconnectedness of various rhodolith bed components.

Acknowledgments

I thank my supervisors Dr. Patrick Gagnon and Dr. Chris Parrish for their positivity, helpfulness, and perseverance throughout this thesis. I will cherish my experiences diving nearby icebergs in freezing temperatures and the countless hours in the fume hood learning the ins and outs of biochemistry. I would also like to thank my committee members, Dr. Suzanne Dufour and Dr. Paul Snelgrove for their guidance throughout the project. I am beyond thankful for the hard work, dedication, and selflessness of Jeanette Wells, Jenna Mackinnon, Camilla Parzanini, Tomer Katan, Alison Pye, Adam Cook, David Bélanger, Anne Provencher St-Pierre, Samantha Trueman, Julie Jacques, Laura Teed, Kaitlyn Graham, Logan Zeinert, Emma Cooke, and Andrew Perry and the FSU for their irreplaceable help with field work, laboratory work, and most importantly, their friendship. Thank you to Dr. David Schneider for his help navigating me through the treacherous world of statistical analyses. I would be remiss not to thank my parents, Karen Hacker and Irving Teper, for their unconditional love and support and for pushing me not only to pursue an M.Sc., but to also complete it! Finally, thank you to my acquaintance, Laurianne Sutton, who was my best cheerleader, listener, and supporter throughout this lengthy and often unpredictable process. This research was supported by Natural Sciences and Engineering Research Council (NSERC-Discovery Grant) to Christopher Parrish and Patrick Gagnon, and by Canada Foundation for Innovation (CFI- Leaders Opportunity Funds), and Research & Development Corporation of Newfoundland and Labrador (Ignite R&D) grants to Patrick Gagnon.

Table of Contents

List of Tables

List of Figures

List of Appendices

Co-Authorship Statement

The work described in the present thesis was conducted by Sean Hacker Teper with guidance from Dr. Patrick Gagnon and Dr. Chris Parrish. Sean Hacker Teper was responsible for the development and execution of all field and laboratory work (with guidance from Dr. Patrick Gagnon and Dr. Chris Parrish). All chapters were written by Sean Hacker Teper with intellectual and editorial input by Dr. Patrick Gagnon, Dr. Chris Parrish, Dr. Suzanne Dufour, and Dr. Paul Snelgrove. Any publication in the primary literature resulting from work in Chapter II or Chapter III will be co-authored by Sean Hacker Teper, Dr. Patrick Gagnon, and Dr. Chris Parrish.

CHAPTER I

General Introduction

1.1. Trophic ecology

Charles Darwin introduced the concept of a food web in 1859 when he suggested that plants and animals "are bound together by a web of complex relations." Lindeman (1942) reimagined this idea, suggesting a concept of "bottom-up" trophodynamics, or energy transfer from producers up to the n^{th} consumer. Trophodynamics describes a specific facet of trophic ecology where energy transfers and flows through ecosystem food webs, organizations of biodiversity and ecosystem function (Thompson et al., 2012). Studying trophodynamics helps understand how underlying biological (i.e. feeding patterns), physical (i.e. seasonal water temperatures), geological (i.e. riverine input) and chemical (i.e. lipid structure) mechanisms affect ecosystem energy flow (Woodward and Hildrew, 2002; Bierwagen et al., 2018). Ultimately, trophodynamics is about understanding how food is acquired through an ecosystem, although this pathway can be particularly difficult to decipher when studying benthic marine ecosystems because these food webs often involve complex pathways of energy flow (Kelly and Scheibling, 2012). For example, marine food can come from both pelagic (e.g. phytoplankton) and benthic (e.g. marine algae) sources, creating multiple pathways from primary producers to their consumers, resulting in an often complicated array of energy pathways. Even when food reaches the benthos, it may not reach a consumer immediately, often recycling through microbial activity, coprophagy, resedimentation, or death (Tenore, 1988; Duffill Telsnig et al., 2019). Thus, it can be difficult to determine the origins of food and trophic positioning without specific trophic ecology techniques.

1.2. Trophic ecology techniques

Recently, an increased emphasis on methodologies and techniques has emerged in the literature to facilitate trophic ecology studies (Garvey and Whiles, 2016). Various methods aim to

test for predator-prey relationships (i.e. interactions), specific food and energy transfers in these relationships (i.e. diet), consequences of these relationships (e.g. changes to lipid composition), and trophic modeling (Majdi et al., 2018). Used in combination, these techniques provide a more comprehensive understanding of trophic interactions in an ecosystem than any standalone technique, yielding information over multiple timescales. As such, this thesis uses a combination of biochemical methodologies and techniques to create a clearer picture of organism relationships, their diets, and diet effect: lipid, fatty acid, and stable isotope analyses.

1.3. Rhodoliths

Rhodoliths are free-living nodules of primarily coralline red algae containing either entirely non-geniculate (i.e. inflexible crusts or plates) coralline or a nucleated core (e.g. mussel shell) (Freiwald and Henrich, 1994; Foster, 2001). Rhodoliths typically grow as balls, branched twigs, or rosettes with highly complex branching lattice structure that form slowly over many years; in Newfoundland, rhodoliths grow about 0.25-0.45 $mm \cdot yr^{-1}$ (Halfar et al., 2000; Teed et al. 2020) and life expectancy of an individual rhodolith exceeds 100 years. Growing evidence suggests rhodoliths are calcium carbonate ($CaCO_3$) bio-factories, producing as much $CaCO_3$ as the world's largest biogenic $CaCO_3$ deposits (Amado-Filho et al., 2012a; Harvey et al., 2017; Teed et al., 2020).

Rhodolith communities often form dense aggregations of rhodoliths known as "rhodolith beds". These beds range in size from 100s of m^2 to 1000s of km^2 and form at depths of up to 150 m in tropical to polar seas (Foster et al., 2007; Steller and Cáceres-Martínez, 2009; Amado-Filho et al., 2012b). Rhodolith beds, together with seagrass meadows, kelp beds and forests, and mangrove forests, are considered the four dominant communities of marine benthic primary producers

(Kharlamenko et al., 2001; Pitt et al., 2009; Kelly and Scheibling, 2012). The complex structure and longevity of rhodoliths create a safe and stable nursery environment for invertebrates. Rhodoliths serve as ecosystem engineers - organisms that positively affect the availability of resources for other species through modification, maintenance, and creation of habitat (Jones et al., 1994). Rhodoliths provide structural complexity that limits physical and biological stress, increases the availability of resources, and even provides food for other organisms (James, 2000; Bruno and Bertness, 2001; Gabara et al., 2018). For example, rhodoliths offer substrata for attachment of hundreds of benthic invertebrates (e.g. Mollusca) (Kamenos et al., 2004a; Steller and Cáceres-Martínez, 2009; Riosmena-Rodriguez and Medina-López, 2010), space for mobile invertebrates (e.g. Annelida and Echinodermata) to burrow or hide (Steller and Cáceres-Martínez, 2009; Bélanger, 2020), habitat for reproduction (Kamenos et al., 2004b; Steller and Cáceres-Martínez, 2009; Gagnon et al., 2012) and foraging in dominant fish and invertebrate species (Steneck, 1986; Gagnon et al., 2012; Teichert et al., 2014), and an environment for recruitment for many organisms during their larval stages (Steller and Cáceres-Martínez, 2009; Riosmena-Rodriguez and Medina-López, 2010; Gagnon et al., 2012).

Rhodoliths have a circumpolar distribution, with extensive populations in Newfoundland and Labrador (Gagnon et al., 2012), the Northeast Atlantic (Grall et al., 2006; Hall-Spencer et al., 2010; Teichert et al., 2014), the Gulf of California (Foster et al., 2007; Riosmena-Rodriguez and Medina-López, 2010), Australia (Harvey and Bird, 2008), and Brazil (Foster, 2001; Amado-Filho et al., 2012a, 2012b). Because rhodoliths are relatively understudied, most publications have focused on categorizing rhodolith community assemblages globally to gain an understanding of their basic ecological role. Studies typically report high biodiversity within rhodoliths, partly due to their structural complexity and role as ecosystem engineers (Jones et al., 1994; Gagnon et al.,

2012; Gabara et al., 2018). As such, little research has focused on feeding relationships among organisms living in rhodolith bed communities; only Grall et al. (2006) and Gabara (2014) have described rhodolith trophodynamics. Rhodolith communities encompass many trophic levels with organisms using a variety of different feeding strategies, among them: primary producers, filter feeders, suspension feeders, deposit feeders, grazers, and predators (Bélanger, 2020). Studying feeding relationships among these organisms is crucial to understanding the structure and function of rhodolith ecosystems.

1.4. Lipids

Lipids are compounds extractable in nonpolar organic solvents. They are the densest form of energy (cal/g) in marine ecosystems (Parrish et al., 2000; Parrish, 2009), they are essential molecules in cell membranes, they provide thermal insulation and buoyancy, and they serve as signaling molecules. In the marine environment, lipids can be separated into classes based on polarity: the least polar structures such as hydrocarbons and simple esters, followed by acids and alcohols, and finally complex polar structures such as glycolipids and phospholipids (Parrish, 2013). Triacylglycerols and phospholipids are among the most important molecules within these classes, providing energy storage and structural integrity to cell membranes, respectively. Structurally, these lipids have two or three fatty acids esterified to their backbone, some of which, along with specific sterols, are considered crucial for marine ecosystem health and stability (Arts et al. 2001; Arts et al. 2009; Parrish 2013). Lipid structure in organisms is defined by the physical characteristics of both their environment and their lifestyle (Lee et al., 2006; Parrish, 2013). Thus, identifying lipid structures among organisms in an ecosystem can provide information about environmental pressures (i.e. seasonal temperatures), food availability (i.e. starvation), or life

cycles (i.e. reproduction) (Lee et al., 2006; Parrish, 2013). As such, analyzing lipids can elucidate trophic relationships and nutritional status.

1.5. Fatty acids

Fatty acids (FA) commonly consist of an even number of 14-24 carbons, but some have more in their structure and some are odd-numbered (Gurr et al., 2002). Each fatty acid has a carbon chain between a terminal methyl group (-CH_3) at one end and a terminal carboxyl group (-COOH) at the other. Fatty acids with no double bonds are saturated, and FA with 1-6 double bonds are unsaturated. In this thesis, the notation used for fatty acids is A:Bωn (e.g. 20:5ω3), where A is the number of carbons, B is the number of double bonds, and n is the location of the first double bond relative to the terminal methyl group (Ackman, 1986; Gurr et al., 2002). Although any given organism can have upwards of 70 fatty acids, only a handful are considered essential in marine diets. Three essential fatty acids (EFAs) are particularly necessary: DHA (docosahexaenoic acid, 22:6ω3), EPA (eicosapentaenoic acid, 20:5ω3), and ARA (arachidonic acid, 20:4ω6) (Müller-Navarra et al., 2000; Castell et al., 2004; Parrish, 2013). These important polyunsaturated fatty acids (PUFA) maintain membrane structure and function in invertebrates and plants (Arts et al., 2009). In the rhodolith community, essential fatty acids are important because most fauna use them for growth and metabolism (Martin-Creuzburg et al., 2009; Parrish, 2009, 2013).

The intake, accumulation, and transferability of fatty acids make them an excellent tool to study trophic pathways (Carreón-Palau et al., 2013; Trueman et al., 2014). Increasingly, researchers use fatty acids as tracers and biomarkers for food sources and nutrition because their composition can show input, cycling, and loss of material within food webs (Kelly and Scheibling, 2012). For example, their accumulation over time as fat stored in organism bodies represents

dietary intake over days, weeks, and even months (Iverson, 2009) and the high variability of fatty acid structures makes them suitable for acquiring unique fatty acid signatures from prey (Budge et al., 2007; Iverson, 2009; Legeżyńska et al., 2014). As biomarkers, specific fatty acid profiles separate classes of primary producers: diatoms, dinoflagellates, bacteria, and macroalgae, each identified by either their specific fatty acid signatures or ratios (Sargent et al., 1987; Parrish et al., 2000; Kelly et al., 2008). Though many trophic studies have used fatty acids to delineate benthic food webs (Budge et al., 2007; Parrish et al., 2009; Mohan et al., 2016), this study is the first to focus on rhodolith bed lipids and fatty acids.

1.6. Stable isotopes

In complex benthic systems such as rhodolith beds, analyzing lipids and fatty acids alone may not give a precise enough model of the energy pathways because some organisms may feed on multiple food sources that have distinct but overlapping fatty acid signatures (Kharlamenko et al., 2001; Pitt et al., 2009; Kelly and Scheibling, 2012). Bulk stable isotope analysis is a useful tool to pair with lipid and fatty acid analyses to help identify trophic relationships (Michener, 1994; Connelly et al., 2014; Hussey et al., 2014), food and carbon sources (Carreón-Palau et al., 2013; Trueman et al., 2014), food web structure (Grall et al., 2006; Linnebjerg et al., 2016), and seasonal variation (Jaschinski et al., 2011). Stable carbon and nitrogen isotopic signatures ($\delta^{15}N$ and $\delta^{13}C$) are typically enriched from prey to consumer by 2 to 4‰ for $\delta^{15}N$, and ~1‰ for $\delta^{13}C$, respectively (DeNiro and Epstein, 1978, 1981; Minagawa and Wada, 1984). The high enrichment of $\delta^{15}N$ between prey and predator makes it a useful indicator of organism trophic level within a food web (Iken et al., 2001; Post, 2002). Distinct $\delta^{13}C$ values of primary producers are reflected in the tissue of their consumers (DeNiro and Epstein, 1978; Riera et al., 1999) and can thus provide dietary

data from the base of the food web (Peterson and Fry, 1987; Post, 2002; Bouillon et al., 2011). Multiple studies have deciphered cold-water benthic food web structure with bulk stable isotope analyses (Iken et al., 2005; Connelly et al., 2014; Linnebjerg et al., 2016), yet only two have focused on rhodolith communities: Grall et al. (2006), and Gabara (2014). Nonetheless, this thesis is the first study to combine lipid, fatty acid, and stable isotope analyses to study a rhodolith community.

1.7. Temporal and spatial studies

Given the complex nature of trophic ecology in benthic marine ecosystems, large-scale spatial and temporal studies provide a more complete representation of trophodynamics than non-continuous sampling studies (Ellis and Schneider, 2008). Many marine processes are complicated or change seasonally and require careful observation. For example, the biannual phytoplankton bloom, once in the spring and once in the fall, affects food availability throughout the entire year. The higher phytoplankton and resulting food availability during blooms creates more complex feeding interactions than outside of blooms; a single snapshot study would not capture this difference (Smetacek, 1984; Christensen and Kanneworff, 1986; Trombetta et al., 2020). Temporal studies are important to capture the diverse diets of organisms living in seasonal waters, which may change seasonally (Kelly and Scheibling, 2012). These studies can help identify seasonal variation in fatty acid composition of microalgae (Galois et al., 1996; Henderson et al., 1998; Connelly et al., 2014) and macroalgae (Honya et al., 1994; Nelson et al., 2002; Dalsgaard et al., 2003), significant sources of food for benthic communities. In addition, large (at least >2 km^2) (Armonies, 2000) spatial scale studies yield a more accurate representation of population dynamics and environmental impact on diet than small-scale studies (Armonies, 2000; Dalsgaard et al., 2003;

Marcelina et al., 2018) because scaling up small-scale studies is not necessarily always accurate (Ellis and Schneider, 2008). Unfortunately, temporal and spatial variability are often poorly represented in food web studies (Thompson et al., 2012). This thesis is the first to study the trophic ecology of a rhodolith ecosystem both seasonally and across multiple sites.

1.8. Study species and area

I studied abundant rhodolith-associated organisms that exhibit different dominant feeding strategies: suspension/filter feeding [daisy brittle star, *Ophiopholis aculeata* and wrinkled rock-borer, *Hiatella arctica* (bivalve)], grazing [chitons *Tonicella* spp. and green sea urchin, *Strongylocentrotus droebachiensis*], and (3) predation [juvenile polychaetes *Nereis* spp. and common sea star, *Asterias rubens*]. I chose these six animal species because they exhibit different dominant feeding strategies defined as per Macdonald et al. (2010), namely suspension/filter feeding, grazing, and predation, while occurring in sufficient abundance to quickly provide sufficient biological material for analyses as per macrofaunal diversity and abundance data for this bed from Gagnon et al. (2012) and Bélanger (2020). Pieces of rhodolith (*Lithothamnion glaciale*), kelp (*Laminaria digitata*), seawater from above the rhodolith bed, and sediment underlying the rhodolith bed were sampled to explore possible benthic-pelagic coupling and how falling nutritional material from pelagic plankton blooms affects diets of benthic organisms.

The study area is located within Conception Bay, Newfoundland, near the coastal community of St. Philip's. The site (47° 35′ 36.5″ N, 52° 53′ 31.0″ W) is located within Broad Cove, a horseshoe-shaped coastline with a river (Broad Cove River) flowing out from a harbour (Figure 1.1.). A large (>500 m^2) rhodolith bed (*L. glaciale*) extends from a depth of 5 m to greater than 25 m. The peripheries of the bed reach to the northeast (47° 35' 39.6" N, 52° 53' 24.6" W),

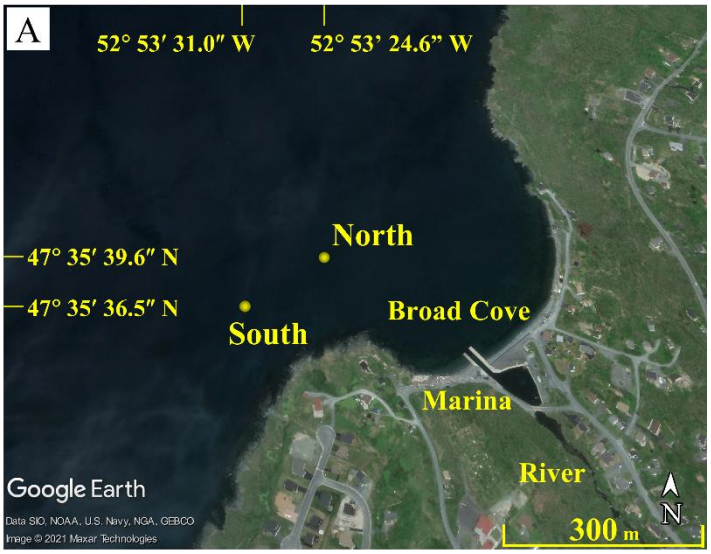
A
52° 53′ 31.0″ W
52° 53’ 24.6” W
North
47° 35′ 39.6″ N
47° 35′ 36.5″ N
South
Broad Cove
Marina
River
Google Earth
Data SIO, NOAA, U.S. Navy, NGA, GEBCO
Image © 2021 Maxar Technologies
N
300 m


B

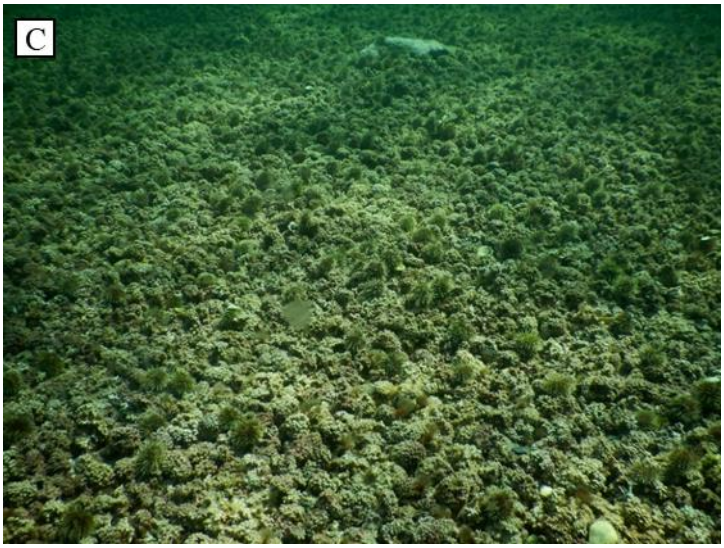
C

Figure 1.1. (A) Location of the two study sites within the rhodolith (*Lithothamnion glaciale*) bed fringing St. Philip's (southeastern Newfoundland) used to study rhodolith bed trophodynamics. Chapter II focuses on the food web at the "South" site in the spring of 2017. The "North" site is included in Chapter III examining spatial and temporal variability in food web structure. Both sites are located at the periphery of Broad Cove, which receives seasonally variable volumes of freshwater from the adjacent marina and river to which it is connected (Image: Google Earth). (B) Staged photograph of rhodoliths (*Lithothamnion glaciale*) and associated macrofauna (pictured: *Ophiopholis aculeata*, *Strongylocentrotus droebachiensis*, and *Tonicella* spp.) out of water from a laboratory bench at the Ocean Sciences Centre. (Image: Sean Hacker Teper). (C) Section of the rhodolith bed at the South site at a depth of ~15 m. Rhodoliths are tightly aggregated, with very little to no epiphytes and a relatively high abundance of green sea urchins (*S. droebachiensis*) moving on the bed surface (the biggest urchins are ~6 cm in test diameter) (Image: Patrick Gagnon).

~300 m from the mouth of the harbour, where rhodoliths become sparser between patches of sediment and scattered bedrock.

1.9. Thesis outline

The general goal of this thesis was to build on previous studies by Gagnon et al. (2012), who first characterized rhodolith morphology and invertebrate diversity in Newfoundland, and by Millar and Gagnon (2018), who then studied how the documented dominant invertebrates affect sedimentation in the bed. I aimed to build on this knowledge and objectively quantify these rhodolith associated invertebrate interactions using a combination of emerging trophic ecology techniques. By combining stable isotope analyses with lipid and fatty acid analyses, this study is the first to provide the resolution necessary to understand better the feeding dynamics in rhodolith beds and some of the expected benthic-pelagic relationships.

Besides the present introductory chapter (I), this thesis contains two data chapters (II and III) and a conclusion and summary chapter (IV). In Chapter II, I combined lipid, fatty acid, and stable isotope techniques and analyses to test the hypotheses that: (1) the lipid composition of organisms generally reflects the predominantly cold-water conditions of Newfoundland; and (2) the food web is mainly controlled from the bottom up by planktivores and detritivores as reflected by high abundance of planktonic and bacterial biomarkers. By testing these hypotheses, I aimed to (1) identify lipid compositions of organisms to understand better if functional strategies relate to organism's environments; and (2) delineate trophic linkages among organisms to understand the nutritional value of their diets and the extent of benthic-pelagic coupling versus strictly benthic interactions. In Chapter III, I increase the temporal and spatial dimensions of Chapter II to explore possible seasonal and spatial trophodynamic variability in the rhodolith bed.

I use the same combination of lipid, fatty acid, and stable isotope techniques and analyses as in Chapter II, but include two additional collections and one additional site to test the hypotheses that: (1) seasonal fluctuations in temperature and food availability affect lipid composition and diets of organisms; and (2) diets of organisms in close proximity to riverine input reflect its freshwater origins. By testing these hypotheses, I aimed to identify (1) temporal dietary changes to understand better how organisms adapt to seasonal fluctuations of food availability; and (2) how riverine input proximity affects both rhodolith community structure and organism lipid composition and diet to characterize how specific *in situ* conditions may affect rhodolith communities. Chapter III is the first study to elucidate how feeding relationships change seasonally and spatially in rhodolith beds. Chapter IV summarizes the results and main conclusions from the two data chapters, the importance of the study, and offers future research potential.

CHAPTER II

Assessing the trophodynamics of a Newfoundland rhodolith (*Lithothamnion glaciale*) bed community using lipid, fatty acid, and stable isotope analyses

2.1. ABSTRACT

Trophic ecology aims to understand relationships and interactions among organisms. Given the high biodiversity of rhodolith beds, combining trophodynamic techniques can help delineate complex trophic interactions. We paired a survey of macrofaunal abundance and rhodolith morphology with lipid, fatty acid, and stable isotope analyses to quantify nutritional patterns and trophic linkages of six dominant echinoderm, bivalve, gastropod, and polychaete species, two macroalgal species, seawater, and underlying sediment in a Newfoundland rhodolith (*Lithothamnion glaciale*) bed. We tested the hypotheses that: (1) the lipid composition of organisms generally reflects the predominantly cold-water conditions of Newfoundland; and (2) the food web is mainly controlled from the bottom up by planktivores and detritivores as reflected by high abundance of planktonic and bacterial biomarkers. We collected rhodoliths from a large (>500 m^2) rhodolith bed in St. Philip's, Newfoundland for all analyses. We observed high densities of chitons (*Tonicella marmorea* and *T. rubra*) and daisy brittle stars (*Ophiopholis aculeata*); overall species composition, morphological traits of rhodoliths (shape and size), and total rhodolith biomass (19.5 kg m^{-2}) were consistent with previous studies from the site, indicating temporal stability. Our lipid and fatty acid analyses revealed high levels of phospholipids and unsaturated fatty acids combined with low sterols in all animal species, indicating adaptability for increased membrane fluidity in response to cold temperatures. Analyses showed that organisms in the rhodolith food web community feed on a shared resource - diatoms. Results also revealed macroalgae-based detritus as a key food source within rhodolith communities. We identified three distinct trophic levels (producers, suspension/filter feeders and grazers, and predators) and potentially discovered a specific link between a macroalgal-based diet and carbon source in bivalves (*Hiatella arctica*), chitons (*Tonicella* spp.), and brittle stars (*O. aculeata*). We conclude Newfoundland rhodolith ecosystem diets reflect cold-water conditions, with significant contributions by planktivores and first-order consumers.

2.2. INTRODUCTION

Trophic ecology is the study of feeding relationships and energy transfers among organisms interacting in a community. In all ecosystems, energy is transferred through feeding from primary producers to primary and higher-order consumers. This transfer is often unclear in marine benthic ecosystems partly because of the broad diets of many species, a large detritus pool, and sometimes complex benthic-pelagic relationships, which can also vary seasonally (Kharlamenko et al., 2001; Pitt et al., 2009; Kelly and Scheibling, 2012). Trophic relationships can be studied with analysis of lipid classes, fatty acids, and stable isotopes. Lipids are the densest form of energy (cal/g) in marine ecosystems, essential for structural integrity, storage, and signaling of molecules in cell membranes (Parrish et al., 2000; Parrish, 2009). Lipids and fatty acids can be used as biomarkers for food sources and nutrition because their composition can show input, cycling, and loss of material within food webs (Kelly and Scheibling, 2012). The intake, accumulation, and transferability of lipids and fatty acids make them an excellent tool to study trophic pathways (Richoux et al., 2005; Drazen et al., 2008a, 2008b). Bulk stable isotope analysis is a useful approach to pair with fatty acid analysis to help identify trophic relationships (Michener, 1994; Connelly et al., 2014), food and carbon sources (Carreón-Palau et al., 2013; Trueman et al., 2014), and food web structure (Grall et al., 2006; Linnebjerg et al., 2016).

Rhodoliths (free-living, non-geniculate red coralline algae growing as balls, branched twigs, or rosettes) often form dense aggregations, known as “rhodolith beds”, at depths of up to 150 m in tropical to polar seas (Foster, 2001; Foster et al., 2007). Rhodolith beds, along with seagrass meadows, kelp beds and forests, and mangrove forests, are one of the four major types of marine benthic primary producers (Foster, 2001; Foster et al., 2007). The relatively complex morphology of rhodoliths creates suitable habitats for attachment (Kamenos et al., 2004a; Steller and Cáceres-Martínez, 2009; Riosmena-Rodriguez and Medina-López, 2010), reproduction

(Kamenos et al., 2004b; Steller and Cáceres-Martínez, 2009; Gagnon et al., 2012), and feeding (Steneck, 1986; Gagnon et al., 2012; Riosmena-Rodríguez et al., 2017) of highly diverse algal and faunal assemblages. The important contribution of rhodolith beds to marine biodiversity (Steller et al., 2003; Gagnon et al., 2012; Riosmena-Rodríguez et al., 2017) and global calcium carbonate ($CaCO_3$) production (Amado-Filho et al., 2012a; Harvey et al., 2017; Teed et al., 2020) has, in part, triggered the recent increase in studies of factors and processes regulating their structure and function (Marrack, 1999; Hinojosa-Arango et al., 2009; Millar and Gagnon, 2018).

Knowledge about trophodynamics in rhodolith beds is limited to only a couple of studies of beds in the northeastern Atlantic (Grall et al., 2006) and the eastern Pacific (Gabara, 2014), suggesting a high importance of suspended particulate organic matter (SPOM), sediment organic matter (SOM), and macroalgae in rhodolith food webs. Both studies based their conclusions on use of bulk stable isotope analysis, in particular consideration of organisms' carbon ($\delta^{13}C$) and nitrogen ($\delta^{15}N$) isotopic signatures (DeNiro and Epstein, 1978, 1981; Minagawa and Wada, 1984) to identify primary producers (Peterson and Fry, 1987; Post, 2002; Bouillon et al., 2011) and trophic levels of consumers (Iken et al., 2001; Post, 2002). As noted by Newell et al. (1995) and Kelly and Scheibling (2012), benthic food webs with significant macroalgal and bacterial components are often too complex to characterize uniquely with stable isotope analysis. This is likely the case for rhodolith beds, in particular those in seasonal seas, where phytoplankton blooms and growth of microalgal and bacterial films on the surface of benthic organisms occur seasonally. In such cases, fatty acid and stable isotope analyses can, in principle, simultaneously help distinguish algal and bacterial inputs (Sargent et al., 1987; Kharlamenko et al., 2001; Kelly and Scheibling, 2012). Our study aims to further knowledge about rhodolith bed trophodynamics by (1) identifying lipid compositions of organisms in order to understand better functional strategies

in relation to organism environments; (2) delineating trophic linkages among organisms to understand the nutritional value of their diets and the extent of benthic-pelagic coupling versus strictly benthic interactions; and (3) investigating specific challenges and requirements for future lipid and stable isotope analyses of rhodolith communities. Thus, by combining stable isotope analyses with lipid and fatty acid analyses, our study is the first to provide a resolution necessary to understand better the feeding dynamics in rhodolith beds and some of the expected benthic-pelagic relationships.

Studies of a large (>500 m^2) bed in St. Philip's, Newfoundland, first characterized rhodolith morphology and invertebrate biodiversity (Gagnon et al., 2012), then addressed how the documented dominant invertebrates affect sedimentation within the bed (Millar and Gagnon, 2018). Building upon these rhodolith-associated invertebrate interactions, our study defines the trophic interactions between said invertebrates and proposes a fundamental rhodolith community food web structure. Lipid class, fatty acid, and stable isotope biomarker analyses in a Newfoundland rhodolith community will elucidate how these food sources affect the diets of rhodolith-associated invertebrates that exhibit different dominant feeding strategies (see section 2.3.1). Our study aims to test the hypotheses that (1) the lipid composition of organisms generally reflects the predominantly cold-water conditions of Newfoundland; and (2) the food web is mainly controlled from the bottom up by planktivores and detritivores as reflected by high abundance of planktonic and bacterial biomarkers. A companion study (Chapter III) based on use of the same and further improved methods of lipid, fatty acid, and stable isotope analyses, increases the temporal and spatial dimensions of the results presented here in order to explore possible seasonal trophodynamic variability.

2.3. MATERIALS AND METHODS

2.3.1. Study site and selection of focal species

Our study was carried out during the spring of 2017 in a rhodolith (*Lithothamnion glaciale*) bed, which extends ~5 to 30 m in depth along the coast of St. Philip's, southeastern Newfoundland, Canada. Consistent with our broader objective of characterizing spatial and temporal variability in rhodolith bed trophodynamics, we chose to study the section of the bed fringing Broad Cove (47° 35′ 36.5″ N, 52° 53′ 31.0″ W; Figure 1.1) because of presumed differences in marine environmental conditions in this area. Broad Cove is connected to a marina, which is the end point of a river originating from several large ponds in the centre of the northern Avalon Peninsula. Volumes of freshwater entering Broad Cove vary seasonally and are generally lowest in summer, when precipitations (ECCC, 2019), and hence river discharge, decrease (P. Gagnon, personal observations). Our study focuses on the southernmost of two sites, i.e. the "South" site (Figure 1.1), which represents a relatively stable environment for the rhodoliths because of low hydrodynamic forces and sedimentation, and nearly unchanged rhodolith size structure over the past few years, as documented in this and other studies of the bed (Gagnon et al., 2012; Millar and Gagnon, 2018). We include the "North" site (Figure 1.1) in a follow up study of trophic variability (Chapter III) because of the presumably greater environmental variability at this site resulting from greater proximity to freshwater input from the marina. This study, therefore, focuses on trophic interactions at one site based on a single point in time, and serves as a baseline for expansion of spatial and temporal dimensions in a follow-up study (Chapter III).

Our food web analyses (described below) focused on the following six animal (1-6; Figure 2.1), two macroalgal (7-8), and two environmental (9-10) components inside (1-6, 8, 10) or outside (7, 9) of the bed: (1) common sea star, *Asterias rubens*; (2) wrinkled rock-borer, *Hiatella*

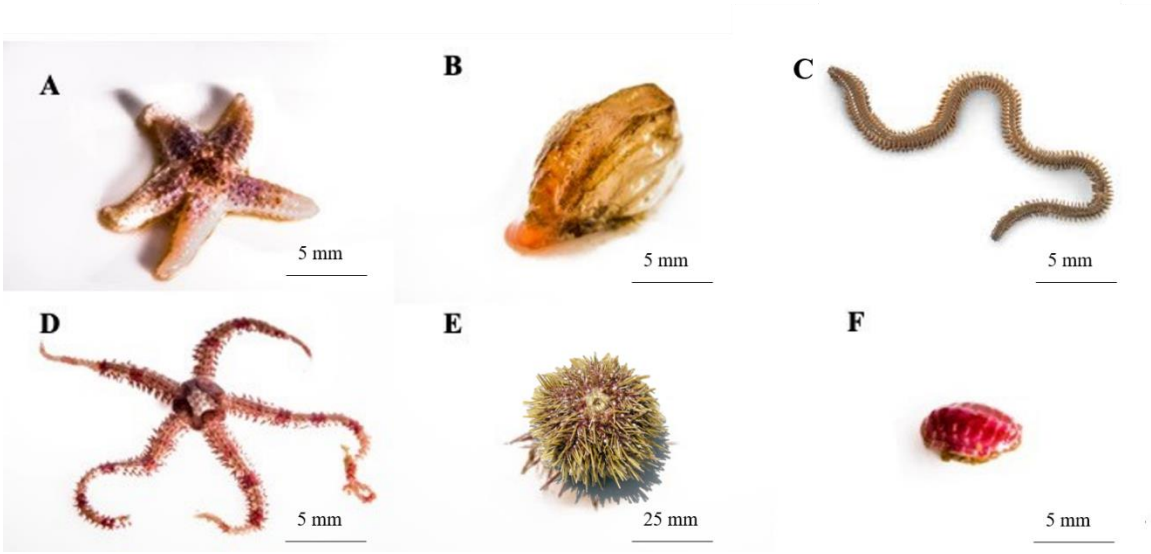

Figure 2.1. The six animal species included in the food web analyses; (A) common sea star, *Asterias rubens*; (B) wrinkled rock-borer, *Hiatella arctica* [bivalve]; (C) *Nereis* spp. [polychaete]; (D) daisy brittle star, *Ophiopholis aculeata*; (E) green sea urchin, *Strongylocentrotus droebachiensis* and (F) Atlantic red chiton, *Tonicella rubra*. (Images: (A), (B), (D), (F) - Sean Hacker Teper; (C) https://www.enasco.com/p/Sandworm-Clam-Worm-Nereis%2C-Preserved%2BLS01292; (E) http://pugetsoundsealife.sseacenter.org/pugetsoundsealife.com/puget_sound_sea_life/Green_Sea_Urchin.html.

arctica [bivalve]; (3) juvenile *Nereis* spp. [polychaetes]; (4) daisy brittle star, *Ophiopholis aculeata*; (5) green sea urchin, *Strongylocentrotus droebachiensis*; (6) red molted chiton, *Tonicella marmorea*, and Atlantic red chiton, *T. rubra*, which were too difficult to distinguish morphologically and hence were pooled; (7) pieces of *Laminaria digitata* [kelp] from nearby kelp beds; (8) *Lithothamnion glaciale* [rhodoliths]; (9) seawater [containing seston] from a few meters above the rhodolith bed; and (10) sediment [containing infauna] underlying the rhodoliths. We chose these six animal species because they exhibit different dominant feeding strategies defined as per Macdonald et al. (2010), namely suspension/filter feeding (2, 4), grazing (5, 6), and predation (1, 3), but occur in sufficient abundance to quickly provide enough biological material for the analyses as per macrofaunal diversity and abundance data for this bed from Gagnon et al. (2012) and Bélanger (2020). Pieces of kelp (8), seawater from above the rhodolith bed (9), and sediment underlying the rhodolith bed (10) were sampled to explore possible benthic-pelagic coupling.

2.3.2. Timing of sampling

To increase the likelihood of detecting benthic-pelagic coupling, we sampled the rhodolith bed during the annual spring phytoplankton bloom in southeastern Newfoundland, when diatom abundance in the water column was predictably highest (Budge and Parrish, 1998; Parrish et al., 2005). Fluorescence data acquired at the study site with a CTD (conductivity, temperature, and depth) profiler equipped with PAR (photosynthetically active radiation) and fluorescence sensors were used to monitor the progression and confirm the occurrence of the bloom (Appendix B). The bloom began in the last few days of March and continued until at least 23 April, 2017

(Appendix B), when we sampled the rhodolith community and collected rhodoliths for food web analyses.

2.3.3. Rhodolith community

In order to broadly characterize the rhodolith community, scuba divers hand collected, on 23 April, 2017, all the rhodoliths from one 30 x 30 cm quadrat placed every 5 m along a 30-m long transect at a depth of ~15 m at the South site (for a total of seven quadrats sampled). We chose to sample this section of the bed because of its relatively homogenous distribution and abundance of rhodoliths (Gagnon et al., 2012; Millar and Gagnon, 2018); Figure 1.1). Rhodoliths and their associated macrofauna were deposited in labelled, sealable plastic bags, with several bags per quadrat. Bags were sealed under water, placed in mesh collection bags, and lifted to a boat where they were stored in plastic bins filled with seawater collected at the site. They were transported to the Ocean Sciences Centre (OSC) of Memorial University of Newfoundland (MUN) within 4 h of collection and placed in large (320-L) holding tanks supplied with running seawater pumped in from the adjacent Logy Bay.

Lengths of the longest, intermediate, and shortest axes, as well as gross weight of the 247 rhodoliths collected were measured with calipers (precision of 0.1 mm) and a balance (precision of 0.1 g; PB3002-S/FACT; Mettler Toldeo). Each rhodolith's linear dimensions and number of rhodoliths in each of the seven quadrats were subsequently used to calculate each rhodolith's sphericity (as per Graham and Midgley (2000) and Sneed and Folk (1958)) or to estimate rhodolith abundance (density) in the bed. Rhodolith shape was plotted with the spreadsheet TRIPLOT (https://www.lboro.ac.uk/microsites/research/phys-geog/tri-plot/tri-plot_v1-4-2.xls (Sneed and Folk, 1958; Graham and Midgley, 2000) as described by Gagnon et al.

(2012). All macrofauna on the external surface and inside of each rhodolith were extracted with tweezers and forceps, breaking rhodoliths in pieces with a screwdriver and a hammer to extract hidden specimens when needed. Organisms were placed in labeled specimen cups filled with a 4% formalin solution prior to permanent changeover after three days into a 70% ethanol solution. Over the following few weeks, preserved macrofauna were identified and counted with a stereomicroscope (DMW-143-N2GG; Motic) at 10 or 20X magnification and weighed with a balance (precision of 0.1 g; PB3002-S/FACT; Mettler Toldeo). Epiphytes and encrusting invertebrates such as bryozoans and sponges were present in trace amounts, and hence excluded from the analysis. For each quadrat, we subsequently subtracted total macrofaunal weight from gross rhodolith weight to obtain net rhodolith weight, which we used to calculate rhodolith abundance (biomass) in the bed.

2.3.4. Collection and preparation of samples for food web analyses

In order to limit influences of manipulation of rhodoliths and their macrofaunal content on data quality, we used a different group of rhodoliths for food web analyses than those sampled to characterize the rhodolith bed community. On 23 April, 2017, divers hand collected ~150 live rhodoliths measuring 8 to 10 cm along the longest axis from the same area where we sampled the associated bed community. Broken rhodoliths and rhodoliths partially buried in sediment or with blackened or whitened tissue on their surface (indicative of stress or necrosis) were not collected because of potential influences on the abundance, diversity, and chemical composition of resident macrofauna. Preliminary analysis indicated that common sea star and green sea urchin biomasses within the rhodoliths were too low to provide the minimum amount of tissues required to run the lipid and stable isotope analyses (see below). We resolved this requirement by collecting an

additional ~10 small individuals (1-2 cm in diameter) from atop the bed for each species. The fronds of three, ~1m long kelp (*L. digitata*) growing on rocks at a depth of ~2 m near the rhodolith bed were also hand collected. Rhodoliths and kelp fronds were placed in plastic bags sealed underwater. We collected seawater a few centimeters above the rhodolith bed with two, 12-L Niskin bottles that we deployed gently to prevent resuspension of sediment from the bed. Water from the bottles was transferred (on the boat) to plastic containers pre-rinsed with distilled water, from which a total of 17 L of seawater was subsequently taken to meet the requirements of the various analyses (see below). Three sediment samples were also scooped from the top (~10 cm) layer of muddy sediment underneath rhodoliths with 15-mL centrifuge tubes.

All rhodoliths and their macrofaunal content, as well as kelp fronds, were transported to the OSC as described above (see section 2.3.3). At the OSC we transferred all the rhodoliths in their sealed plastic bags to large (320-L) holding tanks supplied with running seawater to keep water temperature in the bags naturally low (~0.5 °C), while retaining all macrofauna. Bags were kept sealed in the tanks for 24 h to (1) facilitate stomach emptying of focal species; (2) prevent hypoxia and degradation of biological tissues; and (3) avoid mixing water from St. Philip's [in the bags] with water from Logy Bay [in the holding tanks]. This procedure reduced the likelihood of contaminating the original lipid class, fatty acid, and isotopic signatures of the focal species. After this 24-h resting phase, we removed bags from the tanks and processed them one by one with pre-cleaned/sterilized tools and glassware manipulated with frequently changed nitrile gloves, again to avoid contamination of samples. Test tubes and scintillation vials were heated in an oven for 8 h at 425 °C to remove lipid material, then labeled and weighed. Test tube caps and the tools used to break rhodoliths (hammer, screwdriver, mortar, and pestle) and extract and separate macrofauna (tweezers, forceps, filters) were lipid-cleaned with three rinses each of methanol and

chloroform to remove any residual lipids. Collection and storage items (sealable plastic bags and containers, centrifuge tubes) were rinsed with distilled water.

We extracted the six focal animal species from the surface of rhodoliths with tweezers and forceps, breaking rhodoliths in pieces with a screwdriver and a hammer to extract cryptic specimens when needed. For lipid class and fatty acid analyses, we obtained three replicates of 0.5 to 1.5 g of tissue each (wet weight) for each species from one or several individuals (i.e. pooling tissue as needed). We included whole individuals (i.e. shells, exoskeletons, and internal organs) in the wet weight of lipid class and fatty acid analysis samples. Each replicate was placed in a 40-mL test tube (one replicate per tube) and stored on ice in a cooler until we had collected all replicates. Test tubes were then filled with 8 mL of chloroform, flushed under a gentle stream of nitrogen, capped, sealed with Teflon tape, stored in freezers at -20 °C, and their content analyzed within two months. For stable isotope analysis, we collected ~5 g of tissue, excluding shells and exoskeletons, into one 20-mL scintillation vial for each species to be split into three replicates once dry (see section 2.3.7). Due to the randomness of availability of material of the small, pooled organisms and because lipid extraction may affect $\delta^{15}N$ data (Post et al., 2007), we did not use the same organism material between lipid-extraction and stable isotope analysis (see section 2.3.9.3 for statistical implications). After oven drying for 24 h at 60 °C, at least 1 to 1.5 mg of tissue remained for each replicate. Each scintillation vial was capped with tin foil and a cap, stored in freezers at -80 °C, and their content analyzed within twelve months.

Upon arrival at the OSC, kelp fronds and sediment samples were immediately stored in their individual, sealed plastic bags (kelp) or centrifuge tubes (sediment) in freezers at -80 °C. The same procedures as above were used to prepare rhodolith, kelp, and sediment samples for lipid class, fatty acid, and stable isotope analyses, with the following modifications. Rhodoliths were

first gently scrubbed by hand to remove epibionts, broken off with a screwdriver and a hammer, and ground into a powder with a mortar and a pestle. Rhodolith powder was analyzed; within two (lipid class and fatty acid analyses) or twelve (stable isotopes) months. Kelp fronds (blades and stipes) were gently scrubbed by hand to remove epibionts. Each replicate of sediment for the lipid class and fatty acid analyses weighed 6 to 8 g (wet weight). Kelp and sediment samples were also analyzed within two (lipid class and fatty acid analyses) or twelve (stable isotopes) months.

Seawater samples were processed immediately upon arrival at the OSC. The two plastic containers holding the seawater were shaken to re-suspend any settled materials. This water and its content were transferred with 250- to 500-mL graduated cylinders to a mechanized filtration system, which suctioned water with an aspirator through a 47-mm diameter GF/C filter (Whatman; General Electric) at the bottom of a Büchner funnel. During suction, we washed the contents of graduated cylinders onto the filters with filtered seawater to transfer all lipid material. Visual inspection of the first filter indicated an acceptable accumulation of suspended materials upon completing the filtration of the first 3 L of seawater. Given the total volume of water available (~17 L), three replicates were created for the lipid class and fatty acid analyses; one per each 3 L of filtered seawater. The remaining water, 8 L, was also filtered, yielding three replicates for the stable isotope analysis; one per each 2.5 L of filtered seawater. Each filter used was rolled with tweezers and placed in a 40-mL test tube (one filter per tube) for the lipid class and fatty acid analyses, or in a 20-mL scintillation vial (one filter per vial) for the stable isotope analysis. Test tubes were filled with 8 mL of chloroform, flushed under a gentle stream of nitrogen, capped, sealed with Teflon tape, stored in freezers at -20 °C, and their content analyzed within two months. Vials were capped with tin foil and a cap, stored in freezers at -80 °C, and their content analyzed within twelve months.

2.3.5. Extraction and characterization of lipid classes

Extraction of lipids followed protocols by Folch et al. (1957) with modifications by Parrish (1999). Samples in their test tubes were taken out of the freezers and handled 8 to 16 at a time. Each tube was held in ice and contents were immediately ground to a pulp with a metal-ended rod washed into the tube with ~1 mL of chloroform:methanol (2:1) and 0.5 mL of chloroform-extracted water. The tube was sonicated for 4 min and centrifuged for 3 min at 3000 rpm. The resulting organic layer at the bottom of the tube was completely removed and transferred to a 15-mL vial with a double pipetting technique to bypass the upper aqueous layer and transfer only the lower aqueous layer. After three repetitions, both pipettes were washed into the 15-mL vial with 3 mL of chloroform. All vials were flushed under a gentle stream of nitrogen, capped, sealed with Teflon tape, and stored in freezers at -20 °C. Each vial's content was subsequently transferred to a 2-mL, lipid-clean vial with three or more rinses of 0.5 mL of chloroform, until the chloroform in the 15-mL tube remained transparent. Each 2-mL vial was flushed under a gentle stream of nitrogen, capped, sealed with Teflon tape, and stored in freezers at -20 °C.

We used thin-layer chromatography with flame ionization detection (TLC-FID) to characterize lipid classes (Parrish, 1987). Separation of lipid classes followed a 3-step development method in which four solvent solutions of different polarities were used to obtain three chromatograms per rod (Parrish, 1987). Calibration curves against which samples were compared, were created with a 9-component standard (nonadecane, hydrocarbon; cholesteryl palmitate, steryl ester; 3-hexdecanone, ketone; tripalmitin, triacylglycerol; palmitic acid, free fatty acid; cetyl alcohol, alcohol; cholesterol, sterol; monopalmitoyl glycerol, acetone mobile polar lipid; phosphatidylcoline dipalmitoyl, phospholipid; Sigma Chemicals). Prior to applying samples,

silicic acid-coated quartz rods (Chromarods, Type SV; Iatron Laboratories Inc.) were blank scanned (the process of cleaning and activating rods by burning off any residual lipids from previous samples) three times in an Iatroscan TLC-FID system (Mark VI; Iatron Laboratories Inc.). The Iatroscan operated with a hydrogen flow between 195 and 199 mL min^{-1} and an air flow of 2 L min^{-1} at a room temperature of ~20 °C. After sample application (spotting) and before each development, the rods were dried and conditioned for 5 min in a constant humidity chamber (30%). Samples were spotted individually onto one of 10 rods in each of 2 racks (for a total of 20 rods) with a 25-µL Hamilton syringe (Hamilton Co.). Depending on the lipid concentration of each sample (estimated by colour and confirmed by trial and error), 0.5 to 10 µL was spotted at the origin of each rod (Appendix C). Both racks were then dipped twice into a 100% acetone solution and were removed each time when acetone reached the spotted samples. Rods were then double-developed in a hexane:diethyl ether:formic acid (98.95:1:0.05) solution, for 25 min then for 20 min to separate hydrocarbons (HC), steryl esters (SE), and ethyl and methyl ketones (KET). Each rod was then scanned in the Iatroscan beyond the KET peak to obtain the first chromatogram showing lipid quantities of HC, SE, and KET in each sample.

During the second step, rods were developed for 40 min in a hexane:diethyl ether:formic acid (79:20:1) solution to separate diacyl glyceryl ethers, triacylglycerols (TAG), free fatty acids (FFA), alcohols (ALC), sterols (ST), and diacylglycerols (DG). Each rod was then scanned beyond the DG peak to obtain the second chromatogram showing lipid quantities of TAG, FFA, ALC, ST, and DG in each sample. During the third step, rods were double-developed twice, first in a 100% acetone solution for 15 min each, then in a chloroform:methanol:chloroform-extracted water (5:4:1) solution for 10 min each to separate the most polar lipid classes, acetone-mobile polar lipids

(AMPL), and phospholipids (PL). Finally, each rod was completely scanned to obtain the third and final chromatogram showing lipid quantities of AMPL and PL.

2.3.6. Preparation and characterization of fatty acid methyl esters (FAME)

Fatty acid methyl esters (FAME) of lipids were prepared directly by transesterification from aliquots of lipid extract following a modified procedure described by Christie (1982) and Hamilton (1992). Extracted lipid samples in their 2-mL vials were taken from the freezer and held in ice. Depending on each sample's lipid concentration (estimated by colour and confirmed by trial and error), we transferred 20 to 1000 µL of lipid extract with a 20 to 100 µL Drummond microdispenser (Drummond Scientific) into a lipid-cleaned, 15-mL vial (one sample per vial). The transferred extract was evaporated to dryness under a stream of nitrogen gas, then we added 1.5 mL of dichloromethane and 3 mL of prepared Hilditch reagent (an alkylation derivatization reagent, 1.5 H_2SO_4: 98.5 MeOH). Each vial was vortexed, sonicated for 4 min, flushed with nitrogen gas, heated at 100 °C for one hour, cooled to ambient room temperature, filled with 0.5 mL of a supersaturated sodium bicarbonate solution and 1.5 mL of hexane, and agitated vigorously. This process created an organic layer containing transesterified fatty acids (i.e. converted to fatty acid methyl esters; FAME) at the surface of the solution, which we collected and transferred with a pipette to a lipid-cleaned, 2-mL vial, and evaporated to dryness under a stream of nitrogen gas. Each 2-mL vial was then filled with ~0.5 mL of hexane, flushed with nitrogen, capped, sealed with Teflon tape, and stored in freezers at -20 °C.

We used gas chromatography and flame ionization detection (GC-FID) to characterize fatty acids (Ackman, 1986; Christie, 1989; Budge et al., 2006). FAME samples were analyzed in a HP 6890 GC equipped with an Agilent 7683 autosampler. The GC column was a 30-m long ZB wax+

(Phenomenex) with an internal diameter of 0.32 mm. We introduced each FAME sample individually into a heated injector at 150 °C, which converted the liquid sample to a gaseous state. A stream of hydrogen then carried the sample at a rate of 2 mL min^{-1} through the GC column, which retained FAME depending on their structure. This selective retention resulted in the detection of individually eluted FAME by the FID. The GC-FID was operated as follows: the GC column temperature started at 65 °C for 30 s before it was increased to 195 °C at a rate of 40 °C min^{-1}, held there for 15 min, then increased again to 220 °C at a rate of 2 °C min^{-1}, and held there for 45 s. The initial heated injector's temperature of 150 °C increased to a final temperature of 250 °C at a rate of 120 °C min^{-1}. The detector (FID) temperature remained constant at 260 °C. Fatty acid peaks were identified by comparing retention times in the GC column with those from various standards: FAME mix (47885-U; Supelco), Bacterial acid methyl ester mix (47080-U; Supelco); PUFA 1 (47033; Supelco); and PUFA 3 (47085-U; Supelco). Chromatograms were integrated (quantified by calculating the area underneath a peak/curve) with the software Varian Galaxie Chromatography Data System V1.9.3.2.

2.3.7. Stable isotope preparation and analysis

Samples in their scintillation vials were taken out of the freezers, thawed, and oven dried at 60 °C for 24 h. Each sample was split equally by weight into three new, 20-mL scintillation vials. Each triplicate was ground with a mortar and pestle and rinsed three times with acetone. Ground samples were then each split into two equal parts: one for analysis of carbon content, the other for nitrogen. Vials with samples for nitrogen analysis were each rinsed three times with distilled water to remove salt because halides interfere with the Elemental Analyzer (described below). Samples for carbon analysis were acidified to remove inorganic carbon by adding drops

of 1 M HCl to the vials until no bubbles formed. Vials were left with lids off in a fume hood overnight, rinsed three times with distilled water to remove both HCl and halides, dried again at 60 °C for 24 h, transferred to desiccators, and subsequently taken to The Earth Resources Research and Analysis (TERRA) facility at MUN for analysis. Tools and tin capsules pre-cleaned with acetone were used to extract, weigh, and hold the following quantities of solidified samples from each vial: 1 to 1.5 mg for animals; 4 to 4.5 mg for rhodolith and kelp; 14 to 15 mg for sediment; 5 to 7 mg of filter for seawater $\delta^{13}C$ and carbon content; and 8 to 10 mg of filter for seawater $\delta^{15}N$ and nitrogen content. Tin capsules and their content were held in a desiccator and processed within a month as per the following procedure.

We analyzed bulk stable isotopes and complementary C and N elemental proportions (%) in an Elemental Analyzer (EA) system (NA1500; Carlo-Erba) consisting of an autosampler, an oxidation reactor (oven), a reduction reactor, a water trap, a gas chromatography (GC) column, and a thermal conductivity meter (TCD). The entire EA was flushed continuously with helium gas (He) at a rate of 90 to 110 mL min^{-1}. Each tin capsule with its content was individually dropped onto the oxidation reactor at a temperature of 1050 °C, with simultaneous injection of oxygen and quick flushing with He. This sequence triggered a flash combustion at 1800 °C between the tin capsule and oxygen, creating combustion gases that were pushed through an oxidation catalyst (chromium trioxide, CrO_3) to ensure complete oxidation of the sample and silvered cobaltous/cobaltic oxide, which removes halides and SO_2. The resulting gas mixture passed through the reduction reactor (reduced copper) at 650 °C, which reduces nitrogen oxides to nitrogen gas and absorbs oxygen. The gases then passed through a magnesium perchlorate ($Mg(ClO_4)_2$ water trap, after which the remaining gases (N_2, CO_2) entered a 3 m stainless steel GC column (QS 50/80; Poropak) at 40 to 100 °C. The individual gases were separated as they moved

through the GC column. Upon reaching the TCD, they were detected as separate gas peaks; first N_2, then CO_2. From the TCD, He carried the gases to a ConFloIII interface (Finnigan, Thermo Electron Corporation), which has split tubes, open to the atmosphere, which allow a portion of the He and combustion gases to enter directly into the ion source of the mass spectrometer (MS) (DeltaVPlus; Thermo Scientific) via fused glass capillaries. During operation, He from the EA flowed continuously into the MS. All gases exiting the EA also entered the ion source, but the instrument only recorded signals for the gases of interest, as defined through the software by instrument configuration. Internal and external reference material was used to calibrate MS data. EDTA #2 and D-Fructose were used for carbon isotope calibration, and IAEA-N-1 ($(NH_4)_2SO_4$) and IAEA-N-2 ($(NH_4)_2SO_4$) for nitrogen isotope calibration. NBS-18 ($CaCO_3$), B2150 (high organic sediment), B2151 (high organic sediment), and B2105 (Cystine) were used to aide data interpretation of carbon isotope analyses, and sorghum flour, B2153 (low organic soil), USGS-25 ($(NH_4)_2SO_4$), USGS-26 ($(NH_4)_2SO_4$), sulfanilamide, and BBOT to aide data interpretation of nitrogen isotope analyses. L-glutamic acid and B2155 (protein) were used for both carbon and nitrogen elemental calibration.

2.3.8. Trophic magnification of fatty acids

Stable isotope ratios are expressed in the conventional (δ) notation as parts per thousand (‰) as per the equation of Minagawa and Wada (1984):

$$\delta^{13}C \text{ or } \delta^{15}N(‰) = [\ (R_{sample} / R_{standard}) - 1\ ] \times 1000$$

where R_{sample} and $R_{standard}$ are the ratios of $^{13}C/^{12}C$ or $^{15}N/^{14}N$ of a given sample and corresponding standard, respectively. Results are reported relative to atmospheric N_2 for nitrogen stable isotopes, and Vienna PeeDee Belemnite (VPDB) for carbon stable isotopes. Species trophic position ($TP_{consumer}$) was calculated based on the equation used by Gale et al. (2013), developed by Cabana and Rasmussen (1996):

$$TP_{consumer} = [\ (\delta^{15}N_{consumer} - \delta^{15}N_{base}) / \Delta^{15}N\ ] + TP_{base}$$

where $\delta^{15}N_{consumer}$ is the mean stable N isotope ratio of each species, and $\Delta^{15}N$ is the fractionation factor which, to be consistent with rhodolith food web studies, is 3.4‰ (Grall et al., 2006). $\delta^{15}N_{base}$ and TP_{base} represent the nitrogen stable isotope composition and trophic positions from the base of the food web, respectively. We then calculated a trophic magnification factor (TMF) for fatty acids (FA) correlated with $\delta^{15}N$. This factor quantitatively represents the biomagnification of compounds along a food web (Borgå et al., 2012; Connelly et al., 2014). Compound concentrations often change across trophic levels, thus the equation:

$$FA\% = e^{m \times TP}$$

or

$$\log_e FA\% = (m \times TP) + b$$

and, therefore,

$$TMF = e^{m}$$

where m and b are the slope and intercept of the linear relationship (which strength was determined with conventional Spearman Rank-Order correlation tests) between $\log_e$ FA% and trophic position (TP), respectively. Positive values of m and TMF imply biomagnification throughout the food web, whereas negative values denote proportional depletion. To this extent, we did not use TMF as a tool to see changing concentrations of fatty acids through direct predator-prey relationships among organisms, but rather as a method to assess biomagnification and depletion of fatty acids by comparing fatty acids to one another and to help confirm the presence of key identified biomarkers throughout the food web (Connelly et al., 2014).

2.3.9. Statistical analysis

2.3.9.1. Lipid classes

We used a one-way permutational MANOVA (PERMANOVA) (Euclidean distance matrices with 9999 permutations) with the factor Component (nine of the 10 components of the food web studied [six animal species, kelp, sediment, and seawater]) to examine differences in proportions of lipid classes among samples (N=25, accounting for accidental loss of two samples during the analyses). We excluded the rhodolith component because of insufficient rhodolith tissue for lipid extraction. To limit extraneous data variability while focusing on the most significant lipid classes, our analysis included only lipid classes present in over 50% of the samples. Sample sizes for each food web component (N=2 or 3) was too low to examine differences among specific components. Consequently, for comparison purposes only, we pooled the data into the five following functional groups reflecting the three dominant feeding strategies of the six animal species, one macroalgal species, and two environmental components: (1) suspension/filter feeders [two species]; (2) grazers [two species]; (3) predators [two species]; (4) kelp; and

(5) seawater/sediment [samples combined because of expected benthic-pelagic coupling and to achieve a sufficient sample size for statistical analysis] (see section 2.3.1 for details). We then ran a one-way PERMANOVA with the factor Functional Group (the five groups discussed above). This approach yielded statistically reliable comparisons, except with kelp, for which sample size was too low and could not be pooled with any of the four other groups because of its unique nature. We therefore do not present comparisons with kelp. We examined relationships between total lipid and each of the major lipid classes with conventional Spearman Rank-Order Correlation tests (Zar, 1999).

2.3.9.2. Fatty acids

To examine differences in the proportions of fatty acids among samples (N=25), we used the same statistical approach (two one-way PERMANOVAs; one with Component as factor followed by one with Functional Group as factor) with the same data exclusion and grouping as for the lipid classes analysis. We then used a one-way SIMPER analysis (run on untransformed data with a Bray-Curtis similarity matrix) with the factor Component (nine of the 10 components of the food web studied [six animal species, kelp, sediment, and seawater], to identify potential food sources and the main fatty acids contributing to the lipid composition of each component (Kelly and Scheibling, 2012; Gabara, 2014). To limit extraneous data variability while focusing on the most significant fatty acids, we included only fatty acids contributing to over 70% of the similarities in the SIMPER analysis. We used a follow-up principal coordinates analysis (PCO; also run on untransformed data with a Bray-Curtis similarity matrix) with the factor Component (same as above), mainly for visualization of the feeding relationships among specific groups of organisms (Guest et al., 2008; Drazen et al., 2009). To increase clarity on the PCO, we plotted

only samples with a Pearson coefficient of correlation >65% (plus DHA; 22:6ω3, because of its importance as an essential fatty acid).

2.3.9.3. Stable isotopes

We examined differences in carbon ($\delta^{13}C$) and nitrogen ($\delta^{15}N$) isotope ratios with two one-way PERMANOVAs (one for each type of ratio; both types based on Euclidean distance matrices with 9999 permutations) with Component as factor. The $\delta^{13}C$ isotope ratio analysis (N=27, accounting for accidental loss of three samples during the analyses) included all taxa (six animal species, kelp, and rhodoliths) and both environmental components (seawater and sediment). We included both environmental components and all except one taxon (*Nereis* spp., for which we lacked sufficient amounts of tissues for quantification of stable isotope ratios) in the $\delta^{15}N$ isotope ratio analysis (N=26, accounting for accidental loss of one sample during the analyses). Due to our using separate samples for lipid-extract and stable isotope analyses, we used the averages of stable isotope results of individual components to make comparisons to lipid and fatty acid data. In order to group and map, in the form of a dendrogram, statistically different components of the food web We also carried out a cluster analysis using "Group Average" clustering on $\delta^{13}C$ and $\delta^{15}N$ isotope ratios simultaneously, and complementary SIMPROF test (Euclidian distance matrix with 9999 permutations) (N=23 because of a few unmatched pairs of $\delta^{13}C$ and $\delta^{15}N$ ratios) (Grall et al., 2006; Gabara, 2014). Four main isotopic groups emerged from the SIMPROF test. We therefore ran follow-up one-way PERMANOVAs (one with both isotopic ratios combined, followed by one for each type of isotopic ratio) and complementary one-way ANOVAs and post-hoc tests with the factor Group to identify differences among these four main trophic groups.

2.3.9.4. General aspects of statistical tests

In all PERMANOVAs, data were untransformed and computed on Bray-Curtis similarity or Euclidian distance matrices (9999 permutations) to meet the assumptions of multivariate normal (Gaussian) distribution and homogeneity of the covariance matrices (Budge et al., 2006; Clarke et al., 2006; Hair et al., 2006). All fatty acid multivariate data were computed using Bray-Curtis similarity matrices, while lipid and stable isotope multivariate data were computed using Euclidean distances matrices due to its better ability to handle missing data. Contrary to the recommendation from Kelly and Scheibling (2012), we used untransformed data because the dispersion of variance was equivalent to transformed data and it avoided artificial weighting of fatty acids with smaller proportions on our results compared to transformed data (Carreón-Palau et al., 2017). We used PERMDISP (9999 permutations) to inform our decision ($p=0.391$); we tested for homogeneity of multivariate variances and confirmed all variances were homogenous. We used PCO (principal coordinates analysis) instead of PCA (principal components analysis) to more efficiently account for missing data (Rohlf, 1972). In all ANOVAs, we verified homogeneity of variance and normality of residuals by examining the distribution of the residuals and the normal probability plot of the residuals, respectively (Snedecor and Cochran, 1994). We used a significance level of 0.05 in all analyses and report all means with standard deviation (mean ± SD) unless stated otherwise. We used standard error where applicable for consistency with corresponding literature (Gagnon et al., 2012; Connelly et al., 2014; Parzanini, 2018). We used PRIMER v7 with PERMANOVA+ for multivariate statistical analyses, Minitab 18 for univariate statistical analyses, and Microsoft Excel for descriptive statistics.

2.4. RESULTS

2.4.1. Rhodolith community

Rhodolith biomass at the study site averaged 19.5±0.9 (SE) kg m^{-2}. The 247 rhodoliths sampled varied in size from 11.3 to 65.6 mm, and 24.0 to 116.2 mm along the shortest and longest axes, respectively. Those rhodoliths were predominantly spheroidal and compact (~61%), but otherwise platy (~12%), bladed (~19%), or elongate (~8%) (Figure 2.2). Total macrofaunal biomass averaged 34.5±4.3 g kg^{-1} rhodoliths. The 1,191 animals extracted from the rhodoliths belonged to at least 21 species under six phyla, with echinoderms (452.7±47.0 individuals kg^{-1} rhodoliths) and molluscs (427.6±39.6 individuals kg^{-1} rhodoliths) as the two numerically dominant groups (Table 2.1). Species included in the biochemical analyses were particularly abundant, including *Ophiopholis aculeata* (336.7±30.8 individuals kg^{-1} rhodoliths), *Tonicella marmorea / T. rubra* (191.6±27.2 individuals kg^{-1} rhodoliths) and *Hiatella arctica* (152.8±23.2 individuals kg^{-1} rhodoliths). A few species not included in the analyses were also relatively abundant, including the brittle star, *Ophiura robusta* (72.7±13.8 individuals kg^{-1} rhodoliths), the caridean shrimp, *Pandalus borealis* (36.9±7.5 individuals kg^{-1} rhodoliths), and the polychaete, *Potamilla reniformis* (30.0±10.3 individuals kg^{-1} rhodoliths).

2.4.2. Total lipid content and lipid classes

Of the nine food web components included in the lipid analysis, the three echinoderm species exhibited the highest concentrations of total lipids, ranging from 8.5±2.2 mg g^{-1} (ww) in *A. rubens*, to 13.2±3.7 mg g^{-1} in *O. aculeata* (Table 2.2). The molluscs *H. arctica* and *Tonicella* spp. had, respectively, similarly high and slightly lower concentrations of total lipids, with 6.7±1.6 mg g^{-1} in *Tonicella* spp. (Table 2.2). The polychaete *Nereis* spp. exhibited the lowest concentration among animals, with 6.0±1.9 mg g^{-1}. Kelp (*L. digitata*), seston (from seawater samples), and

A

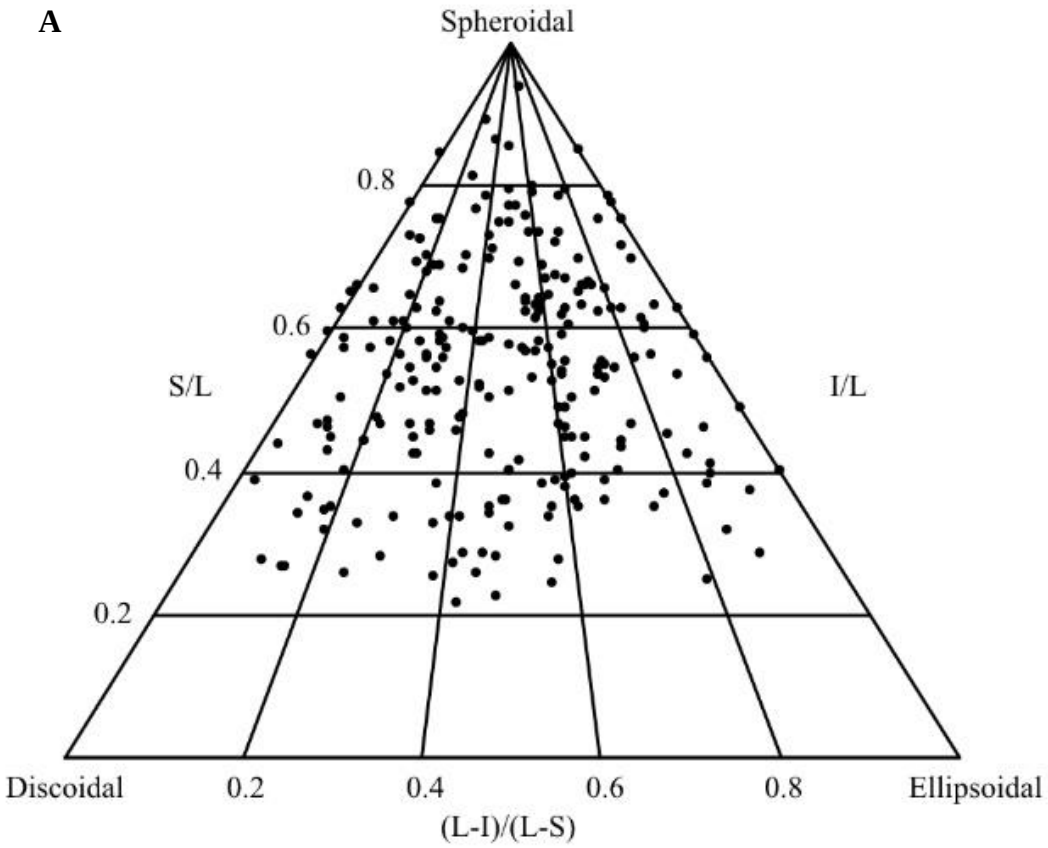
Spheroidal
0.8
0.6
S/L
I/L
0.4
0.2
Discoidal
0.2
0.4
0.6
0.8
Ellipsoidal
(L-I)/(L-S)

B

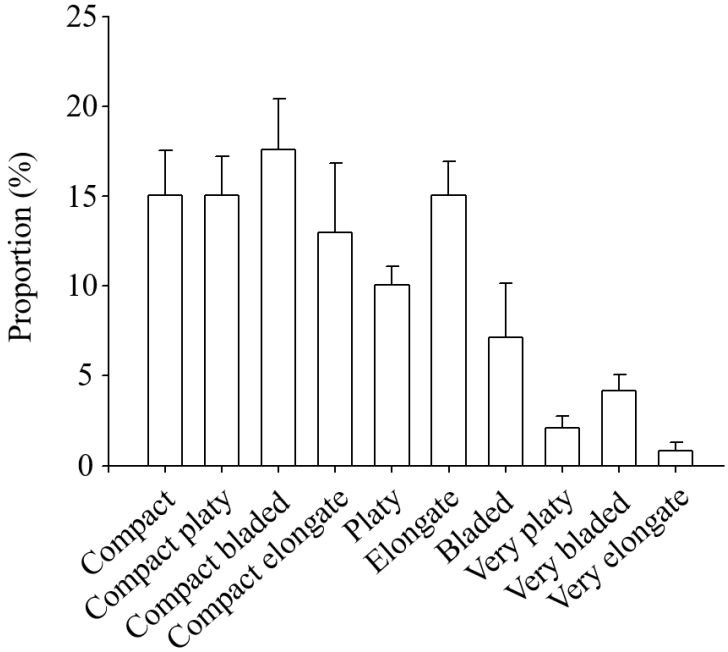
Proportion (%)
25
20
15
10
5
0
Compact
Compact platy
Compact bladed
Compact elongate
Platy
Elongate
Bladed
Very platy
Very bladed
Very elongate

Figure 2.2. (A) Ternary diagram of rhodolith [*Lithothamnion glaciale*] shape relative to purely spheroidal, discoidal, and ellipsoidal rhodoliths [N=247; one dot per rhodolith]. Rhodoliths were collected in April 2017 at the South site (see Figure 1.1). The position of each rhodolith in the diagram is set by its sphericity, calculated from the length of its longest [L], intermediate [I], and shortest [S] axes. (B) Corresponding proportion of rhodoliths under each of 10 finer shape categories as defined by Sneed and Folk (1958).

Table 2.1. Taxonomical breakdown and abundance of invertebrate macrofauna associated with rhodoliths (*Lithothamnion glaciale*) collected in April 2017 at the South site (see Figure 1.1). Each phylum's total abundance (bolded values) includes macrofauna not identified to the genus level.

Phylum / species	Mean (±SE) density (individuals kg^{-1} rhodoliths)
Annelida	**75.9 (8.3)**
Myxicola spp.	8.9 (4.7)
Neridiidae (including *Nereis* spp.)	21.7 (4.7)
Potamilla reniformis	30.0 (10.3)
Arthropoda	**72.8 (13.1)**
Amphipoda	34.1 (12.4)
Cancer irroratus	1.8 (1.0)
Pandalus borealis	36.9 (7.5)
Echinodermata	**452.7 (47.0)**
Asterias rubens	19.7 (4.1)
Ophiopholis aculeata	336.7 (30.8)
Ophiura robusta	72.7 (13.8)
Strongylocentrotus droebachiensis	22.8 (3.7)
Mollusca	**427.6 (39.6)**
Hiatella arctica	152.8 (23.2)
Lacuna vincta	1.8 (1.0)
Margarites costalis	15.8 (3.6)
Modiolus modiolus	14.7 (3.5)
Moelleria costulata	8.6 (3.0)
Puncturella noachina	21.2 (5.4)
Tonicella marmorea / T. rubra	191.6 (27.2)
Turbonilla spp.	3.4 (2.3)
Velutina velutina	2.4 (1.5)
Nemertea	**19.3 (5.5)**
Sipuncula	**5.8 (5.3)**

Table 2.2. Sample size (N), mean wet weight, mean total lipid, and mean proportion (%) of the six dominant lipid classes (PL: phospholipid; TAG: triacylglycerol; FFA: free fatty acid; ST: sterol; AMPL: acetone mobile polar lipid; and HC: hydrocarbon) in the six animal species (common sea star, *Asterias rubens*; wrinkled rock-borer, *Hiatella arctica* [bivalve]; *Nereis* spp. [polychaetes]; daisy brittle star, *Ophiopholis aculeata*; green sea urchin, *Strongylocentrotus droebachiensis*; and chitons, *Tonicella* spp.), two macroalgal species (*Laminaria digitata* [kelp] and *Lithothamnion glaciale* [rhodoliths]), and two environmental components (seawater and sediment) sampled inside (I) or outside (O) of the South site (see Figure 1.1). Each variable's lowest and highest values are bolded.

Component	N	Wet Weight g (±SD)	Total Lipid mg g^{-1} ww (±SD)	PL % (±SD)	TAG % (±SD)	FFA % (±SD)	ST % (±SD)	AMPL % (±SD)	HC % (±SD)
Animal									
A. rubens (I)	3	1.0 (0.2)	8.5 (2.2)	**75.9 (5.2)**	**1.9 (1.5)**	**1.5 (2.0)**	9.8 (2.7)	8.6 (2.6)	0.8 (0.3)
H. arctica (I)	3	1.1 (0.3)	9.2 (3.6)	**45.3 (11.2)**	**34.4 (13.9)**	5.1 (1.3)	7.5 (1.5)	5.4 (0.1)	0.5 (0.3)
Nereis spp. (I)	3	0.9 (0.2)	6.0 (1.9)	63.3 (10.0)	3.9 (5.7)	5.9 (2.1)	**19.2 (4.7)**	**5.0 (3.5)**	1.5 (1.3)
O. aculeata (I)	3	1.3 (0.1)	**13.2 (3.7)**	47.8 (2.6)	25.1 (6.3)	5.5 (4.6)	**5.7 (5.0)**	11.3 (7.3)	**2.9 (1.7)**
S. droebachiensis (I)	2	1.0 (0.2)	10.6 (11.0)	60.8 (3.2)	6.0 (4.7)	0 (0)	14.9 (12.0)	**16.6 (4.3)**	1.2 (1.0)
Tonicella spp. (I)	3	0.7 (0.1)	6.7 (1.6)	49.2 (8.4)	28.9 (2.6)	3.2 (3.0)	10.0 (2.6)	7.3 (4.2)	1.0 (1.2)
Mean		1.0 (0.2)	8.9 (4.2)	56.8 (13.1)	17.3 (14.9)	3.7 (3.1)	11.0 (6.3)	8.6 (5.1)	1.3 (1.2)
Macroalgal									
L. digitata (O)	2	1.6 (0.5)	1.3 (0.1)	49.3 (4.9)	0 (0)	0.4 (0.6)	16.2 (2.8)	32.7 (7.2)	**0.1 (0.2)**
L. glaciale (I)	N/A	N/A	N/A	N/A	N/A	N/A	N/A	N/A	N/A
Mean		1.6 (0.5)	1.3 (0.1)	49.3 (4.9)	0 (0)	0.4 (0.6)	16.2 (2.8)	32.7 (7.2)	0.1 (0.2)
Environmental									
Seawater (O)	3	0.1 (0)	4.1 (1.1)	49.7 (9.9)	0 (0)	**31.2 (3.1)**	10.9 (1.7)	7.0 (12.2)	0 (0)
Sediment (I)	3	6.6 (0.9)	**0.6 (0.5)**	52.7 (45.7)	15.6 (21.9)	4.6 (4.0)	6.0 (3.7)	13.4 (16.5)	0 (0)
Mean		3.3 (3.7)	1.5 (2.1)	51.2 (29.6)	7.8 (16.3)	17.9 (14.9)	8.4 (3.8)	10.2 (13.4)	0 (0)

N/A Data not available

sediment had significantly lower total lipid concentrations than *O. aculeata* (Tukey HSD, $p<0.01$ in all cases) (Table 2.2).

The nine food web components contained nine lipid classes (PL, TAG, FFA, ST, AMPL, HC, SE, KET, and ALC), with six (PL, TAG, FFA, ST, AMPL, and HC) present in >50% of all samples (Table 2.2). PL was the dominant lipid class in every component, with a proportional contribution to total lipid concentration of 48% in *O. aculeata* to 76% in *A. rubens* (Table 2.2). Animal species contained the highest proportion of TAG, ST, and AMPL, with 34% in *H. arctica*, 19% in *Nereis* spp., and 16% in *S. droebachiensis*, respectively. FFA was highest (31%) in seston, lowest (2%) in *A. rubens*, and not detected (0%) in *S. droebachiensis* (Table 2.2). Kelp and seston contained no measurable TAG. Seston lipids were largely PL (50%), FFA (31%), ST (11%), and AMPL (12%). Sediment was dominated by PL (53%), followed by TAG (16%) and AMPL (13%). All components contained PL, ST, and AMPL. Overall, lipid class composition differed significantly among the nine food web components (PERMANOVA; Pseudo-$F_{8,24}$=5.732, P (perm)=0.0003) and five functional groups (suspension/filter feeder, grazer, predator, kelp, and seawater/sediment) studied (PERMANOVA; Pseudo-$F_{4,24}$=3.504, P (perm)=0.0059). Specifically, lipid class composition differed between grazers and predators (t=2.485, p=0.018), and between suspension/filter feeders and predators (t=4.450, p=0.003). Total lipid concentration correlated with ST proportion only (r=-0.469, p=0.018, N=25).

2.4.3. Fatty acid profiles

The nine food web components included in the fatty acid (FA) analysis contained 63 FA, with 43 present in >50% of all samples. Each component exhibited a distinct set of dominant fatty acids and biomarkers (Table 2.3, Figure 2.3). With a proportional contribution to FA profiles ranging from 19% in *H. arctica* to 32% in *A. rubens*, EPA (eicosapentaenoic acid, 20:5ω3; a typical diatom biomarker) was the dominant FA within each of the six animal species sampled

Table 2.3. Mean proportion (%) of each of the 43 dominant fatty acids found in the six animal species, two macroalgal species, and two environmental components (see Table 2.2 for species list) sampled inside (I) or outside (O) of the South site (see Figure 1.1). Each component's highest FA proportion is bolded. Asterisks (*) denote fatty acids that altogether contribute to at least 70% similarity in each food web component (Table D.1). FA are listed in ascending order of retention time from the 30-m long ZB wax+ (Phenomenex) GC column in the Varian Galaxie Chromatography Data System (see section 2.3.6 for details).

	A. rubens **(I; N=3)**	***H. arctica*** **(I; N=3)**	***Nereis* spp.** **(I; N=3)**	***O. aculeata*** **(I; N=3)**	***S. droebachiensis*** **(I; N=2)**	***Tonicella* spp.** **(I; N=3)**	***L. digitata*** **(O; N=2)**	***L. glaciale*** **(I)**	**Seawater (O; N=3)**	**Sediment (I; N=3)**
FA	% (±SD)	% (±SD)	% (±SD)	% (±SD)	% (±SD)	% (±SD)	% (±SD)	% (±SD)	% (±SD)	% (±SD)
14:0	0.6 (0.2)	4.3 (1.1)*	1.2 (0.4)	6.5 (1.3)*	3.2 (1.2)	3.6 (0.4)*	5.2 (0.5)	N/A	0.9 (0.4)	1.7 (0.8)
TMTD†	0.1 (0)	0.4 (0.3)	0 (0)	0 (0)	0.1 (0)	1.2 (0.1)	0 (0)	N/A	0.2 (0.1)	0 (0)
*i*15:0	0.1 (0.1)	0.4 (0.1)	0.1 (0)	0.1 (0)	0.2 (0.1)	0.3 (0)	0.4 (0.1)	N/A	0.1 (0.1)	1.4 (0.4)
*ai*15:0	0.1 (0.1)	0.2 (0.2)	0.1 (0)	0.1 (0)	0.2 (0.1)	0.2 (0)	0 (0)	N/A	0 (0.1)	2.5 (0.4)
15:0	0.3 (0)	0.4 (0.1)	0.8 (0.1)	0.2 (0)	0.4 (0.1)	0.8 (0.1)	0.2 (0)	N/A	0.1 (0.1)	0.8 (0.1)
*i*16:0	0.3 (0)	0.2 (0.2)	0.1 (0)	0 (0)	0.1 (0)	0.2 (0)	0 (0)	N/A	0 (0)	0.4 (0.4)
*ai*16:0	0.2 (0.1)	0.1 (0.1)	0.3 (0.1)	0 (0)	0.1 (0.2)	0.3 (0.4)	0 (0.1)	N/A	0 (0)	1.1 (0.9)
16:0	4.2 (1.6)	16.5 (1.1)*	11.1 (0.6)*	15.5 (14.2)*	8.8 (0.5)*	10.9 (0.8)*	**17.5 (1.2)***	N/A	21.7 (2.8)*	14.6 (0.4)*
16:1ω11	0 (0)	0.2 (0.1)	0.1 (0.1)	0.1 (0.1)	0.3 (0.2)	0.1 (0)	0.8 (0.3)	N/A	0.1 (0)	3.1 (1.7)
16:1ω9	0.1 (0.1)	0.3 (0.1)	0.1 (0.1)	0.1 (0)	0.3 (0.1)	0.3 (0)	0 (0)	N/A	0 (0)	0.9 (0.6)
16:1ω7	1.8 (0.5)	12.7 (0.9)*	3.4 (1.0)	5.9 (0.9*)	4.1 (1.6)*	8.1 (0.4)*	2.4 (0)	N/A	1.2 (0.2)	**20.6 (1.0)***
16:1ω5	0.1 (0.1)	0.6 (0)	0.3 (0)	0.1 (0)	0.4 (0.1)	0.2 (0)	0.1 (0)	N/A	0 (0)	1.4 (0.1)
*i*17:0	0.3 (0.1)	0.8 (0.4)	0.3 (0)	0.3 (0.1)	0.4 (0)	0.2 (0)	1.7 (0.1)	N/A	0.2 (0.1)	0.8 (0.2)
*ai*17:0	0.3 (0.2)	0.5 (0.3)	0.3 (0)	0.3 (0.1)	0.4 (0.1)	0.6 (0.1)	0.3 (0)	N/A	0 (0)	1.2 (0.4)
16:2ω4	0.1 (0.1)	0.8 (0.1)	0.1 (0)	0.8 (0.2)	0.9 (0.5)	0.8 (0.1)	0.2 (0)	N/A	0 (0)	1.0 (0.1)
17:0	0.5 (0.1)	0.4 (0.1)	1.4 (0.2)	0.1 (0.1)	0.1 (0)	0.4 (0.1)	0.1 (0)	N/A	0.1 (0.1)	0.6 (0.1)
16:3ω4	0 (0)	0.2 (0.1)	0 (0)	1.0 (0.6)	0.7 (0.5)	0.8 (0.3)	0 (0)	N/A	0 (0)	2.5 (0.2)*

Table 2.3. (continued)

FA	*A. rubens* (I; N=3) % (±SD)	*H. arctica* (I;N=3) % (±SD)	*Nereis* spp. (I; N=3) % (±SD)	*O. aculeata* (I; N=3) % (±SD)	*S. droebachiensis* (I; N=2) % (±SD)	*Tonicella* spp. (I; N=3) % (±SD)	*L. digitata* (O; N=2) % (±SD)	*L. glaciale* (I) % (±SD)	Seawater (O; N=3) % (±SD)	Sediment (I; N=3) % (±SD)
17:1	9.2 (6.3)*	1.2 (0.2)	1.0 (0.5)	1.1 (1.0)	1.1 (0.5)	0.6 (0.6)	0.7 (0)	N/A	0 (0)	1.0 (0.2)
16:4ω3	1.4 (2.3)	0.1 (0.1)	3.1 (0.6)	0 (0)	0.8 (1.2)	1.4 (0.5)	0 (0)	N/A	0 (0.1)	0.3 (0.4)
16:4ω1	0 (0.1)	0.4 (0.3)	0.1 (0.1)	4.4 (2.0)	1.0 (0.4)	0.7 (0.1)	0.2 (0)	N/A	0.7 (0.2)	2.3 (2.7)
18:0	5.9 (0.8)*	2.7 (0)	4.1 (0.4)*	4.0 (0.6)	2.7 (0.2)	3.0 (0.8)	0.7 (0.1)	N/A	18.2 (2.5)*	3.5 (3.1)
18:1ω11	0.1 (0.1)	0.6 (0.4)	5.3 (0.2)*	1.8 (0.2)	0.5 (0)	0.2 (0.1)	0 (0)	N/A	0 (0)	0 (0.1)
18:1ω9	0.5 (0.5)	1.7 (1.0)	2.2 (0.6)	0.9 (0.1)	1.3 (0.4)	9.0 (1.2)*	13.0 (0.2)*	N/A	**32.9 (12.1)***	5.3 (1.6)*
18:1ω7	2.6 (1.5)	7.0 (1.4)*	6.3 (0.3)*	6.6 (0.9)*	3.5 (0.2)*	6.8 (0.4)*	0.1 (0.1)	N/A	2.0 (1.8)	9.0 (0.6)*
18:2ω6 (LA)	0.1 (0.1)	1.9 (0.3)	1.3 (0.2)	2.6 (0.5)	2.2 (1.6)	0.3 (0)	9.1 (0.2)*	N/A	5.3 (2.0)	1.3 (0.5)
18:2ω4	0 (0)	0.7 (0.1)	0.2 (0)	0.5 (0.1)	0.3 (0.1)	0.5 (0.4)	0 (0)	N/A	0 (0)	0 (0.1)
18:3ω6 (GLA)	0.6 (0.6)	0.2 (0.1)	0 (0)	0.4 (0.1)	0.4 (0.0)	0.4 (0.2)	0.6 (0)	N/A	0 (0)	0.3 (0.2)
18:3ω3 (ALA)	0 (0)	0.8 (0)	0.8 (0.2)	0.5 (0.1)	1.2 (0.2)	0.5 (0.1)	7.5 (0)	N/A	0 (0)	1.1 (0.3)
18:4ω3 (OTA)	0.3 (0.6)	4.5 (1.8)	0.5 (0.2)	5.1 (1.8)*	3.8 (1.1)*	1.3 (0.2)	8.0 (0.4)*	N/A	0.4 (0.4)	1.3 (0.5)
19:3	0 (0)	0 (0)	2.6 (0.6)	0 (0)	0 (0)	0 (0)	0.1 (0.1)	N/A	0 (0)	0 (0)
20:0	0 (0)	0 (0.1)	0 (0)	0.4 (0.2)	1.1 (0.4)	0 (0)	0 (0)	N/A	0.3 (0.3)	0.4 (0.1)
20:1ω11	3.3 (5.7)	0.6 (0.1)	1.6 (0.2)	5.2 (0.9)*	0 (0)	1.0 (0.6)	0 (0)	N/A	0 (0)	0.4 (0.2)
20:1ω9	4.8 (0.4)	0.8 (0.1)	0.8 (0.3)	0.1 (0.1)	1.9 (0.2)	1.2 (1.1)	0 (0)	N/A	0.7 (0.6)	0.1 (0.1)
20:1ω7	0.7 (1.2)	1.6 (1.4)	0.5 (0.1)	1.4 (0.3)	1.5 (0)	0.1 (0.1)	0 (0)	N/A	0 (0)	0.1 (0.1)
20:2ω6	1.8 (0.3)	1.5 (0.4)	1.8 (0.4)	0.3 (0.3)	3.1 (0.3)*	1.5 (0)	0.7 (0)	N/A	0 (0)	1.2 (0.2)
20:4ω6 (ARA)	19.8 (6.3)*	0.6 (0.6)	3.2 (1.6)	0.9 (0.1)	14.5 (2.5)*	4.9 (4.2)	0.1 (0.1)	N/A	0 (0)	3.7 (0.4)*
20:3ω3	0.3 (0.3)	0.1 (0)	1.0 (0.6)	0.1 (0.1)	2.1 (1.3)	0.2 (0.2)	0.6 (0)	N/A	0 (0)	0 (0)
20:4ω3	0.1 (0.2)	0.7 (0.1)	0.3 (0.1)	0.4 (0.1)	1.8 (1.5)	0.8 (0.1)	13.5 (0.8)*	N/A	0 (0)	0 (0)
20:5ω3 (EPA)	**31.6 (1.6)***	**19.3 (3.5)***	**29.3 (4.4)***	**26.8 (5.5)***	**24.8 (2.3)***	**21.8 (0.5)***	0 (0)	N/A	1.2 (0.5)	7.8 (0.9)*
21:5ω3	0.1 (0.1)	1.5 (0.3)	0 (0)	0.8 (0.1)	0.3 (0.2)	0.5 (0)	0 (0)	N/A	0 (0)	0 (0)
22:4ω6	0.1 (0.1)	1.0 (0.7)	4.8 (1.9)*	0 (0)	0.2 (0)	2.8 (0.3)	0 (0)	N/A	0 (0)	0 (0)
22:5ω3 (DPA)	0.1 (0.2)	1.5 (0.6)	4.8 (1.3)*	0.3 (0.2)	0.3 (0.1)	4.7 (0.3)*	0 (0)	N/A	0 (0)	0.9 (1.0)
22:6ω3 (DHA)	5.3 (2.9)	8.9 (1.0)*	1.0 (0.3)	0.6 (0.1)	1.5 (0.6)	0.6 (0)	0 (0)	N/A	1.0 (0.2)	1.4 (0.6)
Total	**97.8**	**98.5**	**93.7**	**98.7**	**92.7**	**93.9**	**83.7**	**N/A**	**87.5**	**96.1**

† Trimethyltridecanoic acid

(A)

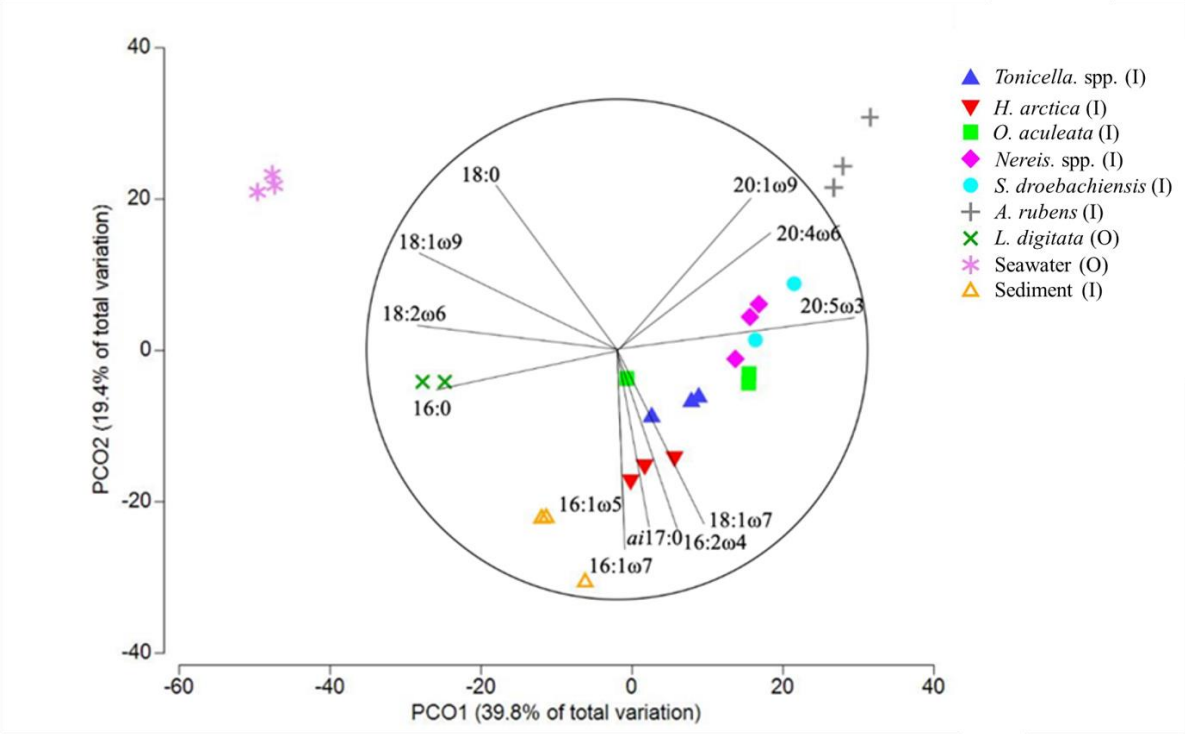

(B)

FA	Biomarker
16:0	Chlorophyta, Flagellates (including Dinoflagellates), Phaeophyta, Rhodophyta
16:1ω5	Bacteria
16:1ω7	Aerobic microorganisms, Diatoms, Rhodophyta
16:2ω4	Bacteria
*ai*17:0	Bacteria
18:0	Detritus
18:1ω9	Crustaceans, Detritus, Dinoflagellates, Phaeophyta
18:1ω7	Aerobic microorganisms, Bacteria, Chlorophyta, Rhodophyta
18:2ω6	Chlorophyta, Terrestrial vegetation
20:1ω9	Amphipods, Copepods (Calanoida)
20:4ω6 (ARA)	Amphipods, Foraminifera, Phaeophyta, Rhodophyta
20:5ω3 (EPA)	Diatoms, Phaeophyta

Figure 2.3. (A) PCO plot (based on Bray-Curtis similarity matrices) of the 12 fatty acids exhibiting at least 70% correlation in the six animal species, two macroalgal species, and two environmental components (see Table 2.2 for species list) sampled inside or outside of the South site (see Figure 1.1). (B) Typical fatty-acid trophic biomarkers for those fatty acids included in the analysis (adapted from Parrish (2013) and Legeżyńska et al. (2014)).

(Table 2.3). ARA (arachidonic acid, 20:4ω6; a kelp and amphipod biomarker), palmitoleic acid (16:1ω7; a diatom biomarker), and palmitic acid (16:0; a flagellate, bacteria, and marine vegetation biomarker) were the next most prominent FA among the animals, with a contribution between 11% and 20% (Table 2.3). Kelp contained mainly palmitic acid (18%), eicosatetraenoic acid (20:4ω3; 14%) and oleic acid (18:1ω9, 13%; a crustacean, detritus, dinoflagellate, and brown seaweed biomarker). Seston FA were largely oleic acid (33%), palmitic acid (22%), and stearic acid (18:0, 18%; a detritus biomarker). Sediment was dominated by palmitoleic acid (21%), palmitic acid (15%), and vaccenic acid (18:1ω7, 9%; an aerobic microorganism, bacteria, and vegetation biomarker) (Table 2.3). Overall, FA composition differed significantly among the nine food web components (PERMANOVA, Pseudo-$F_{8,24}$=26.278, P (perm)<0.001) and five functional groups studied (PERMANOVA, Pseudo-$F_{4,24}$=7.6664, P (perm)=0.001), except kelp whose composition was similar to that of any of the four other functional groups.

Of the three essential fatty acids (EPA, DHA [docosahexaenoic acid], and ARA), EPA was the most prevalent, present in all food web components except kelp and particularly abundant among the six animal species (Table 2.3). ARA was in all components except seston, peaking in *A. rubens* (20%) and *S. droebachiensis* (15%) (Table 2.3). Together, EPA and ARA contributed to 46% and 62% of the similarities in *S. droebachiensis* and *A. rubens* diets, respectively (Table D.1). DHA was present in all components except kelp, and was nevertheless less abundant than EPA and ARA, peaking at 9% in *H. arctica* (Table 2.3).

Animal and kelp FA profiles were generally dominated by polyunsaturated FA (PUFA), which ranged from 44% in *Tonicella* spp. to 65% in *S. droebachiensis*, and to a lesser extent by monounsaturated FA (MUFA), which varied from 17% in *L. digitata* and *S. droebachiensis* to 30% in *Tonicella* spp. (Table 2.4). Animals and kelp contained lower levels of saturated FA (SFA),

Table 2.4. Sample size (N), mean proportional sum (Σ) of saturated (SFA), monounsaturated (MUFA), polyunsaturated (PUFA), ω3 (omega-3), and ω6 (omega-6) fatty acids, and mean ratios of polyunsaturated:saturated (P/S) and DHA:EPA (DHA/EPA), in the six animal species, two macroalgal species, and two environmental components (see Table 2.2 for species list) sampled inside (I) or outside (O) of the South site (see Figure 2.1). Each variable's lowest and highest values are bolded.

		ΣSFA	ΣMUFA	ΣPUFA	Σω3	Σω6	P/S	DHA/EPA
Component	**N**	% (±SD)	% (±SD)	% (±SD)	% (±SD)	% (±SD)	Mean (±SD)	Mean (±SD)
Animal								
A. rubens (I)	3	**11.6 (3.4)**	24.0 (1.2)	63.2 (4.0)	39.4 (5.0)	**22.4 (6.9)**	**5.9 (2.4)**	0.2 (0.1)
H. arctica (I)	3	24.6 (0.9)	27.6 (3.8)	45.7 (4.5)	37.5 (5.8)	5.2 (1.6)	1.9 (0.2)	0.5 (0.0)
Nereis spp. (I)	3	18.6 (0.4)	22 (2.7)	58.2 (2.9)	**40.9 (6.0)**	11.1 (3.8)	3.1 (0.2)	0.0 (0.0)
O. aculeata (I)	3	26.8 (12.7)	24.6 (3.3)	47.8 (10.8)	34.4 (7.4)	**4.2 (0.7)**	2.1 (1.2)	0.0 (0.0)
S. droebachiensis (I)	2	16.6 (1.1)	**16.8 (1.5)**	**65.2 (3.0)**	36.7 (4.4)	20.8 (0.6)	3.9 (0.5)	0.1 (0.0)
Tonicella spp. (I)	3	19.4 (4.0)	30.3 (3.8)	43.9 (0.2)	33.4 (0.2)	10.6 (4.4)	2.3 (0.5)	0.0 (0.0)
Mean		19.8 (7.2)	24.7 (4.8)	53.3 (9.7)	37.1 (5.3)	11.9 (7.8)	3.2 (1.8)	0.1 (0.2)
Macroalgal								
L. digitata (O)	2	23.7 (1.7)	17.2 (0.3)	56.7 (2.2)	29.7 (1.4)	10.5 (0.4)	2.4 (0.3)	**0 (0)**
L. glaciale (I)	N/A	N/A	N/A	N/A	N/A	N/A	N/A	N/A
Mean		23.7 (1.7)	17.2 (0.3)	56.7 (2.2)	29.7 (1.4)	10.5 (0.4)	2.4 (0.3)	0 (0)
Environmental								
Seawater (O)	3	**41.6 (5.4)**	37.9 (12.1)	**20.2 (17.6)**	**2.6 (1.1)**	6.3 (0.3)	**0.5 (0.5)**	**0.9 (0.1)**
Sediment (I)	3	24.2 (2.8)	**42.5 (3.4)**	25.8 (4.9)	13.0 (3.3)	6.6 (0.9)	1.1 (0.3)	0.2 (0.1)
Mean		32.9 (10.3)	40.2 (8.3)	23.0 (12.0)	7.8 (6.1)	6.4 (0.6)	0.8 (0.5)	0.5 (0.4)

N/A Data not available

with lowest and highest proportions in respectively *A. rubens* (11%) and *O. aculeata* (27%) (Table 2.4). Conversely, seston and sediment contained more MUFA (37.9% and 42.5%, respectively) than PUFA (20.2% and 25.9%, respectively) (Table 2.4). SFA levels were higher in seston (41.6%) than sediment (24.2%) (Table 2.4). Animals exhibited the highest ratio of polyunsaturated to unsaturated FA (P/S; 3%), followed by kelp (2%), and seston and sediment (1%) (Table 2.4). All components, except for seawater, had a higher proportion of ω3 (omega-3) fatty acids than ω6 (omega-6). Animals and kelp contained about 3 times as many ω3 fatty acids (37.1% and 29.7%, respectively) than ω6 (11.9% and 10.5%, respectively) and sediment about 2 twice as many ω3 fatty acids (13.0%) than ω6 (6.5%), while seston contained about half as many ω3 fatty acids (2.6%) than ω6 (5.3%) (Table 2.4). The DHA/EPA ratio was highest in seston (0.9), intermediate in sediment, *A. rubens*, *H. arctica*, and *S. droebachiensis* (0.1 to 0.5), low in *Nereis* spp., *O. aculeata*, and *Tonicella* spp. (0.02 to 0.03), and null (0) in kelp (Table 2.4).

2.4.4. Stable isotopes and trophic magnification

Stable carbon isotope ratio ($\delta^{13}C$) differed significantly among the 10 food web components included in the carbon isotope analysis (PERMANOVA, Pseudo-$F_{9,26}$=40.241, P (perm)<0.001), ranging from most depleted in seawater (-26.6‰) to least depleted in *L. glaciale* and *A. rubens* (-18.9‰) (Table 2.5). The stable nitrogen isotope ratio ($\delta^{15}N$), which was lowest in *L. digitata* (3.4‰) and highest in *A. rubens* (11.0‰) (Table 2.5), also differed significantly among the nine food web components included in the nitrogen isotope analysis (i.e. all components except *Nereis* spp.; PERMANOVA, Pseudo-$F_{8,25}$=130.64, P (perm)<0.001), indicating distinct trophic levels (see below). Hierarchical clustering analysis of $\delta^{13}C$ and $\delta^{15}N$ separated the latter nine components in four distinct groups (PERMANOVA, Psuedo-$F_{3,22}$=53.25, P (perm)<0.001;

Table 2.5. Sample size (N), bulk stable isotope ratio ($\delta^{13}C$ and $\delta^{15}N$; ‰), and relative trophic position (TP) in the six animal species, two macroalgal species, and two environmental components (see Table 2.2 for species list) sampled inside (I) or outside (O) of the South site (see Figure 1.1). Trophic position is based on an isotopic model with a $\Delta^{15}N$ fractionation factor of 3.4‰ (see section 2.3.8). Each variable's lowest and highest values are bolded. *Nereis* spp. was not included in the N analysis because of insufficient tissues for quantification.

		Dry weight	Carbon		Dry weight	Nitrogen	TP
Component	**N**	mg (±SD)	$\delta^{13}C$ (±SD)	**N**	mg (±SD)	$\delta^{15}N$ (±SD)	
Animal							
A. rubens (I)	3	1.3 (0.2)	**-18.9 (0.9)**	3	1.4 (0.0)	**11.0 (0.3)**	**3.2**
H. arctica (I)	3	1.1 (0.1)	-20.0 (0.4)	3	1.3 (0.2)	6.3 (0.0)	1.9
Nereis spp. (I)	2	1.3 (0.2)	-22.5 (0.1)	-	N/A	N/A	N/A
O. aculeata (I)	3	1.2 (0.2)	-19.9 (0.3)	3	1.3 (0.1)	8.9 (0.6)	2.6
S. droebachiensis (I)	3	1.2 (0.1)	-19.8 (1.4)	2	1.2 (0.2)	10.0 (0.9)	2.9
Tonicella spp. (I)	3	1.1 (0.0)	-19.3 (0.3)	3	1.2 (0.2)	9.7 (0.3)	2.9
Mean		1.2 (0.1)	-19.9 (1.2)		1.3 (0.1)	9.1 (1.7)	
Macroalgal							
L. digitata (O)	3	1.1 (0.2)	-21.0 (0.5)	3	4.5(0.4)	**3.4 (0.2)**	**1.0**
L. glaciale (I)	1	1.1	**-18.9**	3	4.4 (0.2)	7.3 (0.2)	2.1
Mean		1.1 (0.1)	-20.5 (1.1)		4.4 (0.3)	5.4 (2.1)	
Environmental							
Seawater (O)	3	6.5 (0.4)	**-26.6 (0.1)**	3	9.0 (0.8)	7.0 (0.5)	2.0
Sediment (I)	3	14.2 (0.1)	-22.3 (0.2)	3	14.4 (0.4)	6.3 (0.2)	1.8
Mean		10.4 (4.2)	-24.4 (2.3)		11.7 (3.0)	6.6 (0.5)	

N/A Data not available

Figures D.1 and 2.4). Two of these groups each contained all samples of a single food web component, namely seston (seawater) and *L. digitata* (kelp), hereafter termed respectively Group 1 and Group 4 (Figure 2.4). Group 3 contained three subgroups, each also containing all samples of a single food web component: sediment (Group 3a), *L. glaciale* (rhodolith, Group 3b), and *H. arctica* (Group 3c) (Figure 2.4). Group 2 had four subgroups, of which two were monospecific: *A. rubens* (Group 2a) and *O. aculeata* (Group 2d), and two each contained two species; *A. rubens* and *Tonicella* spp. (Group 2b) and *S. droebachiensis* and *Tonicella* spp. (Group 2c) (Figure 2.4). Group 1 (seston) had a significantly lower $\delta^{13}C$ than all other groups (Tukey HSD, $p<0.001$), yet its $\delta^{15}N$ was similar to that of Group 3 (infauna, *L. glaciale*, *H. arctica*) (Tukey HSD, $p=0.779$) (Figure 2.4). Group 2 (*A. rubens*, *O. aculeata, Tonicella* spp., and *S. droebachiensis*) had a significantly higher $\delta^{15}N$ than Group 1, Group 3, and Group 4 (*L. digitata*) (Tukey HSD, $p<0.001$). Group 2's $\delta^{13}C$ was also significantly more enriched than that of Group 1 (Tukey HSD, $p<0.001$) and Group 3 (Tukey HSD, $p=0.021$), but not Group 4 (Tukey HSD, $p<0.062$). Group 4 had a significantly lower $\delta^{15}N$ than all other groups (Tukey HSD, $p<0.001$) (Figure 2.4).

At our assumed $\Delta^{15}N$ fractionation factor of 3.4‰ (see section 2.3.8), the 10 food web components encompassed over three trophic positions (TP), with kelp (TP=1) and *A. rubens* (TP=3.2) at the base and top of the web, respectively (Table 2.5). Seston (seawater), sediment, rhodoliths (*L. glaciale*), and *H. arctica* occupied intermediate positions ranging from 1.8 to 2.1, whereas the three remaining animal species sampled had similarly high positions of 2.6 to 2.9 (Table 2.5). Thirty-seven (37) fatty acids correlated significantly with $\delta^{15}N$. Of those fatty acids, four (16:4ω3, 20:1ω11, 20:4ω6 [ARA], and 20:5ω3 [EPA]) exhibited a TMF > 1, and hence were biomagnified through trophic levels, whereas 33 had a TMF < 1, indicating biodilution (Table 2.6).

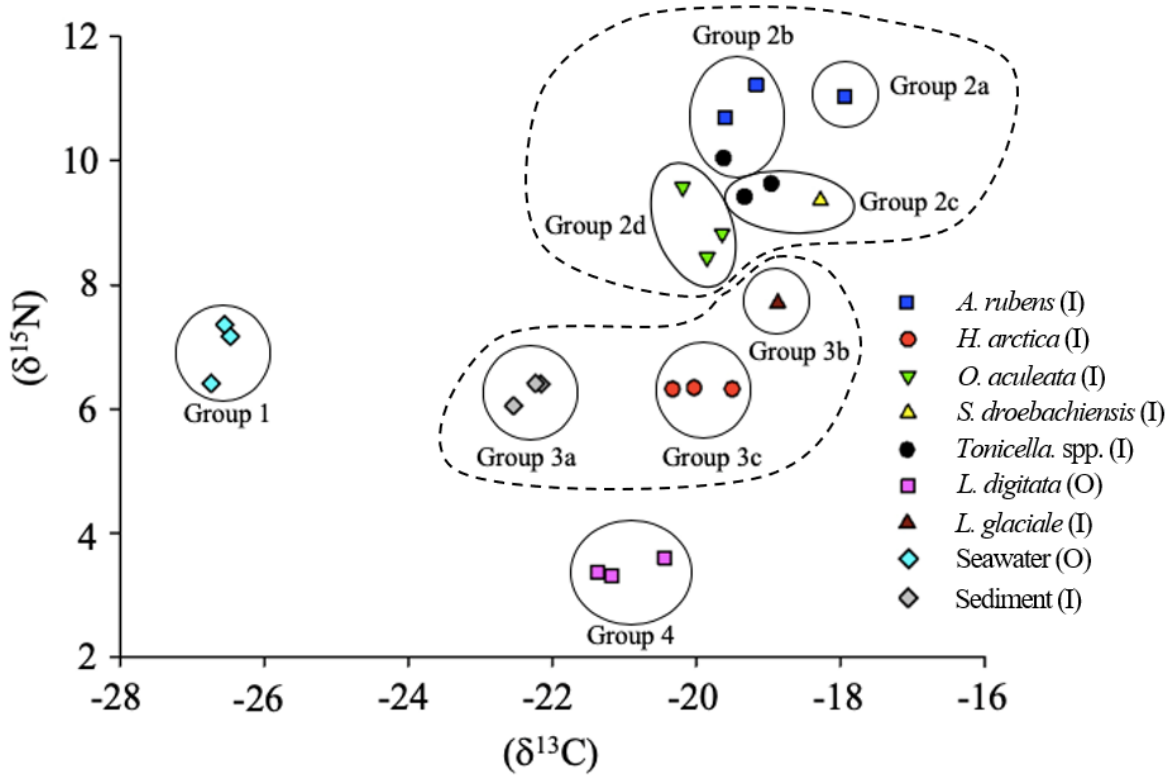

Figure 2.4. Biplot of bulk carbon ($\delta^{13}C$) and nitrogen ($\delta^{15}N$) stable isotope ratios of five animal species, two macroalgal species, and two environmental components (see Table 2.2 for species list) sampled inside or outside of the South site (see Figure 1.1). *Nereis* spp. was not included because of insufficient tissues for quantification in the N analysis. Components grouped (circled) based on agglomerative hierarchical cluster analysis (see Figure E.1).

Table 2.6. Trophic multiplication factor (TMF) of 37 fatty acids (FA) as calculated from the slope (m) of corresponding linear relationship between FA concentration and bulk nitrogen ($\delta^{15}N$) stable isotope ratio (see section 2.3.8). Five animal species, two macroalgal species, and two environmental components (see Table 2.2 for species list) sampled in the South site were included in the analysis (see Figure 1.1). *Nereis* spp. was not included because of insufficient tissues for quantification. Only FA with a statistically significant correlation coefficient (r) are shown.

FA	TMF	m (±SE)	b (±SE)	r	p-value
20:1ω11	1.19	0.2 (0)	7.7 (0.2)	0.4	<0.001
20:4ω6 (ARA)	1.16	0.2 (0)	7.4 (0.2)	0.6	<0.001
20:5ω3 (EPA)	1.15	0.1 (0)	6.0 (0.3)	0.7	<0.001
16:4ω3	1.10	0.1 (0)	8.1 (0.2)	0.2	0.037
18:1ω9	0.95	-0.1 (0)	8.7 (0.2)	-0.2	0.006
22:6ω3 (DHA)	0.93	-0.1 (0)	8.6 (0.2)	-0.2	0.024
22:4ω6	0.90	-0.1 (0)	8.5 (0.2)	-0.3	<0.001
16:0	0.88	-0.1 (0)	9.9 (0.3)	-0.5	<0.001
TMTD†	0.88	-0.1 (0)	8.5 (0.2)	-0.4	<0.001
16:1ω7	0.87	-0.1 (0)	9.2 (0.2)	-0.4	<0.001
21:5ω3	0.87	-0.1 (0)	8.5 (0.2)	-0.4	<0.001
18:1ω11	0.87	-0.1 (0)	8.6 (0.2)	-0.3	<0.001
22:5ω3 (DPA)	0.86	-0.1 (0)	8.6 (0.2)	-0.3	0.003
20:0	0.86	-0.2 (0)	8.5 (0.2)	-0.4	<0.001
20:3ω3	0.85	-0.2 (0)	8.5 (0.2)	-0.4	<0.001
20:4ω3	0.85	-0.2 (0)	8.6 (0.2)	-0.4	<0.001
*ai*16:0	0.83	-0.2 (0)	8.5 (0.2)	-0.4	<0.001
16:1ω9	0.82	-0.2 (0)	8.5 (0.2)	-0.4	<0.001
20:1ω7	0.81	-0.2 (0.1)	8.7 (0.2)	-0.3	<0.001
16:3ω4	0.80	-0.2 (0)	8.6 (0.2)	-0.4	<0.001
18:2ω4	0.79	-0.2 (0)	8.5 (0.2)	-0.4	<0.001
16:4ω1	0.77	-0.3 (0.1)	8.7 (0.2)	-0.4	<0.001
18:3ω6 (GLA)	0.73	-0.3 (0.1)	8.5 (0.2)	-0.3	<0.001
18:4ω3 (OTA)	0.71	-0.3 (0.1)	9.1 (0.2)	-0.4	<0.001
18:2ω6 (LA)	0.69	-0.4 (0.1)	9.0 (0.2)	-0.5	<0.001
*i*16:0	0.67	-0.4 (0.1)	8.5 (0.2)	-0.4	<0.001
18:3ω3 (ALA)	0.62	-0.5 (0.1)	8.8 (0.2)	-0.6	<0.001
16:1ω11	0.58	-0.5 (0.1)	8.7 (0.2)	-0.5	<0.001
*ai*17:0	0.54	-0.6 (0.1)	8.8 (0.2)	-0.3	0.001
*ai*15:0	0.52	-0.7 (0.1)	8.8 (0.2)	-0.6	<0.001
16:2ω4	0.34	-1.1 (0.2)	9.0 (0.2)	-0.5	<0.001
16:1ω5	0.26	-1.4 (0.2)	9.0 (0.2)	-0.6	<0.001
17:0	0.20	-1.6 (0.4)	9.1 (0.2)	-0.3	<0.001
*i*15:0	0.18	-1.7 (0.2)	9.2 (0.2)	-0.6	<0.001
15:0	0.18	-1.7 (0.3)	9.3 (0.2)	-0.4	<0.001
*i*17:0	0.06	-2.8 (0.3)	9.5 (0.2)	-0.6	<0.001

† Trimethyltridecanoic acid

2.5. DISCUSSION

We investigated the trophodynamics of 10 components within a Newfoundland rhodolith bed to provide the first characterization of specific diets based on combined use of lipid, fatty acid, and stable isotope analyses in a rhodolith community. Previous isotope-based rhodolith studies in the Northeast Atlantic (Grall et al., 2006) and California (Gabara, 2014) showed macroalgae-based detritus as a key food source within rhodolith communities. Combined with lipid and fatty acid analyses, our stable isotope analyses supported these findings, while also showing that kelp may not be a significant food source for the components we considered. We identified three distinct trophic levels, and potentially revealed a specific link between a macroalga-based diet and carbon source in *H. arctica*, *Tonicella* spp., and *O. aculeata*.

2.5.1. Rhodolith community

Rhodolith communities vary globally in terms of numerically dominant macrofauna, with gastropods dominating in the Maltese Islands (Sciberras et al., 2009), crustaceans in Santa Catalina Island (Gabara, 2014) and Ireland (de Grave and Whitaker, 1999), echinoderms and annelids in the Gulf of California (Foster et al., 2007), and polychaetes in south Australia (Harvey and Bird, 2008). In Newfoundland, chitons and brittle stars are most common (Gagnon et al., 2012).

The high densities (>80%) of chitons (*Tonicella marmorea and T. rubra*) and daisy brittle stars (*O. aculeata*) at our study site, as well as overall species composition, aligned with the first detailed report from Newfoundland and Labrador (Gagnon et al., 2012). The consistency of chiton and brittle star abundances in conjunction with similar overall species composition in Newfoundland after 8+ years suggest community stability within this rhodolith ecosystem. Moreover, the morphological traits of rhodoliths (shape and size) and total rhodolith biomass (19.5 kg m^{-2}) sampled in this present study further support stability within this rhodolith bed (Gagnon et

al., 2012). We observed many small macrofauna and, although our study did not quantify them, our observations support the literature hypothesizing rhodolith beds as nursery grounds for invertebrates (Foster, 2001; Kamenos et al., 2004b; Steller and Cáceres-Martínez, 2009).

2.5.2. Lipid content and classes

Lipid structure can vary based on environmental conditions, food availability, metabolism, and reproductive strategies (Fraser, 1989; Lloret and Planes, 2003; Parzanini et al., 2018). Low temperatures affect organisms because they can weaken membrane fluidity, structure, and function (Crockett, 1998; Parrish, 2013; Colombo et al., 2017). To accommodate cold temperatures, cold-water ectotherms exhibit homeoviscious adaptation, a process of reducing sterol molecules and lengthening and unsaturating phospholipids (Hazel et al., 1991) to change lipid structure (Hall et al., 2000; Copeman and Parrish, 2003; Parrish, 2009). In our study, although lipid structure of all samples varied by component, their overall high proportions of phospholipids (45 – 76%) and unsaturated fatty acids (58 – 87%), low proportions of sterols (6 – 19%), and a correlation between total lipids and sterol proportions ($p=0.02$) confirmed our hypothesis that lipid composition reflected the cold-water conditions of the Northwest Atlantic in April (0.3°C). These results strongly suggest increased membrane fluidity in these organisms in response to cold temperatures.

Triacylglycerols are a key component of lipid structure and the primary energy storage molecules. They are important to organisms during stressful periods such as limited food availability or reproduction. High variability of TAG content among organisms can occur as a result of differences in allocation strategies (i.e. reproduction, growth, or survival). As such, elevated TAG levels in *H. arctica* (Lebour, 1938), *Tonicella* spp., and *O. aculeata* (Himmelman et al., 2008) likely correspond to an abundance of food (i.e. phytoplankton) or reproductive timing;

organisms increase and maintain their energy storage as they prepare for the reproductive season (Vanderploeg et al., 1992). Given the timing of our study (April during the phytoplankton bloom), high levels of TAG in *H. arctica* (34%), *Tonicella* spp. (29%), and *O. aculeata* (25%) likely demonstrate this energy storage trend and potential benthic-pelagic coupling, utilizing phytoplankton from the water column in the benthos. However, low TAG levels and high PL and ST levels of predatory/omnivorous *A. rubens* (2%, 76%, 10%, respectively), *Nereis* spp. (4%, 63%, and 19%, respectively), and *S. droebachiensis* (6%, 61%, and 15%, respectively) probably link to organisms in search of food for rapid growth during harsh winter conditions (Luis and Passos, 1995; Lee Jr et al., 2006). Over prolonged periods, low TAG levels could indicate stress (Fraser, 1989) (Chapter III).

While seemingly low, lipid content levels of animal samples (~1% g g^{-1} wet weight) were in accordance with those found in literature (Allen, 1968; Parzanini, 2018). In comparison to the animals, seston samples were mainly comprised of PL (50%) and FFA (31%), with no evidence of TAG (0%). This finding contrasts previous reports of Newfoundland seston rich in AMPL and low in FFA (Parrish et al., 1995). Although rare, high levels of FFA could reflect degradation of lipids as a result of sewage runoff from St. Philip's township (Parrish et al., 1992; Galois et al., 1996). Despite the unusual lipid profiles of our seston lipids, total lipid levels (~57 µg L^{-1}) (Appendix F) were comparable to samples collected from a nearby Newfoundland site in 1991 (Parrish et al., 1995), likely evidence of the annual phytoplankton bloom with fresh, lipid rich diatoms (Budge and Parrish, 1998; Kiriakoulakis et al., 2005; Parrish et al., 2005). However, overall low quantities of seston resulting from suboptimal volumes of seawater analyzed may have contributed to our high FFA and low TAG levels. In hindsight, the 3 L of water filtered likely lacked sufficient lipid material for accurate TAG analyses and we therefore recommend at least 10

L for future studies. On the other hand, total lipid content of *L. digitata* samples (~1.3 mg g^{-1} wet weight) were dramatically lower than the wide range of those found in literature (~11 – 60 mg g^{-1}) (Raven et al., 2002; Schall et al., 2010). One could attribute a small part of this difference to variations in technique; gravimetric assays are typically 10 to 15% higher than Iatroscan-derived lipids (Parrish, 2013). Such low lipid contents could also reflect chemical changes of *L. digitata* due to the presence of sea ice; however, brown algae in subarctic cold waters have significantly more total lipid than those in tropical warm waters (Terasaki et al., 2009; Nomura et al., 2013) and brown algae increase their total lipids in winter and under low light conditions (Honya et al., 1994; Nelson et al., 2012; Nomura et al., 2013). This suggests our low total lipid content of *L. digitata* could be due to unknown difficulties with the complete extraction of *L. digitata* lipid material.

2.5.3. Fatty acids and stable isotopes

Higher levels of unsaturated FAs compared to saturated FAs likely result from cold-water conditions (Parrish, 2009). However, unlike lipid structure, which organisms solely regulate (Arts et al., 2009), fatty acid composition also depends on diet, feeding strategy, and phylogeny (Dalsgaard et al., 2003; Makhutova et al., 2011). High levels of ω3 FAs eicosapentaenoic acid (EPA; 20:5ω3) and docosahexaenoic acid (DHA; 22:6ω3), and occasionally ω6 FA arachidonic acid (ARA; 20:4ω6), typically characterize the marine environment. Based on our study, apart from *H. arctica* (9%) and *A. rubens* (5%), only trace amounts of DHA occur within the Newfoundland rhodolith environment. *Hiatella arctica* and *A. rubens* likely require more DHA because mollusks require it for growth (Wacker et al., 2002; Arts et al., 2009) and hatching in copepods (Arendt et al., 2005), which were abundant in the diet of *A. rubens*. The relatively high levels of DHA in *H. arctica* align with the findings of Copeman and Parrish (2003) who reported

that bivalves conserve relatively higher levels of plankton derived DHA and lower ARA than echinoderms. The enhanced trophic relationship (TMF > 1) between *A. rubens* and calanoid copepod-derived lipids such as 20:1ω9 and 20:1ω11 (TMF, 1.19), whether feeding directly or indirectly, follows on the suggestion from Connelly et al. (2014) that organisms can maintain lipid-rich energy stores from copepod-derived lipids in the same way as from DHA. The trophic relationship also aligns with our diatom abundance findings because calanoids in Newfoundland also rely on a diatom-based diet in winter (Urban et al., 1992; Beaugrand et al., 2002). Based on its $\delta^{15}N$ signature (11.0) and TP (3.2), we identified *A. rubens* as the top consumer of the studied components in the rhodolith food web. While we cannot identify with certainty the sources of its diet, its similar FA composition to *H. arctica* combined with the predatory history of *A. rubens* towards mollusks (Allen, 1983) suggests *H. arctica* may be a potential prey item.

EPA was the most abundant FA in each of the six animals sampled (*A. rubens*, 32%; *H. arctica*, 19%; *Nereis* spp., 29%; *O. aculeata*, 27%; *S. droebachiensis*, 25%; and *Tonicella* spp., 22%), suggesting it compensated for DHA deficiency. High levels of essential fatty acids typically reflect the dominant microalgal group (Dalsgaard et al., 2003); EPA levels are consistently high in diatom-dominated environments, whereas DHA prevails where dinoflagellates dominate. We conducted our study at the beginning of the spring phytoplankton bloom, so high concentrations of EPA (diatoms) might overshadow any presence of DHA, such as in *H. arctica* and *A. rubens* (Budge et al., 2001; Dalsgaard et al., 2003). As indicated by its prevalence in all diets, EPA has a high trophic magnification factor (TMF, 1.15). The biomagnification of EPA may confirm our hypothesis of a bottom-up food web in which most organisms rely on a shared resource (diatoms, EPA) passing from first order consumers onto second and third order consumers. The presence of diatom trophic biomarkers 16:0 and 16:1ω7 in sediment and in all animal diets further points to

diatoms as a major food source in this rhodolith community. Although synthesized biomarkers like 16:0 are less useful for understanding dietary intake than externally derived fatty acids like EPA, we feel it is reasonable to not ignore synthesized fatty acids given the large accumulation of them in this study (Wennberg et al., 2009). Interestingly, seawater samples contained little EPA (1.2%) or 16:1ω7 (1.2%), but rather large proportions of 16:0 (21.7%; diatom and particulate macroalgae), 18:1ω9 (32.9%; zooplankton and particulate macroalgae), and 18:0 (18.2%; detrital) biomarkers (Wakeham and Canuel, 1988; Parrish, 2013; Legeżyńska et al., 2014). This is in accordance with Bec et al. (2010) who concluded phytoplankton only explain 27% of the variance in seston. Due to the site's proximity to riverine input, some proportions of 18:1ω9 and 18:2ω6 (5.3%) could also be influenced by conifer pollen found in large quantities during spring (Masclaux et al., 2013; Lichti et al., 2017). Regardless, diatoms help support a rich infaunal community living underneath rhodoliths which likely depend on deposition of organic material both at the rhodolith layer and into the sediment (Steller et al., 2003; Grall et al., 2006; Berlandi et al., 2012). However, diatoms may provide more than just food to rhodolith beds, in that Steller and Cáceres-Martínez (2009) suggest diatom films on rhodoliths could also promote larval settlement of invertebrates (Morse et al., 1988; Daume et al., 1999; Huggett et al., 2006).

Although not as common as EPA or DHA, some marine organisms also require ARA as an essential fatty acid. ARA is especially important for echinoderms (Copeman and Parrish, 2003) to regulate metabolic activities (Ciapa et al., 1995) and to maintain membrane structure and function (Parrish, 2009). In our study, ARA was highest in the echinoderms *A. rubens* (20%) and *S. droebachiensis* (15%). These high levels of ARA in sampled urchins were higher than those reported by Kelly et al. (2008) from both a coralline barren and kelp bed (*Laminaria digitata*). *Laminaria digitata*, a common food source for *S. droebachiensis,* is typically rich in ARA

(Fleurence et al., 1994; Schmid et al., 2014) and its low nitrogen ($\delta^{15}N$) signature (3.4) places it at the base of our food web (TP: 1.0). However, our kelp samples contained only 0.1% of ARA proportionally, making it an unlikely source of ARA throughout our food web. Nevertheless, high levels of a fatty acid precursor to ARA, 18:2ω6 (9%) marked FA profiles of *L. digitata*. The ability of *S. droebachiensis* to synthesize ARA from 18:2ω6 complicates biomarker identification from algal fatty acids (Kelly et al., 2008). Combining fatty acid analyses with stable isotope analyses can increase the resolution of organism diets. Thus, given some similarities of carbon ($\delta^{13}C$) signatures, *S. droebachiensis* (-19.8‰) may consume *L. digitata* (-21.0‰); however, $\delta^{13}C$ signatures of *L. digitata* were degraded compared to literature (Raven et al., 2002; Schaal et al., 2010). Although we could not identify the dietary source of ARA among sampled components, we believe amphipods represent a potential source of ARA in the rhodolith system because of both their high abundance in the rhodolith community and their typical ARA richness (Guerra-García et al., 2004). Given its biomagnification across diets (TMF, 1.16), ARA likely represents a key essential FA in the rhodolith food web and should be a focus of future studies.

Three potential photosynthetic carbon sources exist within a rhodolith bed: macroalgae (including the coralline alga itself), phytoplankton, and microphytobenthos (Grall et al., 2006). Similarly to *S. droebachiensis*, the carbon signature (-19.3‰) of *Tonicella* spp. proximated that of rhodoliths (-18.9‰) and not kelp, suggesting that our focal grazing species feed directly on coralline algae with little to no dietary input from kelp. *Strongylocentrotus droebachiensis* often leaves star-shaped tooth marks on rhodoliths (personal observation) and are known to consume coralline algae and microalgal films in coralline barrens, though confining their bites to tips of rhodolith branches (Steneck, 1990; Scheibling et al., 1999; Lauzon-Guay and Scheibling, 2007). *Tonicella* spp. occurs in high abundance, often on the outside of rhodoliths. Although their

bite marks are not as evident as those of *S. droebachiensis*, their articulating plates give them the unique ability to graze between rhodolith branches (Steneck, 1990). In addition to eating the coralline, these grazers may also feed on diatom films on the surface of the rhodoliths (James, 2000). Because of negligible lipid concentration, we were not confident in the accuracy of our rhodolith lipid and fatty acid results, and therefore cannot compare these compositions with those of *S. droebachiensis* and *Tonicella.* spp. Whereas Kelly et al. (2008) sampled a blend of coralline algae taxa, our study was the first to explore lipids in a single rhodolith species, and we were uncertain how much rhodolith material our lipid analyses would require. We determined that 3-5 g of rhodolith material resulted in negligible lipid concentrations and based on our subsequent calculations and findings that rhodoliths are 85% $CaCO_3$ by weight (Teed et al. 2020), we recommend a minimum of 12-15 g of rhodolith material (organic and inorganic, combined) for future analyses. As mentioned above, $\delta^{13}C$ signatures of *L. digitata* were lower compared to literature. We hypothesize sea ice contributed to its carbon depletion by either causing bacterial degradation of the kelp, by causing the kelp to produce new fronds on stored photosynthate containing little nutritional value, or by creating low phytosynthetic conditions (Fredriksen, 2003; Vanderklift and Bearham, 2014). Similarly, nitrogen ($\delta^{15}N$) signatures are influenced by light availability (Vanderklift and Bearham, 2014) and nutrient status (Gagné et al., 1982; Schaal et al., 2009), thus sea ice may have also contributed to the unusually low $\delta^{15}N$ signatures of *L. digitata* (3.4‰) compared to literature (Raven et al., 2002; Schall et al., 2010). Combined with our abnormally low total lipid levels of *L. digitata*, we do not recommend a change in analysis for kelp material, but rather additional samplings (Chapter III) to determine the reliability of variation seen in our samples.

FA profiles of *H. arctica*, *O. aculeata*, and *Tonicella* spp. were influenced by bacterial (16:2ω4 and *i*17:0) and red and green alga (18:1ω7) trophic biomarkers. $\delta^{15}N$ signatures identified *H. arctica* (6.3‰) as a first order consumer and *O. aculeata* (9.0‰) and *Tonicella* spp. (9.7‰) as second order consumers. Though their trophic levels varied (TP, 1.9, 2.6, and 2.9, respectively), the similar $\delta^{13}C$ signatures (-19.3 – -20.0‰) in the three species indicate similar carbon sources. We combined fatty acid and stable isotope analyses to identify similarities between the diets of non-predatory benthic organisms that suggest a resource partitioning relationship wherein animals consume different elements of the same foods (i.e. particulate algae, microphytobenthos, phytoplankton) at different times using different strategies (filter feeding, suspension feeding, and grazing, respectively) resulting in the effective use of the majority of the food source (Hines, 1982; Parrish et al., 2009). In this instance, the feeding strategy of *O. aculeata* offers a possible explanation for the feeding relationship described above. Although brittle stars shared a nearly identical $\delta^{13}C$ signature to *H. arctica* (-19.9‰ and -20.0‰, respectively), their stronger $\delta^{15}N$ signature (9.0‰ versus 6.3‰, respectively), presumably results from POM enrichment as it settles on the seafloor (Iken et al., 2001). Therefore, *O. aculeata* likely consumes the same material as *H. arctica*, but as resuspended matter rather than through direct filter feeding, and thus benefitting from the particulate leftover from *H. arctica*. Additionally, *Tonicella* spp. may graze on larger particulate material inaccessible to *O. aculeata*, potentially breaking it down into smaller pieces for consumption by *O. aculeata*. Indeed *O. aculeata* utilizes several different suspension feeding mechanisms to collect enriched particles resuspended into the water surrounding the rhodoliths (Labarbera, 1978). The species may therefore enhance benthic-pelagic coupling in transferring organic material from the pelagic zone to the benthos (Guerra-García et al., 2004). These results

align with Grall et al. (2006) who demonstrated that rhodolith beds offer potential for both pelagic (Herman et al., 2000) and benthic algae-based feeding (Takai et al., 2004).

2.5.4. Conclusion and future research directions

Our study confirms the hypotheses that (1) the lipid composition of organisms generally reflects the predominantly cold-water conditions of Newfoundland; and (2) bottom-up planktivores and detritivores largely control the rhodolith bed food web as reflected by high abundance of planktonic and bacterial biomarkers. Our lipid and fatty acid analyses revealed high levels of phospholipids and unsaturated fatty acids combined with low sterols in all animal species. These findings indicate a need for increased membrane fluidity in response to cold temperatures. Our fatty acid and stable isotope analyses demonstrated that many organisms in the rhodolith food web community rely on a shared resource - diatoms. We also elucidated a potential resource partitioning feeding relationship between first- (*H. arctica*) and second- (*O. aculeata* and *Tonicella* spp.) order consumers, in that organisms consume different variations of the same organic and inorganic material so that each organism receives food by benefiting off the feeding strategies of another organism.

Our study documents, for the first time, specific diets of organisms in a Newfoundland rhodolith community. Because of the complexity of diets in the benthic community (Kharlamenko et al., 2001; Pitt et al., 2009; Kelly and Scheibling, 2012) and uncertainty in the volume of sample material required for some components (seawater and *L. glaciale*), we could not decipher all potential links among studied components within the rhodolith community. In future studies, we recommend the aformentioned minimal sampling material requirements, We also recommend expanding the breadth of species to include organisms such as amphipods and copepods that may

influence rhodolith community diets (Guerra-García et al., 2004; Pakhomov et al., 2004). To understand better how the sediment beneath the rhodolith bed affects the trophodynamics of the rhodolith ecosystem, we suggest future studies examine bacteria and microbe composition and their production of fatty acids (e.g. 16:0, 16:1ω7, and 18:1ω7) (Fullarton et al., 1995). We also suggest temporal and spatial investigations to understand better how the rhodolith community trophodynamics function (Chapter III).

Chapter III

Spatio-temporal variation in a Newfoundland rhodolith bed food web inferred from lipid, fatty acid, and stable isotope analyses

3.1. ABSTRACT

Temporal and spatial studies provide a detailed representation of trophodynamics in benthic marine ecosystems with complex interactions such as in rhodolith communities. Food availability and physiochemical conditions can impact organism lipid composition and diet. To test the hypotheses that: (1) seasonal fluctuations in temperature and food availability affect lipid composition and diets of organisms; and (2) diets of organisms near riverine input reflect its freshwater origins, we sampled rhodoliths (*Lithothamnion glaciale*) from two sites in a large (>500 m^2) rhodolith bed in St. Philip's, Newfoundland that presumably differed in physicochemical characteristics in April, July, and December 2017 to capture the spring and fall phytoplankton blooms. Rhodolith size and abundance of epiphytes differed significantly between sites despite similar biomasses of rhodoliths and cryptofauna. We showed strong benthic-pelagic coupling, seasonal changes in trophodynamics, and species-specific dietary changes based on food availability and life-history requirements. Our analyses revealed overall community shifts in diet from a diatom-based food web following the spring phytoplankton bloom to a kelp/algae-based food web during the fall months. This finding suggests that EPA (20:5ω3) is of much higher value than DHA (22:6ω3) to the Newfoundland rhodolith community. We identified a resource partitioning feeding relationship in which first- and second- order consumers share a common resource (diatoms or kelp). Our analyses showed fluctuations in diets (i.e. *Tonicella* spp.) reflecting life-history requirements. Diets were not impacted by riverine input proximity. Given a significant reliance on water-column processes (i.e. phytoplankton blooms) and ongoing global climate change, we conclude that a shift in availability or timing of resources may affect the health and stability of rhodolith bed communities.

3.2. INTRODUCTION

Trophic ecology is the study of feeding relationships and energy transfers among organisms interacting in a community. Lipid classes, fatty acids, and stable isotopes offer powerful approaches to the study of trophic relationships. These dietary linkages largely remain unresolved in marine benthic ecosystems because of the broad range of diets of many species and sometimes complex benthic-pelagic relationships, which can further vary seasonally (Kharlamenko et al., 2001; Pitt et al., 2009; Kelly and Scheibling, 2012).

Prevailing environmental conditions strongly influence temporal and spatial variation in marine benthic ecosystems (McConnico et al., 2017). Changes in temperature (Schiel et al., 2004), salinity (Steneck, 1986; Gagnon et al., 2012; Teichert et al., 2014), and chlorophyll (Górska and Włodarska-Kowalczuk, 2017) can affect invertebrate abundance, biomass, and feeding patterns (Parrish, 2013) in shallow benthic communities. To cope with these changing physical conditions, organisms can alter their diet (Kelly and Scheibling, 2012), and therefore their lipid class (Honya et al., 1994), fatty acid (Nelson et al., 2002), and stable isotope composition (Pakhomov et al., 2004). Although analyzing lipids, fatty acids and stable isotopes (listed in increasing order of broadness of dietary time-scale) provides a detailed snapshot of feeding relationships at a period in time, seasonal and temporal studies can capture diet alteration in relation to changing environmental conditions and thus provide a more comprehensive ecological perspective. Therefore, combining lipid class, fatty acid, and stable isotope analyses with seasonal and temporal aspects can assist in defining a more accurate representation of food webs.

Rhodoliths (free-living, non-geniculate red coralline algae growing as balls, branched twigs, or rosettes) often form dense aggregations, known as “rhodolith beds,” at depths of up to 150 m in tropical to polar seas (Foster, 2001; Foster et al., 2007). Rhodolith beds, together with seagrass meadows, kelp beds and forests, and mangrove forests, are considered the four dominant

types of marine communities that rely upon benthic primary producers (Foster, 2001; Foster et al., 2007). The relatively complex morphology of rhodoliths creates suitable habitats for attachment (Kamenos et al., 2004a; Steller and Cáceres-Martínez, 2009; Riosmena-Rodriguez and Medina-López, 2010), reproduction (Kamenos et al., 2004b; Steller and Cáceres-Martínez, 2009; Gagnon et al., 2012), and feeding (Steneck, 1986; Gagnon et al., 2012; Teichert et al., 2014) of highly diverse algal and faunal assemblages. The important contribution of rhodolith beds to marine biodiversity (Steller et al., 2003; Gagnon et al., 2012; Riosmena-Rodríguez et al., 2017) and global calcium carbonate ($CaCO_3$) production (Amado-Filho et al., 2012a; Harvey et al., 2017; Teed et al., 2020) has helped motivate the recent increase in studies of factors and processes regulating their structure and function (Marrack, 1999; Hinojosa-Arango et al., 2009; Millar and Gagnon, 2018).

Knowledge about rhodolith community dynamics is limited to shifts in macroalgal (Piazzi et al., 2002; McConnico et al., 2017) and invertebrate (Gabara, 2014) assemblages, as well as the negative effects of human disturbance to rhodolith ecosystems (Steller et al., 2003; Gabara et al., 2018). These aforementioned studies broadly quantify changes in rhodolith-associated organisms at the community level, however, they do not clarify how these organisms interact with their changing environment. Given the intricacy of benthic and rhodolith communities, where macroalgae and bacterial components contribute just as significantly to nutrition as the macroinvertebrates themselves (Newell et al., 1995), quantifying diversity and abundance may not offer a complete representation of the interconnections in the rhodolith community (Kelly and Scheibling, 2012). This caveat has particular relevance to mid to high latitude seasonal seas, where phytoplankton bloom and microalgal and bacterial films on the surface of benthic organisms grow seasonally. As conditions shift seasonally, so may community dynamics. Specifically, diets shift

as resource availability changes (McMeans et al., 2015). Understanding the complexity of the system requires evaluating effects of seasonality and bottom substrate in supporting production for different trophic levels. Our study aims to further knowledge about rhodolith bed trophodynamics by: (1) investigating temporal dietary changes to understand better how organisms adapt to seasonal fluctuations in food availability; (2) investigating how riverine input proximity affects rhodolith community structure as well as organism lipid composition and diet to characterize how specific *in situ* conditions may affect rhodolith communities. Thus, by extending lipid, fatty acid, and stable isotope analyses to different time periods, our study is the first to elucidate how feeding dynamics change seasonally and spatially in rhodolith beds.

Chapter II built on previous studies of a large (>500 m^2) rhodolith bed in St. Philip's, Newfoundland that first characterized rhodolith morphology and invertebrate biodiversity (Gagnon et al., 2012), and addressed how the dominant invertebrates affect sedimentation within the bed (Millar and Gagnon, 2018). Specifically, Chapter II: 1) identified lipid composition of organisms to understand better if functional strategies relate to organism's environments; 2) delineated trophic linkages among organisms to understand the nutritional value of their diets and the extent of benthic-pelagic coupling versus strictly benthic interactions; and 3) investigated specific challenges and requirements for lipid, fatty acid, and stable isotope analyses in rhodolith communities. Our present study increases the temporal and spatial dimensions of Chapter II to explore possible trophodynamic variability in the rhodolith bed. Specifically, we aim to test the hypotheses that: (1) seasonal fluctuations in temperature and food availability affect lipid composition and diets of organisms; (2) diets of organisms in close proximity to riverine input reflect its freshwater origins.

3.3. MATERIALS AND METHODS

For consistency with Chapter II, we used the same materials and methods, including laboratory and statistical analyses, as described in section 2.3. This present study increases the temporal and spatial dimensions of Chapter II. As such, only differences between section 2.3 and section 3.3, including seasonal sampling in April, July, and December and the addition of a second collection site, are presented below.

3.3.1. Study sites and selection of focal species

We completed our field work during the spring, summer, and fall of 2017 in a rhodolith (*Lithothamnion glaciale*) bed, which extends ~5 to 30 m in depth along the coast of St. Philip's, southeastern Newfoundland, Canada. Consistent with our broader objective of characterizing spatial and temporal variability in rhodolith bed trophodynamics and presumed differences in marine environmental conditions in this area, we chose to study two sections of the bed fringing Broad Cove (South: 47° 35′ 36.5″ N, 52° 53′ 31.0″ W and North: 47° 35' 39.6" N, 52° 53' 24.6" W; Figure 1.1). The present study follows up on the "South" site study in Chapter II. Adding the "North" site (Figure 1.1) allowed us to investigate trophic variability because of the presumably greater environmental variability at this site resulting from greater proximity to freshwater input from the marina. This study addresses trophic interactions at both sites across three seasons and thereby expands our knowledge of spatial and temporal dimensions in the Broad Cove rhodolith bed. See section 2.3.1 for full details.

3.3.2. Timing of sampling

In order to examine how benthic-pelagic coupling might change during different phytoplankton bloom events, we sampled the rhodolith bed during and at the end of the annual

spring phytoplankton bloom in southeastern Newfoundland, when we anticipated peak diatom abundance in the water column (Budge and Parrish, 1998; Parrish et al., 2005), and at the end of annual fall phytoplankton bloom, when we expected peak dinoflagellate abundance (Parrish et al., 1995). The bloom began in the last few days of March and persisted through 23 April, 2017, when we sampled the rhodolith community and collect rhodoliths for food web analyses. When we sampled the bloom on 10 July, 2017, the bloom was dwindling. We also sampled on 2 December, 2017, at the end of the fall bloom (Appendix B). See section 2.3.2 for full details.

3.3.3. Rhodolith community

In order to broadly characterize the rhodolith community, scuba divers hand collected, on 23 April, 2017, all the rhodoliths from one 30 x 30 cm quadrat placed every 5 m along a 30-m long transect at a depth of ~15 m at the South site and North site (for a total of seven quadrats sampled at each site). In contrast, we chose the North section of the bed for its relative proximity to freshwater input and its perceived higher sediment abundance around rhodoliths (personal observations). See section 2.3.3 for full details.

3.3.4. Rhodolith percent cover and epiphyte coverage

In order to investigate rhodolith epiphyte coverage differences between sites (personal observation), on 29 September, 2018, scuba divers took photos of rhodoliths from one 30 x 30 cm quadrat placed every 5 m along each of four 15-m long transects at a depth of ~15 m at the South site and North site (for a total of 24 quadrat photographs each; we took photographs with a Canon PowerShot D30). From each photograph, we estimated epiphyte coverage on rhodoliths and percent cover of rhodolith, sediment, and macroalgae (kelp and algae) using the point intercept

method. A 7 x 7 grid was overlaid onto each photo in Adobe Photoshop and the element present underneath each grid intercept was recorded (i.e. rhodolith, sediment, or macroalgal). We marked rhodolith intercepts for presence or absence of epiphytes. We measured epiphyte coverage only using intercepts overlaying rhodoliths. The 7 x 7 grid yielded 49 intercepts on each image, each representing ~2.1% cover. The outline of the 30 x 30 quadrat frame provided a reference scale. We used Microsoft Excel for descriptive statistics (see section 2.3.9.4).

3.3.5. Collection and preparation of samples for food web analyses

On 23 April, 10 July, and 2 December, 2017, divers hand collected ~150 live rhodoliths measuring 8 to 10 cm along the longest axis, we collected seawater a few centimeters above the rhodolith bed with two, 12-L Niskin bottles that were deployed gently to prevent resuspension of sediment from the bed, and we collected three sediment samples that were scooped from the top (~10 cm) layer of muddy sediment underneath rhodoliths with 15-mL centrifuge tubes. See section 2.3.4 for full details.

3.3.6. Extraction and characterization of lipid classes

Extraction of lipids followed protocols by Folch et al. (1957) with modifications by Parrish (1999). See section 2.3.5 for full details.

3.3.7. Preparation and characterization of fatty acid methyl esters (FAME)

Fatty acids methyl esters (FAME) of lipids were prepared directly by transesterification from aliquots of lipid extract following a modified procedure described by Christie (1982) and Hamilton (1992). See section 2.3.6 for full details.

3.3.8. Stable Isotope Preparation and Analysis

Samples in their scintillation vials were prepared separately for carbon and nitrogen analyses, transferred to desiccators, and subsequently taken to the Earth Resources Research and Analysis (TERRA) facility at MUN for analysis. See section 2.3.7 for full details.

3.3.9. Trophic magnification of fatty acids

We calculated a trophic magnification factor (TMF) for fatty acids (FA) correlated with $\delta^{15}N$. This factor quantitatively represents the biomagnification of compounds along a food web (Borgå et al., 2012; Connelly et al., 2014). See section 2.3.8 for full details.

3.3.10. Statistical analysis

3.3.10.1. Lipid classes

We used two separate two-way permutational MANOVAs (PERMANOVA) (Euclidean distance matrices with 9999 permutations) to test total lipid (N=139) and lipid classes (N=147) for temporal and spatial differences with the factors Month (April, July, and December) and Site (North and South). We also used separate one-way PERMANOVAs with the factor Component (each of the 10 components of the food web studied [six animal species, two macroalgal species, and two environmental components]) to examine differences in proportions of total lipid (and overall lipid classes among samples, accounting for accidental loss of samples during the analyses). To limit extraneous data variability while focusing on the most significant lipid classes, only lipid classes present in over 50% of the samples were included in the analysis. For consistency with Chapter II and for comparison purposes, we pooled the data into the five following functional

groups reflecting the three dominant feeding strategies of the six animal species, two macroalgal species, and two environmental components: (1) suspension/filter feeders [two species]; (2) grazers [two species]; (3) predators [two species]; (4) kelp and rhodolith; and (5) seawater/sediment [samples combined because of expected benthic-pelagic coupling] (see section 3.3.1 for details). We then ran a one-way PERMANOVA with the factor Functional Group (the five groups discussed above). We ran one-way ANOVAs to test for relationships between individual components and total lipid or individual lipid classes. We examined relationships between total lipid and each of the major lipid classes with conventional Spearman Rank-Order Correlation tests (Zar, 1999).

3.3.10.2. Fatty acids

We used the same statistical approach (one two-way PERMANOVA with the factors Month and Site, and two one-way PERMANOVAs; one with the factor Component followed by one wit the factor Functional Group), with data exclusion to account for samples lost during analyses, to examine differences in the proportions of fatty acids and their proportional sums among samples (N=142). We then used a one-way SIMPER analysis (run on untransformed data with a Bray-Curtis similarity matrix) with the factor Component (each of the 10 components of the food web studied [six animal species, two macroalgal species, and two environmental components]), to identify potential food sources and the main fatty acids contributing to the lipid structure of each component (Kelly and Scheibling, 2012; Gabara, 2014). To limit extraneous data variability while focusing on the most significant fatty acids, only fatty acids contributing to over 70% of the similarities were included in the SIMPER analysis. We used a follow-up principal coordinates analysis (PCO; also run on untransformed data with a Bray-Curtis similarity matrix)

with the factor Component (same as above), mainly for visualization of the feeding relationships among specific groups of organisms (Guest et al., 2008; Drazen et al., 2009). To increase clarity on the PCO, only samples with a Pearson coefficient of correlation > 65%). We ran two-way ANOVAs to test if individual fatty acid composition among all components changed by month or by site. We also ran individual two-way ANOVAs to test if proportions of the 8 fatty acids (16:0, 16:1ω7, 18:0, 18:1ω9, 18:1ω7, 20:1ω11, 20:4ω6 [ARA], and 20:5ω3 [EPA]) exhibiting at least 70% correlation changed significantly seasonally or temporally by specific components.

3.3.10.3. Stable isotopes

We examined differences in carbon ($\delta^{13}C$) and nitrogen ($\delta^{15}N$) isotope ratios with two one-way PERMANOVAs (one for each type of ratio; both types based on Euclidean distance matrices with 9999 permutations) with the factor Component and two two-way PERMANOVAs with the factors Month and Site. All taxa (six animal species, kelp, and rhodoliths) and both environmental components (seawater and sediment) were included in the $\delta^{13}C$ isotope ratio analysis (N=128, accounting for accidental loss of samples during the analyses). All components were also included in the $\delta^{15}N$ isotope ratio analysis (N=161), accounting for accidental loss of samples during the analyses). We also carried out a cluster analysis (with the "Group Average" clustering method) on $\delta^{13}C$ and $\delta^{15}N$ isotope ratios simultaneously, and complementary SIMPROF test (Euclidian distance matrix with 9999 permutations) (N=120 because of a few unmatched pairs of $\delta^{13}C$ and $\delta^{15}N$ ratios), to group and map, in the form of a dendrogram, statistically different components of the food web (Grall et al., 2006; Gabara, 2014). Seven main isotopic groups emerged from the SIMPROF test. We therefore ran a follow-up one-way PERMANOVA with both isotopic ratios

combined and complementary one-way ANOVAs and post-hoc tests with the factor Group to examine differences among these seven main trophic groups.

3.3.10.4. General aspects of statistical tests

In all PERMANOVAs, data were untransformed and computed to Bray-Curtis similarity or Euclidian distance matrices (9999 permutations). All fatty acid multivariate data were computed using Bray-Curtis similarity matrices, while lipid and stable isotope multivariate data were computed using Euclidean distances matrices. We used PERMDISP (9999 permutations) to inform our decision ($p=0.3236$); we tested for homogeneity of multivariate variances and confirmed all variances were homogenous. We used PCO (principal coordinate analysis) instead of PCA (principal component analysis) to more efficiently account for missing data (Rohlf, 1972). We combined the North site and the South site in all figures because of their absence of statistical variation. In all ANOVAs, we verified homogeneity of variance and normality of residuals by examining the distribution of the residuals and the normal probability plot of the residuals, respectively (Snedecor and Cochran, 1994). We used a significance level of 0.05 in all analyses and report all means with standard deviation (mean ± SD) unless stated otherwise. We used standard error where applicable for consistency with corresponding literature (Gagnon et al., 2012; Connelly et al., 2014; Parzanini, 2018). We used PRIMER v7 with PERMANOVA+ for multivariate statistical analyses, Minitab 18 for univariate statistical analyses, and Microsoft Excel for descriptive statistics. See section 2.3.9.4 for full details.

3.4. RESULTS

3.4.1. Rhodolith community

Average rhodolith biomass was consistent between the South (19.5±0.1 (SE) kg m^{-2}) and North sites (20.2±0.2 kg m^{-2}). However, the significantly fewer rhodoliths (N=163, $p<0.001$) at the North site were significantly bigger (114.1±9.9 cm^3, $p<0.001$) than the 247 rhodoliths at the South site (70.0±4.5 cm^3). North site rhodoliths averaged from 12.1 to 68.7 mm, and 25.4 to 153.1 mm along the shortest and longest axes, respectively, whereas South site rhodoliths averaged from 11.3 to 65.6 mm, and 24.0 to 116.2 mm along the shortest and longest axes, respectively. Rhodolith shape did not vary significantly between sites; together they were predominantly spheroidal and compact (~62%), but otherwise platy (~11%), bladed (~16%), or elongate (~6%) (Figure 3.1). Sediment ($p=0.264$) and rhodolith ($p=0.074$) percent cover did not vary significantly between sites, but epiphyte coverage per rhodolith was significantly higher ($p<0.001$) at the North site (33.0±3.0%) than the South site (14.1±2.4%) (Figure 3.2**)**. Total macrofaunal biomass differed significantly between sites ($p=0.024$); South site biomass (34.5±4.3 g kg^{-1} rhodoliths) nearly doubled North site biomass (18.8±8.4 g kg^{-1} rhodoliths). In total, the 2918 animals extracted from the rhodoliths from the North (N=1727) and South (N=1191) sites did not differ significantly in terms of total animal abundance, but included at least 21 species representing six phyla. Echinoderms (527.9±60.8 individuals kg^{-1} rhodoliths) and molluscs (515.6±52.9 individuals kg^{-1} rhodoliths) dominated both sites numerically (Table 3.1). Species included in the biochemical analyses were particularly abundant at both sites, including *Ophiopholis aculeata* (359.2±58.0 individuals kg^{-1} rhodoliths), *Tonicella marmorea / T. rubra* (226.2±25.2 individuals kg^{-1} rhodoliths) and *Hiatella arctica* (161.9±31.5 individuals kg^{-1} rhodoliths). A few species not included in the analyses were also relatively abundant, including the brittle star *Ophiura robusta* (133.1±27.3 individuals kg^{-1} rhodoliths), caridean shrimp *Pandalus borealis* (64.2±12.2

A

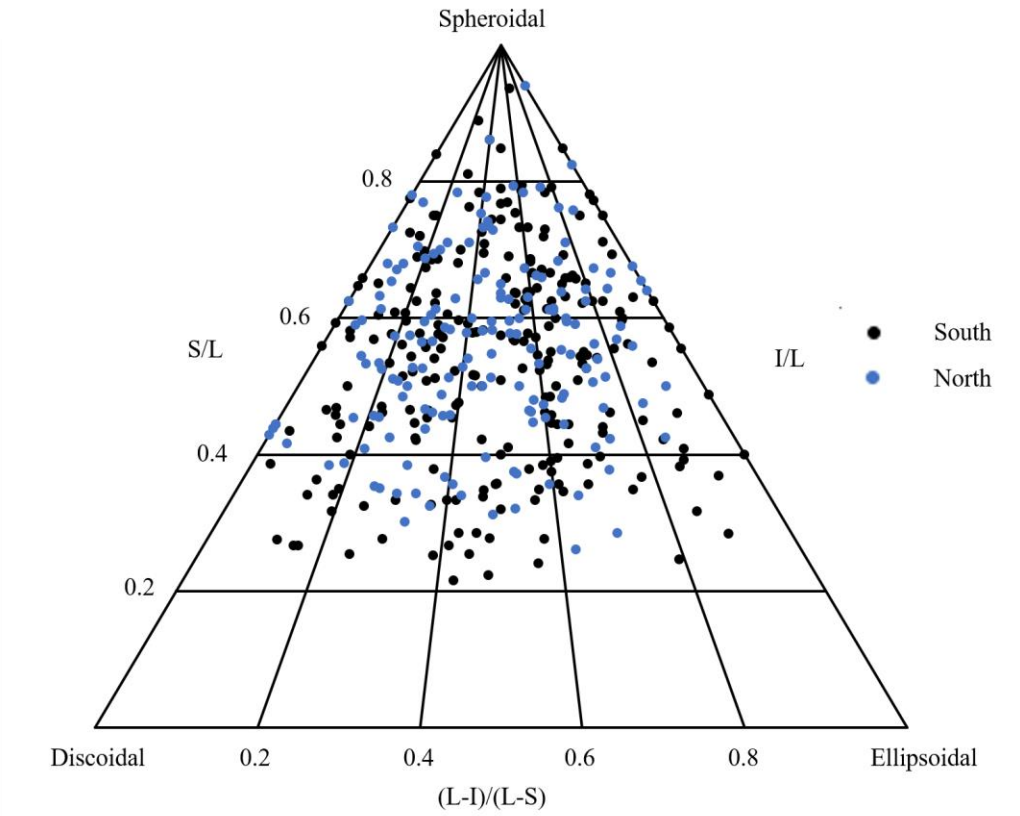
Spheroidal
0.8
0.6
0.4
0.2
S/L
I/L
South
North
Discoidal
0.2
0.4
0.6
0.8
Ellipsoidal
(L-I)/(L-S)

B

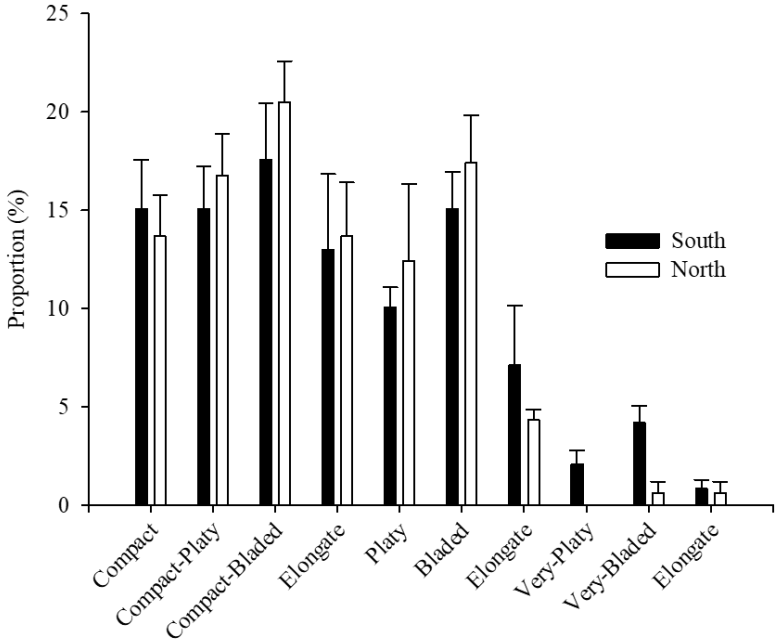
25
20
15
10
5
0
Proportion (%)
South
North
Compact
Compact-Platy
Compact-Bladed
Elongate
Platy
Bladed
Elongate
Very-Platy
Very-Bladed
Elongate

Figure 3.1. (A) Ternary diagram of rhodolith [*Lithothamnion glaciale*] shape relative to purely spheroidal, discoidal, and ellipsoidal rhodoliths [North N=156, South N=247; one dot per rhodolith;]. Rhodoliths were collected in April 2017 at the South and North sites (see Figure 1.1). The position of each rhodolith in the diagram is set by its sphericity, calculated from the length of its longest [L], intermediate [I], and shortest [S] axes. (B) Corresponding proportion of rhodoliths under each of 10 finer shape categories as defined by Sneed and Folk (1958).

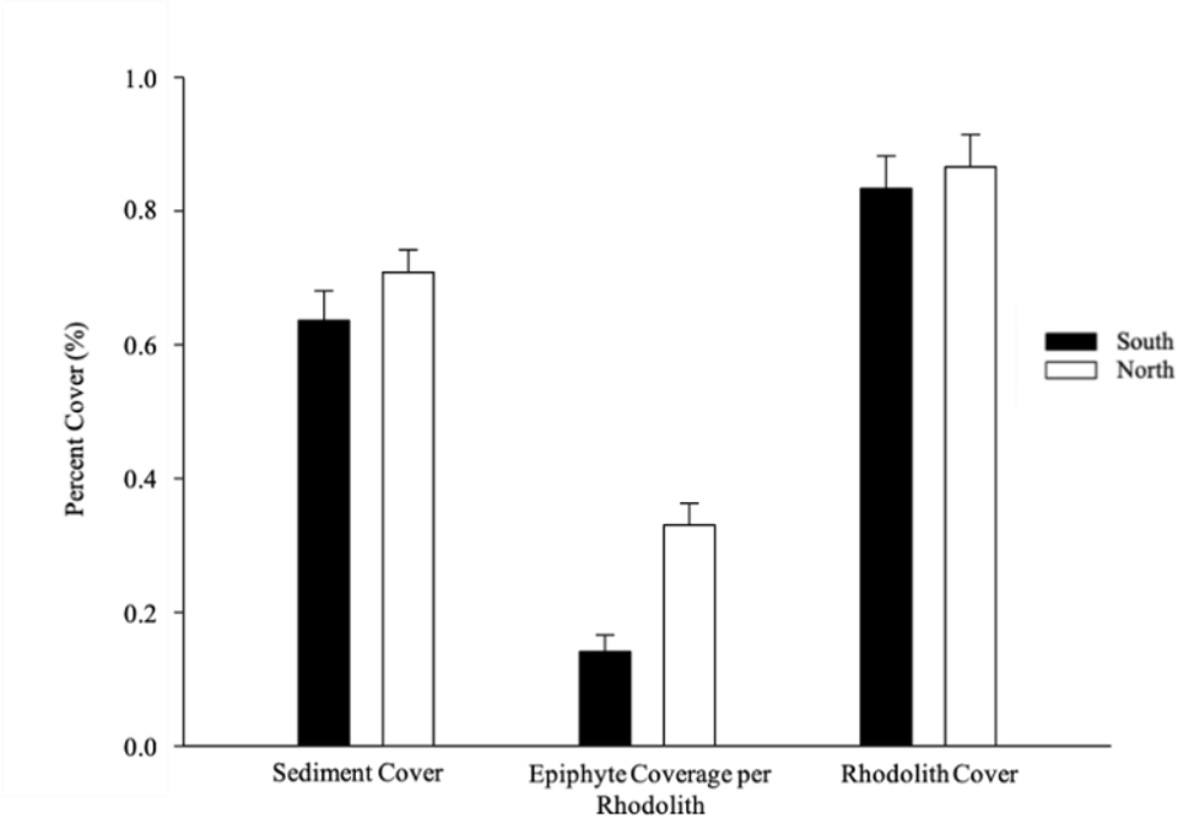

Figure 3.2. Percent coverage of sediment, rhodoliths (*Lithothamnion glaciale*), and epiphyte coverage per rhodolith estimated from photographs taken in September 2018 at the South and North Sites (see Figure 1.1).

Table 3.1. Taxonomical breakdown and abundance of invertebrate macrofauna associated with rhodoliths (*Lithothamnion glaciale*) collected in April 2017 at the South and North sites (see Figure 1.1). Each phylum's total abundance (bolded values) includes macrofauna that could not be identified to the genus level.

Phylum / species	Mean (±SE) density (individuals kg^{-1} rhodoliths)	
	South	**North**
Annelida	**75.9 (8.3)**	**88.1 (21.5)**
Myxicola spp.	8.9 (4.7)	6.7 (3.0)
Neridídae (including *Nereis* spp.)	21.7 (4.7)	17.8 (4.4)
Potamilla reniformis	30.0 (10.3)	41.0 (13.7)
Arthropoda	**72.8 (13.1)**	**125.8 (19.2)**
Amphipoda	34.1 (12.4)	29.7 (9.1)
Cancer irroratus	1.8 (1.0)	4.6 (2.2)
Pandalus borealis	36.9 (7.5)	91.5 (16.3)
Echinodermata	**452.7 (47.0)**	**603.1 (97.4)**
Asterias rubens	19.7 (4.1)	10.8 (4.2)
Ophiopholis aculeata	336.7 (30.8)	381.7 (68.9)
Ophiura robusta	72.7 (13.8)	193.5 (37.7)
Strongylocentrotus droebachiensis	22.8 (3.7)	17.2 (6.2)
Mollusca	**427.6 (39.6)**	**603.7 (78.2)**
Hiatella arctica	152.8 (23.2)	171.0 (26.6)
Lacuna vincta	1.8 (1.0)	2.6 (1.5)
Margarites costalis	15.8 (3.6)	33.9 (4.8)
Modiolus modiolus	14.7 (3.5)	22.1 (5.4)
Moelleria costulata	8.6 (3.0)	11.0 (3.6)
Puncturella noachina	21.2 (5.4)	51.3 (9.1)
Tonicella marmorea / T. rubra	191.6 (27.2)	260.9 (36.2)
Turbonilla spp.	3.4 (2.3)	5.6 (2.9)
Velutina velutina	2.4 (1.5)	3.5 (1.5)
Nemertea	**19.3 (5.5)**	**19.5 (4.7)**
Sipuncula	**5.8 (5.3)**	**6.9 (3.6)**

individuals kg^{-1} rhodoliths), and polychaete *Potamilla reniformis* (35.5±8.8 individuals kg^{-1} rhodoliths).

3.4.2. Total lipid content and lipid classes

Of the ten food web components included in the lipid analysis, the brittle star *O. aculeata* contained the highest average concentrations of total lipids (9.8±4.1 mg g^{-1} [ww]), ranging from 8.9±1.6 mg g^{-1} at the North site in December to 15.0±5.5 mg g^{-1} at the South site in July (Table 3.2). The polychaete *Nereis* spp. had similarly high average concentrations of total lipids (9.7±4.4 mg g^{-1}), ranging from 6.0±1.9 mg g^{-1} at the South site in April to 12.9±5.9 mg g^{-1} at the North site in July. (Table 3.2). The molluscs *Tonicella* spp. and *H. arctica* had respectively high and low concentrations of total lipids averaging 9.1±4.1 mg g^{-1} and 6.7±3.3 mg g^{-1}, respectively. The sea urchin *S. droebachiensis* exhibited the lowest concentrations among animals, averaging 4.9±3.7 mg g^{-1}, a significantly lower total lipid concentration than *O. aculeata* (t=4.8212, $p<0.01$). Kelp (*L. digitata*), rhodolith (*L. glaciale*), seston (from seawater samples), and sediment had the lowest average total lipid concentrations of all components, ranging from 0.4±0.1 mg g^{-1} and 0.4±0.3 mg g^{-1} in *L. glaciale* and sediment, respectively, to 2.7±3.0 mg g^{-1} in seawater (Table 3.2). Both the macroalgal and environmental groups had significantly lower total lipid concentrations than the animal group ($t>4.29$, $p<0.01$ in all cases). Total lipid varied significantly by component (PERMANOVA; Pseudo-$F_{9,129}$=12.225, P (perm)<0.01), but not between sites (PERMANOVA; Pseudo-$F_{1,138}$=0.321, P (perm)=0.55) nor among months (PERMANOVA; Pseudo-$F_{2,138}$=0.813, P (perm)=0.16). The interaction was also not significant.

The ten food web components contained nine lipid classes (PL, TAG, FFA, ST, AMPL, HC, SE, KET, and ALC), with six (PL, TAG, FFA, ST, AMPL, and HC) present in >50% of all

Table 3.2. Sample size (N), mean wet weight, mean total lipid, and mean proportion (%) of the six dominant lipid classes (PL: phospholipid; TAG: triacylglycerol; FFA: free fatty acid; ST: sterol; AMPL: acetone mobile polar lipid; and HC: hydrocarbon) in the six animal species, two macroalgal species, and two environmental components (see Table 2.2 for species list) sampled in April, July, and December 2017 inside (I) or outside (O) of the South and North sites (see Figure 1.1). Each component group (animal, macroalgal, environmental) variable's lowest and highest values are bolded.

				Wet Weight	Total Lipid	PL	TAG	FFA	ST	AMPL	HC
Component	**Site**	**Collection Month**	**N**	g (±SD)	mg g^{-1} ww (±SD)	% (±SD)	% (±SD)	% (±SD)	% (±SD)	% (±SD)	% (±SD)
Animal											
A. rubens (I)	South	April	3	1.0 (0.2)	8.5 (2.2)	**75.9 (5.2)**	1.9 (1.5)	1.5 (2.0)	9.8 (2.7)	8.6 (2.6)	0.8 (0.3)
		July	3	0.7 (0)	9.3 (3.6)	69.3 (14.9)	7.0 (4.2)	1.9 (2.4)	11.7 (2.6)	9.0 (9.1)	0.3 (0.4)
		December	2	0.8 (0.3)	8.6 (1.4)	62.9 (7.5)	6.1 (8.6)	0.9 (1.3)	15.1 (2.7)	11.3 (5.3)	1.1 (1.1)
	North	April	3	0.8 (0.2)	5.2 (2.7)	68.9 (4.0)	0.9 (1.5)	2.7 (3.7)	16.8 (3.3)	7.3 (1.3)	1.8 (1.9)
		July	3	1.0 (0.3)	9.4 (3.2)	68.5 (10.0)	6.6 (2.3)	**8.2 (10.0)**	12.5 (1.3)	3.7 (3.2)	0.3 (0.5)
		December	3	0.9 (0.2)	6.3 (0.4)	68.7 (5.9)	1.3 (2.1)	4.5 (4.7)	13.9 (1.5)	10.6 (2.8)	0.4 (0.5)
Mean			17	0.9 (0.2)	7.9 (2.7)	69.1 (8.2)	4.0 (4.0)	3.3 (5.0)	13.3 (3.1)	8.4 (4.7)	0.8 (1.0)
H. arctica (I)	South	April	3	1.1 (0.3)	9.2 (2.1)	45.3 (11.2)	34.4 (13.9)	5.1 (1.3)	7.5 (1.5)	5.4 (0.1)	0.5 (0.3)
		July	3	0.9 (0.2)	**3.3 (1.6)**	42.7 (10.5)	31.8 (5.0)	4.5 (4.4)	14.6 (7.2)	4.0 (1.9)	1.8 (3.0)
		December	3	0.9 (0.2)	6.2 (1.0)	42.0 (4.2)	28.7 (6.7)	6.8 (2.3)	10.7 (1.4)	7.7 (3.6)	2.1 (1.1)
	North	April	3	1.2 (0.1)	7.5 (2.4)	51.1 (2.6)	30.8 (5.9)	2.3 (1.8)	6.2 (2.4)	5.9 (3.5)	1.6 (1.4)
		July	3	0.9 (0.1)	5.3 (1.6)	55.6 (16.4)	23.5 (9.6)	0.8 (1.4)	10.2 (1.5)	3.6 (4.1)	1.6 (1.5)
		December	3	1.0 (0.3)	8.9 (6.2)	46.6 (6.8)	23.2 (4.5)	3.5 (4.3)	7.6 (5.4)	8.4 (0.2)	1.3 (0.9)
Mean			18	1.0 (0.2)	6.7 (3.3)	47.2 (9.6)	28.7 (8.2)	3.9 (3.1)	9.5 (4.4)	5.9 (2.9)	1.5 (1.7)
Nereis spp. (I)	South	April	3	0.9 (0.2)	6.0 (1.9)	63.3 (10.0)	3.9 (5.7)	5.9 (2.1)	19.2 (4.7)	5.0 (3.5)	1.5 (1.3)
		July	2	0.9 (0.3)	12.2 (10.9)	44.7 (20.8)	29.1 (26.4)	5.5 (0.8)	15.6 (6.3)	4.2 (0.2)	0.3 (0.5)
		December	3	0.9 (0.2)	8.2 (1.1)	64.0 (7.2)	3.6 (1.0)	6.1 (2.6)	19.6 (3.6)	4.4 (1.2)	1.6 (1.8)
	North	April	3	0.6 (0)	8.8 (1.9)	61.2 (2.8)	7.4 (3.8)	3.9 (1.4)	19.3 (4.2)	5.2 (1.3)	1.2 (1.4)
		July	3	1.0 (0.3)	12.9 (5.9)	53.3 (12.6)	19.6 (16.0)	2.6 (2.7)	15.0 (3.6)	5.6 (2.5)	3.4 (3.7)
		December	3	1.0 (0.3)	11.3 (1.8)	52.4 (9.0)	11.2 (2.3)	8.1 (1.6)	16.8 (3.7)	9.8 (5.9)	1.6 (1.6)
Mean			17	0.9 (0.2)	9.7 (4.4)	56.5 (11.1)	12.5 (12.6)	5.4 (2.5)	17.6 (4.0)	5.7 (3.3)	1.7 (1.9)

Table 3.2. (continued):

				Wet Weight	Total Lipid	PL	TAG	FFA	ST	AMPL	HC
Component	**Site**	**Collection Month**	**N**	g (±SD)	mg g^{-1} ww (±SD)	% (±SD)	% (±SD)	% (±SD)	% (±SD)	% (±SD)	% (±SD)
O. aculeata (I)	South	April	3	1.3 (0.1)	13.2 (3.7)	47.8 (2.6)	25.1 (6.3)	5.4 (4.6)	5.7 (5.0)	11.3 (7.3)	2.9 (1.7)
		July	3	1.4 (0.1)	**15.0 (5.5)**	37.9 (11.6)	36.4 (12.7)	8.0 (2.4)	9.7 (0.8)	6.4 (1.5)	1.4 (0.9)
		December	3	0.7 (0.3)	9.3 (1.4)	44.1 (9.0)	29 (13.5)	2.1 (2.2)	16.7 (1.5)	5.6 (4.5)	1.2 (1.0)
	North	April	3	1.0 (0.1)	9.8 (4.8)	49.5 (10.8)	24.9 (4.2)	4.4 (4.8)	10.6 (4.1)	8.6 (1.9)	0.8 (0.4)
		July	2	1.2 (0.2)	10.4 (5.7)	35.9 (3.4)	41.2 (0.5)	5.3 (2.9)	8.7 (1.5)	5.9 (1.5)	1.3 (1.0)
		December	3	1.1 (0.3)	8.9 (1.6)	51.0 (14.8)	26.4 (10.8)	6.9 (3.3)	10.2 (2.3)	3.6 (1.6)	1.6 (1.1)
Mean			17	1.1 (0.3)	9.8 (4.1)	44.4 (10.1)	30.5 (10.0)	5.4 (3.6)	10.3 (4.3)	6.9 (4.1)	1.5 (1.1)
S. droebachiensis (I)	South	April	2	1.1 (0.2)	10.6 (11.0)	60.8 (3.2)	6.0 (4.7)	**0 (0)**	14.9 (8.5)	**16.6 (4.3)**	1.2 (1.0)
		July	3	1.1 (0.4)	4.0 (1.5)	63.1 (11.0)	9.4 (0.5)	1.1 (2.0)	**23.5 (10.8)**	2.4 (2.1)	0 (0)
		December	3	0.9 (0.2)	3.7 (1.4)	66.3 (8.5)	1.6 (1.9)	2.7 (2.3)	22.7 (6.0)	4.8 (4.2)	0.5 (0.5)
	North	April	3	1.1 (0.2)	4.5 (0.6)	52.1 (12.2)	18.3 (11.6)	3.0 (3.5)	16.4 (2.0)	4.6 (0.7)	0.6 (0.6)
		July	3	1.0 (0.3)	4.6 (1.3)	67.7 (10.3)	10.7 (2.3)	**0 (0)**	18.8 (8.4)	**1.6 (0.7)**	1.0 (0.5)
		December	2	0.7 (0.2)	3.6 (1.0)	65.3 (10.7)	**1.0 (1.4)**	4.9 (5.9)	26.0 (1.1)	5.1 (7.2)	1.0 (1.0)
Mean			16	1.0 (0.3)	4.9 (3.7)	62.6 (10.0)	7.8 (7.7)	2.0 (3.2)	20.4 (7.4)	5.8 (5.4)	0.7 (0.7)
Tonicella spp. (I)	South	April	3	0.7 (0.1)	6.7 (1.6)	49.2 (8.4)	28.9 (2.6)	3.2 (3.0)	10.0 (2.6)	7.3 (4.2)	1.0 (1.2)
		July	3	0.6 (0.1)	13.5 (0.9)	36.8 (4.5)	40.7 (6.1)	5.9 (1.8)	9.2 (1.1)	5.3 (1.6)	0.7 (0.2)
		December	3	0.6 (0)	6.2 (1.5)	59.6 (15.5)	12.8 (6.2)	2.5 (2.8)	14.5 (5.7)	5.2 (3.2)	1.5 (2.0)
	North	April	N/A	N/A	N/A	N/A	N/A	N/A	N/A	N/A	N/A
		July	3	0.7 (0.1)	13.9 (2.8)	**33.4 (2.4)**	**49.9 (3.1)**	2.8 (2.4)	**4.5 (3.9)**	3.3 (1.4)	0.2 (05)
		December	3	0.6 (0)	5.4 (0.5)	58.4 (9.8)	8.8 (3.8)	5.2 (3.0)	15.9 (0.6)	4.5 (3.2)	0 (0)
Mean			15	0.6 (0.1)	9.1 (4.1)	47.5 (13.6)	28.2 (16.8)	3.9 (2.6)	10.8 (5.1)	5.1 (2.8)	0.7 (1.1)

Table 3.2. (continued):

Component	Site	Collection Month	N	Wet Weight g (±SD)	Total Lipid mg g^{-1} ww (±SD)	PL % (±SD)	TAG % (±SD)	FFA % (±SD)	ST % (±SD)	AMPL % (±SD)	HC % (±SD)
Macroalgal											
L. digitata (O)	South	April	2	1.6 (0.5)	1.3 (0.1)	49.3 (4.9)	**0 (0)**	**0.4 (0.6)**	**16.2 (2.8)**	**32.7 (7.2)**	0 (0)
		July	3	N/A	N/A	**83.4 (4.0)**	0.6 (1.0)	2.7 (2.3)	**6.8 (3.0)**	**4.1 (3.9)**	0 (0)
		December	3	1.3 (0.3)	**2.1 (0.5)**	**39.8 (8.9)**	**28.5 (5.6)**	2.1 (1.2)	6.9 (6)	19 (3.8)	0 (0)
	North	April	N/A	N/A	N/A	N/A	N/A	N/A	N/A	N/A	N/A
		July	N/A	N/A	N/A	N/A	N/A	N/A	N/A	N/A	N/A
		December	N/A	N/A	N/A	N/A	N/A	N/A	N/A	N/A	N/A
Mean			8	1.4 (0.4)	1.7 (0.6)	57.5 (21.7)	9.7 (14.9)	1.7 (1.7)	9.9 (5.7)	18.6 (12.6)	0
L. glaciale (I)	South	April	N/A	N/A	N/A	N/A	N/A	N/A	N/A	N/A	N/A
		July	3	12.5 (1.2)	0.5 (0.1)	52.9 (6.4)	8.9 (1.0)	6.0 (0.9)	8.3 (1.7)	15.8 (1.1)	4.0 (1.0)
		December	N/A	N/A	N/A	N/A	N/A	N/A	N/A	N/A	N/A
	North	April	N/A	N/A	N/A	N/A	N/A	N/A	N/A	N/A	N/A
		July	3	11.2 (0.6)	**0.3 (0.1)**	48.7 (4)	11.4 (2.9)	**7.4 (3.2)**	7.0 (3.1)	18.0 (1.4)	4.4 (3.8)
		December	N/A	N/A	N/A	N/A	N/A	N/A	N/A	N/A	N/A
Mean			6	11.9 (1.1)	0.4 (0.1)	50.8 (5.3)	10.1 (2.4)	6.7 (2.2)	7.6 (2.3)	16.9 (1.7)	4.1 (2.5)

Table 3.2. (continued):

Component	Site	Collection Month	N	Wet Weight g (±SD)	Total Lipid mg g^{-1} ww (±SD)	PL % (±SD)	TAG % (±SD)	FFA % (±SD)	ST % (±SD)	AMPL % (±SD)	HC % (±SD)
Environmental											
Seawater (O)	South	April	3	0.1 (0)	4.1 (1.2)	49.7 (9.9)	0 (0)	31.2 (3.1)	**10.9 (1.8)**	7.0 (7.0)	0 (0)
		July	3	0.1 (0)	4.7 (0.9)	60.1 (19.2)	0 (0)	**36.6 (18.0)**	2.3 (1.2)	0 (0)	0 (0)
		December	3	0 (0)	**6.3 (5.6)**	93.0 (4.4)	0 (0)	0	5.1 (6.1)	0 (0)	0 (0)
	North	April	3	0.1 (0)	2.9 (0.5)	53.8 (10.2)	0 (0)	34.5 (8.6)	10.7 (1.5)	0 (0)	0 (0)
		July	3	0.1 (0)	2.2 (0.1)	66.7 (10.0)	0 (0)	26.5 (8.4)	5.9 (5.1)	0 (0)	0 (0)
		December	2	0.1 (0)	3.0 (0.7)	**93.5 (2.1)**	0 (0)	0	4.0 (5.6)	0 (0)	0 (0)
Mean			17	0.1 (0)	2.7 (3)	69.5 (19.9)	0 (0)	21.5 (17.3)	6.5 (4.7)	**1.2 (1.2)**	0 (0)
Sediment (I)	South	April	3	6.6 (0.8)	0.6 (0.5)	52.7 (45.7)	**15.6 (21.9)**	4.6 (4.0)	6.0 (3.7)	13.4 (16.5)	0 (0)
		July	3	N/A	N/A	**46.0 (40.5)**	12.0 (5.1)	10.4 (18.1)	6.5 (11.3)	14.2 (4.5)	0.4 (0.8)
		December	2	9.7 (1.6)	0.5 (0.2)	70.2 (5.1)	**7.6 (3.6)**	7.5 (4.8)	**0.9 (1.3)**	9.9 (3.0)	2.2 (0.4)
	North	April	1	5.1	0.4	81.5	3.4	1.6	0.5	11.8	1.3
		July	3	N/A	N/A	68.0 (8.4)	9.6 (2.9)	**1.4 (1.6)**	0 (0)	**18.4 (4.4)**	0.1 (0.1)
		December	3	14.5 (1.8)	**0.2 (0)**	65.5 (14.3)	8.9 (7.5)	3.4 (4.1)	3.0 (2.7)	12.7 (5.4)	3.5 (2.6)
Mean			15	9.3 (3.7)	0.4 (0.3)	60.5 (26.3)	9.5 (9.7)	4.8 (8.0)	2.8 (5.3)	13.4 (7.5)	1.2 (1.8)

N/A Data not available

samples (Table 3.2). PL was present and the dominant lipid class in every component, except for *O. aculeata* (North site, 35.9±3.4%) and *Tonicella* spp. (South, 36.8±4.5%; North, 33.4±2.4%) in July, with an average proportional contribution to total lipid concentration of 44% in *O. aculeata* to 70% in seawater (Table 3.2). Proportions of PL of all combined components did not vary by site nor month; however, *Tonicella* spp. (ANOVA, $F_{2.14}$=10.84, p<0.01), *L. digitata* (ANOVA, $F_{2.7}$=35.98, p<0.01), and seawater (ANOVA, $F_{2.16}$=22.80, p<0.01) each significantly varied monthly individually. High average proportions of TAG were most common in animal species, with 30% in *O. aculeata*, 29% in *H. arctica*, and 28.2% in *Tonicella* spp. (Table 3.2). TAG proportions varied significantly among some individual components; *Tonicella* spp. (ANOVA, $F_{2,14}$=57.47, p<0.01), Neretidae (ANOVA, $F_{2,16}$=4.25, p=0.038), and *S. droebachiensis* (ANOVA, $F_{2,15}$=4.61, p=0.033). ST was most prevalent in animal species, with average high proportions of 20% in *S. droebachiensis* and 18% in *Nereis* spp. (Table 3.2). ST proportions varied significantly among some individual components; *Tonicella* spp. (ANOVA, $F_{2.14}$=8.26, p=0.006) and seawater (ANOVA, $F_{2,16}$=5.48, p=0.019). PL to ST ratios in animal species significantly varied from April to December (pairwise PERMANOVA, t=2.6363, P (perm)=0.005) and nearly significantly from April to July (pairwise PERMANOVA, t=1.8437, P (perm)=0.055), but not between July and December (pairwise PERMANOVA, t=0.9321, P (perm)=0.373). AMPL peaked in macroalgal components, with ~9% in *L. digitata* and 17% in *L. glaciale* (Table 3.2). FFA was highest (22%) in seston and lowest (~2%) in *L. digitata* (Table 3.2). Seston lipids contained no TAG, and were dominated by PL (70%), FFA (22%), and ST (7%) (Table 3.2). Sediment lipids were largely comprised of PL (60%), AMPL (13%), TAG (10%), and FFA (5%) (Table 3.2).

Overall lipid class composition varied significantly among components (PERMANOVA; Pseudo-$F_{9,137}$=40.385, P (perm)<0.01) and five functional groups (suspension/filter feeder, grazer, predator, macroalgal, and environmental components) studied (PERMANOVA; Pseudo-$F_{4,142}$=19.363, P (perm)<0.01), but did not vary monthly (PERMANOVA; Pseudo-$F_{2,146}$=0.568, P

(perm)=0.68) nor between sites (PERMANOVA; Pseudo-$F_{1,146}$=0.121, P (perm)=0.94). The interaction was also not significant. Total lipid concentration significantly correlated with PL (r=0.094, p=0.036, N=138), TAG (r=0.409, p<0.01, N=138), FFA (r=-0.115, p<0.01, N=138), and ST (r=-0.095, p=0.02, N=138).

3.4.3. Fatty acid profiles

The ten food web components included in the fatty acid (FA) analysis contained 63 FA, with 50 present in >50% of all samples. Each component exhibited a distinct set of dominant fatty acids and biomarkers (Table 3.3, Figure 3.3). With a proportional contribution to FA profiles ranging from 14% in *H. arctica* in December to 32% in *A. rubens* in April, EPA (eicosapentaenoic acid, 20:5ω3; a typical diatom biomarker) was typically the dominant FA within each of the six animal species sampled (Table 3.3). In December, ARA (arachidonic acid, 20:4ω6; a kelp and amphipod biomarker) and DHA (docosahexaenoic acid, 22:6ω3; a dinoflagellate biomarker) were respectively the most abundant FA in *S. droebachiensis* (~25%) and *H. arctica* (~20 to 24%). Across all months, ARA, vaccenic acid (18:1ω7; an aerobe, bacteria, and marine vegetation biomarker), palmitoleic acid (16:1ω7; a diatom biomarker), and palmitic acid (16:0; a flagellate and marine vegetation biomarker) were the next most prominent FA among the animals, with peaking contributions between 8 and 25% (Table 3.3). Macroalgal components were rich in palmitic acid (18 to 31%) and EPA (9 to 23%) (Table 3.3). Additionally, large proportions of oleic acid (18:1ω9, 8 to 18%; a crustacean, detritus, dinoflagellate, and brown seaweed biomarker) and linoleic acid (18:2ω6, 4 to 14%; a marine vegetation biomarker) were present in kelp, while palmitoleic acid (5 to 8%) was abundant in rhodoliths (Table 3.3). Seston FA were dominated by stearic acid (18:0, 18 to 33%; a detritus biomarker), palmitic acid (15 to 34%), and oleic acid (8 to 33%) (Table 3.3). Overall, FA composition differed significantly among the ten food web

Table 3.3. Mean proportion (%) of each of the 50 dominant fatty acids found in the six animal species, two macroalgal species, and two environmental components (see Table 2.2 for species list) sampled in April, July, and December 2017 inside (I) or outside (O) of the South and North sites (see Figure 1.1). Each component's highest FA proportion is bolded. FA are listed in ascending order of retention time from the 30-m long ZB wax+ (Phenomenex) GC column in the Varian Galaxie Chromatography Data System (see section 2.3.6 for details).

	A. rubens (I)						*H. arctica* (I)					
Site	**South**			**North**			**South**			**North**		
Collection Month	**Apr**	**Jul**	**Dec**	**Apr**	**Jul**	**Dec**	**Apr**	**Jul**	**Dec**	**Apr**	**Jul**	**Dec**
N	**3**	**3**	**2**	**3**	**3**	**3**	**3**	**3**	**3**	**3**	**3**	**3**
FA	**% (±SD)**						**% (±SD)**					
14:0	0.6 (0.3)	2.4 (1.2)	0.3 (0)	0.5 (0.3)	1.1 (0.6)	0.4 (0.1)	4.3 (1.1)	3.0 (0.6)	3.9 (0.2)	3.8 (1.2)	2.9 (0.2)	3.7 (0.2)
TMTD†	0.1 (0.1)	0.1 (0.1)	0 (0)	0.0 (0.1)	0 (0)	0.1 (0.2)	0.4 (0.3)	0.5 (0.4)	0.3 (0.1)	0.3 (0.2)	0.6 (0.1)	0.3 (0.1)
14:1	0 (0)	0 (0)	0 (0)	0.1 (0.1)	0 (0)	0.1 (0.1)	0.2 (0)	0 (0)	0 (0)	0.1 (0.1)	0 (0)	0 (0)
*i*15:0	0.1 (0.1)	0.2 (0.2)	0.2 (0.1)	0.1 (0.1)	0.2 (0.1)	0.4 (0.1)	0.4 (0.1)	0.4 (0.1)	0.9 (0.1)	0.3 (0)	0.3 (0.1)	0.7 (0.1)
*ai*15:0	0.1 (0.1)	0 (0)	0.1 (0)	0.1 (0.2)	0.1 (0)	0.1 (0)	0.2 (0.2)	0.2 (0.1)	0.2 (0)	0 (0)	0.1 (0)	0.1 (0.1)
15:0	0.3 (0.1)	0.3 (0)	0.3 (0)	0.2 (0.2)	0.3 (0)	0.3 (0.1)	0.4 (0.1)	0.4 (0)	0.6 (0)	0.3 (0)	0.3 (0)	0.6 (0)
*i*16:0	0.3 (0.1)	0.3 (0.3)	0.2 (0)	0.2 (0.1)	0.2 (0.1)	0.4 (0.2)	0.2 (0.2)	0.3 (0.1)	0.4 (0)	0.2 (0.1)	0.2 (0)	0.2 (0.2)
*ai*16:0	0.2 (0.2)	0.2 (0.3)	0.8 (0.1)	0.1 (0.1)	0.1 (0.2)	0.9 (0.2)	0.1 (0.1)	0.1 (0.2)	0 (0)	0.2 (0.1)	0.3 (0.3)	0 (0)
16:0	4.2 (2.7)	4.2 (1.5)	1.6 (0.2)	3.4 (0.4)	3.5 (1.9)	2.0 (0.4)	16.5 (1.1)	12.6 (1.2)	10.8 (0.3)	14.0 (1.4)	11.5 (0.3)	11.3 (1.3)
16:1ω11	0 (0.1)	0.3 (0.3)	0.6 (0.1)	0 (0)	0.1 (0.1)	0.7 (0.1)	0.2 (0.1)	0.3 (0)	0.5 (0.1)	0.1 (0.1)	0.1 (0.1)	0.4 (0.1)
16:1ω9	0.1 (0.2)	0 (0.1)	0.1 (0.1)	0.3 (0.5)	0.1 (0.3)	0.1 (0)	0.3 (0.1)	0.1 (0.2)	0.4 (0)	0 (0)	0.1 (0.1)	0.4 (0)
16:1ω7	1.8 (0.9)	2.4 (1.1)	0.4 (0.1)	1.5 (0.3)	1.6 (1.1)	0.3 (0)	12.7 (0.9)	9.7 (1.8)	3.9 (0.5)	11.9 (2.1)	8.1 (0.7)	4.7 (1.5)
16:1ω5	0.1 (0.2)	0.2 (0.2)	0.1 (0)	0 (0)	0.2 (0.1)	0.2 (0.1)	0.6 (0)	0.6 (0.1)	0.5 (0.1)	0.6 (0.1)	0.5 (0)	0.5 (0)
*i*17:0	0.3 (0.1)	0.1 (0.1)	0.2 (0)	0.2 (0.1)	0.1 (0)	0.2 (0.1)	0.8 (0.4)	0.5 (0.2)	0.6 (0)	0.3 (0)	0.4 (0.1)	0.6 (0)
*ai*17:0	0.3 (0.4)	0.6 (0.6)	1.7 (0.2)	0.3 (0.3)	0.7 (0.2)	1.5 (0.2)	0.5 (0.3)	0.8 (0.2)	1.1 (0)	0.3 (0.1)	0.5 (0.1)	1.0 (0.1)
16:2ω4	0.1 (0.1)	0.3 (0.1)	0.1 (0)	0.1 (0.1)	0.2 (0.1)	0.3 (0.3)	0.8 (0.1)	0.7 (0.1)	0.5 (0.1)	0.7 (0.1)	0.4 (0.2)	0.5 (0.1)
17:0	0.5 (0.1)	0.4 (0.1)	0.3 (0.1)	0.4 (0)	0.4 (0.1)	0.3 (0)	0.4 (0.1)	0.4 (0.1)	0.7 (0)	0.3 (0)	0.4 (0)	0.7 (0)
16:3ω4	0 (0)	0 (0)	0.5 (0.1)	0 (0)	0.7 (1.2)	0 (0)	0.2 (0.1)	0.3 (0.2)	0.1 (0)	0 (0)	0.3 (0.4)	0.1 (0.1)
17:1	9.2 (6.3)	2.8 (2.5)	0.2 (0.1)	8.9 (0.8)	1.6 (2.6)	0.2 (0.1)	1.2 (0.2)	0.1 (0.1)	0.1 (0)	0.9 (0.4)	0.8 (1.4)	0.1 (0.1)
16:3ω3	0.1 (0.1)	0 (0)	0 (0.1)	0 (0)	0 (0)	0.1 (0)	0.1 (0)	0.1 (0)	0.3 (0)	0 (0)	0.1 (0.2)	0.2 (0)
16:4ω3	1.4 (2.3)	5.6 (2.4)	12.9 (0.1)	0 (0)	7.7 (2.9)	12.4 (1.4)	0.1 (0.1)	1.9 (0.8)	2.5 (0.2)	0.5 (0.4)	1.1 (0.4)	2.3 (0.7)
16:4ω1	0 (0.1)	0.5 (0.4)	0 (0)	0.1 (0.1)	0.1 (0.2)	0 (0)	0.4 (0.3)	0.4 (0)	0 (0)	0.9 (0.5)	0.3 (0)	0.1 (0.1)
18:0	5.9 (0.8)	7.1 (0.4)	4.8 (0)	5.1 (0.9)	6.4 (0.8)	4.8 (0.3)	2.7 (0)	4.3 (0.4)	5.1 (0.2)	2.9 (0.5)	4.8 (0.4)	4.8 (0.6)
18:1ω11	0.1 (0.1)	0.9 (0.3)	0.2 (0.1)	0.2 (0.1)	0.9 (0.2)	0.2 (0.1)	0.6 (0.4)	0.6 (0.3)	0 (0)	0.3 (0.2)	0.4 (0)	0.6 (1.1)
18:1ω9	0.5 (0.5)	0.7 (0.3)	0.7 (0.1)	1.2 (0.6)	0.6 (0.3)	0.6 (0.1)	1.7 (1.0)	1.6 (0.5)	1.9 (0)	0.8 (0.3)	1.2 (0)	2.4 (1.7)
18:1ω7	2.6 (1.5)	5.3 (1.5)	1.6 (0.2)	2.0 (0.9)	3.5 (0.3)	1.9 (0.8)	7.0 (1.4)	6.7 (1.4)	3.0 (0.2)	5.8 (1.4)	5.5 (0.2)	2.2 (1.6)

Table 3.3. (continued):

	A. rubens (I)						*H. arctica* (I)					
Site	**South**			**North**			**South**			**North**		
Collection Month	**Apr**	**Jul**	**Dec**	**Apr**	**Jul**	**Dec**	**Apr**	**Jul**	**Dec**	**Apr**	**Jul**	**Dec**
N	**3**	**3**	**2**	**3**	**3**	**3**	**3**	**3**	**3**	**3**	**3**	**3**
FA	**% (±SD)**						**% (±SD)**					
18:1ω5	0.2 (0.2)	0.3 (0.3)	0.3 (0)	0.1 (0.2)	0.2 (0.2)	0.4 (0.1)	0.2 (0.2)	0.3 (0)	0 (0)	0 (0)	0.3 (0)	0 (0)
18:2ω6	0.1 (0.1)	0.1 (0.1)	0.6 (0)	1.0 (1.5)	0.3 (0.3)	0.9 (0.4)	1.9 (0.3)	1.2 (0.3)	0.7 (0)	1.6 (0.2)	1.0 (0.3)	0.7 (0.1)
18:2ω4	0 (0)	0.2 (0.2)	0.1 (0)	0 (0)	0.2 (0.2)	0.1 (0.1)	0.7 (0.1)	0.3 (0.3)	0.3 (0)	0.7 (0)	0.5 (0)	0.3 (0.1)
18:3ω6	0.6 (0.6)	0.4 (0.4)	0.8 (0)	0.8 (0.1)	0.8 (0.2)	0.9 (0)	0.2 (0.1)	0.1 (0.1)	0.2 (0.1)	0.2 (0)	0.2 (0)	0.2 (0)
18:3ω3	0 (0)	0 (0)	0 (0)	0 (0)	0 (0)	0.1 (0.1)	0.8 (0)	0.6 (0.1)	1.4 (0)	0.7 (0.1)	0.5 (0.0)	1.3 (0.1)
18:4ω3	0.3 (0.6)	0.7 (0.2)	0.4 (0)	0.2 (0.3)	0.6 (0.5)	0.7 (0.4)	4.5 (1.8)	2.4 (0.3)	4.3 (0.3)	5.3 (0.5)	2.6 (0.4)	4.4 (0.5)
18:4ω1	0 (0)	0 (0)	0.4 (0.2)	0 (0)	0 (0)	0.3 (0.1)	0.4 (0.1)	0.1 (0.1)	0 (0.1)	0.5 (0.2)	0.1 (0.1)	0.2 (0.2)
20:0	0 (0)	0 (0)	0.3 (0)	0 (0)	0 (0)	0.4 (0.1)	0 (0.1)	0 (0)	0.2 (0)	0 (0)	0 (0)	0.1 (0.1)
20:1ω11	3.3 (5.7)	10.6 (1.0)	11.8 (0.2)	12.3 (0.8)	10.6 (1.6)	10.8 (2.1)	0.6 (0.1)	1.1 (0.3)	0.8 (0)	0.5 (0.1)	1.1 (0.3)	0.8 (0)
20:1ω9	4.8 (0.4)	3.1 (0.7)	2.9 (0.1)	4.1 (0.3)	2.5 (0.3)	2.4 (0.2)	0.8 (0.1)	0.8 (0.1)	2.4 (0.1)	0.8 (0.2)	1.1 (0.1)	2.2 (0.1)
20:1ω7	0.7 (1.2)	2.4 (0.7)	1.7 (0.2)	1.9 (0.2)	2.3 (0.5)	1.5 (0.4)	1.6 (1.4)	3.4 (0.7)	3.3 (0.3)	3.2 (0.6)	4.6 (0.3)	3.7 (0.1)
20:2*a*	1.1 (1.8)	1.6 (1.4)	3.4 (0.4)	1.9 (1.6)	2.7 (0.6)	3.6 (0.6)	0 (0)	1.2 (0.6)	0 (0)	1.0 (0.2)	1.5 (0.4)	0.4 (0.1)
20:2*b*	0 (0)	0.2 (0.3)	0.3 (0.1)	0.2 (0.3)	0.5 (0.4)	0.2 (0)	0 (0)	0.9 (0.3)	0 (0)	0.9 (0.3)	0.9 (0.2)	0 (0)
20:2ω6	1.8 (0.3)	1.6 (0.3)	1.3 (0)	1.8 (0.2)	1.4 (0)	1.0 (0.3)	1.5 (0.4)	1.1 (0.2)	1.4 (0.1)	1.2 (0.1)	1.2 (0)	1.3 (0.1)
20:3ω6	0.1 (0.1)	0 (0)	0.1 (0.1)	0 (0)	0 (0)	0 (0)	0.2 (0.1)	0 (0)	0.1 (0.1)	0 (0)	0.7 (1.1)	0 (0.1)
20:4ω6	19.8 (6.3)	12.6 (2.0)	17.2 (2.5)	18.5 (1.5)	14.2 (4.9)	15.4 (2.6)	0.6 (0.6)	1.6 (0.2)	1.9 (0.2)	1.2 (0.3)	1.7 (0.3)	1.8 (0.5)
20:3ω3	0.3 (0.3)	0 (0)	0.3 (0.2)	0.1 (0.1)	0 (0)	0.2 (0.2)	0.1 (0)	0 (0)	0.2 (0)	0 (0)	0 (0)	0.2 (0)
20:4ω3	0.1 (0.2)	0 (0)	0 (0)	0.1 (0.1)	0 (0)	0 (0)	0.7 (0.1)	0.4 (0.1)	0.9 (0)	0.7 (0)	0.4 (0.3)	1.0 (0.2)
20:5ω3	**31.6 (1.6)**	**26.0 (3.2)**	**20.6 (0.9)**	**27.8 (1.7)**	**26.3 (2.2)**	**22.4 (2.3)**	**19.3 (3.5)**	**21.3 (2.8)**	14.1 (0.7)	**21.1 (1.5)**	**23.6 (1.7)**	16.4 (2.0)
22:2NIMD*a*	0 (0)	0 (0)	0.6 (0.1)	0 (0)	0 (0)	0.5 (0.1)	0 (0)	0.8 (0.3)	0.7 (0.1)	0 (0)	0.9 (0.3)	0.9 (0.4)
21:5ω3	0.1 (0.1)	0 (0)	0 (0)	0 (0)	0 (0)	0 (0)	1.5 (0.3)	1.2 (0.4)	1.6 (0)	1.5 (0)	1.6 (0.1)	1.4 (0.1)
22:4ω6	0.1 (0.1)	0 (0)	0.5 (0)	0 (0)	0 (0)	0.3 (0)	1.0 (0.7)	0.9 (0.8)	0.5 (0.1)	0.5 (0.2)	0.5 (0.2)	0.5 (0.2)
22:5ω3	0.1 (0.2)	0.5 (0.4)	0.5 (0.2)	0.5 (0.2)	0.8 (0.3)	0.4 (0.2)	1.5 (0.6)	1.5 (0.6)	1.3 (0.1)	1.0 (0.1)	1.3 (0.2)	1.3 (0.1)
22:6ω3	5.3 (2.9)	3.2 (0.9)	3.8 (1.3)	3.2 (1.6)	3.7 (0.5)	4.5 (1.2)	8.9 (1.0)	11.2 (2.3)	**23.8 (1.3)**	11.3 (3.1)	12.4 (1.1)	**20.4 (4.4)**

† Trimethyltridecanoic acid

Table 3.3. (continued):

	Nereis spp. (I)						*O. aculeata* (I)					
Site	**South**			**North**			**South**			**North**		
Collection Month	**Apr**	**Jul**	**Dec**	**Apr**	**Jul**	**Dec**	**Apr**	**Jul**	**Dec**	**Apr**	**Jul**	**Dec**
N	**3**	**2**	**2**	**3**	**3**	**3**	**3**	**3**	**3**	**3**	**2**	**2**
FA	**% (±SD)**						**% (±SD)**					
14:0	1.2 (0.4)	1.9 (0.4)	1.2 (0)	2.1 (0.2)	1.8 (0.6)	1.5 (0.1)	6.5 (1.3)	7.8 (0.6)	6.4 (1.6)	6.0 (0.9)	7.2 (1.2)	7.4 (1.2)
TMTD†	0 (0)	0 (0)	0 (0)	0 (0)	0 (0)	0 (0)	0 (0)	0 (0)	0 (0)	0 (0)	0 (0)	0 (0)
14:1	0 (0)	0 (0)	0 (0)	0 (0)	0 (0.1)	0 (0)	0 (0)	0 (0)	0 (0)	0 (0)	0 (0)	0 (0)
*i*15:0	0.1 (0)	0.1 (0)	0.1 (0)	0.2 (0)	0.1 (0)	0.1 (0)	0.1 (0)	0.3 (0)	0.4 (0)	0.1 (0)	0.2 (0)	0.3 (0.1)
*ai*15:0	0.1 (0)	0.1 (0)	0.1 (0)	0 (0)	0 (0)	0.1 (0)	0.1 (0)	0.2 (0)	0.3 (0)	0.1 (0)	0.2 (0)	0.3 (0)
15:0	0.8 (0.1)	0.5 (0.1)	0.7 (0)	0.6 (0)	0.5 (0.1)	0.7 (0)	0.2 (0)	0.2 (0)	0.3 (0)	0.2 (0)	0.2 (0)	0.3 (0)
*i*16:0	0.1 (0)	0.1 (0)	0.1 (0)	0.1 (0.1)	0.1 (0)	0.1 (0.1)	0 (0)	0.1 (0)	0.1 (0)	0 (0)	0.1 (0)	0.1 (0)
*ai*16:0	0.3 (0.1)	0 (0.1)	0.5 (0)	0.2 (0.2)	0.1 (0.1)	0.4 (0.1)	0 (0)	0.2 (0)	0 (0)	0 (0)	0.1 (0)	0.1 (0)
16:0	11.1 (0.6)	14.8 (5.7)	10.3 (0.4)	12.2 (0.6)	12.2 (2.7)	12.6 (1.4)	15.5 (14.2)	7.9 (0.2)	6.3 (1.2)	7.2 (1.0)	3.7 (5.2)	7.2 (1.2)
16:1ω11	0.1 (0.1)	0.4 (0.1)	0.2 (0)	0.2 (0.1)	0.3 (0.1)	0.3 (0)	0.1 (0.1)	0.4 (0)	0.1 (0.1)	0 (0)	0.3 (0)	0.2 (0)
16:1ω9	0.1 (0.1)	0.3 (0)	0.1 (0)	0.1 (0.2)	0.2 (0.1)	0.1 (0.1)	0.1 (0)	0.1 (0.1)	0.2 (0)	0 (0)	0.1 (0.1)	0.1 (0)
16:1ω7	3.4 (1.0)	4.1 (0.5)	2.2 (0.3)	4.8 (1.1)	4.5 (1.8)	3.4 (0.2)	5.9 (0.9)	6.0 (0.4)	4.4 (1.2)	5.9 (0.8)	5.4 (0.6)	4.9 (0.6)
16:1ω5	0.3 (0)	0.3 (0)	0.3 (0)	0.4 (0.2)	0.4 (0.1)	0.3 (0.1)	0.1 (0)	0.2 (0)	0.2 (0)	0.1 (0)	0.2 (0)	0.2 (0)
*i*17:0	0.3 (0)	0.2 (0)	0.3 (0)	0.4 (0)	0.3 (0)	0.4 (0.1)	0.3 (0.1)	0.3 (0)	0.2 (0)	0.3 (0)	0.2 (0)	0.2 (0.1)
*ai*17:0	0.3 (0)	0.3 (0.2)	0.5 (0)	0.2 (0.1)	0.3 (0.1)	0.5 (0.1)	0.3 (0.1)	0.3 (0)	0.3 (0)	0.2 (0)	0.3 (0)	0.2 (0.1)
16:2ω4	0.1 (0)	0.1 (0)	0 (0)	0.2 (0.1)	0.2 (0)	0.1 (0)	0.8 (0.2)	0.7 (0)	0.5 (0.2)	0.7 (0.1)	0.7 (0)	0.6 (0)
17:0	1.4 (0.2)	0.7 (0.3)	1.0 (0)	1.0 (0.1)	0.9 (0.2)	1.0 (0.1)	0.1 (0.1)	0.1 (0)	0.2 (0)	0.1 (0)	0.1 (0)	0.2 (0)
16:3ω4	0 (0)	0.2 (0)	0.1 (0.2)	0 (0)	0.2 (0)	0.3 (0)	1.0 (0.6)	0.9 (0)	0.6 (0.2)	0.7 (0.1)	0.8 (0)	0.7 (0.1)
17:1	1.0 (0.5)	0.6 (0.2)	0.3 (0.1)	2.4 (1.2)	1.0 (0.8)	0.1 (0)	1.1 (1.0)	0.4 (0.2)	0 (0)	1.5 (0.7)	0.4 (0.3)	0 (0)
16:3ω3	0.1 (0.1)	0.1 (0.1)	0.1 (0)	0.1 (0.1)	0.1 (0)	0.1 (0)	0 (0)	0 (0)	0 (0)	0 (0)	0 (0)	0 (0)
16:4ω3	3.1 (0.6)	3.2 (1.9)	6.2 (0.4)	0.8 (1.1)	2.8 (1.0)	4.9 (0.5)	0 (0)	2.2 (0.3)	4.3 (0.8)	1.1 (1.2)	2.2 (0.6)	2.0 (2.9)
16:4ω1	0.1 (0.1)	0 (0)	0 (0)	0 (0.1)	0.1 (0)	0 (0)	4.4 (2.0)	3.9 (0.1)	2.7 (0.8)	2.1 (1.8)	3.6 (0)	3.3 (0.6)
18:0	4.1 (0.4)	1.9 (2.7)	3.9 (0.3)	4.2 (0.1)	3.8 (1.0)	3.6 (0.2)	4.0 (0.6)	4.8 (0.2)	4.8 (0.3)	4.9 (0.3)	5.2 (0.2)	5.1 (0.7)
18:1ω11	5.3 (0.2)	5.3 (1.2)	5.4 (0.3)	5.3 (0.3)	5.7 (0.9)	5.8 (0.8)	1.8 (0.2)	2.4 (0.4)	2.1 (0.5)	2.1 (0.3)	2.3 (0.1)	2.4 (0.1)
18:1ω9	2.2 (0.6)	3.4 (3.0)	2.5 (0)	2.7 (0.5)	2.0 (0.3)	2.2 (0.1)	0.9 (0.1)	0.9 (0.1)	1.7 (0.2)	0.9 (0)	0.8 (0.1)	1.5 (0.2)
18:1ω7	6.3 (0.3)	7.1 (7.4)	5.2 (0.2)	6.8 (1.1)	7.3 (1.5)	6.5 (1.3)	6.6 (0.9)	7.5 (0.2)	6.6 (1.1)	7.3 (0.6)	7.5 (0.7)	7.7 (0.9)
18:1ω5	0.4 (0)	0.4 (0.1)	0.3 (0.1)	0.3 (0.2)	0.4 (0.1)	0.4 (0)	0.1 (0.1)	0.2 (0)	0.1 (0.1)	0.1 (0.1)	0.2 (0.1)	0.2 (0.1)
18:2ω6	1.3 (0.2)	1.0 (0.5)	0.9 (0.1)	2.2 (0.8)	0.9 (0.5)	0.9 (0.1)	2.6 (0.5)	1.7 (0.2)	1.6 (0.4)	2.6 (0.3)	1.8 (0.1)	1.8 (0.2)

Table 3.3. (continued):

	Nereis spp. (I)						*O. aculeata* (I)					
Site	**South**			**North**			**South**			**North**		
Collection Month	**Apr**	**Jul**	**Dec**	**Apr**	**Jul**	**Dec**	**Apr**	**Jul**	**Dec**	**Apr**	**Jul**	**Dec**
N	**3**	**2**	**2**	**3**	**3**	**3**	**3**	**3**	**3**	**3**	**2**	**2**
FA	**% (±SD)**						**% (±SD)**					
18:2ω4	0.2 (0)	0.3 (0.1)	0.2 (0)	0.2 (0)	0.2 (0.0)	0.2 (0)	0.5 (0.1)	0.5 (0)	0.4 (0.1)	0.5 (0)	0.6 (0)	0.5 (0.1)
18:3ω6	0 (0)	0.1 (0.1)	0.1 (0)	0.1 (0.1)	0.1 (0.1)	0.1 (0)	0.4 (0.1)	0.4 (0)	0.3 (0.1)	0.4 (0)	0.4 (0)	0.4 (0)
18:3ω3	0.8 (0.2)	0.8 (0)	0.8 (0.1)	1.3 (0.2)	1.0 (0.1)	1.1 (0.4)	0.5 (0.1)	0.3 (0)	0.3 (0)	0.4 (0.2)	0.3 (0.1)	0.3 (0.1)
18:4ω3	0.5 (0.2)	0.5 (0)	0.4 (0)	1.2 (0.3)	0.6 (0.1)	0.4 (0.1)	5.1 (1.8)	3.9 (0.2)	3.7 (0.7)	4.3 (0.2)	4.0 (0.2)	3.6 (0.2)
18:4ω1	0 (0)	0 (0)	0.1 (0.1)	0 (0)	0 (0)	0.2 (0.2)	0 (0)	0.5 (0.1)	0.9 (0.2)	0.2 (0.4)	0.5 (0.1)	0.7 (0.3)
20:0	0 (0)	0 (0)	0.1 (0)	0 (0)	0 (0)	0.1 (0)	0.4 (0.2)	0.3 (0.3)	0.1 (0.2)	0 (0)	0.4 (0)	0.2 (0)
20:1ω11	1.6 (0.2)	2.7 (0.2)	2.4 (0.2)	2.0 (0.3)	2.2 (0.2)	2.6 (0.3)	5.2 (0.9)	5.2 (2.8)	8.7 (0.8)	4.5 (3.9)	6.6 (0.7)	9.4 (0.2)
20:1ω9	0.8 (0.3)	1.2 (0.6)	0.7 (0.1)	1.0 (0.2)	0.9 (0.1)	0.9 (0.2)	0.1 (0.1)	0 (0)	0 (0)	0.5 (0.9)	0 (0)	0.1 (0.1)
20:1ω7	0.5 (0.1)	0.8 (0.1)	0.6 (0.1)	0.5 (0.1)	0.7 (0.1)	0.8 (0.1)	1.4 (0.3)	1.9 (0.1)	1.5 (0.3)	1.0 (0.9)	2.1 (0.1)	1.7 (0.2)
20:2*a*	0 (0)	0.5 (0.5)	0.1 (0)	0 (0)	0.5 (0.7)	0.2 (0.1)	0.7 (1.0)	0.2 (0)	1.4 (0.5)	0.5 (0.7)	0.2 (0)	1.6 (0.1)
20:2*b*	0 (0)	0.3 (0.2)	0.2 (0)	0 (0)	0.2 (0.1)	0.3 (0.1)	0.9 (0.7)	1.7 (0.2)	0 (0)	1.2 (0.6)	1.5 (0.1)	0.1 (0.1)
20:2ω6	1.8 (0.4)	1.9 (0)	1.9 (0)	2.5 (0.2)	2.0 (0.3)	2.0 (0.4)	0.3 (0.3)	0.4 (0.1)	0.5 (0.1)	0.4 (0.3)	0.5 (0.1)	0.5 (0.1)
20:3ω6	0 (0.1)	0.1 (0)	0.1 (0.1)	0.1 (0.1)	0.1 (0.1)	0.1 (0.1)	0 (0)	0 (0)	0 (0)	0 (0)	0 (0)	0.1 (0.1)
20:4ω6	3.2 (1.6)	2.1 (1.1)	4.5 (1.4)	2.9 (0.5)	2.1 (0.4)	4.6 (0.6)	0.9 (0.1)	1.0 (0.1)	2.3 (0.6)	1.0 (0.9)	1.2 (0)	2.3 (0.6)
20:3ω3	1.0 (0.6)	0.6 (0.1)	0.8 (0.2)	0.8 (0.1)	0.8 (0.2)	1.0 (0.2)	0.1 (0.1)	0.1 (0)	0 (0.1)	0.1 (0.1)	0.1 (0)	0.1 (0.2)
20:4ω3	0.3 (0.1)	0.4 (0.3)	0.2 (0)	0.6 (0.2)	0.4 (0)	0.3 (0.1)	0.4 (0.1)	0.3 (0)	0.2 (0.1)	9.5 (16.0)	0.3 (0)	0.1 (0.2)
20:5ω3	**29.3 (4.4)**	**20.5 (5.2)**	**21.6 (0.4)**	**26.2 (2.1)**	**24.6 (3.4)**	**22.5 (1.9)**	**26.8 (5.5)**	**26.6 (0.5)**	**23.3 (1.3)**	**17.3 (15.0)**	**25.7 (1.5)**	**22.4 (1.4)**
22:2NIMD*a*	3.1 (0.3)	3.4 (0.1)	3.9 (0.3)	2.3 (2.0)	3.1 (0.2)	0.2 (0)	0.5 (0.5)	1.0 (0.1)	1.4 (0.1)	2.7 (2.9)	1.1 (0.2)	1.6 (0.1)
21:5ω3	0 (0)	0.6 (0)	0.5 (0)	0 (0)	0.7 (0.1)	0.5 (0)	0.8 (0.1)	0.7 (0.1)	0.5 (0.2)	0.5 (0.5)	0.7 (0)	0.5 (0.1)
22:4ω6	4.8 (1.9)	4.9 (1.3)	7.4 (0.8)	5.2 (1.2)	5.4 (0.7)	6.9 (0.1)	0 (0)	0 (0)	0 (0)	0 (0)	0 (0)	0.1 (0)
22:5ω3	4.8 (1.3)	4.1 (0.2)	4.2 (0.6)	4.0 (0.3)	4.6 (0.4)	3.7 (1.0)	0.3 (0.2)	0.4 (0)	0.3 (0.1)	0.2 (0.2)	0.5 (0)	0.3 (0.1)
22:6ω3	1.0 (0.3)	1.2 (0.1)	1.0 (0)	1.5 (0.6)	1.2 (0.2)	0.9 (0.3)	0.6 (0.1)	0.7 (0.1)	0.9 (0.2)	0.2 (0.3)	0.8 (0.3)	0.6 (0.1)

† Trimethyltridecanoic acid

Table 3.3. (continued):

	S. droebachiensis (I)						*Tonicella* spp. (I)					
Site	**South**			**North**			**South**			**North**		
Collection Month	**Apr**	**Jul**	**Dec**	**Apr**	**Jul**	**Dec**	**Apr**	**Jul**	**Dec**	**Apr**	**Jul**	**Dec**
N	**2**	**3**	**3**	**3**	**3**	**3**	**3**	**3**	**3**	**N/A**	**3**	**3**
FA	**% (±SD)**						**% (±SD)**					
14:0	3.2 (1.2)	2.5 (0.7)	2.0 (0.2)	2.6 (0.6)	2.7 (1.0)	2.1 (0.3)	3.6 (0.4)	4.4 (0.5)	2.3 (0.5)	N/A	5.1 (0.2)	2.6 (0.1)
TMTD†	0.1 (0)	0 (0)	0 (0)	0 (0)	0 (0)	0 (0)	1.2 (0.1)	0.4 (0)	0.9 (0.2)	N/A	0.4 (0.1)	0.9 (0.2)
14:1	0 (0)	0 (0)	0 (0)	0 (0)	0 (0)	0 (0)	0.1 (0)	0.1 (0)	0 (0)	N/A	0.1 (0)	0.1 (0.1)
*i*15:0	0.2 (0.1)	0.2 (0)	0.4 (0.1)	0.1 (0.1)	0.2 (0)	0.2 (0)	0.3 (0)	0.3 (0)	0.3 (0)	N/A	0.3 (0)	0.3 (0.1)
*ai*15:0	0.2 (0.1)	0.1 (0)	0.2 (0.0)	0.1 (0.1)	0.1 (0)	0.2 (0)	0.2 (0)	0.2 (0)	0.3 (0.1)	N/A	0.2 (0)	0.5 (0.3)
15:0	0.4 (0.1)	0.4 (0.1)	0.6 (0.1)	0.2 (0.2)	0.4 (0.1)	0.7 (0.1)	0.8 (0.1)	0.7 (0)	0.8 (0)	N/A	0.7 (0)	0.6 (0.5)
*i*16:0	0.1 (0)	0 (0)	0 (0)	0 (0)	0.1 (0.1)	0.6 (0.5)	0.2 (0)	0.2 (0)	0.1 (0.1)	N/A	0.2 (0)	0.2 (0.1)
*ai*16:0	0.1 (0.2)	0.4 (0.5)	0.1 (0)	0 (0)	0.3 (0.3)	0 (0)	0.3 (0.4)	0.1 (0.1)	0 (0)	N/A	0.1 (0)	0.7 (1.1)
16:0	8.8 (0.5)	9.1 (0.1)	8.6 (0.4)	8.0 (0.5)	8.5 (0.3)	9.2 (0.5)	10.9 (0.8)	11.4 (0.6)	10.1 (0.4)	N/A	12.3 (0.2)	11.4 (1.6)
16:1ω11	0.3 (0.2)	0.2 (0.1)	0.9 (0.1)	0 (0)	0.1 (0.1)	0.9 (1.3)	0.1 (0)	0.1 (0)	0.1 (0.1)	N/A	0.1 (0)	0.1 (0)
16:1ω9	0.3 (0.1)	0.1 (0.2)	0.4 (0.1)	0 (0)	0 (0)	0 (0)	0.3 (0)	0.3 (0)	0 (0)	N/A	0.2 (0)	0.1 (0.2)
16:1ω7	4.1 (1.6)	3.0 (0.8)	1.5 (0)	3.2 (1.1)	3.8 (0.5)	1.4 (0.1)	8.1 (0.4)	8.2 (0.4)	4.4 (1.0)	N/A	10.6 (0.9)	4.4 (0.3)
16:1ω5	0.4 (0.1)	0.2 (0.1)	0.3 (0)	0.4 (0.2)	0.2 (0.1)	0.3 (0.1)	0.2 (0)	0.2 (0)	0.1 (0.1)	N/A	0.2 (0)	0.1 (0.1)
*i*17:0	0.4 (0)	0.1 (0.1)	0.2 (0)	0.2 (0)	0.1 (0.1)	0.1 (0.1)	0.2 (0)	0.2 (0)	0.2 (0)	N/A	0.2 (0)	0.2 (0.1)
*ai*17:0	0.4 (0.1)	0.4 (0.4)	2.1 (0.3)	0.1 (0.1)	0.5 (0.2)	0.8 (0.6)	0.6 (0.1)	0.8 (0.2)	1.0 (0)	N/A	0.6 (0)	0.8 (0.1)
16:2ω4	0.9 (0.5)	0.6 (0.1)	0.4 (0.2)	0.5 (0.4)	0.6 (0.1)	0.7 (0.2)	0.8 (0.1)	0.7 (0)	0.3 (0.1)	N/A	0.6 (0.1)	0.3 (0)
17:0	0.1 (0)	0.2 (0.1)	0.2 (0)	0.1 (0)	0.2 (0)	0.1 (0.1)	0.4 (0.1)	0.4 (0)	0.7 (0.1)	N/A	0.3 (0)	0.7 (0)
16:3ω4	0.7 (0.5)	0.2 (0.2)	0 (0)	0 (0)	0.1 (0.2)	0 (0)	0.8 (0.3)	0.6 (0)	0.5 (0.2)	N/A	0.6 (0.1)	0.4 (0.2)
17:1	1.1 (0.5)	1.3 (1.3)	0 (0)	2.5 (0.6)	1.2 (1.0)	0 (0)	0.6 (0.6)	0.2 (0.2)	0 (0)	N/A	0.2 (0.2)	0.1 (0.2)
16:3ω3	0 (0)	0.3 (0.5)	0 (0)	0 (0)	0.1 (0.3)	0 (0)	0 (0)	0 (0)	0 (0)	N/A	0 (0)	0 (0)
16:4ω3	0.8 (1.2)	2.4 (2.4)	5.0 (0.1)	0.4 (0.6)	2.8 (1.1)	5.6 (0.5)	1.4 (0.5)	1.3 (0.1)	4.1 (0.6)	N/A	1.2 (0.1)	2.7 (2.3)
16:4ω1	1.0 (0.4)	0.3 (0.3)	0 (0)	0.4 (0.3)	0.5 (0.1)	0 (0)	0.7 (0.1)	0.6 (0.1)	0.1 (0.1)	N/A	0.6 (0.1)	1.0 (1.7)
18:0	2.7 (0.2)	4.0 (0.8)	3.2 (0)	2.6 (0.4)	3.4 (0.4)	2.6 (2.3)	3.0 (0.8)	2.0 (1.6)	4.9 (0.4)	N/A	2.9 (0.1)	4.2 (0.7)
18:1ω11	0.5 (0)	0.8 (0.2)	0.3 (0)	0.7 (0)	0.7 (0.1)	1.4 (1.7)	0.2 (0.1)	1.1 (1.7)	0 (0)	N/A	0.4 (0)	0.1 (0.1)
18:1ω9	1.3 (0.4)	1.0 (0.3)	0.9 (0.3)	1.4 (0.4)	0.8 (0.1)	0.4 (0.4)	9.0 (1.2)	7.4 (6.1)	6.8 (1.1)	N/A	10.9 (0.9)	7.0 (0.6)
18:1ω7	3.5 (0.2)	3.2 (0.1)	2.4 (0.4)	2.8 (0.4)	3.4 (0.7)	3.0 (2.3)	6.8 (0.4)	7.9 (2.7)	7.7 (0.2)	N/A	7.3 (0.1)	8.2 (0.3)
18:1ω5	0 (0)	0 (0)	0 (0)	0 (0)	0 (0)	0 (0)	0.2 (0.2)	0.2 (0.1)	0.2 (0.1)	N/A	0.2 (0.1)	0.2 (0.2)
18:2ω6	2.2 (1.6)	1.3 (1.0)	2.5 (0.8)	1.5 (1.1)	0.9 (0.4)	0.3 (0.3)	0.3 (0)	0.4 (0.1)	0.4 (0.1)	N/A	0.3 (0)	0.3 (0)

Table 3.3. (continued):

	***S. droebachiensis* (I)**						***Tonicella* spp. (I)**					
Site	**South**			**North**			**South**			**North**		
Collection Month	**Apr**	**Jul**	**Dec**	**Apr**	**Jul**	**Dec**	**Apr**	**Jul**	**Dec**	**Apr**	**Jul**	**Dec**
N	**2**	**3**	**3**	**3**	**3**	**3**	**3**	**3**	**3**	**N/A**	**3**	**3**
FA	**% (±SD)**						**% (±SD)**					
18:2ω4	0.3 (0.1)	0.1 (0.1)	0 (0)	0.1 (0.1)	0.1 (0.1)	0 (0)	0.5 (0.4)	0.6 (0.1)	0.4 (0.1)	N/A	0.5 (0)	0.4 (0)
18:3ω6	0.4 (0.0)	0.4 (0.1)	0.6 (0.1)	0.4 (0)	0.5 (0)	0.6 (0.2)	0.4 (0.2)	0.3 (0)	0.1 (0.1)	N/A	0.3 (0)	0.2 (0)
18:3ω3	1.2 (0.2)	0.4 (0.3)	0.6 (0.8)	1.1 (0.3)	0.8 (0.5)	0.1 (0.2)	0.5 (0.1)	0.6 (0.1)	0.5 (0.1)	N/A	0.6 (0)	0.4 (0.1)
18:4ω3	3.8 (1.1)	1.0 (0.8)	0.8 (0.4)	3.0 (1.1)	1.5 (0.7)	0.4 (0.5)	1.3 (0.2)	1.5 (0.2)	0.6 (0.1)	N/A	1.4 (0.2)	0.5 (0.1)
18:4ω1	0.1 (0)	0 (0)	0.4 (0.6)	0 (0)	0 (0)	0 (0)	0.5 (0.1)	0.4 (0.1)	0.2 (0)	N/A	0.4 (0.1)	0.2 (0.1)
20:0	1.1 (0.4)	0.6 (0.2)	0.7 (0.1)	1.0 (0.1)	0.7 (0.1)	0.5 (0.4)	0 (0)	0 (0)	0 (0)	N/A	0 (0)	0.2 (0.3)
20:1ω11	0 (0)	10.6 (1.8)	9.0 (1.0)	8.2 (1.5)	9.1 (0.8)	9.7 (0.6)	1.0 (0.6)	0.7 (0.1)	1.4 (0.1)	N/A	0.7 (0.1)	1.4 (0.1)
20:1ω9	1.9 (0.2)	1.9 (0.3)	1.9 (0.1)	2.3 (0.7)	1.5 (0.5)	0.8 (1.1)	1.2 (1.1)	1.3 (0.1)	1.6 (0)	N/A	1.3 (0.1)	1.8 (0.2)
20:1ω7	1.5 (0)	1.3 (0.2)	1.6 (0.3)	1.0 (0.1)	1.3 (0.2)	0.8 (0.7)	0.1 (0.1)	0.1 (0)	0 (0)	N/A	0.1 (0)	1.0 (1.6)
20:2*a*	2.8 (0.2)	2.9 (0.5)	0 (0)	3.4 (0.9)	2.9 (0.6)	0 (0)	1.9 (0.2)	1.7 (0.1)	0.1 (0.1)	N/A	1.5 (0.2)	0.1 (0.2)
20:2*b*	1.4 (0.1)	1.2 (0.2)	0 (0)	1.1 (0.2)	1.1 (0.3)	0 (0)	0 (0)	0.1 (0.1)	0.2 (0.2)	N/A	0.2 (0)	0.1 (0.2)
20:2ω6	3.1 (0.3)	1.9 (0.3)	3.7 (0.4)	2.4 (0.6)	1.7 (0.2)	2.0 (0.1)	1.5 (0)	1.3 (0.1)	1.8 (0.1)	N/A	1.2 (0.1)	1.6 (0.1)
20:3ω6	0.4 (0)	0 (0)	0.2 (0.3)	0 (0)	0 (0)	0.1 (0.1)	0.7 (0)	0.6 (0)	0.7 (0.2)	N/A	0.6 (0.1)	0.8 (0.1)
20:4ω6	14.5 (2.5)	16.6 (2.8)	**24.7 (0.9)**	14.6 (3.6)	15.8 (0.8)	**24.9 (0.7)**	4.9 (4.2)	6.7 (0.3)	12.1 (1.0)	N/A	5.8 (0.3)	10.8 (2.4)
20:3ω3	2.1 (1.3)	0.8 (0.8)	1.0 (0.2)	1.9 (0.7)	1.4 (0.1)	1.0 (0.3)	0.2 (0.2)	0.2 (0)	0.3 (0.1)	N/A	0.2 (0)	0.3 (0)
20:4ω3	1.8 (1.5)	0.3 (0.5)	0 (0)	1.0 (0.4)	0.2 (0.3)	0.1 (0.2)	0.8 (0.1)	0.7 (0.1)	0.7 (0.1)	N/A	0.7 (0)	0.6 (0)
20:5ω3	**24.8 (2.3)**	**21.3 (0.6)**	15.8 (1.2)	**21.4 (1.7)**	**22.9 (2.2)**	20.6 (1.2)	**21.8 (0.5)**	**20.8 (1.4)**	**17.5 (0.3)**	N/A	**19.2 (0.5)**	**16.2 (2.7)**
22:2NIMD*a*	0.2 (0.1)	3.5 (0.8)	2.8 (0.6)	2.3 (0.2)	3.5 (0.5)	3.4 (0.2)	1.6 (1.4)	1.6 (0.1)	4.4 (0.7)	N/A	1.5 (0.1)	4.5 (0.3)
21:5ω3	0.3 (0.2)	0 (0)	0 (0)	0 (0)	0 (0)	0 (0)	0.5 (0)	0.4 (0.0)	0 (0)	N/A	0.3 (0)	0.2 (0.3)
22:4ω6	0.2 (0)	0 (0)	0 (0)	0 (0)	0 (0)	0 (0)	2.8 (0.3)	2.3 (0.1)	4.5 (0.5)	N/A	2.0 (0.2)	4.2 (0.7)
22:5ω3	0.3 (0.1)	0 (0)	0.1 (0.1)	0 (0)	0 (0)	0 (0)	4.7 (0.3)	4.1 (0.3)	5.9 (0.3)	N/A	3.8 (0.2)	5.5 (0.8)
22:6ω3	1.5 (0.6)	1.4 (0.2)	1.2 (0.9)	5.2 (7.3)	1.4 (0.4)	0.8 (0.7)	0.6 (0)	0.7 (0.1)	0.5 (0.1)	N/A	0.5 (0)	0.4 (0.1)

† Trimethyltridecanoic acid

Table 3.3. (continued):

	L. digitata (O)						*L. glaciale* (I)					
Site	**South**			**North**			**South**			**North**		
Collection Month	**Apr**	**Jul**	**Dec**	**Apr**	**Jul**	**Dec**	**Apr**	**Jul**	**Dec**	**Apr**	**Jul**	**Dec**
N	**2**	**3**	**2**	**N/A**	**N/A**	**N/A**	**N/A**	**3**	**N/A**	**N/A**	**3**	**N/A**
FA	**% (±SD)**						**% (±SD)**					
14:0	5.2 (0.5)	1.7 (0.4)	4.7 (0)	N/A	N/A	N/A	N/A	3.0 (0.3)	N/A	N/A	2.7 (0.2)	N/A
TMTD†	0 (0)	0.3 (0.4)	0 (0)	N/A	N/A	N/A	N/A	0.1 (0)	N/A	N/A	0 (0)	N/A
14:1	0 (0)	0.1 (0.1)	0.2 (0)	N/A	N/A	N/A	N/A	0.7 (0.3)	N/A	N/A	0.3 (0.1)	N/A
*i*15:0	0.4 (0.1)	0.8 (0.9)	0.3 (0)	N/A	N/A	N/A	N/A	0.8 (0.2)	N/A	N/A	0.6 (0.1)	N/A
*ai*15:0	0 (0)	0.1 (0.1)	0.3 (0)	N/A	N/A	N/A	N/A	0.8 (0.3)	N/A	N/A	0.5 (0)	N/A
15:0	0.2 (0)	0.2 (0.2)	0.3 (0)	N/A	N/A	N/A	N/A	0.4 (0)	N/A	N/A	0.4 (0)	N/A
*i*16:0	0 (0)	1.8 (1.6)	0.1 (0)	N/A	N/A	N/A	N/A	0.5 (0.2)	N/A	N/A	0.3 (0.1)	N/A
*ai*16:0	0 (0.1)	0.3 (0.2)	0.6 (0)	N/A	N/A	N/A	N/A	0.6 (0.3)	N/A	N/A	0.6 (0.1)	N/A
16:0	**17.5 (1.2)**	**30.5 (12.3)**	**19.0 (0.2)**	N/A	N/A	N/A	N/A	**21.6 (1.9)**	N/A	N/A	20.9 (1.7)	N/A
16:1ω11	0.8 (0.3)	4.2 (5.6)	1.2 (0)	N/A	N/A	N/A	N/A	1.0 (0.5)	N/A	N/A	0.5 (0.1)	N/A
16:1ω9	0 (0)	0.3 (0.5)	0.2 (0.3)	N/A	N/A	N/A	N/A	0.6 (0.1)	N/A	N/A	0.4 (0)	N/A
16:1ω7	2.4 (0)	0.3 (0.1)	0.2 (0.3)	N/A	N/A	N/A	N/A	5.4 (0.3)	N/A	N/A	7.6 (0.0)	N/A
16:1ω5	0.1 (0)	0.2 (0.1)	0.4 (0.1)	N/A	N/A	N/A	N/A	0.1 (0)	N/A	N/A	0.3 (0)	N/A
*i*17:0	1.7 (0.1)	1.7 (0.9)	0.5 (0)	N/A	N/A	N/A	N/A	0.2 (0)	N/A	N/A	0.5 (0.1)	N/A
*ai*17:0	0.3 (0)	0.3 (0.3)	0.1 (0)	N/A	N/A	N/A	N/A	2.8 (0.8)	N/A	N/A	1.2 (0)	N/A
16:2ω4	0.2 (0)	0 (0)	0.3 (0)	N/A	N/A	N/A	N/A	0.6 (0)	N/A	N/A	0.6 (0.3)	N/A
17:0	0.1 (0)	0.1 (0.0)	0.1 (0)	N/A	N/A	N/A	N/A	0.3 (0)	N/A	N/A	0.3 (0)	N/A
16:3ω4	0 (0)	1.2 (1.0)	0 (0)	N/A	N/A	N/A	N/A	0.2 (0)	N/A	N/A	0.4 (0.1)	N/A
17:1	0.7 (0)	0 (0)	0.4 (0.2)	N/A	N/A	N/A	N/A	0.3 (0.1)	N/A	N/A	0.3 (0.1)	N/A
16:3ω3	0 (0)	1.7 (2.8)	0.2 (0.3)	N/A	N/A	N/A	N/A	0.7 (0.1)	N/A	N/A	0.5 (0.1)	N/A
16:4ω3	0 (0)	0.6 (1.1)	0 (0)	N/A	N/A	N/A	N/A	0.4 (0.1)	N/A	N/A	0.8 (0)	N/A
16:4ω1	0.2 (0)	0 (0)	0.3 (0.1)	N/A	N/A	N/A	N/A	0.3 (0)	N/A	N/A	0.1 (0.1)	N/A
18:0	0.7 (0.1)	0.6 (0.4)	1.4 (0)	N/A	N/A	N/A	N/A	3.5 (0.5)	N/A	N/A	2.0 (0.4)	N/A
18:1ω11	0 (0)	1.6 (2.8)	0 (0)	N/A	N/A	N/A	N/A	0.2 (0)	N/A	N/A	0.4 (0.1)	N/A
18:1ω9	13.0 (0.2)	8.1 (1.6)	18.4 (0.1)	N/A	N/A	N/A	N/A	3.8 (0.2)	N/A	N/A	2.3 (0.2)	N/A
18:1ω7	0.1 (0.1)	0 (0)	0.2 (0.1)	N/A	N/A	N/A	N/A	2.7 (0.4)	N/A	N/A	3.7 (0.4)	N/A
18:1ω5	0 (0.1)	0 (0)	0 (0)	N/A	N/A	N/A	N/A	0.2 (0)	N/A	N/A	0.2 (0.2)	N/A
18:2ω6	9.1 (0.2)	3.8 (1.2)	14.0 (0.5)	N/A	N/A	N/A	N/A	3.4 (0.6)	N/A	N/A	2.3 (0)	N/A

Table 3.3. (continued):

	L. digitata (O)						*L. glaciale* (I)					
Site	**South**			**North**			**South**			**North**		
Collection Month	**Apr**	**Jul**	**Dec**	**Apr**	**Jul**	**Dec**	**Apr**	**Jul**	**Dec**	**Apr**	**Jul**	**Dec**
N	**2**	**3**	**2**	**N/A**	**N/A**	**N/A**	**N/A**	**3**	**N/A**	**N/A**	**3**	**N/A**
FA	**% (±SD)**						**% (±SD)**					
18:2ω4	0 (0)	0 (0)	0 (0)	N/A	N/A	N/A	N/A	0.6 (0)	N/A	N/A	0.3 (0.1)	N/A
18:3ω6	0.6 (0)	0.5 (0.2)	0.9 (0)	N/A	N/A	N/A	N/A	1.8 (0.2)	N/A	N/A	1.5 (0.2)	N/A
18:3ω3	7.5 (0)	5.1 (2.6)	5.8 (0)	N/A	N/A	N/A	N/A	0.4 (0.1)	N/A	N/A	0.7 (0.1)	N/A
18:4ω3	8.0 (0.4)	7.5 (5.9)	6.6 (0.1)	N/A	N/A	N/A	N/A	0.5 (0.1)	N/A	N/A	1.1 (0.1)	N/A
18:4ω1	0 (0)	0 (0)	0 (0)	N/A	N/A	N/A	N/A	0.0 (0)	N/A	N/A	0 (0)	N/A
20:0	0 (0)	0.5 (0.6)	1.0 (0)	N/A	N/A	N/A	N/A	0.3 (0)	N/A	N/A	0.3 (0)	N/A
20:1ω11	0 (0)	0 (0)	0 (0)	N/A	N/A	N/A	N/A	0.2 (0.1)	N/A	N/A	0.3 (0)	N/A
20:1ω9	0 (0)	0 (0)	0 (0)	N/A	N/A	N/A	N/A	0.6 (0.1)	N/A	N/A	0.5 (0)	N/A
20:1ω7	0 (0)	0 (0)	0 (0)	N/A	N/A	N/A	N/A	0.1 (0.1)	N/A	N/A	0.3 (0)	N/A
20:2*a*	0 (0)	2.0 (3.4)	0 (0)	N/A	N/A	N/A	N/A	0 (0)	N/A	N/A	0.1 (0)	N/A
20:2*b*	0.3 (0.1)	0 (0)	0 (0)	N/A	N/A	N/A	N/A	0.1 (0)	N/A	N/A	0.1 (0)	N/A
20:2ω6	0.7 (0)	0.6 (0.4)	0.3 (0)	N/A	N/A	N/A	N/A	0.6 (0.1)	N/A	N/A	0.6 (0.1)	N/A
20:3ω6	0 (0)	0.2 (0.2)	0.2 (0)	N/A	N/A	N/A	N/A	2.1 (0.2)	N/A	N/A	2.1 (0)	N/A
20:4ω6	0.1 (0.1)	5.6 (2.7)	10.1 (0.2)	N/A	N/A	N/A	N/A	0.1 (0)	N/A	N/A	0.1 (0)	N/A
20:3ω3	0.6 (0)	0 (0.1)	0.2 (0)	N/A	N/A	N/A	N/A	0.2 (0)	N/A	N/A	0.1 (0)	N/A
20:4ω3	13.5 (0.8)	0.5 (0.1)	0.5 (0.2)	N/A	N/A	N/A	N/A	0.5 (0)	N/A	N/A	0.5 (0)	N/A
20:5ω3	0 (0)	9.0 (6.5)	9.3 (0.2)	N/A	N/A	N/A	N/A	20.6 (1.1)	N/A	N/A	**23.1 (2.9)**	N/A
22:2NIMD*a*	0 (0)	0 (0)	0 (0)	N/A	N/A	N/A	N/A	0.2 (0.1)	N/A	N/A	0.3 (0.1)	N/A
21:5ω3	0 (0)	0 (0)	0.1 (0)	N/A	N/A	N/A	N/A	0.4 (0)	N/A	N/A	0 (0)	N/A
22:4ω6	0 (0)	0.1 (0.2)	0 (0)	N/A	N/A	N/A	N/A	0.4 (0.1)	N/A	N/A	0.8 (0.1)	N/A
22:5ω3	0 (0)	0.4 (0.4)	0 (0)	N/A	N/A	N/A	N/A	1.2 (0.1)	N/A	N/A	1.3 (0.1)	N/A
22:6ω3	0 (0)	3.6 (4.1)	0 (0.1)	N/A	N/A	N/A	N/A	0.7 (0.2)	N/A	N/A	1.6 (0)	N/A

† Trimethyltridecanoic acid

Table 3.3. (continued):

	Seawater (O)						Sediment (I)					
Site	**South**			**North**			**South**			**North**		
Collection Month	**Apr**	**Jul**	**Dec**	**Apr**	**Jul**	**Dec**	**Apr**	**Jul**	**Dec**	**Apr**	**Jul**	**Dec**
N	**3**	**3**	**3**	**3**	**3**	**N/A**	**3**	**3**	**3**	**N/A**	**3**	**3**
FA	**% (±SD)**						**% (±SD)**					
14:0	0.9 (0.4)	0.6 (0.4)	4.6 (2.8)	0.9 (0.8)	1.2 (0.5)	N/A	1.7 (0.8)	3.8 (0.5)	2.6 (0.5)	N/A	2.9 (0.5)	2.4 (0.2)
TMTD†	0.2 (0.1)	0 (0)	0.1 (0)	0.1 (0.2)	0 (0)	N/A	0 (0)	0 (0)	0 (0)	N/A	0.2 (0.3)	0.1 (0.2)
14:1	0 (0)	0.3 (0.1)	0.4 (0.2)	0.1 (0.1)	0.1 (0)	N/A	0.1 (0.1)	0.1 (0.1)	0 (0.1)	N/A	0.1 (0)	0 (0)
*i*15:0	0.1 (0.1)	0 (0)	0.3 (0.1)	0.1 (0.0)	0.1 (0)	N/A	1.4 (0.4)	1.9 (0.2)	2.2 (0.2)	N/A	2.0 (0.2)	2.0 (0.2)
*ai*15:0	0 (0.1)	0 (0)	0.3 (0.2)	0 (0)	0.1 (0)	N/A	2.5 (0.4)	4.5 (0.6)	4.5 (0.4)	N/A	3.0 (0.3)	4.0 (0.2)
15:0	0.1 (0.1)	0.2 (0.1)	1.2 (0.6)	0.2 (0.1)	0.3 (0.1)	N/A	0.8 (0.1)	1.6 (0.4)	1.4 (0.3)	N/A	1.1 (0.2)	1.5 (0.4)
*i*16:0	0 (0)	0.5 (0.5)	0.3 (0.1)	0.1 (0.2)	0 (0)	N/A	0.4 (0.4)	0.7 (0.2)	0.9 (0.1)	N/A	0.7 (0.2)	0.7 (0.2)
*ai*16:0	0 (0)	0.1 (0.1)	0.1 (0.1)	0.1 (0.1)	0 (0)	N/A	1.1 (0.9)	0.3 (0.2)	1.0 (0)	N/A	0.6 (0.4)	1.1 (0.2)
16:0	21.7 (2.8)	17.1 (5.5)	**34.4 (11.1)**	21.0 (3.6)	14.8 (2.4)	N/A	14.6 (0.4)	18.0 (3.8)	15.0 (0.7)	N/A	16.1 (1.6)	16.0 (1.5)
16:1ω11	0.1 (0)	0.1 (0)	0.1 (0.1)	0.1 (0.1)	0 (0)	N/A	3.1 (1.7)	0.5 (0.2)	1.7 (0.2)	N/A	1.0 (0.3)	2.5 (0.5)
16:1ω9	0 (0)	0.3 (0.1)	1.0 (0.3)	0.1 (0.1)	0.3 (0.1)	N/A	0.9 (0.6)	0.5 (0.4)	0.5 (0.4)	N/A	0.4 (0.2)	0.7 (0)
16:1ω7	1.2 (0.2)	0.7 (0.1)	1.1 (0.3)	1.3 (0.7)	0.8 (0.3)	N/A	**20.6 (1.0)**	**18.9 (5.6)**	**23.8 (0.3)**	N/A	**17.5 (0.7)**	**20.1 (1.8)**
16:1ω5	0 (0)	0.1 (0.1)	0.1 (0.1)	0.1 (0.1)	0.1 (0)	N/A	1.4 (0.1)	0.8 (0.6)	1.6 (0.1)	N/A	1.6 (0.1)	2.0 (0.9)
*i*17:0	0.2 (0.1)	0.3 (0.4)	0.2 (0.1)	0.2 (0.1)	0.1 (0)	N/A	0.8 (0.2)	0.7 (0.2)	0.5 (0)	N/A	0.6 (0.1)	0.5 (0.6)
*ai*17:0	0 (0)	0.1 (0.1)	0.3 (0.1)	0.1 (0.1)	0.1 (0)	N/A	1.2 (0.4)	1.1 (0.2)	0.8 (0.3)	N/A	1.0 (0.4)	0.6 (0.7)
16:2ω4	0 (0)	0.4 (0.4)	0.9 (0.6)	0.5 (0.4)	0.4 (0)	N/A	1.0 (0.1)	0.7 (0.6)	1.0 (0)	N/A	0.9 (0)	1.2 (0.4)
17:0	0.1 (0.1)	0.2 (0)	0.6 (0.1)	0.3 (0.1)	0.2 (0)	N/A	0.6 (0.1)	0.7 (0.2)	0.6 (0.1)	N/A	0.8 (0.3)	1.1 (0.3)
16:3ω4	0 (0)	0 (0)	0 (0)	0 (0.1)	0 (0)	N/A	2.5 (0.2)	1.5 (1.3)	2.1 (1.3)	N/A	1.7 (0.7)	1.8 (0.9)
17:1	0 (0)	0 (0)	0.2 (0.1)	0 (0)	0 (0)	N/A	1.0 (0.2)	0.7 (0.1)	1.1 (0.2)	N/A	1.1 (0.4)	0.9 (1.0)
16:3ω3	0 (0)	0.4 (0.7)	0.2 (0)	0 (0.1)	0.1 (0.1)	N/A	0.3 (0.1)	0.3 (0.2)	0.3 (0.1)	N/A	0.1 (0.1)	0 (0)
16:4ω3	0 (0.1)	0.1 (0.1)	0.2 (0)	0.6 (0.6)	0.2 (0.1)	N/A	0.3 (0.4)	0.3 (0.1)	0.1 (0.2)	N/A	0.2 (0.1)	0 (0)
16:4ω1	0.7 (0.2)	1.4 (0.3)	1.0 (1.1)	1.0 (1.1)	1.1 (0.2)	N/A	2.3 (2.7)	0.3 (0.4)	0.9 (0.6)	N/A	0.7 (0.1)	1.0 (0.3)
18:0	18.2 (2.5)	**24.2 (3.6)**	23.1 (2.3)	**33.0 (0.9)**	**21.3 (4.2)**	N/A	3.5 (3.1)	6.2 (1.5)	5.1 (2.1)	N/A	5.7 (0.8)	7.7 (1.4)
18:1ω11	0 (0)	0 (0)	0 (0)	0 (0)	0 (0)	N/A	0 (0.1)	0.3 (0.1)	0.2 (0.2)	N/A	1.6 (2.2)	0 (0)
18:1ω9	**32.9 (12.1)**	18.8 (8.2)	8.4 (1.3)	20.1 (7.0)	19.7 (5.5)	N/A	5.3 (1.6)	1.6 (1.1)	3.7 (0.9)	N/A	3.3 (0.5)	3.1 (2.7)
18:1ω7	2.0 (1.8)	0.6 (0.2)	0.5 (0.1)	0.5 (0.4)	0.4 (0.1)	N/A	9.0 (0.6)	4.7 (1.7)	9.3 (0.2)	N/A	7.3 (0.8)	9.9 (0.7)
18:1ω5	0 (0)	0 (0)	0.1 (0.1)	0 (0.1)	0 (0)	N/A	0.3 (0.2)	5.9 (6.1)	0.2 (0.3)	N/A	0.3 (0.2)	0 (0)
18:2ω6	5.3 (2.0)	2.8 (0.8)	1.3 (0.5)	3.7 (1.7)	1.9 (0.5)	N/A	1.3 (0.5)	0.8 (0.6)	1.8 (0.1)	N/A	1.8 (0.7)	1.3 (0.4)

Table 3.3. (continued):

	Seawater (O)						Sediment (I)					
Site	**South**			**North**			**South**			**North**		
Collection Month	**Apr**	**Jul**	**Dec**	**Apr**	**Jul**	**Dec**	**Apr**	**Jul**	**Dec**	**Apr**	**Jul**	**Dec**
N	**3**	**3**	**3**	**3**	**3**	**N/A**	**3**	**3**	**3**	**N/A**	**3**	**3**
FA	**% (±SD)**						**% (±SD)**					
18:2ω4	0 (0)	2.0 (0.1)	1.3 (1.5)	1.1 (1.1)	2.4 (0.5)	N/A	0 (0.1)	0.2 (0.3)	0.2 (0)	N/A	0.2 (0.1)	0 (0)
18:3ω6	0 (0)	0 (0)	0 (0.1)	0 (0)	0 (0.1)	N/A	0.3 (0.2)	0.2 (0.2)	0.2 (0.1)	N/A	0.2 (0.1)	0 (0)
18:3ω3	0 (0)	0.3 (0.1)	0.4 (0.2)	0.1 (0.1)	0.3 (0.1)	N/A	1.1 (0.3)	0.5 (0.4)	0.7 (0.2)	N/A	0.5 (0.1)	0.5 (0.6)
18:4ω3	0.4 (0.4)	0.7 (0.1)	1.1 (0.3)	0.8 (0.4)	0.6 (0.2)	N/A	1.3 (0.5)	1.1 (0.8)	0.8 (0.1)	N/A	0.7 (0.1)	0.6 (0.1)
18:4ω1	0 (0)	1.8 (0.6)	2.2 (1.5)	0.2 (0.2)	2.0 (0.3)	N/A	0.5 (0.4)	1.3 (1.0)	0.7 (0.2)	N/A	0.3 (0.3)	0.6 (0.6)
20:0	0.3 (0.3)	0.4 (0)	0.6 (0.2)	0.3 (0.3)	0.4 (0.1)	N/A	0.4 (0.1)	1.0 (0.5)	0.8 (0.1)	N/A	0.6 (0.6)	0.8 (0.4)
20:1ω11	0 (0)	0.1 (0.1)	0.1 (0.2)	0 (0)	0.1 (0)	N/A	0.4 (0.2)	0.5 (0.1)	0.1 (0.2)	N/A	0.3 (0.1)	0 (0)
20:1ω9	0.7 (0.6)	0.3 (0.1)	0.2 (0.1)	0.4 (0)	0.1 (0)	N/A	0.1 (0.1)	0.6 (0.2)	0.3 (0.1)	N/A	0.2 (0.1)	0 (0)
20:1ω7	0 (0)	0.2 (0.3)	0.1 (0.1)	0 (0)	0 (0)	N/A	0.1 (0.1)	0.6 (0.4)	0.1 (0.1)	N/A	0.2 (0.1)	0 (0)
20:2*a*	0 (0)	0.7 (0.6)	0.2 (0.2)	0.1 (0.2)	0 (0)	N/A	0 (0)	0 (0)	0 (0.0)	N/A	0.1 (0.2)	0 (0)
20:2*b*	0 (0)	0 (0)	0.1 (0.1)	0 (0)	0 (0)	N/A	0 (0)	0.5 (0.5)	0.5 (0.7)	N/A	0 (0)	0 (0)
20:2ω6	0 (0)	0 (0)	0 (0.1)	0 (0)	0 (0)	N/A	1.2 (0.2)	0.5 (0.2)	0.9 (1.2)	N/A	1.2 (0.8)	0.9 (0.7)
20:3ω6	0 (0)	3.9 (0.2)	2.0 (2.1)	2.0 (2.2)	5.3 (1.7)	N/A	0 (0)	0 (0.1)	0 (0)	N/A	0 (0)	0 (0)
20:4ω6	0 (0)	0.2 (0)	0.2 (0.2)	0 (0)	0 (0.1)	N/A	3.7 (0.4)	1.8 (1.4)	1.7 (1.1)	N/A	1.9 (0.6)	3.7 (0.4)
20:3ω3	0 (0)	0 (0)	0 (0)	0.1 (0.1)	0 (0)	N/A	0 (0)	0.3 (0)	0 (0)	N/A	0 (0.1)	0 (0)
20:4ω3	0 (0)	0.9 (0.8)	0.4 (0.1)	0.2 (0.3)	0.1 (0)	N/A	0 (0)	0.1 (0.1)	0.1 (0.1)	N/A	0.2 (0.1)	0 (0)
20:5ω3	1.2 (0.5)	5.7 (0.5)	1.4 (0.8)	3.0 (1.8)	7.2 (1.3)	N/A	7.8 (0.9)	4.6 (3.9)	2.0 (1.4)	N/A	5.0 (2.0)	4.2 (0.2)
22:2NIMD*a*	11.5 (19.9)	0.1 (0.2)	0 (0.1)	0 (0)	0 (0)	N/A	0 (0)	0.5 (0.5)	0 (0.1)	N/A	0.1 (0.1)	0 (0)
21:5ω3	0 (0)	3.3 (0.4)	1.7 (2.0)	1.6 (1.7)	5.6 (1.8)	N/A	0 (0)	0 (0.1)	0 (0)	N/A	0.2 (0.4)	0 (0)
22:4ω6	0 (0)	0.1 (0.2)	0.1 (0.1)	0 (0)	0 (0)	N/A	0 (0)	0.4 (0.3)	0 (0)	N/A	0 (0)	0 (0)
22:5ω3	0 (0)	3.2 (0.3)	1.6 (1.9)	1.5 (1.5)	4.9 (1.6)	N/A	0.9 (1.0)	0.1 (0.2)	0 (0)	N/A	0.2 (0)	0 (0)
22:6ω3	1.0 (0.2)	1.5 (0.6)	1.5 (0.5)	0.9 (0.2)	1.2 (0.5)	N/A	1.4 (0.6)	1.1 (0.6)	0.5 (0.2)	N/A	1.1 (0.4)	1.6 (0.9)

† Trimethyltridecanoic acid

(A)

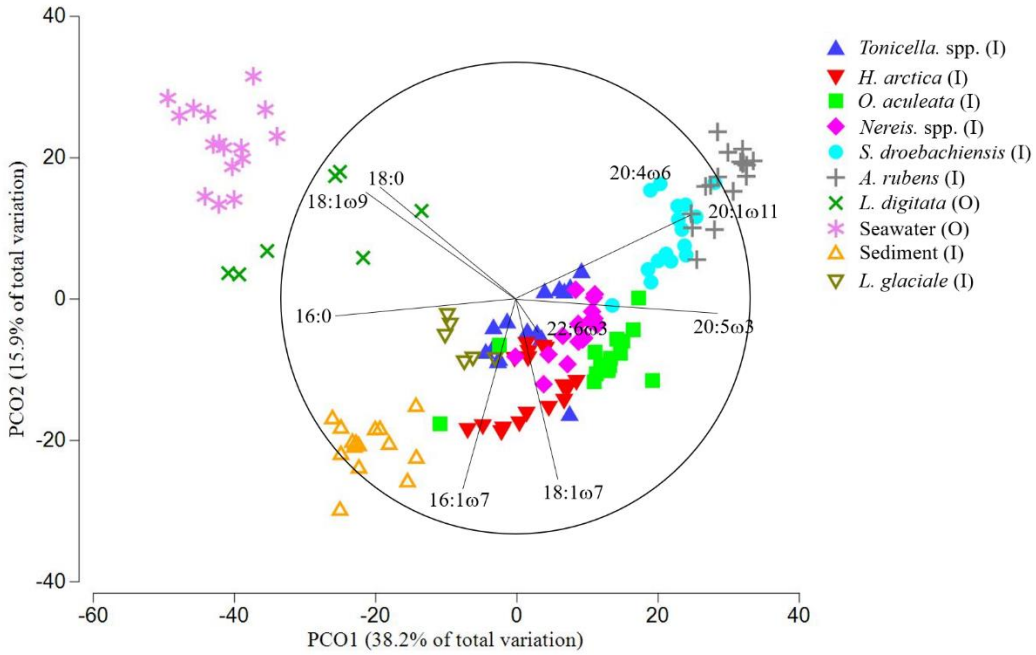

(B)

FA	Biomarker
16:0	Chlorophyta, Flagellates (including Dinoflagellates), Phaeophyta, Rhodophyta
16:1ω7	Aerobic microorganisms, Diatoms, Rhodophyta
18:0	Detritus
18:1ω9	Crustaceans, Detritus, Dinoflagellates, Phaeophyta
18:1ω7	Aerobes, Bacteria, Chlorophyta, Rhodophyta
20:1ω11	Copepods
20:4ω6 (ARA)	Amphipods, Foraminifera, Phaeophyta, Rhodophyta
20:5ω3 (EPA)	Diatoms, Phaeophyta
22:6ω3 (DHA)	Flagellates (including Dinoflagellates)

Figure 3.3. (A) PCO plot (based on Bray-Curtis similarity matrices) of the 8 fatty acids exhibiting at least 70% correlation and DHA which had 21% correlation in the six animal species, two macroalgal species, and two environmental components (see Table 2.2 for species list) sampled in April, July, and December 2017 inside (I) or outside (O) of the South and North sites (see Figure 1.1). (B) Typical fatty-acid trophic biomarkers for those fatty acids included in the analysis (adapted from Parrish (2013) and Legeżyńska et al. (2014).

components (PERMANOVA; Pseudo-$F_{9,132}$=53.596, P (perm)<0.01) and five functional groups studied (PERMANOVA, Pseudo-$F_{4,137}$=27.898, P (perm)<0.01). FA composition changed significantly monthly (PERMANOVA, Pseudo-$F_{2,141}$=2.09, P (perm)=0.025), but a subsequent pairwise test revealed specifically only between April and December (PERMANOVA, t=1.769, P (perm)=0.0123). FA at each site were not significantly different (PERMANOVA, Pseudo-$F_{1,141}$=1.575, P (perm)=0.14), nor was the interaction effect. In addition to the slight significant changes between months, 12 individual FA profiles significantly differed seasonally (Table 3.4). Of the eight FA which exhibited at least 70% correlation in the ten components (Figure 3.3), seven (16:1ω7, 18:0, 18:1ω9, 18:1ω7, 20:1ω11, 20:5ω3 [EPA], and 20:4ω6 [ARA]) showed significant changes among individual components (Table 3.5).

Of the three essential fatty acids (EPA, DHA [docosahexaenoic acid], and ARA), EPA was the most abundant, present in all food web components, but particularly among the six animal species (Table 3.3). ARA was in all components, except for trace amounts in seston, peaking in December in *S. droebachiensis* (25%) at higher proportions than EPA (Table 3.3). All components had DHA, which was typically less abundant than EPA and ARA, except in *H. arctica*, which peaked at both sites in December with proportions higher than EPA (20 – 24%) (Table 3.3). Animal FA profiles were richest in polyunsaturated FA (PUFA), which ranged from 38% in *Tonicella* spp. in July to 67% in *A. rubens* in December (Table 3.6). Monounsaturated FA (MUFA) were lower, varying from 17% in *S. droebachiensis* in April to *S. droebachiensis* to 35% in *Tonicella* spp. in July, but were nevertheless still generally most abundant than saturated FA (SFA), ranging from 8% in *A. rubens* in December to 27% in *Nereis* spp. in April (Table 3.6). Environmental components and *L. glaciale* presented lower levels of PUFA than the animals, ranging from 15% in seston in December to 39% in *L. glaciale* in July, and typically contained higher proportions of

Table 3.4. Significant seasonal changes of all fatty acids in the six animal species, two macroalgal species, and two environmental components (see Table 2.2 for species list) sampled in April, July, and December 2017 inside (I) or outside (O) of the South and North sites (see Figure 1.1) .

FA	Significance	F value	P value
14:1	Month	3.24	0.036
i15:0	Month	3.46	0.035
15:0	Month	6.84	<0.010
*ai*17:0	Month	9.02	<0.010
17:0	Month	3.90	0.023
17:1	Month	12.87	<0.010
16:4ω3	Month	18.33	<0.010
20:3ω6	Month	4.80	0.010
20:4ω3	Month	3.30	0.032

Table 3.5. Significant seasonal changes of specific components within the 8 fatty acids exhibiting at least 70% correlation in the six animal species, two macroalgal species, and two environmental components (see Table 2.2 for species list) sampled in April, July, and December 2017 inside (I) or outside (O) of the South and North sites (see Figure 1.1).

FA	Component	Significance	F value	P value
16:1ω7	*Tonicella* spp.	Month	51.96	<0.010
16:1ω7	*H. arctica*	Month	50.22	<0.010
16:1ω7	*S. droebachiensis*	Month	10.60	0.003
16:1ω7	*A. rubens*	Month	6.31	0.015
18:0	*Tonicella* spp.	Month	8.60	<0.010
18:0	*H. arctica*	Month	49.64	<0.010
18:0	*A. rubens*	Month	12.84	<0.010
18:0	Seawater	Month	12.82	<0.010
18:1ω9	*S. droebachiensis*	Month	4.77	0.035
18:1ω7	*H. arctica*	Month	19.62	<0.010
18:1ω7	*A. rubens*	Month	9.75	<0.010
18:1ω7	Sediment	Month	17.27	<0.010
20:1ω11	*Tonicella* spp.	Month	10.31	<0.010
20:1ω11	*H. arctica*	Month	12.26	<0.010
20:1ω11	*Nereis* spp.	Month	14.10	<0.010
20:1ω11	*S. droebachiensis*	Month	35.5	<0.010
20:1ω11	Sediment	Month	12.55	<0.010
20:5ω3	*Tonicella* spp.	Month	12.21	<0.010
20:5ω3	*H. arctica*	Month	16.80	<0.010
20:5ω3	*Nereis* spp.	Month	5.15	0.029
20:5ω3	*S. droebachiensis*	Month	12.99	<0.010
20:5ω3	*A. rubens*	Month	18.68	<0.010
20:5ω3	Seawater	Month	35.86	<0.010
20:5ω3	Sediment	Month	8.64	0.010
20:4ω6	*Tonicella* spp.	Month	13.55	<0.010
20:4ω6	*H. arctica*	Month	12.41	<0.010
20:4ω6	*Nereis* spp.	Month	7.44	0.010
20:4ω6	*S. droebachiensis*	Month	29.14	<0.010
20:4ω6	*L. digitata*	Month	13.31	0.017

Table 3.6. Sample size (N), mean proportional sum (Σ) of saturated (SFA), monounsaturated (MUFA), polyunsaturated (PUFA), ω3 (omega-3), and ω6 (omega-6) fatty acids, and mean ratios of polyunsaturated:saturated (P/S) and DHA:EPA (DHA/EPA), in the six animal species, two macroalgal species, and two environmental components (see Table 2.2 for species list) sampled in April, July, and December 2017 inside (I) or outside (O) of the South and North sites (see Figure 1.1). Each component group (animal, macroalgal, environmental) variable's lowest and highest values are bolded.

				ΣSFA	ΣMUFA	ΣPUFA	Σω3	Σω6	P/S	DHA/EPA
Component	**Site**	**Collection Month**	**N**	% (±SD)	% (±SD)	% (±SD)	% (±SD)	% (±SD)	Mean (±SD)	Mean (±SD)
Animal										
A. rubens	South	April	3	11.6 (3.4)	24.0 (1.2)	63.2 (4.0)	39.4 (5.0)	22.5 (6.9)	5.9 (2.4)	0.2 (0.1)
		July	3	14.6 (2.7)	29.2 (5.2)	54.7 (6.5)	36.1 (2.6)	14.7 (2.1)	3.9 (1.1)	0.1 (0.1)
		December	2	**7.9 (0.1)**	22.2 (0.3)	**66.8 (0)**	38.5 (2.3)	20.5 (2.7)	**8.5 (0.1)**	0.2 (0.1)
	North	April	3	9.7 (1.1)	33.2 (1.8)	56.2 (1.0)	32.0 (3.6)	22.0 (3.2)	5.9 (0.6)	0.1 (0.1)
		July	3	11.7 (2.6)	25.7 (1.5)	61.2 (2.2)	39.0 (2.0)	16.7 (4.9)	5.4 (1.2)	0.1 (0)
		December	3	8.6 (0.7)	21.1 (1.0)	66.7 (0.4)	40.8 (4.0)	18.6 (2.9)	7.8 (0.6)	0.2 (0.1)
Mean			17	10.8 (2.9)	26.1 (4.8)	61.2 (5.6)	37.6 (4.2)	19.1 (4.6)	6.1 (1.9)	0.2 (0.1)
H. arctica	South	April	3	24.6 (0.9)	27.6 (3.8)	45.7 (4.5)	37.5 (5.8)	5.3 (1.6)	1.9 (0.2)	0.5 (0)
		July	3	21.1 (1.0)	25.5 (3.5)	51.1 (4.7)	40.7 (4.7)	4.9 (1.1)	2.4 (0.3)	0.5 (0.1)
		December	3	21.6 (0.1)	17.0 (0.8)	58.2 (0.8)	**50.4 (0.6)**	5.1 (0.3)	2.7 (0)	**1.7 (0.2)**
	North	April	3	21.5 (1.3)	25.0 (2.8)	52.1 (3.7)	42.2 (4.1)	4.7 (0.3)	2.4 (0.3)	0.5 (0.1)
		July	3	20.7 (0.4)	23.8 (0.8)	54.4 (0.8)	43.7 (1.3)	5.3 (1.2)	2.6 (0.1)	0.5 (0.1)
		December	3	21.7 (1.2)	18.3 (2.2)	57.3 (3.2)	49.0 (2.7)	4.7 (0.7)	2.7 (0.3)	1.3 (0.4)
Mean			18	21.9 (1.5)	22.9 (4.5)	53.1 (5.2)	43.9 (5.6)	5.0 (0.9)	2.5 (0.4)	0.8 (0.5)
Nereis spp.	South	April	3	18.6 (0.4)	22.0 (2.7)	58.2 (2.9)	40.9 (6.0)	11.1 (3.8)	3.1 (0.2)	0 (0)
		July	2	19.9 (8.4)	29.5 (2.9)	49.8 (11.1)	31.8 (6.7)	13.2 (7.2)	2.9 (1.8)	0.1 (0)
		December	3	17.7 (0.6)	20.4 (0.5)	60.3 (0.1)	35.8 (1.6)	14.9 (2.4)	3.4 (0.1)	0 (0)
	North	April	3	20.1 (0.7)	26.5 (2.6)	52.4 (3.0)	36.3 (1.8)	12.9 (0.7)	2.6 (0.2)	0.1 (0)
		July	3	19.2 (2.4)	25.6 (3.6)	54.2 (5.7)	36.7 (4.8)	10.8 (1.5)	2.9 (0.6)	0 (0)
		December	3	19.6 (1.3)	23.6 (2.5)	55.3 (4.0)	35.3 (2.7)	14.6 (1.1)	2.8 (0.4)	0 (0)
Mean			17	19.2 (2.5)	24.6 (3.6)	55.0 (5.3)	36.5 (4.4)	12.8 (3.0)	2.9 (0.6)	0 (0)

Table 3.6. (continued):

				ΣSFA	**ΣMUFA**	**ΣPUFA**	**Σω3**	**Σω6**	**P/S**	**DHA/EPA**
Component	**Site**	**Collection Month**	**N**	% (±SD)	% (±SD)	% (±SD)	% (±SD)	% (±SD)	Mean (±SD)	Mean (±SD)
O. aculeata	South	April	3	**26.8 (12.7)**	24.6 (3.3)	47.8 (10.8)	34.4 (7.4)	4.2 (0.7)	2.1 (1.2)	0 (0)
		July	3	21.2 (0.9)	26.9 (3.2)	50.6 (3.2)	37.4 (3.1)	**3.5 (0.3)**	2.4 (0.2)	0 (0)
		December	3	18.3 (2.7)	32.5 (5.2)	47.9 (2.6)	33.6 (1.4)	4.8 (0.3)	2.6 (0.3)	0 (0)
	North	April	3	18.4 (0.4)	28.1 (2.5)	52.7 (2.8)	34.3 (1.3)	4.4 (1.0)	2.9 (0.2)	0 (0)
		July	2	20.5 (1.1)	27.7 (0.2)	50.7 (0.9)	34.5 (2.3)	3.9 (0.2)	2.5 (0.2)	0 (0)
		December	3	20.6 (3.1)	32.2 (0.1)	46.1 (3.2)	31.8 (3.8)	5.2 (0.2)	2.3 (0.5)	0 (0)
Mean			17	21.0 (5.7)	28.5 (4.0)	49.4 (5.0)	34.5 (3.6)	4.3 (0.7)	2.5 (0.5)	0 (0)
S. droebachiensis	South	April	2	16.6 (1.1)	**16.8 (1.5)**	65.2 (3.0)	36.7 (4.4)	20.8 (0.6)	3.9 (0.5)	0.1 (0)
		July	3	16.8 (0.3)	25.0 (3.0)	57.1 (2.1)	28.1 (3.7)	20.2 (1.9)	3.4 (0.1)	0.1 (0)
		December	3	16.5 (0.3)	20.2 (1.2)	60.4 (0.4)	**24.5 (1.8)**	**31.7 (0.1)**	3.7 (0)	0.1 (0.1)
	North	April	3	14.5 (1.1)	24.2 (1.3)	60.8 (2.3)	34.0 (3.7)	18.8 (2.1)	4.2 (0.5)	0.3 (0.4)
		July	3	16.0 (1.2)	23.6 (1.3)	59.1 (1.7)	31.2 (2.2)	19.0 (0.5)	3.7 (0.4)	0.1 (0)
		December	2	16.8 (3.1)	20.2 (1.6)	61.2 (1.9)	28.7 (2.7)	28.6 (1.1)	3.7 (0.9)	0 (0)
Mean			16	16.2 (1.6)	22.1 (3.2)	60.3 (2.2)	30.5 (4.6)	22.8 (5.2)	3.8 (0.5)	0.1 (0.2)
Tonicella spp.	South	April	3	19.4 (4.0)	30.3 (3.8)	43.9 (0.2)	33.4 (0.2)	10.6 (4.4)	2.3 (0.5)	0 (0)
		July	3	21.1 (2.3)	32.0 (0.8)	39.9 (3.3)	31.3 (1.9)	13.8 (3.8)	1.9 (0.3)	0 (0)
		December	3	24.6 (1.0)	26.0 (1.7)	44.7 (1.2)	30.9 (0.9)	19.5 (1.6)	1.8 (0)	0 (0)
	North	April	N/A	N/A	N/A	N/A	N/A	N/A	N/A	N/A
		July	3	20.4 (0.3)	**34.5 (0.8)**	**37.8 (0.8)**	28.7 (0.5)	10.4 (0.6)	1.9 (0)	0 (0)
		December	3	24.6 (0.7)	28.4 (3.9)	41.3 (4.9)	28.6 (3.8)	18.0 (3.1)	**1.7 (0.2)**	0.9 (1.5)
Mean			15	22.0 (1.7)	30.2 (0.3)	41.5 (3.5)	30.6 (4.6)	14.4 (2.7)	1.9 (0.3)	0.2 (0)

Table 3.6. (continued):

				ΣSFA	**ΣMUFA**	**ΣPUFA**	**Σω3**	**Σω6**	**P/S**	**DHA/EPA**
Component	**Site**	**Collection Month**	**N**	% (±SD)	% (±SD)	% (±SD)	% (±SD)	% (±SD)	Mean (±SD)	Mean (±SD)
Macroalgal										
		April	2	23.7 (1.7)	17.2 (0.3)	**56.7 (2.2)**	**29.7 (1.4)**	10.5 (0.4)	**2.4 (0.3)**	0 (0)
	South	July	3	34.8 (14.7)	17.5 (3.1)	42.7 (16.7)	28.6 (11.6)	11.3 (3.4)	1.5 (1.1)	**0.7 (0.7)**
		December	3	27.4 (0.1)	21.7 (0.3)	48.9 (0.2)	**22.8 (0.5)**	**25.7 (0.7)**	1.8 (0)	0 (0)
L. digitata		April	N/A	N/A	N/A	N/A	N/A	N/A	N/A	N/A
	North	July	N/A	N/A	N/A	N/A	N/A	N/A	N/A	N/A
		December	N/A	N/A	N/A	N/A	N/A	N/A	N/A	N/A
Mean			8	29.5 (10.0)	18.6 (2.8)	48.5 (11.5)	27.2 (7.4)	15.2 (7.4)	1.9 (0.8)	0.3 (0.5)
		April	N/A	N/A	N/A	N/A	N/A	N/A	N/A	N/A
	South	July	3	**40.9 (2.1)**	**16.6 (1.0)**	**36.8 (0.5)**	25.6 (0.7)	8.4 (0.4)	**0.9 (0.1)**	0 (0)
		December	N/A	N/A	N/A	N/A	N/A	N/A	N/A	N/A
L. glaciale		April	N/A	N/A	N/A	N/A	N/A	N/A	N/A	N/A
	North	July	3	**18.2 (0.7)**	**40.6 (3.1)**	39.0 (2.8)	28.2 (2.8)	**7.5 (0.2)**	2.1 (0.1)	0.1 (0)
		December	N/A	N/A	N/A	N/A	N/A	N/A	N/A	N/A
Mean			6	29.5 (12.5)	28.6 (13.3)	37.9 (2.1)	26.9 (2.3)	8.0 (0.6)	1.5 (0.7)	0.1 (0)

Table 3.6. (continued):

				ΣSFA	**ΣMUFA**	**ΣPUFA**	**Σω3**	**Σω6**	**P/S**	**DHA/EPA**
Component	**Site**	**Collection Month**	**N**	% (±SD)	% (±SD)	% (±SD)	% (±SD)	% (±SD)	Mean (±SD)	Mean (±SD)
Environmental										
Seawater	South	April	3	41.6 (5.4)	37.9 (12.1)	20.2 (17.6)	**2.6 (1.1)**	6.3 (0.3)	0.5 (0.5)	0.9 (0.1)
		July	3	43.0 (9.2)	22.0 (8.3)	33.9 (2.2)	16.1 (0.3)	7.0 (0.6)	0.8 (0.2)	0.3 (0.1)
		December	3	**65.1 (14.1)**	**13.0 (0.9)**	20.5 (15.3)	8.6 (5.4)	**3.8 (3.0)**	**0.4 (0.4)**	**1.2 (0.3)**
	North	April	3	56.2 (3.4)	23.8 (8.1)	19.5 (10.4)	8.7 (4.9)	6.9 (1.0)	**0.4 (0.2)**	0.4 (0.3)
		July	3	38.8 (5.0)	22.6 (6.2)	**38.3 (6.6)**	**20.2 (3.7)**	**7.4 (1.3)**	1.0 (0.3)	**0.2 (0.1)**
		December	N/A	N/A	N/A	N/A	N/A	N/A	N/A	N/A
Mean			17	46.9 (14.6)	26.6 (15.1)	26.5 (13.0)	10.7 (7.2)	6.6 (2.2)	0.6 (0.4)	0.6 (0.5)
Sediment	South	April	3	**24.2 (2.8)**	42.5 (3.4)	25.8 (4.9)	13.0 (3.3)	6.6 (0.9)	**1.1 (0.3)**	0.2 (0.1)
		July	3	35.6 (8.9)	37.4 (2.1)	17.9 (8.0)	8.4 (6.1)	4.6 (0.9)	0.6 (0.4)	0.3 (0.1)
		December	2	29.7 (0.8)	**43.5 (0.3)**	17.6 (0.9)	5.3 (0.1)	4.6 (2.0)	0.6 (0)	**0.2 (0)**
	North	April	N/A	N/A	N/A	N/A	N/A	N/A	N/A	N/A
		July	3	33.0 (2.0)	39.4 (3.5)	19.7 (0.6)	9.6 (1.6)	5.1 (1.1)	0.6 (0)	**0.2 (0)**
		December	3	34.6 (1.3)	39.3 (2.7)	**17.3 (1.9)**	6.9 (1.3)	5.9 (0.9)	0.5 (0.1)	0.4 (0.2)
Mean			15	31.3 (5.6)	39.9 (3.4)	20.6 (5.8)	9.6 (4.6)	5.5 (1.2)	0.7 (0.3)	0.3 (0.1)

N/A Data not available

MUFA (35 – 43% in infauna) and SFA (17 – 65% in seston) (Table 3.6). Animals exhibited the highest ratio of polyunsaturated to unsaturated FA, particularly *A. rubens* and *S. droebachiensis* (P/S; 3 - 9%), followed by macroalgal (2%), and seston and infauna (1%) (Table 3.6). All components, except for seawater, had an average higher proportion of ω3 (omega-3) fatty acids than ω6 (omega-6), although *S. droebachiensis* had higher ω6 proportions at the South site in December. The filter feeders *H. arctica* and *O. aculeata* contained about 9 times as many ω3 fatty acids (43.9% and 34.5%, respectively) than ω6 (5.0% and 4.3%, respectively), whereas the rest of the animals and macroalgal components were between 2 and 3 times as many ω3 than ω6. Conversely, seston and sediment were more proportional (10.7 and 9.6% ω3; 6.6 and 5.5% ω6, respectively) (Table 3.6). The average DHA/EPA ratio was significantly higher in December than in April (pairwise PERMANOVA, t=2.7807, P (perm)=0.01) and July (pairwise PERMANOVA, t=2.7852, P (perm)=0.01) and was highest in *H. arctica* and seston (0.8 and 0.6, respectively) with both peaking in December at the South site. Contrarily, the DHA/EPA ratio showed low values in sediment, *L. digitata*, *Tonicella* spp., *A. rubens*, *S. droebachiensis* and *L. glaciale* (0.1 to 0.3); and null (0) values for *Nereis* spp. and *O. aculeata* (Table 3.6). Proportional sums of FA varied significantly among the 10 components (PERMANOVA; Pseudo-$F_{9,132}$=37.054, P (perm)<0.01) and five functional groups studied (PERMANOVA, Pseudo-$F_{4,137}$=45.993, P (perm)<0.01), but not by site (PERMANOVA, Pseudo-$F_{1,141}$=1.759, P (perm)=0.18) nor month (PERMANOVA, Pseudo-$F_{2,141}$=0.41, P (perm)=0.77). The interaction was also not significant.

3.4.4. Stable isotopes and trophic magnification

Stable carbon and nitrogen isotope ratios ($\delta^{13}C$ and $\delta^{15}N$) showed no significant seasonal or temporal changes, except in kelp, which was less carbon depleted in July and December

(-15.2‰) than in April (-21.0‰) ($\delta^{13}C$, PERMANOVA, Pseudo-$F_{2,6}$=332.97, P (perm)=0.013), and increased its trophic position from 1 to ~1.98 during the same time period ($\delta^{15}N$, PERMANOVA, Pseudo-$F_{2,6}$=300.97, P (perm)=0.005). Stable carbon isotope ratio ($\delta^{13}C$) differed significantly among the 10 food web components included in the carbon isotope analysis (PERMANOVA, Pseudo-$F_{9,118}$=50.929, P (perm)<0.001), ranging from most depleted in seawater in December at the North site (-27.5‰) to least depleted in *L. digitata* in July at the South site (-15.1‰) (Table 3.7). Stable nitrogen isotope ratio ($\delta^{15}N$), which was lowest in *L. digitata* in April (3.4‰) and highest in *A. rubens* in April and December (11.4‰) (Table 3.7), also differed significantly among the ten food web components included in the nitrogen isotope analysis (PERMANOVA, Pseudo-$F_{9,151}$=135.15, P (perm) < 0.001), indicating distinct trophic levels (see below). Hierarchical clustering analysis of $\delta^{13}C$ and $\delta^{15}N$ separated the ten components in seven distinct groups (PERMANOVA, Psuedo-$F_{6,113}$=127.29, P (perm)<0.001; Figure 3.4 and Table 3.8). Two of these groups each contained all samples of a single food web component, namely *L. digitata* (kelp) and *A. rubens* (sea star), hereafter termed respectively Group 1 and Group 6 (Figure 3.4 and Table 3.8). Group 2 also had only a single food web component, seawater (seston), but was separated into two sub-groups (Groups 2a and 2b). Group 3 contained four subgroups of which only one was monospecific, but each included at least one of *Nereis* (polychaete) (Groups 3a and 3c), seawater (seston) (Groups 3a, 3b, and 3c), or sediment (Groups 3b and 3d) (Figure 3.4 and Table 3.8). Group 5 also included four subgroups with each containing at least one of *A. rubens* (Groups 5a and 5c), *Nereis* spp. (Groups 5a and 5b), *O. aculeata* (Groups 5a and 5b), *S. droebachiensis* (Groups 5c and 5d), or *Tonicella* spp. (Groups 5a and 5d) (Figure 3.4 and Table 3.8). Groups 4 and 7 each had two distinct subgroups of monospecific components: *H. arctica* (Group 4a), *L. glaciale* (Group 4b), *Tonicella* spp. (Group 7a), and *L. digitata* (Group 7b) (Figure

Table 3.7. Sample size (N), bulk stable isotope ratio ($\delta^{13}C$ and $\delta^{15}N$; ‰), and relative trophic position (TP) in the six animal species, two macroalgal species, and two environmental components (see Table 2.2 for species list) sampled in April, July, and December 2017 inside (I) or outside (O) of the South and North sites (see Figure 1.1). Trophic position is based on an isotopic model with a $\Delta^{15}N$ fractionation factor of 3.4‰ (see section 2.3.8). Each component group (animal, macroalgal, environmental) variable's lowest and highest values are bolded.

				Dry Weight	Carbon		Dry Weight	Nitrogen	TP
Component	**Site**	**Collection Month**	**N**	mg (±SD)	$\delta^{13}C$ (±SD)	**N**	mg (±SD)	$\delta^{15}N$ (±SD)	
Animal									
A. rubens	South	April	3	1.3 (0.2)	-18.9 (0.9)	3	1.4 (0)	11.0 (0.3)	3.22
		July	2	1.0 (0)	**-15.7 (3.6)**	3	1.2 (0.1)	**11.4 (0.4)**	3.34
		December	1	1.12	-19.4	3	1.3 (0.2)	11.3 (0.1)	3.33
	North	April	3	1.4 (0.1)	-17.5 (3.1)	3	1.2 (0.1)	11.3 (0.4)	3.30
		July	2	1.1 (0.1)	-20.1 (1.7)	3	1.2 (0.1)	**11.4 (0.5)**	**3.36**
		December	1	1.0	-20.0	3	1.3 (0.2)	**11.4 (0.1)**	3.34
Mean			12	1.2 (0.2)	-18.4 (2.4)	18	1.3 (0.1)	11.3 (0.3)	3.31
H. arctica	South	April	3	1.1 (0.1)	-20.0 (0.4)	3	1.3 (0.2)	**6.3 (0)**	**1.85**
		July	3	1.1 (0.1)	-21.1 (0.4)	3	1.2 (0.1)	7.1 (0)	2.09
		December	3	1.1 (0.1)	-21.4 (0.2)	3	1.2 (0.2)	6.9 (0.3)	2.03
	North	April	3	1.1 (0.1)	-19.9 (0.6)	2	1.2 (0.1)	7.1 (0.6)	2.09
		July	2	1.1 (0)	-20.7 (0.4)	3	1.3 (0.1)	6.6 (0.1)	1.93
		December	3	1.1 (0.1)	-20.9 (0.6)	3	1.2 (0.1)	7.2 (0)	2.10
Mean			17	1.1 (0.1)	-20.7 (0.7)	17	1.2 (0.1)	6.9 (0.4)	2.02
Nereis spp.	South	April	2	1.3 (0.2)	**-22.5 (0.1)**	N/A	N/A	N/A	N/A
		July	2	1.1 (0.2)	-22.0 (2.4)	3	1.2 (0.1)	8.9 (0.1)	2.61
		December	3	1.4 (0)	-21.9 (0.6)	2	1.4 (0.1)	10.1 (0.6)	2.95
	North	April	2	1.3 (0)	-21.8 (0.1)	N/A	N/A	N/A	N/A
		July	3	1.2 (0.2)	-21.9 (1.4)	3	1.2 (0.2)	9.0 (0.1)	2.63
		December	3	1.3 (0.2)	-21.7 (0.6)	3	1.3 (0.1)	9.3 (1.1)	2.74
Mean			15	1.3 (0.2)	-22.0 (0.9)	11	1.3 (0.1)	9.2 (0.7)	2.73

Table 3.7. (continued):

Component	Site	Collection Month	N	Dry Weight mg (±SD)	Carbon $\delta^{13}C$ (±SD)	N	Dry Weight mg (±SD)	Nitrogen $\delta^{15}N$ (±SD)	TP
O. aculeata	South	April	3	1.2 (0.2)	-19.9 (0.3)	3	1.3 (0.1)	8.9 (0.6)	2.63
		July	1	1.4	-20.3	3	1.3 (0.1)	8.3 (0.2)	2.43
		December	N/A	N/A	N/A	3	1.2 (0.1)	8.5 (0.2)	2.49
	North	April	3	1.2 (0.1)	-20.9 (0.8)	3	1.1 (0.1)	9.6 (0.6)	2.82
		July	1	1.0	-20.7	3	1.3 (0.2)	8.7 (0.4)	2.54
		December	N/A	N/A	N/A	3	1.1 (0)	9.1 (0.4)	2.66
Mean			8	1.2 (0.1)	-20.4 (0.7)	18	1.2 (0.1)	8.8 (0.6)	2.59
S. droebachiensis	South	April	3	1.2 (0.1)	-19.8 (1.4)	2	1.2 (0.2)	10.0 (0.9)	2.93
		July	N/A	N/A	N/A	3	1.3 (0.2)	9.4 (0.3)	2.75
		December	N/A	N/A	N/A	3	1.3 (0.2)	9.5 (0.4)	2.78
	North	April	N/A	N/A	N/A	3	1.3 (0.2)	10.0 (0.2)	2.94
		July	N/A	N/A	N/A	3	1.3 (0.1)	9.1 (0.3)	2.68
		December	N/A	N/A	N/A	3	1.3 (0.1)	9.4 (0.3)	2.75
Mean			3	1.19 (0)	-19.8 (0.8)	17	1.3 (0.1)	9.5 (0.5)	2.80
Tonicella spp.	South	April	3	1.1 (0)	-19.3 (0.3)	3	1.2 (0.2)	9.7 (0.3)	2.85
		July	2	1.1 (0)	-19.2 (0.4)	3	1.2 (0.2)	9.5 (0.1)	2.77
		December	2	1.3 (0.2)	-20.2 (1.6)	3	1.4 (0)	9.5 (0.2)	2.79
	North	April	3	1.2 (0.1)	-16.4 (2.9)	2	1.2 (0.2)	9.9 (0)	2.90
		July	3	1.1 (0)	-19.1 (0.3)	3	1.2 (0.2)	9.5 (0.1)	2.77
		December	3	1.2 (0.1)	-17.5 (0.9)	3	1.2 (0.2)	8.9 (0.7)	2.60
Mean			16	1.2 (0.1)	-18.5 (1.8)	17	1.2 (0.1)	9.5 (0.4)	2.78

Table 3.7. (continued):

Component	Site	Collection Month	N	Dry Weight mg (±SD)	Carbon $\delta^{13}C$ (±SD)	N	Dry Weight mg (±SD)	Nitrogen $\delta^{15}N$ (±SD)	TP
Macroalgal									
L. digitata	South	April	3	1.1 (0.2)	**-21.0 (0.5)**	3	4.5 (0.4)	**3.4 (0.2)**	**1.00**
		July	3	1.2 (0.2)	**-15.1 (0.2)**	3	4.3 (0.1)	7.0 (0.2)	2.06
		December	3	1.1 (0.1)	-15.3 (0.1)	3	3.9 (1.6)	6.5 (0.2)	1.90
	North	April	N/A	N/A	N/A	N/A	N/A	N/A	N/A
		July	N/A	N/A	N/A	N/A	N/A	N/A	N/A
		December	N/A	N/A	N/A	N/A	N/A	N/A	N/A
Mean			9	1.1 (0.1)	-17.2 (2.9)	9	4.2 (0.9)	5.6 (1.7)	1.65
L. glaciale	South	April	1	1.1	-18.9	3	4.4 (0.4)	7.3 (0.4)	2.14
		July	2	1.1 (0)	-18.6 (0.2)	3	4.6 (0.2)	7.1 (0.1)	2.07
		December	2	1.1 (0.1)	-19.0 (0)	3	4.3 (0.4)	7.3 (0.2)	2.15
	North	April	1	1.1	-18.9	3	4.6 (0.5)	7.2 (0.3)	2.10
		July	3	1.0 (0)	-19.1 (0.1)	3	4.6 (0.3)	7.4 (0.5)	2.18
		December	3	1.2 (0.1)	-18.7 (0)	3	4.5 (0.5)	**7.6 (0.2)**	**2.23**
Mean			12	1.1 (0)	-18.9 (0.1)	18	4.5 (0.3)	7.3 (0.3)	2.15

Table 3.7. (continued):

				Dry Weight	Carbon		Dry Weight	Nitrogen	TP
Component	**Site**	**Collection Month**	**N**	mg (±SD)	$\delta^{13}C$ (±SD)	**N**	mg (±SD)	$\delta^{15}N$ (±SD)	
Environmental									
Seawater	South	April	3	6.5 (0.4)	-26.6 (0.1)	3	9.0 (0.8)	7.0 (0.5)	2.05
		July	3	6.2 (1.0)	-26.6 (0.1)	3	9.1 (0.5)	7.8 (0.2)	1.98
		December	3	5.9 (0.9)	-24.4 (1.7)	3	9.4 (0.5)	8.0 (0.4)	2.29
	North	April	3	5.8 (0.6)	-25.6 (0.7)	3	9.5 (0.2)	6.7 (0.2)	2.27
		July	3	5.9 (0.3)	-26.3 (0.5)	3	8.9 (0.7)	7.7 (0.8)	2.35
		December	3	5.8 (0.7)	**-27.5 (0.5)**	3	9.0 (0.6)	**8.1 (0.2)**	**2.37**
Mean			18	6.0 (0.6)	-26.2 (1.2)	18	9.1 (0.5)	7.6 (0.6)	2.22
Sediment	South	April	3	14.2 (0.1)	**-22.3 (0.2)**	3	14.4 (0.4)	6.3 (0.2)	1.84
		July	3	14.2 (0.1)	**-22.3 (0.3)**	3	14.5 (0.3)	6.3 (0.2)	1.85
		December	3	13.6 (0.4)	-23.6 (0.5)	3	14.7 (0.2)	6.5 (0)	1.89
	North	April	3	14.4 (0.4)	-22.8 (0.9)	3	14.3 (0.3)	**5.5 (0.1)**	**1.61**
		July	3	14.3 (0.2)	-24.0 (0.8)	3	14.6 (0.1)	5.9 (0.2)	1.74
		December	3	14.4 (0.4)	-24.8 (0)	3	14.5 (0.3)	6.1 (0.2)	1.79
Mean			18	14.2 (0.4)	-23.3 (1.0)	18	14.5 (0.3)	6.1 (0.4)	1.79

N/A Data not available

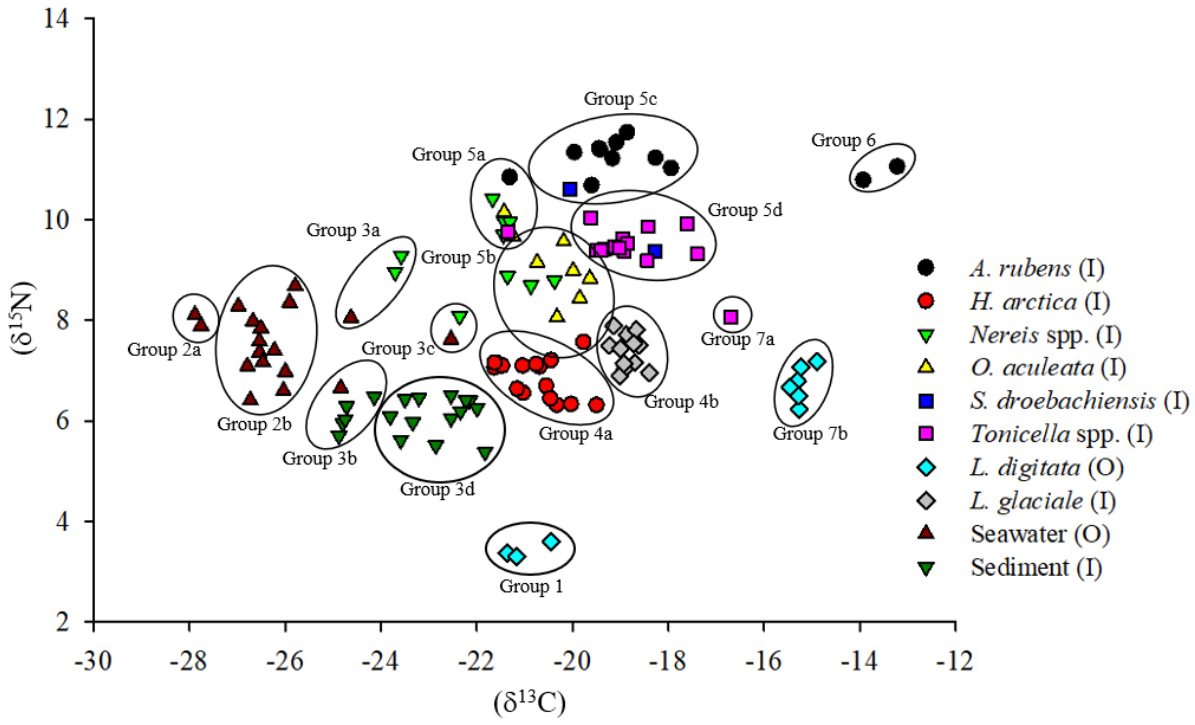

Figure 3.4. Biplot of bulk carbon ($\delta^{13}C$) and nitrogen ($\delta^{15}N$) stable isotope ratios of six animal species, two macroalgal species, and two environmental components (see Table 2.2 for species list) sampled in April, July, and December 2017 inside (I) or outside (O) of the South and North sites (see Figure 1.1). Components grouped (circled) based on agglomerative hierarchical cluster analysis.

Table 3.8. Tukey HSD test of bulk carbon ($\delta^{13}C$) and nitrogen ($\delta^{15}N$) stable isotope ratio groups based on agglomerative hierarchical cluster analysis. The six animal species, two macroalgal species, and two environmental components (see Table 2.2 for species list) sampled in April, July, and December 2017 inside (I) or outside (O) of the South and North sites (see Figure 1.1) were included in the analysis.

.

Component	Group	Sub-Group	($\delta^{13}C$) Tukey HSD	($\delta^{15}N$) Tukey HSD
L. digitata	1	-	C	D
Seawater	2	a	A	B
Seawater		b		
Seawater, *Nereis* spp.	3	a	B	C
Seawater, Sediment		b		
Seawater, *Nereis* spp.		c		
Sediment		d		
H. arctica	4	a	C	B, C
L. glaciale		b		
A. rubens, *Nereis* spp., *O. aculeata*, *Tonicella* spp.	5	a	C	A
Nereis spp., *O. aculeata*		b		
A. rubens, *S. droebachiensis*		c		
Tonicella spp., *S. droebachiensis*		d		
A. rubens	6	-	D	A
Tonicella spp.	7	a	D	B, C
L. digitata		b		

3.4 and Table 3.8). Group 1 contained *L. digitata* sampled in April, while Group 7b contained *L. digitata* sampled in July and December. 20:5ω3 [EPA], and 22:4ω6) exhibited a TMF > 1, and hence were biomagnified through trophic levels, whereas 21 had a TMF < 1, indicating biodilution (Table 3.9).

3.5. DISCUSSION

We investigated the seasonal and temporal trophodynamics of 10 components within a Northern and Southern site within the St. Philip's, Newfoundland rhodolith bed. This study extends Chapter II to provide the first characterization of temporal and spatial patterns of specific diets based on lipid, fatty acid, and stable isotope analyses in a rhodolith community. In Chapter II, we identified macroalgal-based detritus, but not kelp, as a key rhodolith community food source, identified 3 distinct trophic levels, and potentially revealed a specific link between an algal-based diet and carbon source in 3 species (*H. arctica*, *Tonicella* spp., *O. aculeata*). Here, we build on these findings and showed potentially strong benthic-pelagic coupling, seasonal changes to trophodynamics, and species-specific dietary changes based on food availability, including kelp.

3.5.1. Rhodolith community

Macroalgal and species composition commonly shifts seasonally in rhodolith beds because of changing environmental conditions such as water temperature and nutrient availability (Steller et al., 2003; Foster et al., 2007). In the Gulf of California, foliose red algae presence was significantly greater in the winter (Steller et al., 2003); however, in St. Philip's, epiphytic foliose red algae were apparent only in the fall (September and October, personal observations). This difference likely reflects greater light availability in the Newfoundland summer (Bélanger and Gagnon, 2020) and similar temperature conditions in both studies, where annual summer water

Table 3.9. Trophic multiplication factor (TMF) of 33 fatty acids (FA) as calculated from the slope (m) of corresponding linear relationship between FA concentration and bulk nitrogen ($\delta^{15}N$) stable isotope ratio (see section 2.3.8). Six animal species, two macroalgal species, and two environmental components (see Table 2.2 for species list) sampled in April, July, and December 2017 inside (I) or outside (O) of the South and North sites (see Figure 1.1) were included in the analysis. Only FA with a statistically significant correlation coefficient (r) are shown.

FA	TMF	m (±SE)	b (±SE)	r	p-value
20:3ω3	2.76	1.0 (0.3)	8.1 (0.2)	0.3	<0.001
20:1ω9	2.65	1.0 (0.1)	7.3 (0.2)	0.6	<0.001
18:3ω6	2.58	0.9 (0.4)	8.0 (0.2)	0.3	0.015
20:2ω6	2.50	0.9 (0.2)	7.3 (0.2)	0.4	<0.001
20:2*a*	2.11	0.7 (0.1)	7.7 (0.2)	0.6	<0.001
16:4ω3	1.41	0.3 (0)	7.6 (0.2)	0.5	<0.001
17:1	1.33	0.3 (0.1)	8.1 (0.2)	0.1	<0.001
20:1ω11	1.32	0.3 (0)	7.4 (0.1)	0.7	<0.001
18:1ω11	1.24	0.2 (0.1)	8.2 (0)	0.4	0.023
22:4ω6	1.21	0.2 (0.1)	8.2 (0.2)	0.1	0.020
20:4ω6	1.17	0.2 (0)	7.4 (0.2)	0.6	<0.001
20:5ω3	1.14	0.1 (0)	6.2 (0.2)	0.6	<0.001
18:1ω9	0.95	-0.1 (0)	8.7 (0.2)	-0.4	0.002
22:6ω3	0.94	-0.1 (0)	8.6 (0.2)	0.0	0.044
16:0	0.87	-0.1 (0)	10.2 (0.2)	-0.7	<0.001
16:1ω7	0.87	-0.1 (0)	9.2 (0.2)	-0.4	<0.001
14:0	0.85	-0.2 (0.1)	8.9 (0.3)	-0.2	0.032
*i*15:0	0.85	-0.2 (0.2)	9.1 (0.2)	-0.5	<0.001
18:4ω3	0.76	-0.3 (0.1)	8.9 (0.2)	-0.3	<0.001
21:5ω3	0.71	-0.3 (0.1)	8.6 (0.2)	-0.2	0.011
16:1ω11	0.64	-0.5 (0.1)	8.6 (0.2)	-0.4	0.001
18:4ω1	0.58	-0.6 (0.2)	8.6 (0.2)	-0.2	0.028
18:3ω3	0.57	-0.6 (0.1)	8.8 (0.2)	-0.3	<0.001
*ai*15:0	0.51	-0.7 (0.1)	8.8 (0.2)	-0.3	<0.001
16:3ω3	0.50	-0.7 (0.3)	8.5 (0.2)	-0.4	0.035
16:3ω4	0.48	-0.7 (0.2)	8.7 (0.2)	-0.3	0.001
*i*16:0	0.34	-1.1 (0.4)	8.7 (0.2)	-0.2	0.005
15:0	0.32	-1.1 (0.4)	9.0 (0.2)	-0.1	0.004
16:2ω4	0.22	-1.5 (0.4)	9.1 (0.3)	-0.3	0.001
16:1ω5	0.16	-1.8 (0.3)	9.1 (0.2)	-0.4	<0.001
16:1ω9	0.13	-2.1 (0.5)	8.9 (0.2)	-0.4	<0.001
14:1	0.07	-2.6 (1.0)	8.6 (0.2)	-0.2	0.011
*i*17:0	0.07	-2.7 (0.3)	9.4 (0.2)	-0.5	<0.001

temperatures in St. Philip's reach highs of 17°C (de Young and Sanderson, 1995) and annual winter water temperatures in the Gulf of California reach lows of 18 °C (Robles-Tamayo et al., 2018). Interestingly, foliose red algae coverage was one of the few species that differed significantly between our North (33.0%) and South (14.1%) sites. We cannot explain this phenomenon. We hypothesized the potential influence of freshwater feeding directly into the North site bed because Smith et al. (1999) attributed increased biomass of marine epiphytic algae in coastal marine systems to eutrophication. However, low abundance of terrestrial fatty acid biomarkers (18:2ω6 and 18:3ω3) and larger rhodoliths at the North site (114.1±9.9 cm^3) compared to the South site (70.0±4.5 cm^3) suggest otherwise; Bélanger and Gagnon (2020) showed that eutrophication inhibits rhodolith growth. After preliminary visual diving observations of sediment patches between rhodoliths, we also hypothesized that North site rhodoliths were larger due to an increased sedimentary load from the riverine source; sediment acts as protection from turbulence-induced movement and subsequent abrasion or breakage preventing growth (Gagnon et al., 2012). However, statistical tests revealed no significant differences in sediment cover between North (26%) and South (31%) sites. Additionally, the larger rhodoliths at the North site contained lower macrofaunal biomass (18.8 g kg^{-1} rhodoliths) than the smaller rhodoliths at the South site (34.5 g kg^{-1} rhodoliths). We hypothesize that hollow, nucleated, or less structurally complex larger rhodoliths offer fewer places for organisms to settle and hide than smaller rhodoliths. Regardless, we recommend that further studies investigate this trend by analyzing epiphyte coverage and macrofaunal biomass in closer proximity to the freshwater input.

3.5.2. Lipid content and classes

Lipid content fluctuates in organisms, including seasonal variability associated with changing environmental conditions, food availability, metabolic states, or reproductive status (Lloret and Planes, 2003; Meador, 2003; Parzanini et al., 2018). In our study, although individual lipid class of some individual components fluctuated seasonally (TAG in *Nereis spp.*, *S. droebachiensis*, *L. digitata*; ST in *O. aculeata*; AMPL in *S. droebachiensis*; PL in *L. digitata*; and HC in seawater), a significant overall lipid content change occurred in *Tonicella* spp. We detected significantly higher total lipid (13.7 mg g^{-1}) and lower PL levels (35.1%) simultaneously with elevated levels of TAG (45.3%) in July than in April or December. This change in lipid content offers evidence of a seasonal diet shift to accommodate reproductive timing. A decrease in long-term storage reserves (PL) and an increase in short-term reserves (TAG) indicates expending PL and replacement with TAG to enable rapid turnover of energy required for reproduction (Lee et al., 2006). Langer (1978) observed peak gonad index in April and May in Maine, indicating reproductive timing of *Tonicella marmorea*, one of our sampled species. Based on the geographical difference between Maine and Newfoundland and lipid class changes in our study, reproductive season of *T. marmorea* may begin later in Newfoundland.

In addition to organisms changing their lipid composition in response to their reproductive needs, we also expected to see lipid composition changes based on prevailing environmental conditions. In Chapter II, we suggested that high proportions of phospholipids and unsaturated fatty acids and low proportions of sterols reflected the cold-water conditions of the Northwest Atlantic in April (0.3 °C). As such, the warmer waters of July (6-8 °C) and December (4.4 °C) should have resulted in a less fluid lipid membrane consisting of lower proportions of phospholipids and unsaturated fatty acids and higher proportions of sterols and saturated fatty acids (Graf, 1992). We observed a decrease of phospholipid to sterol ratios from April (9.1) to July (6.3)

to December (5.9), but not of polyunsaturated to saturated fatty acid ratios (2.6 vs. 2.2 vs. 2.7). This trend could suggest that the more rigid membrane lipid structure of organisms in July and December reflects the warming temperatures, whereas the unchanged fatty acid composition suggests strong-benthic pelagic coupling and a reliance on the polyunsaturated fatty acids available as main food sources (diatoms as EPA or dinoflagellates as DHA).

3.5.3. Fatty acids

As discussed in Chapter II, high average levels of EPA (17.9%) and low average levels of DHA (2.8%) in April characterized our study sites, probably resulting from the spring diatom phytoplankton bloom (~0.4 mg/m^3). Our study documented similarly high average levels of EPA (18.2%) and low average levels of DHA (2.6%) at the end of the phytoplankton bloom in July (~0.07 mg/m^3), likely a result of the continuous sinking and seabed accumulation of phytoplankton and, ultimately, the organisms that utilize these resources; in shallow waters, diatoms often reach the benthos intact following the spring bloom (Graf, 1992). However, after the fall dinoflagellate phytoplankton bloom in December (nearly 0 mg/m^3), we observed lower average levels of EPA (14.1%) and higher average levels of DHA (3.5%) resulting in a significantly higher ratio of DHA compared to EPA (0.47 vs. 0.19 and 0.23). Combined with a lack of overall seasonal change between April and July, this change in diet suggests organisms prioritize EPA and its availability over DHA. Although these trends were consistent across our entire sample set, a few species, *H. arctica, O. aculeata, and A. rubens*, exemplify this phytoplankton and fatty acid biomarker shift. In particular, *H. arctica* decreased in the proportion of EPA from April (20.2%) and July (21.9%) to December (15.3%) combined with a substantial increase in the proportion of DHA from April (10.1%) and July (11.9%) to December (22.1%). This change in fatty acid biomarker provides

evidence of a strong benthic-pelagic coupling link that resulted in filter and suspension feeding invertebrates utilizing the available phytoplankton; feeding is likely based on a "bloom" vs. "no bloom" scenario rather than on distinct seasons (Iken et al., 2001). In Chapter II we suggested that *A. rubens* preys on *H. arctica* given their similar FA compositions and *A. rubens* preference of mollusks (Allen, 1983). Consistent levels of DHA in *A. rubens* from April through December compared to high levels of DHA observed in *H. arctica* support our hypothesis that *H. arctica* represents a major food source for *A. rubens*. However, while we cannot explain why little DHA appeared in the diets of other invertebrates, the increase in overall ARA from April (5.6%) and July (5.0%) to December (8.2%) offers one explanation for the low levels of DHA observed in most sampled invertebrates. For example, in *O. aculeata*, the proportion of EPA decreased from April (22%) and July (26%) to December (15%) and the proportion of ARA doubled from April (0.9%) and July (1.1%) to December (1.9%). Similar increases in proportional ARA also occurred in *Tonicella. spp.*, *Nereis spp.*, and *S. droebachiensis*. These increases in ARA rather than DHA suggest that, in the absence of abundant diatoms (EPA), organisms in the Newfoundland rhodolith community actively select an algal and kelp-derived (ARA) diet rather than feeding on abundant dinoflagellates (DHA). Additionally, kelp becomes more abundant in the summer and fall months, offering an alternative food source for primary consumers (Ramshaw et al., 2017). Building on Chapter II, we hypothesize that a resource partitioning relationship may exist where multiple species utilize different forms of the same food (i.e. algae/kelp and particulate algae/kelp) through various feeding strategies (i.e. suspension feeding and grazing), where the organisms benefit from the residual food from their co-habitants. In this instance, because suspension-feeding *O. aculeata* and grazing *Tonicella. spp*. likely cannot utilize large pieces of drift kelp, they could potentially utilize residual feeding matter in the form of particulate kelp after *S. droebachiensis* or other larger

organisms have grazed upon and broken it down (Krumhansl and Scheibling, 2012; Yorke et al., 2019). On the one hand, the complex structure of rhodoliths might trap algal particulates that subsequently become more enriched through microbial activity, resulting in increased nutritive value via increased nitrogen content (Tenore et al., 1984; Duggins and Eckman, 1997). On the other hand, *Nereis* spp. may not require large amounts on DHA (Narciso and da Fonseca, 2000) and given the similarity of its fatty acid profile to *O. aculeata* and *Tonicella* spp., likely receives ARA by preying or scavenging on organisms in the rhodolith community rather than feeding directly on a kelp source. However, depending on the specific *Nereis* species and population, we propose at least three different foraging strategies; *Nereis spp.* could: (1) simply prey on rhodolith biota (Copeland and Wieman, 1924), (2) swallow detrital and microbenthic algae in the uppermost sediment layer (Fauchald and Jumars, 1979) or, (3) filter feed on phytoplankton (Nielsen et al., 1995). Some populations may switch from one mode to another (Fauchald and Jumars, 1979). In fact, *N. diversicolor* can change its feeding strategy from predatory to suspension-feeding (Nielsen et al., 1995), whereas juvenile *N. virens* feed on detritus (Olivier et al., 1993) and feeding on plant matter promotes its growth (Olivier et al., 1996). In any case, the diverse fatty acid assemblage of *Nereis* spp. suggests the (presumably) juvenile samples we analysed likely fed on a mixture of prey, detritus, and phytoplankton.

Given proximity to riverine input and the observed statistical differences in rhodolith size, macrofauna abundance, and rhodolith foliose coverage between sites, we expected to see some variation in trophodynamics between sites. Instead, the few trophodynamic differences between sites and the lack of terrestrial biomarkers at the North site reject our hypothesis that riverine input affects trophodynamics of this rhodolith ecosystem. The rejection of the hypothesis may be due to the potential low-quality of terrestrial sources (i.e. refractory carbon) (Schlacher et al., 2009)

compared to the abundant availability of nutritious phytoplankton. Few terrestrial biomarkers in seawater samples also could indicate limited mixing between riverine and marine systems or destruction of terrestrial matter upon entering the ocean (Hedges et al., 1997). To detect potential abundances of terrestrial matter and to determine the nutrient flow into Broad Cove and its availability to the rhodolith ecosystem, we suggest analyzing water in the river, water where the mouth of the river meets the marina, and water at the mouth of the marina (Figure 1.1).

3.5.4. Stable isotopes

Although organisms such as *A. rubens*, *H. arctica*, and *O. aculeata* altered their diets following the spring phytoplankton bloom, the overall $\delta^{13}C$ and $\delta^{15}N$ isotopic signature values did not change seasonally or spatially. This lack of seasonal change in $\delta^{13}C$ suggests a two-tier dietary preference whereby the overall components of an organisms' food source (i.e. phytoplankton or bacteria) remain consistent throughout the year, but the specific components of their food source (i.e. diatom vs. dinoflagellate) changes. In addition, the unchanged seasonal $\delta^{15}N$ signatures of our focal species support this hypothesis because organisms did not drastically alter their diets, but rather adjusted to available resources.

Although no significant overall changes occurred seasonally, we observed some variation among individual organism $\delta^{13}C$ and $\delta^{15}N$ signatures. Small variations within individual organisms likely reflect food obtained during different stages of the recycling pathway outlined above. Because POM degrades as it settles on the seafloor, organisms feeding during later stages of the pathway (i.e. consuming resuspended material or predation) typically exhibit greater enrichment in $\delta^{13}C$ and $\delta^{15}N$ than organisms feeding on sinking POM (Iken et al., 2001). Furthermore, overlap in $\delta^{15}N$ values indicates reliance on similar food sources and fierce

competition for food (Iken et al., 2001). For example, samples of *Nereis* spp. split into four different bulk isotope subgroups (3a, 3c, 5a, 5b). We hypothesize this variation in isotope signature reflects opportunistic feeding, where *Nereis* spp. is not a major predator in this system but rather an opportunist. Similarly, the isotopic signatures of *A. rubens* varied greatly. Most notably, two *A. rubens* samples had far more enriched $\delta^{13}C$ signatures (13.6‰) than the majority of *A. rubens* samples (19.3‰). The former *A. rubens* likely obtained their food from sources outside the recyclable macroalgae pathway outlined above and therefore probably do not fall within the benthic-pelagic coupling link we proposed for other focal community members. Instead, given their enriched signatures, we hypothesize that these individuals preyed on organisms in a kelp rather than phytoplankton-based food web (Miller and Page, 2012). However, a seasonal species, (Schaffelke and Lüning, 1994), *L. digitata*, had the largest seasonal isotopic difference, with $\delta^{13}C$ values jumping from -21.0‰ in April to -15.2‰ in July and December, and its $\delta^{15}N$ increased from 3.4‰ in April to ~6.7‰ in July and December. Low values in April compared to both our seasonal samples and typical averages (-12‰ to -15‰ for $\delta^{13}C$ and 6.6‰ to 7‰ for $\delta^{15}N$) (Raven et al., 2002; Schaal et al., 2010) could reflect a March sea ice event inhibiting *L. digitata* photosynthesis and growth; prolonged sea ice limits light availability and thus may inhibit metabolic process resulting in stunted growth, reduced carbon uptake, a less enriched $\delta^{13}C$ value, and a lower $\delta^{15}N$ value (Hepburn et al., 2007). Given the abnormal April values of *L. digitata* and its effect on trophodynamic interpretation, it may be appropriate to remove them from this study (Appendix G). A removal of these samples would not change the dynamics of the food web, but would rather consolidate first- and second-order consumers, further emphasizing the ecosystem's interdependence, potential resource partitioning, and reliance on a shared resource -

phytoplankton. Confirmation of this anomaly in data will require further investigation of bulk isotope values of *L. digitata* in the spring months.

3.5.5. Conclusion and future research directions

Our study confirms our hypothesis that seasonal fluctuations in temperature and food availability affect lipid composition and diets of organisms. Our analyses revealed overall community shifts in diet from a diatom-based food web following the spring phytoplankton bloom to a kelp/algae-based food web during the fall months. We conclude that EPA is of much higher value than DHA to the Newfoundland rhodolith community. Our fatty acid and stable isotope analyses revealed additional evidence to support our Chapter II conclusion that organisms in the rhodolith food web community potentially feed in a resource partitioning relationship whereby first- and second- order consumers share a common resource (i.e. diatoms or kelp). Our seasonal studies also showed fluctuations in individual organism diets (i.e. *Tonicella* spp.) that reflected specific life-cycle requirements. However, these finding do not support our hypothesis that diets of organisms in close proximity to riverine input reflect freshwater influences. We suggest that future studies should compare more spatially distant sites that offer a stronger contrast in environmental conditions. Overall, our study expands the growing library of specific dietary patterns and trophodynamics of rhodolith communities.

Chapter IV

Summary and general conclusions

4.1 Overall objectives of the study

Researchers study trophic ecology to understand better energy transfer and feeding dynamics among organisms interacting in a community. An emerging variety of techniques and methodologies can elucidate these organismal relationships (Garvey and Whiles, 2016). Combining select techniques can yield a more comprehensive understanding of these interactions. As such, combining lipid, fatty acid, and stable isotope analyses can create a clearer delineation of organism interactions (e.g. predator-prey relationships), their diets (i.e. food and energy transfer), and dietary effects (e.g. changes to lipid structure) (Majdi et al., 2018).

Rhodoliths build important benthic community habitats globally (Foster, 2001; Gagnon et al., 2012). Their complex lattice structure and dense aggregations, termed rhodolith beds, create habitat for diverse assemblages of flora and fauna (Foster, 2001; Foster et al., 2007). Their contribution to marine biodiversity has prompted studies of rhodolith communities in the northeastern Atlantic (Grall et al., 2006; Hall-Spencer et al., 2010; Teichert et al., 2014), the Gulf of California (Foster et al., 2007; Riosmena-Rodriguez and Medina-López, 2010), Australia (Harvey and Bird, 2008), and Brazil (Foster, 2001; Amado-Filho et al., 2012b, 2012a). However, knowledge about trophodynamics in rhodolith beds is limited to isotopic studies in the northeastern Atlantic (Grall et al., 2006) and in the eastern Pacific (Gabara, 2014).

Several recent studies of rhodolith (*Lithothamnion glaciale*) beds in Newfoundland examined rhodolith morphology and macrofaunal diversity (Gagnon et al., 2012; Bélanger, 2020), sedimentation (Millar and Gagnon, 2018), eutrophication (Bélanger and Gagnon, 2020), and $CaCO_3$ production (Teed et al., 2020). This thesis aimed to build on both the broad global knowledge base and the rhodolith communities in Newfoundland by quantifying invertebrate interactions using a combination of modern trophic ecology techniques. By combining stable

isotope analyses with lipid and fatty acid analyses, this study is the first to provide the comprehensive resolution necessary to understand better the feeding dynamics and invertebrate interactions in rhodolith beds.

Overall, this thesis addressed three objectives: (1) to identify lipid composition of organisms to understand better if they prioritize functional strategies in relation to their environment; (2) to delineate trophic linkages among organisms to understand the nutritional value of their diets and the extent of benthic-pelagic coupling versus strictly benthic interactions; and (3) to describe how organisms respond to temporal (seasonal) and spatial (riverine input proximity) variation. My research involved laboratory analyses (fatty acid, lipid, and stable isotope) and a survey of macrofaunal abundance and rhodolith morphology of a rhodolith bed off St. Philip's in Conception Bay, Newfoundland (see Chapter II).

4.2 Trophodynamics of a Newfoundland rhodolith bed community (Chapter II)

Chapter II quantified nutritional patterns and trophic linkages of six dominant echinoderm, bivalve, gastropod, and polychaete species in a Newfoundland rhodolith bed to increase knowledge of trophic relationships in cold-water rhodolith communities. I paired a survey of macrofaunal abundance and rhodolith morphology with lipid, fatty acid, and stable isotope analyses to test the hypotheses that: (1) the lipid composition of organisms generally reflects the predominantly cold-water conditions of Newfoundland; and (2) bottom up by planktivores and detritivores largely control the food web. I collected rhodoliths from a large (>500 m^2) rhodolith bed in St. Philip's, Newfoundland for the survey and all trophodynamic analyses. From my abundance survey, I documented high densities of (>80%) of chitons (*Tonicella marmorea* and *T. rubra*) and daisy brittle stars (*O. aculeata*) as well as overall species composition, morphological

traits of rhodoliths (shape and size), and total rhodolith biomass (19.5 kg m^{-2}); all findings aligned with those of Gagnon et al. (2012). My lipid and fatty acid analyses demonstrated high levels of phospholipids and unsaturated fatty acids combined with low sterols in all animal species. These findings indicate a need for increased membrane fluidity in response to cold temperatures. My fatty acid and stable isotope analyses demonstrated that many organisms in the rhodolith food web community feed on a shared resource - diatoms. Fatty acid and stable isotope analyses also revealed algae-based detritus as a key food source within rhodolith communities. We identified three distinct trophic levels (producers, suspension/filter feeders and grazers, and predators), and potentially discovered a specific link between an algae-based diet and carbon source in clams (*H. arctica*), chitons (*Tonicella* spp.), and brittle stars (*O. aculeata*).

4.3 Spatio-temporal variation of trophodynamics in a Newfoundland rhodolith bed community (Chapter III)

Chapter III extended on the findings of Chapter II by examining spatio-temporal variation in nutritional patterns and trophic linkages among common macrofauna and flora from a Newfoundland rhodolith bed. I tested hypotheses that: (1) seasonal fluctuations in temperature and food availability affect lipid composition and diets of organisms; (2) diets of organisms near riverine input reflect its freshwater origins. To this end, I sampled rhodoliths at two sites in the bed that presumably differed in physicochemical characteristics in April, July, and December 2017 to capture the spring and fall phytoplankton blooms. Rhodolith size and abundance of epiphytes differed significantly between sites despite similar biomass of rhodoliths and cryptofauna. I showed potentially strong benthic-pelagic coupling, seasonal changes to trophodynamics, and species-specific dietary changes based on food availability. The fatty acid and stable isotope

analyses revealed overall community shifts in diet from a diatom-based food web following the spring phytoplankton bloom to a kelp/algae-based food web during the fall months. This comparison also demonstrated the greater value of EPA (20:5ω3) than DHA (22:6ω3) to the Newfoundland rhodolith community. These analyses further supported findings of Chapter II that organisms in the rhodolith food web community potentially feed in a resource partitioning relationship whereby first- and second- order consumers share a common resource (i.e. diatoms or kelp). My seasonal study showed fluctuations in individual organism diets (i.e. *Tonicella* spp.) reflecting their life-cycle requirements. However, my study does not support my hypothesis that diets of organisms near riverine input reflect its freshwater origins.

4.4 Importance of this study

This study expands on an increasing number of rhodolith bed ecological studies by examining trophodynamics within a Newfoundland rhodolith bed. This is the first rhodolith-based study to combine stable isotope analyses with lipid and fatty acid analyses and thus yields a more comprehensive assessment of rhodolith bed ecology. My findings help further understand linkages between water-column productivity processes (i.e. phytoplankton blooms) and subtidal benthic communities. Rhodolith beds serve as important ecosystem engineers for a diverse group of organisms (Jones et al., 1994; Gagnon et al., 2012). My study revealed the essential nutrients required by specific organisms in this ecosystem. The findings of this study may be used to monitor the health of the rhodolith bed communities.

Based on my findings, I conceptualized a partial food web detailing the interpreted linkages among food sources and organisms in the studied rhodolith bed (Figure 4.1). This proposed food web may help understand the direct linkages and relationships among organisms and essential

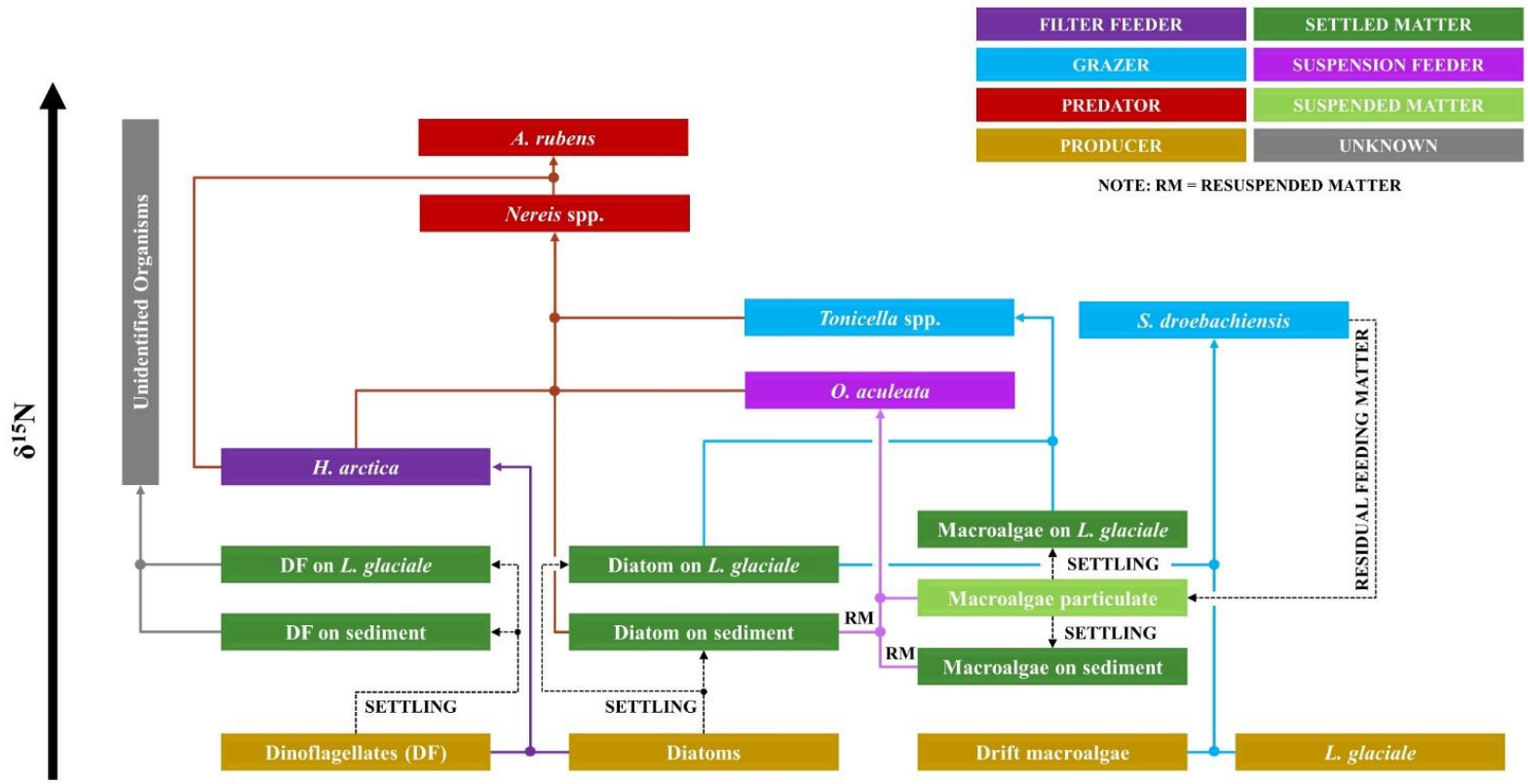
FILTER FEEDER
SETTLED MATTER
GRAZER
SUSPENSION FEEDER
PREDATOR
SUSPENDED MATTER
PRODUCER
UNKNOWN
NOTE: RM = RESUSPENDED MATTER
δ15N
Unidentified Organisms
A. rubens
Nereis spp.
Tonicella spp.
S. droebachiensis
O. aculeata
H. arctica
RESIDUAL FEEDING MATTER
Macroalgae on L. glaciale
DF on L. glaciale
Diatom on L. glaciale
SETTLING
Macroalgae particulate
DF on sediment
Diatom on sediment
RM
SETTLING
RM
Macroalgae on sediment
SETTLING
SETTLING
Dinoflagellates (DF)
Diatoms
Drift macroalgae
L. glaciale

Figure 4.1. Rhodolith community food web model based on fatty acid and bulk stable isotope ($\delta^{13}C$ and $\delta^{15}N$) results of six animal species, two macroalgal species, and two environmental components (see Table 2.2 for species list) sampled in April, July, and December 2017 at the South and North sites (see Figure 1.1). Flow of energy follows the $\delta^{15}N$ values on the isotope biplot (see Figure 3.4). Dotted lines represent settling and residual feeding matter. RM = Resuspended matter. DF = Dinoflagellates. Unidentified organisms refers to organisms not sampled in the present study but that are likely using this resource.

nutrients, and it demonstrates the interconnectedness of the rhodolith ecosystem. My results confirm previous studies that showed algae-based detritus as a key food source within rhodolith beds (Grall et al., 2006; Gabara, 2014) and supports the dominance of chitons (*Tonicella marmorea* and *T. rubra*) and daisy brittle stars (*Ophiopholis aculeata*) in rhodolith beds, as previously documented by Gagnon et al. (2012) and Bélanger (2020). Findings indicate that certain organisms (e.g. *H. arctica* and *O. aculeata*) in Newfoundland rhodolith beds transfer energy from the water column to the benthos (i.e. benthic-pelagic coupling) by utilizing phytoplankton as a primary food source during blooms (Figure 4.1) (Griffiths et al., 2017; Bélanger, 2020). Additionally, these organisms may change their lipid composition in response to seasonal water temperatures and life-cycle requirements. This finding has significant implications for these organisms on a regional scale given ongoing global climate change; a shift in availability or timing of resources may affect the health and function of the entire community.

4.5 Future directions

My study provides a detailed account of rhodolith community feeding relationships and interactions based on a portion of the larger community. I focused on the most abundant species and habitat components of the rhodolith bed (common sea star, *Asterias rubens*; wrinkled rock-borer, *Hiatella arctica*; daisy brittle star, *Ophiopholis aculeata*; polychaetes, *Nereis* spp.; green sea urchin, *Strongylocentrotus droebachiensis*; chitons, *Tonicella* spp., rhodolith, *Lithothamnion glaciale*; kelp, *Laminaria digitata*, seawater from above the rhodolith bed, and sediment underlying the rhodolith bed), which together represent about 7% of the 109 taxa Bélanger (2020) identified in his earlier study of the same rhodolith bed. To gain a more comprehensive understanding of the multiple interactions among organisms in the rhodolith community, future

studies should focus on additional organisms not sampled (for a list refer to Tables 2.1 and 3.1) as well as a more detailed analysis of the underlying sediment. In Chapter II, I discussed the potential of amphipods and copepods as important food sources and thus recommend a more thorough investigation of amphipod and copepod trophodynamics and their potential relationship to the rest of the rhodolith community.

Temporal analysis (Chapter III) revealed a strong seasonal component to diet; I demonstrated a strong link between seasonal phytoplankton blooms and food availability and intake. Moreover, this is the first study to investigate seasonal trophodynamics in a rhodolith bed. However, I was only able to capture data from one seasonal cycle (late spring, early summer, late fall) which included a sea ice event anomaly in March. Furthermore, phytoplankton blooms can vary in timing and magnitude (Friedland et al., 2018). On the one hand, to understand how organisms continually cope with changing environments, future studies could focus on longer time scales over multiple years. On the other hand, studies looking for more precise shifts in diet could sample organisms monthly, necessitating greater time commitments and financial resources. As discussed, my study only sampled organisms during or following a phytoplankton event and subsequently demonstrated the necessity of phytoplankton in diets of rhodolith associated organisms. To understand how organisms alter their diet outside of a phytoplankton bloom during periods of limited resource availability, I recommend that future studies of temporal seas sample outside of phytoplankton blooms (i.e. the winter months).

Spatial analysis showed no clear relationship between organism diet and proximity to freshwater input. I attribute this outcome to the close proximity of our two study sites; we tried to sample opposite ends of the large St. Philip's rhodolith bed, but this distance was probably insufficient. Bélanger and Gagnon (2020) demonstrated that natural eutrophication conditions

affect rhodolith growth. Eutrophication should, in principle, influence rhodolith-associated organism diet (van der Lee et al., 2020). Sampling distinct rhodolith beds in conjunction with monitoring eutrophication levels would provide more concrete answers regarding the relationship between freshwater input and rhodolith community health. Furthermore, because this is the first comprehensive trophodynamic analysis of rhodolith beds, there was very little literature available for comparison. My study may be used as a steppingstone for future studies on rhodolith bed trophodynamics, and to eventually create a dataset of global rhodolith bed community interactions. Discovering the true importance of these unique ecosystems to the future health of our planet crucially hinges upon understanding how different rhodolith communities interact with their surrounding environments.

Literature Cited

Ackman, R.G., 1986. WCOT (capillary) gas-liquid chromatography. Analysis of Oils and Fats 137–206.

Allen, P.L., 1983. Feeding behaviour of *Asterias rubens* (L.) on soft bottom bivalves: a study in selective predation. Journal of Experimental Marine Biology and Ecology 70, 79–90.

Allen, W.V., 1968. Fatty-acid synthesis in the echinoderms: *Asterias rubens*, *Echinus esculentus* and *Holothuria forskali*. Journal of the Marine Biological Association of the United Kingdom 48, 521-533.

Amado-Filho, G.M., Moura, R.L., Bastos, A.C., Salgado, L.T., Sumida, P.Y., Guth, A.Z., Francini-Filho, R.B., Pereira-Filho, G.H., Abrantes, D.P., Brasileiro, P.S., 2012a. Rhodolith beds are major $CaCO_3$ bio-factories in the tropical South West Atlantic. PloS one 7, e35171.

Amado-Filho, G.M., Pereira-Filho, G.H., Bahia, R.G., Abrantes, D.P., Veras, P.C., Matheus, Z., 2012b. Occurrence and distribution of rhodolith beds on the Fernando de Noronha Archipelago of Brazil. Aquatic Botany 101, 41–45.

Arendt, K.E., Jónasdóttir, S.H., Hansen, P.J., Gärtner, S., 2005. Effects of dietary fatty acids on the reproductive success of the calanoid copepod *Temora longicornis*. Marine Biology 146, 513–530.

Armonies, W., 2000. On the spatial scale needed for benthos community monitoring in the coastal North Sea. Journal of Sea Research 43, 121–133.

Arts, M.T., Ackman, R.G., Holub, B.J., 2001. "Essential fatty acids" in aquatic ecosystems: a crucial link between diet and human health and evolution. Canadian Journal of Fisheries and Aquatic Sciences 58, 122–137.

Arts, M.T., Brett, M.T., Kainz, M.J., 2009. Lipids in aquatic ecosystems. Lipids in Aquatic Ecosystems xv–xx.

Beaugrand, G., Ibañez, F., Lindley, J.A., Reid, P.C., 2002. Diversity of calanoid copepods in the North Atlantic and adjacent seas: species associations and biogeography. Marine Ecology Progress Series 232, 179-195.

Bec, A., Perga, M.E., Desvilettes, C., Bourdier, G., 2010. How well can the fatty acid content of lake seston be predicted from its taxonomic composition? Freshwater Biology 55, 1958-1972.

Bélanger, D., 2020. Growth controls of rhodoliths (*Lithothamnion glaciale*) and relationships between structural complexity and macrofaunal diversity in subarctic rhodolith beds (Doctoral dissertation). Memorial University of Newfoundland, St. John's, NL.

Bélanger, D., Gagnon, P., 2020. Low growth resilience of subarctic rhodoliths (*Lithothamnion glaciale*) to coastal eutrophication. Marine Ecology Progress Series 642, 117–132.

Berlandi, R.M., de O. Figueiredo, M.A., Paiva, P.C., 2012. Rhodolith morphology and the diversity of polychaetes off the southeastern Brazilian coast. Journal of Coastal Research 28, 280–287.

Bierwagen, S.L., Heupel, M.R., Chin, A., Simpfendorfer, C.A., 2018. Trophodynamics as a tool for understanding coral reef ecosystems. Frontiers in Marine Science 5, 24.

Borgå, K., Kidd, K.A., Muir, D.C.G., Berglund, O., Conder, J.M., Gobas, F.A.P.C., Kucklick, J., Malm, O., Powell, D.E., 2012. Trophic magnification factors: considerations of ecology, ecosystems, and study design. Integrated Environmental Assessment and Management 8, 64–84.

Bouillon, S., Connolly, R.M., Gillikin, D.P., 2011. 7.07 Use of stable isotopes to understand food webs and ecosystem functioning in estuaries. Treatise on Estuarine and Coastal Science 7.

Bruno, J., Bertness, M.D., 2001. Positive interactions, facilitations and foundation species. Marine Community Ecology 201–220.

Budge, S.M., Iverson, S.J., Koopman, H.N., 2006. Studying trophic ecology in marine ecosystems using fatty acids: A primer on analysis and interpretation. Marine Mammal Science.

Budge, S.M., Parrish, C.C., 1998. Lipid biogeochemistry of plankton, settling matter and sediments in Trinity Bay, Newfoundland. II. Fatty acids. Organic Geochemistry 29, 1547–1559.
Budge, S.M., Parrish, C.C., Mckenzie, C.H., 2001. Fatty acid composition of phytoplankton, settling particulate matter and sediments at a sheltered bivalve aquaculture site. Marine Chemistry 76, 285–303.
Budge, S.M., Springer, A.M., Iverson, S.J., Sheffield, G., 2007. Fatty acid biomarkers reveal niche separation in an Arctic benthic food web. Marine Ecology Progress Series 336, 305–309.
Cabana, G., Rasmussen, J.B., 1996. Comparison of aquatic food chains using nitrogen isotopes. Proceedings of the National Academy of Sciences 93, 10844–10847.
Carreón-Palau, L., Parrish, C.C., del Angel-Rodríguez, J.A., Pérez-España, H., Aguiñiga-García, S., 2013. Revealing organic carbon sources fueling a coral reef food web in the Gulf of Mexico using stable isotopes and fatty acids. Limnology and Oceanography 58, 593–612.
Carreón-Palau, L., Parrish, C.C., Perez-Espana, H., 2017. Urban sewage lipids in the suspended particulate matter of a coral reef under river influence in the South West Gulf of Mexico. Water research 123, 192-205.
Castell, J.D., Kennedy, E.J., Robinson, S.M.C., Parsons, G.J., Blair, T.J., Gonzalez-Duran, E., 2004. Effect of dietary lipids on fatty acid composition and metabolism in juvenile green sea urchins (*Strongylocentrotus droebachiensis*). Aquaculture 242, 417–435.
Christensen, H., Kanneworff, E., 1986. Sedimentation of phytoplankton during a spring bloom in the Øresund. Ophelia 26, 109–122.
Christie, W.W., 1989. Gas chromatographic analysis of fatty acid derivatives. Gas Chromatography and Lipids: A Practical Guide 85–128.
Christie, W.W., 1982. A simple procedure for rapid transmethylation of glycerolipids and cholesteryl esters. Journal of Lipid Research 23, 1072–1075.
Ciapa, B., Allemand, D., de Renzis, G., 1995. Effect of arachidonic acid on Na^+/H^+ exchange and neutral amino acid transport in sea urchin eggs. Experimental Cell Research 218, 248–254.
Clarke, K.R., Somerfield, P.J., Chapman, M.G., 2006. On resemblance measures for ecological studies, including taxonomic dissimilarities and a zero-adjusted Bray–Curtis coefficient for denuded assemblages. Journal of Experimental Marine Biology and Ecology 330, 55–80.
Colombo, S.M., Wacker, A., Parrish, C.C., Kainz, M.J., Arts, M.T., 2017. A fundamental dichotomy in long-chain polyunsaturated fatty acid abundance between and within marine and terrestrial ecosystems. Environmental Reviews 25, 163–174.
Connelly, T.L., Deibel, D., Parrish, C.C., 2014. Trophic interactions in the benthic boundary layer of the Beaufort Sea shelf, Arctic Ocean: Combining bulk stable isotope and fatty acid signatures. Progress in Oceanography 120, 79–92.
Copeland, M., Wieman, H.L., 1924. The chemical sense and feeding behavior of *Nereis virens*. Sars. The Biological Bulletin 47, 231–238.
Copeman, L.A., Parrish, C.C., 2003. Marine lipids in a cold coastal ecosystem: Gilbert Bay, Labrador. Marine Biology 143, 1213–1227.
Crockett, E.L., 1998. Cholesterol function in plasma membranes from ectotherms: membrane-specific roles in adaptation to temperature. American Zoologist 38, 291–304.
Dalsgaard, J., st. John, M., Kattner, G., Müller-Navarra, D., Hagen, W., 2003. Fatty acid trophic markers in the pelagic marine environment. Advances in Marine Biology.
Daume, S., Brand-Gardner, S., Woelkerling, W.J., 1999. Settlement of abalone larvae (*Haliotis laevigata Donovan*) in response to non-geniculate coralline red algae (Corallinales, Rhodophyta). Journal of Experimental Marine Biology and Ecology 234, 125–143.

de Grave, S., Whitaker, A., 1999. A census of maërl beds in Irish waters. Aquatic Conservation: Marine and Freshwater Ecosystems 9, 303–311.
de Young, B., Sanderson, B., 1995. The circulation and hydrography of Conception Bay, Newfoundland. Atmosphere-Ocean 33, 135–162.
DeNiro, M.J., Epstein, S., 1981. Influence of diet on the distribution of nitrogen isotopes in animals. Geochimica et Cosmochimica Acta 45, 341–351.
DeNiro, M.J., Epstein, S., 1978. Influence of diet on the distribution of carbon isotopes in animals. Geochimica et Cosmochimica Acta 42, 495–506.
Drazen, J.C., Phleger, C.F., Guest, M.A., Nichols, P.D., 2009. Lipid composition and diet inferences in abyssal macrourids of the eastern North Pacific. Marine Ecology Progress Series 387, 1–14.
Drazen, J.C., Phleger, C.F., Guest, M.A., Nichols, P.D., 2008a. Lipid, sterols and fatty acids of abyssal polychaetes, crustaceans, and a cnidarian from the northeast Pacific Ocean: food web implications. Marine Ecology Progress Series 372, 157–167.
Drazen, J.C., Phleger, C.F., Guest, M.A., Nichols, P.D., 2008b. Lipid, sterols and fatty acid composition of abyssal holothurians and ophiuroids from the North-East Pacific Ocean: food web implications. Comparative Biochemistry and Physiology Part B: Biochemistry and Molecular Biology 151, 79–87.
Duffill Telsnig, J.I., Jennings, S., Mill, A.C., Walker, N.D., Parnell, A.C., Polunin, N.V.C., 2019. Estimating contributions of pelagic and benthic pathways to consumer production in coupled marine food webs. Journal of Animal Ecology 88, 405–415.
Duggins, D.O., Eckman, J.E., 1997. Is kelp detritus a good food for suspension feeders? Effects of kelp species, age and secondary metabolites. Marine Biology 128, 489–495.
Ellis, J., Schneider, D.C., 2008. Spatial and temporal scaling in benthic ecology. Journal of Experimental Marine Biology and Ecology 366, 92–98.
Fauchald, K., Jumars, P.A., 1979. The diet of worms: a study of polychaete feeding guilds. Oceanography and Marine Biology Annual Review.
Fleurence, J., Gutbier, G., Mabeau, S., Leray, C., 1994. Fatty acids from 11 marine macroalgae of the French Brittany coast. Journal of Applied Phycology 6, 527–532.
Folch, J., Lees, M., Sloane Stanley, G.H., 1957. A simple method for the isolation and purification of total lipides from animal tissues. The Journal of Biological Chemistry 226, 497–509.
Foster, M.S., 2001. Rhodoliths: Between rocks and soft places. Journal of Phycology.
Foster, M.S., McConnico, L.C., Lundsten, L., Wadsworth, T., Kimball, T., Brooks, L.B., Medina-López, M., Riosmena-Rodríguez, R., Hernandez-Carmona, G., Vásquez-Elizondo, R.M., 2007. Diversity and natural history of a *Lithothamnion muelleri-Sargassum horridum* community in the Gulf of California. Ciencias Marinas 33, 367–384.
Fraser, A.J., 1989. Triacylglycerol content as a condition index for fish, bivalve, and crustacean larvae. Canadian Journal of Fisheries and Aquatic Sciences 46, 1868–1873.
Fredriksen, S., 2003. Food web studies in a Norwegian kelp forest based on stable isotope ($\delta^{13}C$ and $\delta^{15}N$) analysis. Marine Ecology Progress Series 260, 71-81.
Freiwald, A., Henrich, R., 1994. Reefal coralline algal build-ups within the Arctic Circle: morphology and sedimentary dynamics under extreme environmental seasonality. Sedimentology 41, 963–984.
Friedland, K.D., Mouw, C.B., Asch, R.G., Ferreira, A.S.A., Henson, S., Hyde, K.J.W., Morse, R.E., Thomas, A.C., Brady, D.C., 2018. Phenology and time series trends of the dominant seasonal phytoplankton bloom across global scales. Global Ecology and Biogeography 27, 551–569.

Fullarton, J.G., Dando, P.R., Sargent, J.R., Southwards, A.J., Southward, E.C., 1995. Fatty acids of hydrothermal vent *Ridgeia piscesae* and inshore bivalves containing symbiotic bacteria. Journal of the Marine Biological Association of the United Kingdom 75, 455–468.

Gabara, S.S., 2014. Community structure and energy flow within rhodolith habitats at Santa Catalina Island, CA. San José State University, San José, CA.

Gabara, S.S., Hamilton, S.L., Edwards, M.S., Steller, D.L., 2018. Rhodolith structural loss decreases abundance, diversity, and stability of benthic communities at Santa Catalina Island, CA. Marine Ecology Progress Series 595, 71–88.

Gagné, J.A., Mann, K.H. and Chapman, A.R.O., 1982. Seasonal patterns of growth and storage in *Laminaria longicruris* in relation to differing patterns of availability of nitrogen in the water. Marine Biology 69. 91-101.

Gagnon, P., Matheson, K., Stapleton, M., 2012. Variation in rhodolith morphology and biogenic potential of newly discovered rhodolith beds in Newfoundland and Labrador (Canada). Botanica Marina 55, 85–99.

Gale, K.S.P., Hamel, J.-F., Mercier, A., 2013. Trophic ecology of deep-sea Asteroidea (Echinodermata) from eastern Canada. Deep Sea Research Part I: Oceanographic Research Papers 80, 25–36.

Galois, R., Richard, P., Fricourt, B., 1996. Seasonal variations in suspended particulate matter in the Marennes-Oleron Bay, France, using lipids as biomarkers. Estuarine, Coastal and Shelf Science 43, 335–357.

Garvey, J.E., Whiles, M., 2016. Trophic ecology. CRC Press.

Górska, B., Włodarska-Kowalczuk, M., 2017. Food and disturbance effects on Arctic benthic biomass and production size spectra. Progress in Oceanography 152, 50–61.

Graf, G., 1992. Benthic-pelagic coupling: a benthic view. Oceanography and Marine Biology: An Annual Review.

Graham, D.J., Midgley, N.G., 2000. Graphical representation of particle shape using triangular diagrams: an Excel spreadsheet method. Earth Surface Processes and Landforms 25, 1473–1477.

Grall, J., Leloch, F., Guyonnet, B., Riera, P., 2006. Community structure and food web based on stable isotopes ($\delta^{15}N$ and $\delta^{13}C$) analysis of a North Eastern Atlantic maërl bed. Journal of Experimental Marine Biology and Ecology 338, 1–15.

Griffiths, J.R., Kadin, M., Nascimento, F.J.A., Tamelander, T., Törnroos, A., Bonaglia, S., Bonsdorff, E., Brüchert, V., Gårdmark, A., Järnström, M., 2017. The importance of benthic–pelagic coupling for marine ecosystem functioning in a changing world. Global Change Biology 23, 2179–2196.

Guerra-García, J.M., Martínez-Pita, I., Pita, M.L., 2004. Fatty acid composition of the Caprellidea (Crustacea: Amphipoda) from the Strait of Gibraltar. Scientia Marina 68, 501–510.

Guest, M.A., Nichols, P.D., Frusher, S.D., Hirst, A.J., 2008. Evidence of abalone (*Haliotis rubra*) diet from combined fatty acid and stable isotope analyses. Marine Biology 153, 579–588.

Gurr, M.I., Harwood, J.L., Frayn, K.N., 2002. Lipid biochemistry. Springer.

Hair, J.F., Black, W.C., Babin, B.J., Anderson, R.E., Tatham, R., 2006. Multivariate data analysis. Uppersaddle River.

Halfar, J., Zack, T., Kronz, A., Zachos, J.C., 2000. Growth and high-resolution paleoenvironmental signals of rhodoliths (coralline red algae): a new biogenic archive. Journal of Geophysical Research: Oceans 105, 22107–22116.

Hall, J.M., Parrish, C.C., Thompson, R.J., 2000. Importance of unsaturated fatty acids in regulating bivalve and finfish membrane fluidity in response to changes in environmental temperature. Seafood in Health and Nutrition, 435–448.

Hall-Spencer, J.M., Kelly, J., Maggs, C.A., 2010. Background document for maërl. OSPAR Commission, 491.
Hamilton, S., 1992. Extraction of lipids and derivative formation. Lipid Analysis: A Practical Approach, 13–64.
Harvey, A.S., Bird, F.L., 2008. Community structure of a rhodolith bed from cold-temperate waters (southern Australia). Australian Journal of Botany 56, 437–450.
Harvey, A.S., Harvey, R.M., Merton, E., 2017. The distribution, significance and vulnerability of Australian rhodolith beds: a review. Marine and Freshwater Research 68, 411–428.
Hazel, J.R., Williams, E.E., Livermore, R., Mozingo, N., 1991. Thermal adaptation in biological membranes: functional significance of changes in phospholipid molecular species composition. Lipids 26, 277–282.
Hedges, J.I., Keil, R.G., Benner, R., 1997. What happens to terrestrial organic matter in the ocean? Organic geochemistry 27, 195-212.
Henderson, R.J., Hegseth, E.N., Park, M.T., 1998. Seasonal variation in lipid and fatty acid composition of ice algae from the Barents Sea. Polar Biology 20, 48–55.
Hepburn, C.D., Holborow, J.D., Wing, S.R., Frew, R.D., Hurd, C.L., 2007. Exposure to waves enhances the growth rate and nitrogen status of the giant kelp *Macrocystis pyrifera*. Marine Ecology Progress Series 339, 99–108.
Herman, P.M.J., Middelburg, J.J., Widdows, J., Lucas, C.H., Heip, C.H.R., 2000. Stable isotopes as trophic tracers: combining field sampling and manipulative labelling of food resources for macrobenthos. Marine Ecology Progress Series 204, 79–92.
Himmelman, J.H., Dumont, C.P., Gaymer, C.F., Vallières, C., Drolet, D., 2008. Spawning synchrony and aggregative behaviour of cold-water echinoderms during multi-species mass spawnings. Marine Ecology Progress Series 361, 161–168.
Hines, A.H., 1982. Coexistence in a kelp forest: size, population dynamics, and resource partitioning in a guild of spider crabs (Brachyura, Majidae). Ecological Monographs 52, 179-198.
Hinojosa-Arango, G., Maggs, C.A., Johnson, M.P., 2009. Like a rolling stone: the mobility of maërl (Corallinaceae) and the neutrality of the associated assemblages. Ecology 90, 517–528.
Historical Data - Climate - Environment and Climate Change Canada [WWW Document], n.d. URL https://climate.weather.gc.ca/historical_data/search_historic_data_e.html#. (accessed 9.19.19).
Honya, M., Kinoshita, T., Ishikawa, M., Mori, H., Nisizawa, K., 1994. Seasonal variation in the lipid content of cultured *Laminaria japonica*: fatty acids, sterols, β-carotene and tocopherol. Journal of Applied Phycology 6, 25–29.
Huggett, M.J., Williamson, J.E., de Nys, R., Kjelleberg, S., Steinberg, P.D., 2006. Larval settlement of the common Australian sea urchin *Heliocidaris erythrogramma* in response to bacteria from the surface of coralline algae. Oecologia 149, 604–619.
Hussey, N.E., Macneil, M.A., Mcmeans, B.C., Olin, J.A., Dudley, S.F.J., Cliff, G., Wintner, S.P., Fennessy, S.T., Fisk, A.T., 2014. Rescaling the trophic structure of marine food webs. Ecology Letters 17, 239–250.
Iken, K., Bluhm, B.A., Gradinger, R., 2005. Food web structure in the high Arctic Canada Basin: evidence from $\delta^{13}C$ and $\delta^{15}N$ analysis. Polar Biology 28, 238–249.
Iken, K., Brey, T., Wand, U., Voigt, J., Junghans, P., 2001. Food web structure of the benthic community at the Porcupine Abyssal Plain (NE Atlantic): a stable isotope analysis. Progress in Oceanography 50, 383–405.
Iverson, S.J., 2009. Tracing aquatic food webs using fatty acids: from qualitative indicators to quantitative determination. Lipids in Aquatic Ecosystems, 281–308.

James, D.W., 2000. Diet, movement, and covering behavior of the sea urchin *Toxopneustes roseus* in rhodolith beds in the Gulf of California, México. Marine Biology 137, 913–923.
Jaschinski, S., Brepohl, D.C., Sommer, U., 2011. Seasonal variation in carbon sources of mesograzers and small predators in an eelgrass community: stable isotope and fatty acid analyses. Marine Ecology Progress Series 431, 69–82.
Jones, C.G., Lawton, J.H., Shachak, M., 1994. Organisms as ecosystem engineers, in: Ecosystem Management 130–147.
Kamenos, N A, Moore, P.G., Hall-Spencer, J.M., 2004a. Attachment of the juvenile queen scallop (*Aequipecten opercularis* (L.)) to maërl in mesocosm conditions; juvenile habitat selection. Journal of Experimental Marine Biology and Ecology 306, 139–155.
Kamenos, Nicholas A., Moore, P.G., Hall-Spencer, J.M., 2004b. Nursery-area function of maërl grounds for juvenile queen scallops *Aequipecten opercularis* and other invertebrates. Marine Ecology Progress Series 274, 183–189.
Kelly, J.R., Scheibling, R.E., 2012. Fatty acids as dietary tracers in benthic food webs. Marine Ecology Progress Series 446, 1–22.
Kelly, J.R., Scheibling, R.E., Iverson, S.J., Gagnon, P., 2008. Fatty acid profiles in the gonads of the sea urchin *Strongylocentrotus droebachiensis* on natural algal diets. Marine Ecology Progress Series 373, 1–9.
Kharlamenko, V.I., Kiyashko, S.I., Imbs, A.B., Vyshkvartzev, D.I., 2001. Identification of food sources of invertebrates from the seagrass *Zostera marina* community using carbon and sulfur stable isotope ratio and fatty acid analyses. Marine Ecology Progress Series 220, 103–117.
Kiriakoulakis, K., Fisher, E., Wolff, G.A., Freiwald, A., Grehan, A., Roberts, J.M., 2005. Lipids and nitrogen isotopes of two deep-water corals from the North-East Atlantic: initial results and implications for their nutrition. Cold-water corals and ecosystems, 715-729.
Krumhansl, K.A., Scheibling, R.E., 2012. Production and fate of kelp detritus. Marine Ecology Progress Series 467, 281–302.
Labarbera, M., 1978. Particle capture by a Pacific brittle star: experimental test of the aerosol suspension feeding model. Science 201, 1147–1149.
Langer, P.D., 1978. Some aspects of the biology of three Northwestern Atlantic Chitons: *Tonicella rubra*, *Tonicella marmorea*, and *Ischnochiton albus* (Mollusca: Polyplacophora).
Lauzon-Guay, J.-S., Scheibling, R.E., 2007. Seasonal variation in movement, aggregation and destructive grazing of the green sea urchin (*Strongylocentrotus droebachiensis*) in relation to wave action and sea temperature. Marine Biology 151, 2109–2118.
Lebour, M. v, 1938. Notes on the breeding of some lamellibranchs from Plymouth and their larvae. Journal of the Marine Biological Association of the United Kingdom 23, 119–144.
Lee Jr, R.E., Damodaran, K., Yi, S.-X., Lorigan, G.A., 2006. Rapid cold-hardening increases membrane fluidity and cold tolerance of insect cells. Cryobiology 52, 459–463.
Lee, R.F., Hagen, W., Kattner, G., 2006. Lipid storage in marine zooplankton. Marine Ecology Progress Series 307, 273–306.
Legeżyńska, J., Kędra, M., Walkusz, W., 2014. Identifying trophic relationships within the high Arctic benthic community: How much can fatty acids tell? Marine Biology.
Lichti, D.A., Rinchard, J., Kimmel, D.G., 2017. Changes in zooplankton community, and seston and zooplankton fatty acid profiles at the freshwater/saltwater interface of the Chowan River, North Carolina. PeerJ 5, e3667.
Lindeman, R.L., 1942. The trophic-dynamic aspect of ecology. Ecology 23, 399–417.

Linnebjerg, J.F., Hobson, K.A., Fort, J., Nielsen, T.G., Møller, P., Wieland, K., Born, E.W., Rigét, F.F., Mosbech, A., 2016. Deciphering the structure of the West Greenland marine food web using stable isotopes ($\delta^{13}C$, $\delta^{15}N$). Marine Biology 163, 230.

Lloret, J., Planes, S., 2003. Condition, feeding and reproductive potential of white seabream *Diplodus sargus* as indicators of habitat quality and the effect of reserve protection in the northwestern Mediterranean. Marine Ecology Progress Series 248, 197–208.

Luis, O.J., Passos, A.M., 1995. Seasonal changes in lipid content and composition of the polychaete *Nereis (Hediste) diversicolor*. Comparative Biochemistry and Physiology Part B: Biochemistry and Molecular Biology 111, 579–586.

Macdonald, T.A., Burd, B.J., Macdonald, V.I., van Roodselaar, A., 2010. Taxonomic and feeding guild classification for the marine benthic macroinvertebrates of the Strait of Georgia, British Columbia. Fisheries and Oceans Canada= Pêches et Océans Canada.

Majdi, N., Hette-Tronquart, N., Auclair, E., Bec, A., Chouvelon, T., Cognie, B., Danger, M., Decottignies, P., Dessier, A., Desvilettes, C., 2018. There's no harm in having too much: A comprehensive toolbox of methods in trophic ecology. Food Webs 17, e00100.

Makhutova, O.N., Sushchik, N.N., Gladyshev, M.I., Ageev, A. v, Pryanichnikova, E.G., Kalachova, G.S., 2011. Is the fatty acid composition of freshwater zoobenthic invertebrates controlled by phylogenetic or trophic factors? Lipids 46, 709–721.

Marcelina, Z., Adam, S., Pierre, R., 2018. Spatial and temporal variability of organic matter sources and food web structure across benthic habitats in a low diversity system (southern Baltic Sea). Journal of Sea Research 141, 47–60.

Marrack, E.C., 1999. The relationship between water motion and living rhodolith beds in the southwestern Gulf of California, Mexico. Palaios 14, 159–171.

Martin-Creuzburg, D., von Elert, Ervin., Elert, El, 2009. Ecological Significance of Sterols in Aquatic Food Webs. Lipids in Aquatic Ecosystems 43–64.

Masclaux, H., Perga, M.E., Kagami, M., Desvilettes, C., Bourdier, G., Bec, A., 2013. How pollen organic matter enters freshwater food webs. Limnology and Oceanography 58, 1185-1195.

McConnico, L.A., Carmona, G.H., Morales, J.S.M., Rodríguez, R.R., 2017. Temporal variation in seaweed and invertebrate assemblages in shallow rhodolith beds of Baja California Sur, México. Aquatic Botany 139, 37–47.

McMeans, B.C., McCann, K.S., Humphries, M., Rooney, N., Fisk, A.T., 2015. Food Web Structure in Temporally-Forced Ecosystems. Trends in Ecology and Evolution.

Meador, J.P., 2003. Bioaccumulation of PAHs in Marine Invertebrates. PAHs: An Ecotoxicological Perspective 147.

Michener, M., 1994. Stable isotope ratios as tracers in marine aquatic food webs. Stable Isotopes in Ecology and Environmental Science 138–186.

Millar, K.R., Gagnon, P., 2018. Mechanisms of stability of rhodolith beds: sedimentological aspects. Marine Ecology Progress Series 594, 65–83.

Miller, R.J., Page, H.M., 2012. Kelp as a trophic resource for marine suspension feeders: a review of isotope-based evidence. Marine Biology 159, 1391–1402.

Minagawa, M., Wada, E., 1984. Stepwise enrichment of ^{15}N along food chains: further evidence and the relation between $\delta^{15}N$ and animal age. Geochimica et Cosmochimica Acta 48, 1135–1140.

Mohan, S.D., Connelly, T.L., Harris, C.M., Dunton, K.H., McClelland, J.W., 2016. Seasonal trophic linkages in Arctic marine invertebrates assessed via fatty acids and compound-specific stable isotopes. Ecosphere 7.

Morse, D.E., Hooker, N., Morse, A.N.C., Jensen, R.A., 1988. Control of larval metamorphosis and recruitment in sympatric agariciid corals. Journal of Experimental Marine Biology and Ecology 116, 193–217.

Müller-Navarra, D.C., Brett, M.T., Liston, a M., Goldman, C.R., 2000. A highly unsaturated fatty acid predicts carbon transfer between primary producers and consumers. Nature 403, 74–77.

Narciso, L., da Fonseca, L.C., 2000. Growth, survival and fatty acid profile of *Nereis diversicolor* (OF Müller, 1776) fed on six different diets. Bulletin of Marine Science 67, 337–343.

Nelson, M.M., Phleger, C.F., Nichols, P.D., 2002. Seasonal lipid composition in macroalgae of the northeastern Pacific Ocean. Botanica Marina 45, 58–65.

Newell, R.I.E., Marshall, N., Sasekumar, A., Chong, V.C., 1995. Relative importance of benthic microalgae, phytoplankton, and mangroves as sources of nutrition for penaeid prawns and other coastal invertebrates from Malaysia. Marine Biology 123, 595–606.

Nielsen, A.M., Eriksen, N.T., Iversen, J.J.L., Riisgård, H.U., 1995. Feeding, growth and respiration in the polychaetes *Nereis diversicolor* (facultative filter-feeder) and *N. virens* (omnivorous) - a comparative study. Marine Ecology Progress Series 125, 149–158.

Nomura, M., Kamogawa, H., Susanto, E., Kawagoe, C., Yasui, H., Saga, N., Hosokawa, M., Miyashita, K., 2013. Seasonal variations of total lipids, fatty acid composition, and fucoxanthin contents of *Sargassum horneri* (Turner) and *Cystoseira hakodatensis* (Yendo) from the northern seashore of Japan. Journal of Applied Phycology 25, 1159-1169.

Olivier, M., Desrosiers, G., Caron, A., Retière, C., 1996. Juvenile growth of the polychaete *Nereis virens* feeding on a range of marine vascular and macroalgal plant sources. Marine Biology 125, 693–699.

Olivier, M., Desrosiers, G., Retière, C., Brêthes, J.-C., 1993. Variations spatio-temporelles de l'alimentation du polychète *Nereis virens* en zone intertidale (Estuaire maritime du saint-Laurent, Québec). Vie et Milieu/Life & Environment 1–12.

Pakhomov, E.A., McClelland, J.W., Bernard, K., Kaehler, S., Montoya, J.P., 2004. Spatial and temporal shifts in stable isotope values of the bottom-dwelling shrimp *Nauticaris marionis* at the sub-Antarctic archipelago. Marine Biology 144, 317–325.

Parrish, C.C., 2013. Lipids in Marine Ecosystems. ISRN Oceanography 2013, 1–16.

Parrish, C.C., 2009. Essential fatty acids in aquatic food webs, in: Lipids in Aquatic Ecosystems. 309–326.

Parrish, C.C., 1999. Determination of Total Lipid, Lipid Classes, and Fatty Acids in Aquatic Samples. Lipids in Freshwater Ecosystems 4–20.

Parrish, C.C., 1987. Time series of particulate and dissolved lipid classes during spring phytoplankton blooms in Bedford Basin, a marine inlet. Marine Ecology Progress Series 35, 10.

Parrish, C.C., Abrajano, T. a, Budge, S.M., Helleur, R.J., Hudson, E.D., 2000. Lipid and phenolic biomarkers in marine ecosystems: Analysis and applications. The Handbook of Environmental Chemistry Vol 5 Part D Marine Chemistry 5, 193–223.

Parrish, C.C., Bodennec, G., Macpherson, E.J., Ackman, R.G., 1992. Seawater fatty acids and lipid classes in an urban and a rural Nova Scotia inlet. Lipids 27, 651.

Parrish, C.C., Deibel, D., Thompson, R.J., 2009. Effect of sinking spring phytoplankton blooms on lipid content and composition in suprabenthic and benthic invertebrates in a cold ocean coastal environment. Marine Ecology Progress Series 391, 33–51.

Parrish, C.C., McKenzie, C.H., MacDonald, B.A., Hatfield, E.A., 1995. Seasonal studies of seston lipids in relation to microplankton species composition and scallop growth in South Broad Cove, Newfoundland. Marine Ecology Progress Series 129, 151–164.

Parrish, C.C., Thompson, R.J., Deibel, D., 2005. Lipid classes and fatty acids in plankton and settling matter during the spring bloom in a cold ocean coastal environment. Marine Ecology Progress Series 286, 57–68.

Parzanini, C., 2018. An integrated approach to studying the trophic ecology of a deep-sea faunal assemblage from the Northwest Atlantic (Doctoral dissertation). Memorial University of Newfoundland, St. John's, NL.

Parzanini, C., Parrish, C.C., Hamel, J.-F., Mercier, A., 2018. Functional diversity and nutritional content in a deep-sea faunal assemblage through total lipid, lipid class, and fatty acid analyses. PloS one 13, e0207395.

Peterson, B.J., Fry, B., 1987. Stable isotopes in ecosystem studies. Annual review of Ecology and Systematics 18, 293–320.

Piazzi, L., Pardi, G., Cinelli, F., 2002. Structure and temporal dynamics of a macroalgal assemblage associated with a rhodolith bed of the Tuscan archipelago (Tyrrhenian Sea). Atti della Società Toscana di Scienze Naturali, Memorie 5–10.

Pitt, K.A., Connolly, R.M., Meziane, T., 2009. Stable isotope and fatty acid tracers in energy and nutrient studies of jellyfish: A review. Hydrobiologia, 119–132.

Post, D.M., 2002. Using stable isotopes to estimate trophic position: models, methods, and assumptions. Ecology 83, 703–718.

Post, D.M., Layman, C.A., Arrington, D.A., Takimoto, G., Quattrochi, J., Montana, C.G., 2007. Getting to the fat of the matter: models, methods and assumptions for dealing with lipids in stable isotope analyses. Oecologia, 179-189.

Ramshaw, B.C., Pakhomov, E.A., Markel, R.W., Kaehler, S., 2017. Quantifying spatial and temporal variations in phytoplankton and kelp isotopic signatures to estimate the distribution of kelp-derived detritus off the west coast of Vancouver Island, Canada. Limnology and Oceanography 62, 2133–2153.

Raven, J.A., Johnston, A.M., Kübler, J.E., Korb, R., McInroy, S.G., Handley, L.L., Scrimgeour, C.M., Walker, D.I., Beardall, J., Vanderklift, M., 2002. Mechanistic interpretation of carbon isotope discrimination by marine macroalgae and seagrasses. Functional Plant Biology 29, 355–378.

Richoux, N.B., Deibel, D., Thompson, R.J., Parrish, C.C., 2005. Seasonal and developmental variation in the fatty acid composition of *Mysis mixta* (Mysidacea) and *Acanthostepheia malmgreni* (Amphipoda) from the hyperbenthos of a cold-ocean environment (Conception Bay, Newfoundland). Journal of Plankton Research 27, 719–733.

Riera, P., Stal, L.J., Nieuwenhuize, J., Richard, P., Blanchard, G., Gentil, F., 1999. Determination of food sources for benthic invertebrates in a salt marsh (Aiguillon Bay, France) by carbon and nitrogen stable isotopes: importance of locally produced sources. Marine Ecology Progress Series 187, 301–307.

Riosmena-Rodriguez, R., Medina-López, M.A., 2010. The role of rhodolith beds in the recruitment of invertebrate species from the southwestern Gulf of California, Mexico. Seaweeds and Their Role in Globally Changing Environments, 127–138.

Riosmena-Rodríguez, R., Nelson, W., Aguirre, J., 2017. Rhodolith/maërl beds: a global perspective. Springer.

Robles-Tamayo, C.M., Valdez-Holguín, J.E., García-Morales, R., Figueroa-Preciado, G., Herrera-Cervantes, H., López-Martínez, J., Enríquez-Ocaña, L.F., 2018. Sea surface temperature (SST) variability of the eastern coastal zone of the gulf of California. Remote Sensing 10, 1434.

Rohlf, F.J., 1972. An empirical comparison of three ordination techniques in numerical taxonomy. Systematic Zoology 21, 271–280.

Sargent, J.R., Parkes, R.J., Mueller-Harvey, I., Henderson, R.J., 1987. Lipid biomarkers in marine ecology. Microbes in the Sea, 119–138.
Schaal, G., Riera, P., Leroux, C., 2009. Trophic significance of the kelp Laminaria digitata (Lamour.) for the associated food web: a between-sites comparison. Estuarine, Coastal and Shelf Science 85, 565-572.
Schaal, G., Riera, P., Leroux, C., 2010. Trophic ecology in a Northern Brittany (Batz Island, France) kelp (*Laminaria digitata*) forest, as investigated through stable isotopes and chemical assays. Journal of Sea Research 63, 24–35.
Schaffelke, B., Lüning, K., 1994. A circannual rhythm controls seasonal growth in the kelps *Laminaria hyperborea* and *L. digitata* from Helgoland (North Sea). European Journal of Phycology 29, 49–56.
Scheibling, R.E., Hennigar, A.W., Balch, T., 1999. Destructive grazing, epiphytism, and disease: the dynamics of sea urchin-kelp interactions in Nova Scotia. Canadian Journal of Fisheries and Aquatic Sciences 56, 2300–2314.
Schiel, D.R., Steinbeck, J.R., Foster, M.S., 2004. Ten years of induced ocean warming causes comprehensive changes in marine benthic communities. Ecology 85, 1833–1839.
Schlacher, T.A., Connolly, R.M., Skillington, A.J., Gaston, T.F., 2009. Can export of organic matter from estuaries support zooplankton in nearshore, marine plumes? Aquatic Ecology 43, 383-393.
Schmid, M., Guihéneuf, F., Stengel, D.B., 2014. Fatty acid contents and profiles of 16 macroalgae collected from the Irish Coast at two seasons. Journal of Applied Phycology 26, 451–463.
Sciberras, M., Rizzo, M., Mifsud, J.R., Camilleri, K., Borg, J.A., Lanfranco, E., Schembri, P.J., 2009. Habitat structure and biological characteristics of a maërl bed off the northeastern coast of the Maltese Islands (central Mediterranean). Marine biodiversity 39, 251–264.
Smetacek, V., 1984. The supply of food to the benthos. Flows of Energy and Materials in Marine Ecosystems, 517–547.
Smith, V.H., Tilman, G.D., Nekola, J.C., 1999. Eutrophication: impacts of excess nutrient inputs on freshwater, marine, and terrestrial ecosystems. Environmental Pollution 100, 179–196.
Snedecor, G.W., Cochran, W.G., 1994. Statistical methods, 8th edn. Affiliated East.
Sneed, E.D., Folk, R.L., 1958. Pebbles in the lower Colorado River, Texas a study in particle morphogenesis. The Journal of Geology 66, 114–150.
Steller, D.L., Cáceres-Martínez, C., 2009. Coralline algal rhodoliths enhance larval settlement and early growth of the pacific calico scallop *Argopecten ventricosus*. Marine Ecology Progress Series 396, 49–60.
Steller, D.L., Riosmena-Rodriguez, R., Foster, M.S., Roberts, C.A., 2003. Rhodolith bed diversity in the Gulf of California: The importance of rhodolith structure and consequences of disturbance. Aquatic Conservation: Marine and Freshwater Ecosystems 13, 5–20.
Steneck, R.S., 1990. Herbivory and the evolution of nongeniculate coralline algae (Rhodophyta, Corallinales) in the North Atlantic and North Pacific. Evolutionary Biogeography of the Marine Algae of the North Atlantic, 107–129.
Steneck, R.S., 1986. The ecology of coralline algal crusts: convergent patterns and adaptative strategies. Annual review of Ecology and Systematics 17, 273–303.
Takai, N., Yorozu, A., Tanimoto, T., Hoshika, A., Yoshihara, K., 2004. Transport pathways of microphytobenthos-originating organic carbon in the food web of an exposed hard bottom shore in the Seto Inland Sea, Japan. Marine Ecology Progress Series 284, 97–108.

Teed, L., Bélanger, D., Gagnon, P., Edinger, E., 2020. Calcium carbonate ($CaCO_3$) production of a subpolar rhodolith bed: Methods of estimation, effect of bioturbators, and global comparisons. Estuarine, Coastal and Shelf Science 242, 106822.

Teichert, S., Woelkerling, W., Rüggeberg, A., Wisshak, M., Piepenburg, D., Meyerhöfer, M., Form, A., Freiwald, A., 2014. Arctic rhodolith beds and their environmental controls (Spitsbergen, Norway). Facies 60, 15–37.

Tenore, K.R., 1988. Nitrogen in benthic food chains. Nitrogen Cycling in Coastal Marine Environments 191–206.

Tenore, K.R., Hanson, R.B., McClain, J., Maccubbin, A.E., Hodson, R.E., 1984. Changes in composition and nutritional value to a benthic deposit feeder of decomposing detritus pools. Bulletin of Marine Science 35, 299–311.

Terasaki, M., Hirose, A., Narayan, B., Baba, Y., Kawagoe, C., Yasui, H., Saga, N., Hosokawa, M. and Miyashita, K., 2009. Evaluation of recoverable functional lipid components of several brown seaweeds (Phaeophyta) from Japan with special reference to fucoxanthin and fucosterol contents. Journal of phycology 45, 974-980.

Thompson, R.M., Brose, U., Dunne, J.A., Hall Jr, R.O., Hladyz, S., Kitching, R.L., Martinez, N.D., Rantala, H., Romanuk, T.N., Stouffer, D.B., 2012. Food webs: reconciling the structure and function of biodiversity. Trends in Ecology and Evolution 27, 689–697.

Trombetta, T., Vidussi, F., Roques, C., Scotti, M., Mostajir, B., 2020. Marine Microbial Food Web Networks During Phytoplankton Bloom and Non-bloom Periods: Warming Favors Smaller Organism Interactions and Intensifies Trophic Cascade. Frontiers in Microbiology 11.

Trueman, C.N., Johnston, G., O'Hea, B., MacKenzie, K.M., 2014. Trophic interactions of fish communities at midwater depths enhance long-term carbon storage and benthic production on continental slopes. Proceedings of the Royal Society B: Biological Sciences 281.

Urban, J.L., McKenzie, C.H., Deibel, D., 1992. Seasonal differences in the content of *Oikopleura vanhoeffeni* and *Calanus finmarchicus* faecal pellets: illustrations of zooplankton food web shifts in coastal Newfoundland waters. Marine Ecology Progress Series, 255-264.

van der Lee, G.H., Arie Vonk, J., Verdonschot, R.C.M., Kraak, M.H.S., Verdonschot, P.F.M., Huisman, J., 2020. Eutrophication induces shifts in the trophic position of invertebrates in aquatic food webs. Ecology, e03275.

Vanderklift, M.A., Bearham, D., 2014. Variation in $\delta^{13}C$ and $\delta^{15}N$ of kelp is explained by light and productivity. Marine Ecology Progress Series 515, 111-121.

Vanderploeg, H.A., Bolsenga, S.J., Fahnenstiel, G.L., Liebig, J.R., Gardner, W.S., 1992. Plankton ecology in an ice-covered bay of Lake Michigan: Utilization of a winter phytoplankton bloom by reproducing copepods. Hydrobiologia 243, 175–183.

Wacker, A., Becher, P., von Elert, E., 2002. Food quality effects of unsaturated fatty acids on larvae of the zebra mussel *Dreissena polymorpha*. Limnology and Oceanography 47, 1242–1248.

Wakeham, S.G. and Canuel, E.A., 1988. Organic geochemistry of particulate matter in the eastern tropical North Pacific Ocean: Implications for particle dynamics. Journal of Marine Research 46, 183-213.

Wennberg, M., Vessby, B., Johansson, I., 2009. Evaluation of relative intake of fatty acids according to the Northern Sweden FFQ with fatty acid levels in erythrocyte membranes as biomarkers. Public health nutrition 12, 1477-1484.

Woodward, G.U.Y., Hildrew, A.G., 2002. Food web structure in riverine landscapes. Freshwater Biology 47, 777–798.

Yorke, C.E., Page, H.M., Miller, R.J., 2019. Sea urchins mediate the availability of kelp detritus to benthic consumers. Proceedings of the Royal Society B 286, 20190846.
Zar, J.H., 1999. Biostatistical analysis. Pearson Education India.

Appendices

Appendix A

List of abbreviations and symbols

AMPL	Acetone mobile polar lipid(s)
ALC	Alcohol(s)
ARA	Arachidonic acid
°C	Degrees Celsius
cm	Centimetres
CTD	Conductivity, Temperature, and Depth Instrument
DG	Diacylglycerol(s)
DHA	Docosahexaenoic acid
DHA/EPA	Docosahexaenoic acid:eicosapentaenoic acid ratio
EPA	Eicosapentaenoic acid
EA	Elemental analyzer
FA	Fatty acid(s) [notation: A:Bωn (e.g.. 20:5ω3)]
FAME	Fatty acid methyl ester(s)
A:Bωn	Fatty acid notation
FID	Flame ionization detection
FFA	Free fatty acid(s)
g	Grams
GC	Gas chromatography
GC-FID	Gas chromatography and flame ionization detection
h	Hours
HC	Hydrocarbon(s)
KET	Ketone(s)
kg	Kilograms
L	Litres
MS	Mass Spectrometer

MUN	Memorial University of Newfoundland
m	Metres
μL	Microlitres
mL	Millilitres
mm	Millimetres
min	Minutes
MUFA	Monounsaturated fatty acid(s)
ω3	Omega-3 fatty acid(s)
ω6	Omega-6 fatty acid(s)
OSC	Ocean Sciences Centre
PL	Phospholipid(s)
PAR	Photosynthetically Active Radiation
PUFA	Polyunsaturated fatty acid(s)
P/S	Polyunsaturated:saturated fatty acid ratio
PCO	Principal coordinates analysis
rpm	Revolutions per minute
SFA	Saturated fatty acid(s)
$\delta^{13}C$	Stable carbon isotope ratio
$\delta^{15}N$	Stable nitrogen isotope ratio
SD	Standard deviation
SE	Standard error
ST	Sterol(s)
TERRA	The Earth Resources Research and Analysis facility
TCD	Thermal conductivity meter
TLC-FID	Thin-layer chromatography with flame ionization detection
TAG	Triacylglycerol(s)
TMF	Trophic multiplication factor
TP	Trophic position

Appendix B

General physicochemical environment and timing of phytoplankton bloom at the study site

The timing of the phytoplankton bloom at the study sites was confirmed by casting a CTD (conductivity, temperature, and depth) instrument (SBE - 19 PLUS; Seabird) with PAR (QSP2300; Biospherical Instruments Inc.) and fluorescence sensors (FLRT; WETstar fluorometer), every few days from 1 to 29 March, 2017, and again from 23 to 26 April, 2017; from 30 May, 2017 to 10 July, 2017; from 12 October to 26 October, 2017, and again on 02 December, 2017. Ice covered the sea surface from 30 March to 22 April, preventing CTD casts during this period. Personal injury prevented data collection between 27 October and 01 December; Fluorescence sensor issues prevented accurate fluorescence data during the fall collection until 02 December. For each cast we lowered the instrument from the ocean surface down to the surface of the rhodolith bed at a speed of ~1 m s^{-1}. Data collected by the CTD across the water column (i.e. PAR, fluorescence, pressure (depth), temperature, and salinity) were plotted with Ocean Data View V4.0 (https://odv.awi.de/) and SigmaPlot V11.0 and used to characterize the general physicochemical environment at the study site. Fluorescence data within the first 3 m above the rhodolith bed (i.e. between 12 and 15 m deep) were used to monitor the progression, and confirm the occurrence of, the bloom. Below we present fluorescence (Figures B.1-2), temperature (Figure B.3-5), and salinity (Figure B.6-8) data from the sea surface down to the rhodolith bed from each of the three progressions, except for fluorescence data leading up to the collection on 02 December, 2017. We also present the final fluorescence, temperature, and salinity data (Table B.1) from the monthly

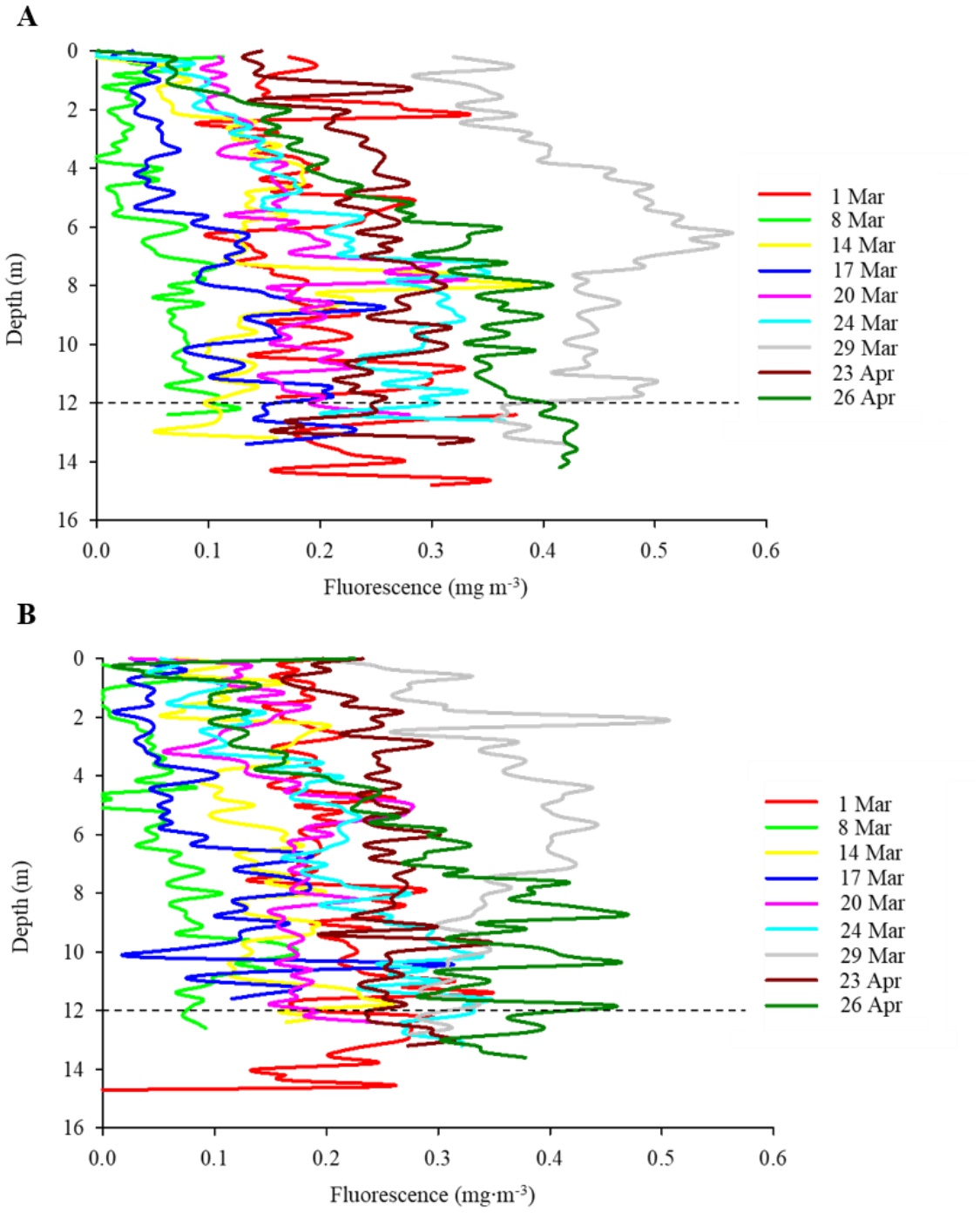

Figure B.1. Fluorescence between the sea surface and rhodolith bed at 15 m depth at our (A) South site and (B) North site through March 2017 and end of April 2017. The horizontal dashed line indicates the depth (12 m) below which fluorescence was considered in determining the timing of the phytoplankton bloom.

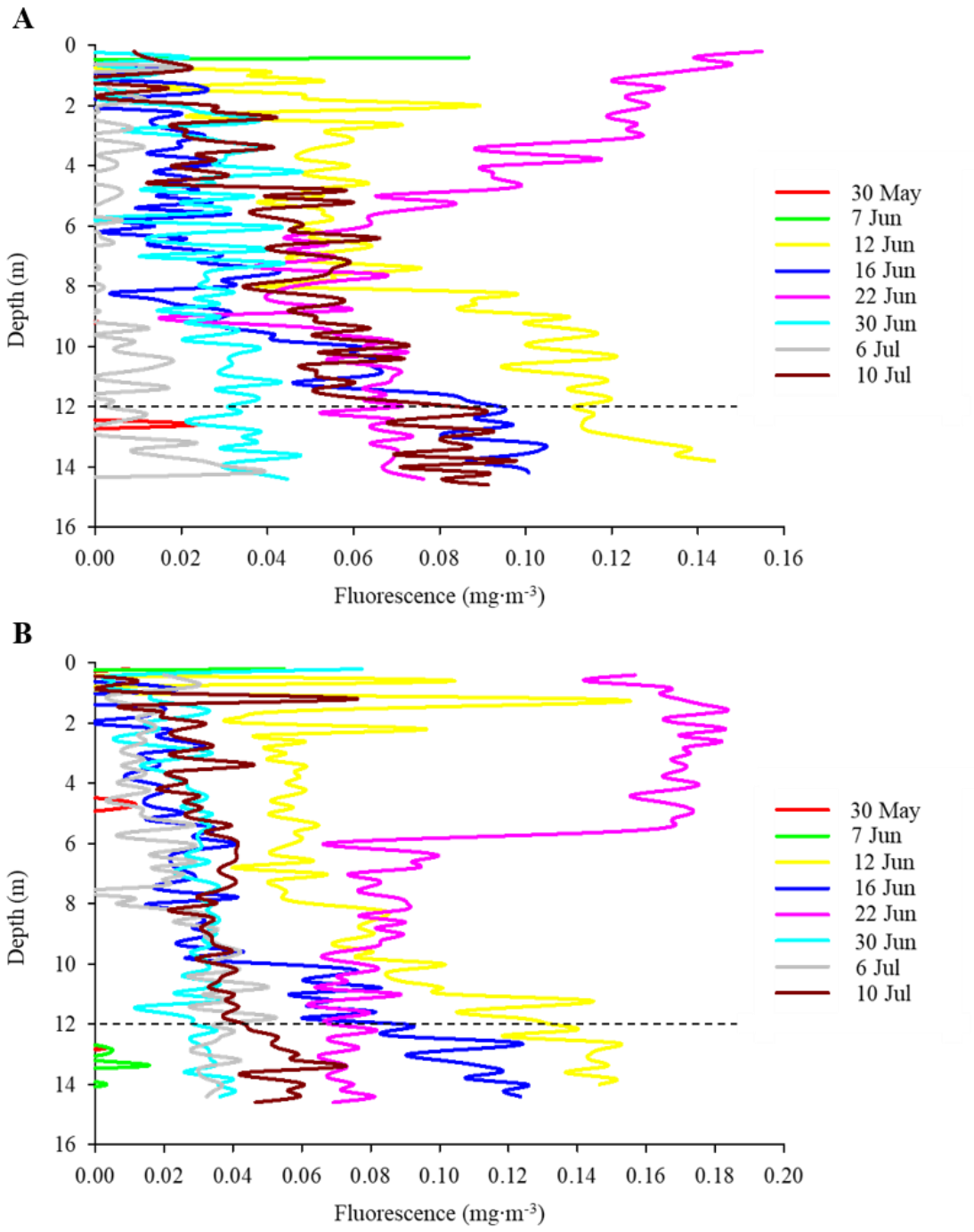

Figure B.2. Fluorescence between the sea surface and rhodolith bed at 15 m depth at our (A) South site and (B) North site through May 2017 to July 2017. The horizontal dashed line indicates the depth (12 m) below which fluorescence was considered in determining the timing of the phytoplankton bloom.

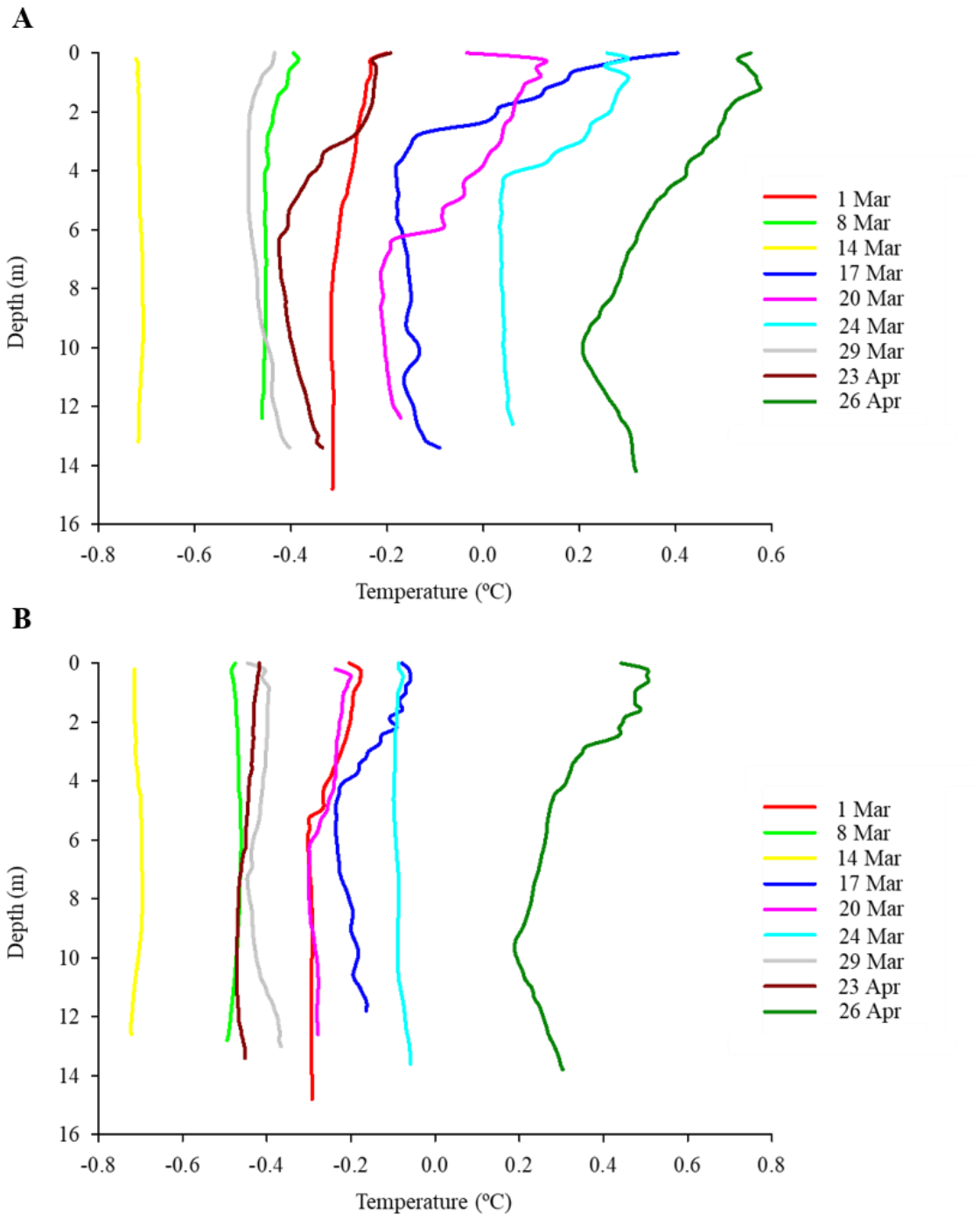

Figure B.3. Temperature between the sea surface and rhodolith bed at 15 m depth at our (A) South site and (B) North site through March 2017 and end of April 2017.

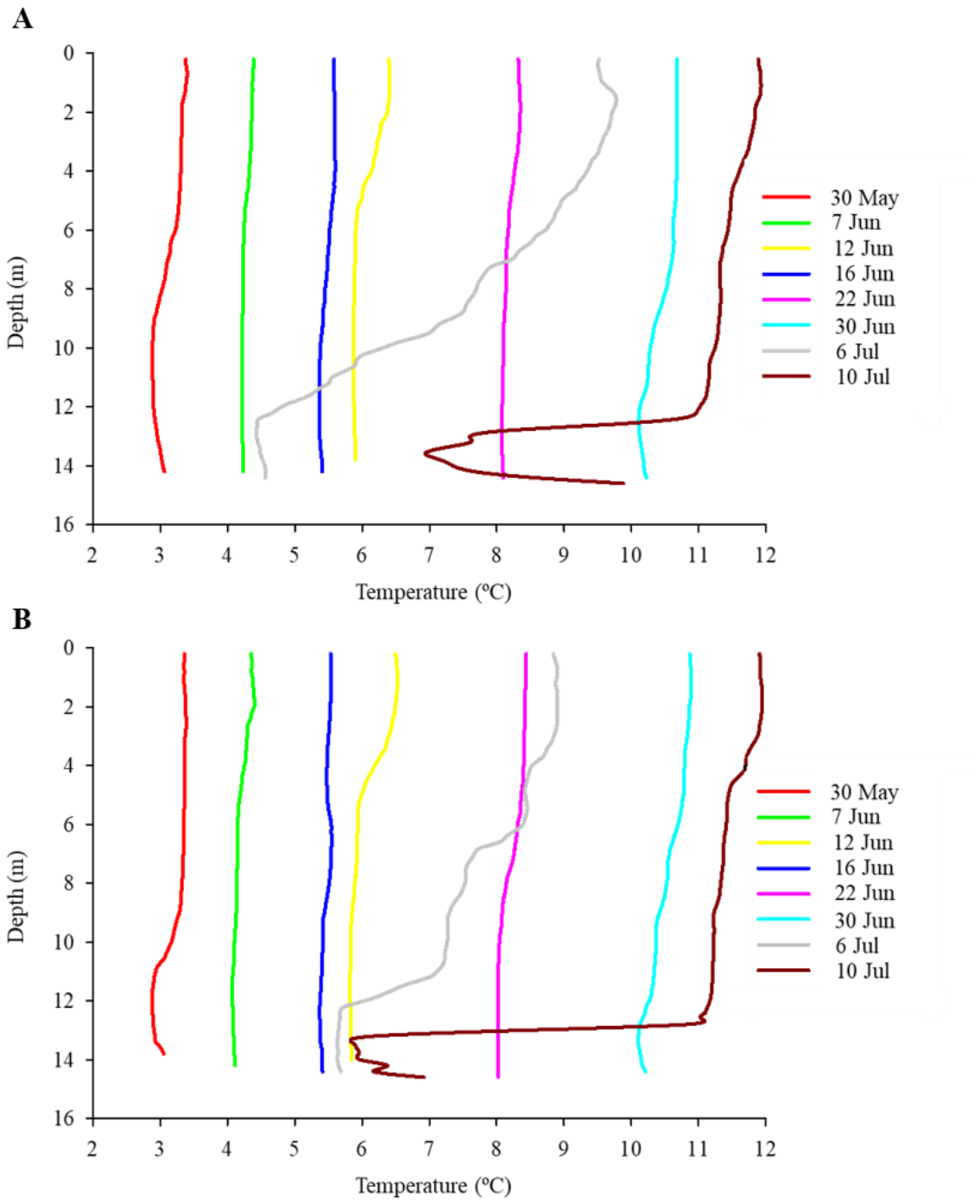

Figure B.4. Temperature between the sea surface and rhodolith bed at 15 m depth at our (A) South site and (B) North site through May 2017 to July 2017.

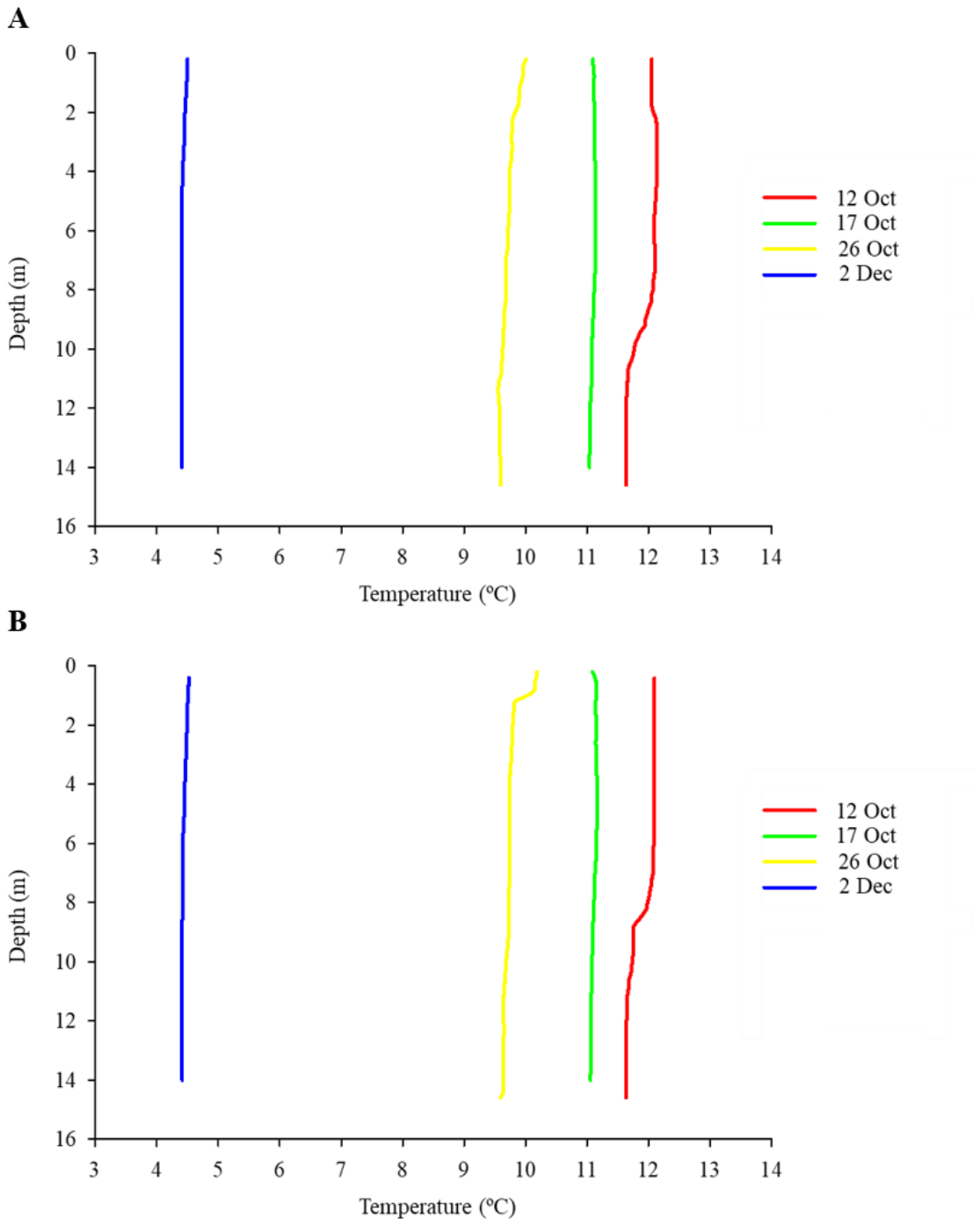

Figure B.5. Temperature between the sea surface and rhodolith bed at 15 m depth at our (A) South site and (B) North site through October and beginning of December 2017.

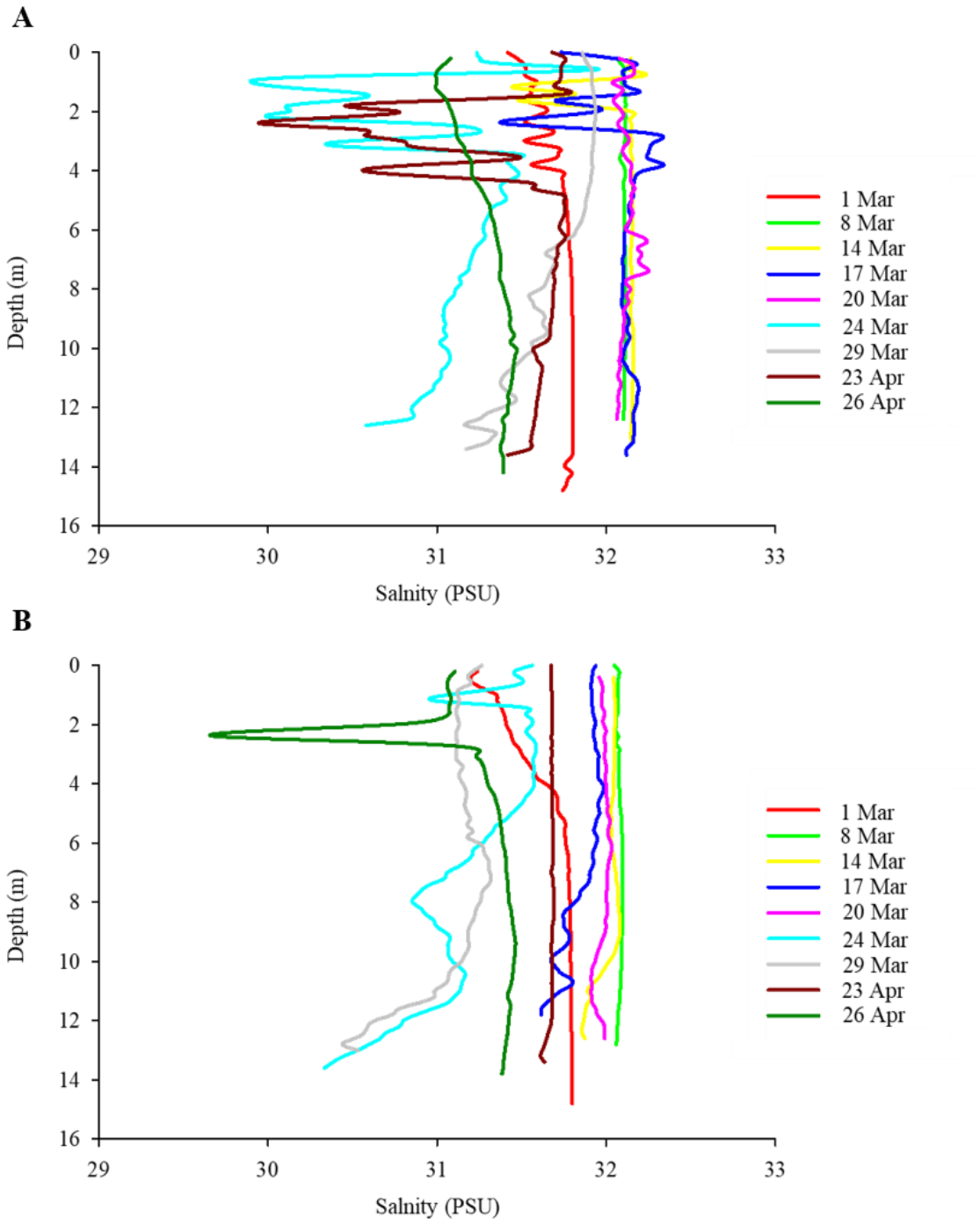

Figure B.6. Salinity between the sea surface and rhodolith bed at 15 m depth at our (A) South site and (B) North site through March 2017 and end of April 2017.

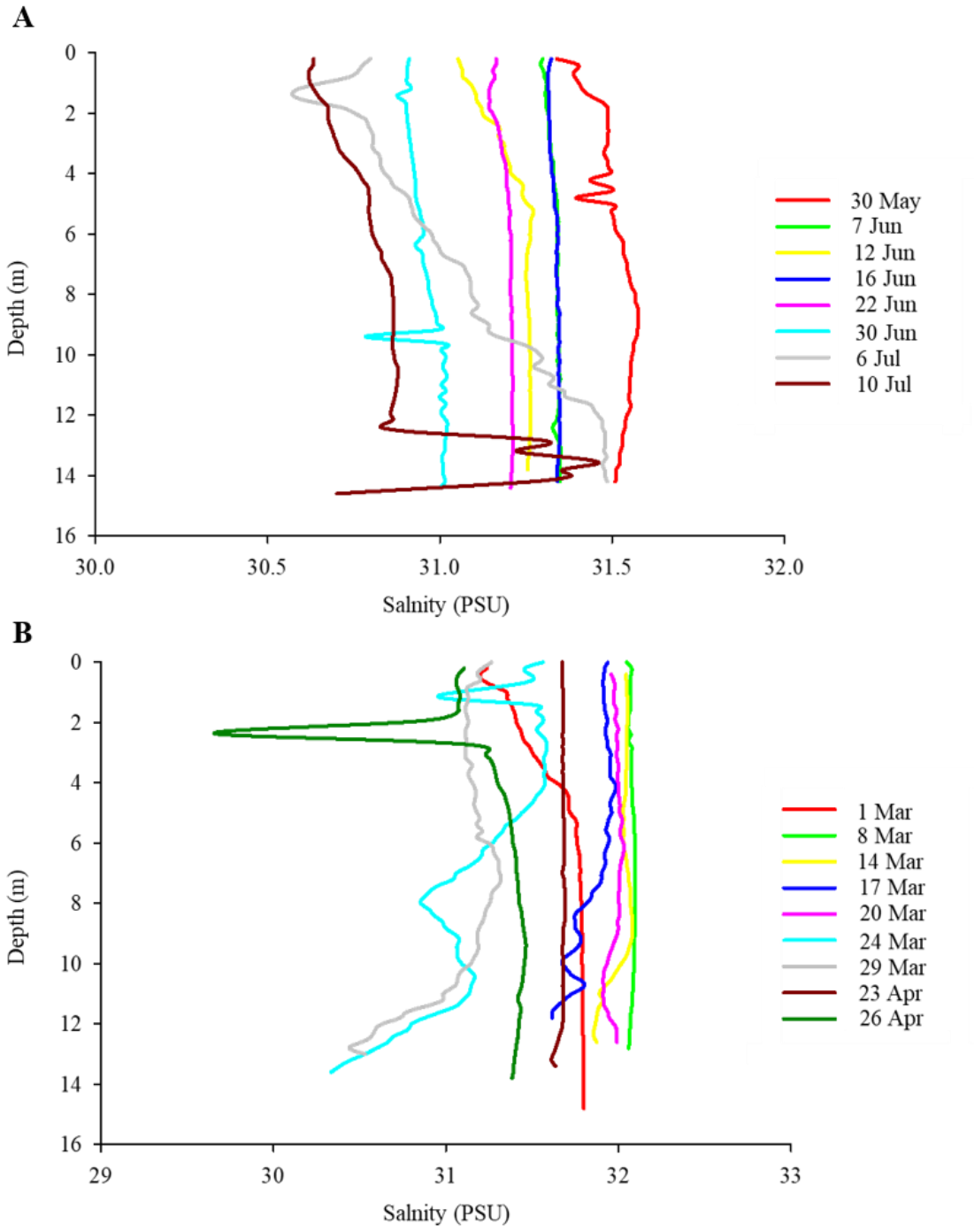

Figure B.7. Salinity between the sea surface and rhodolith bed at 15 m depth at our (A) South site and (B) North site through May 2017 to July 2017.

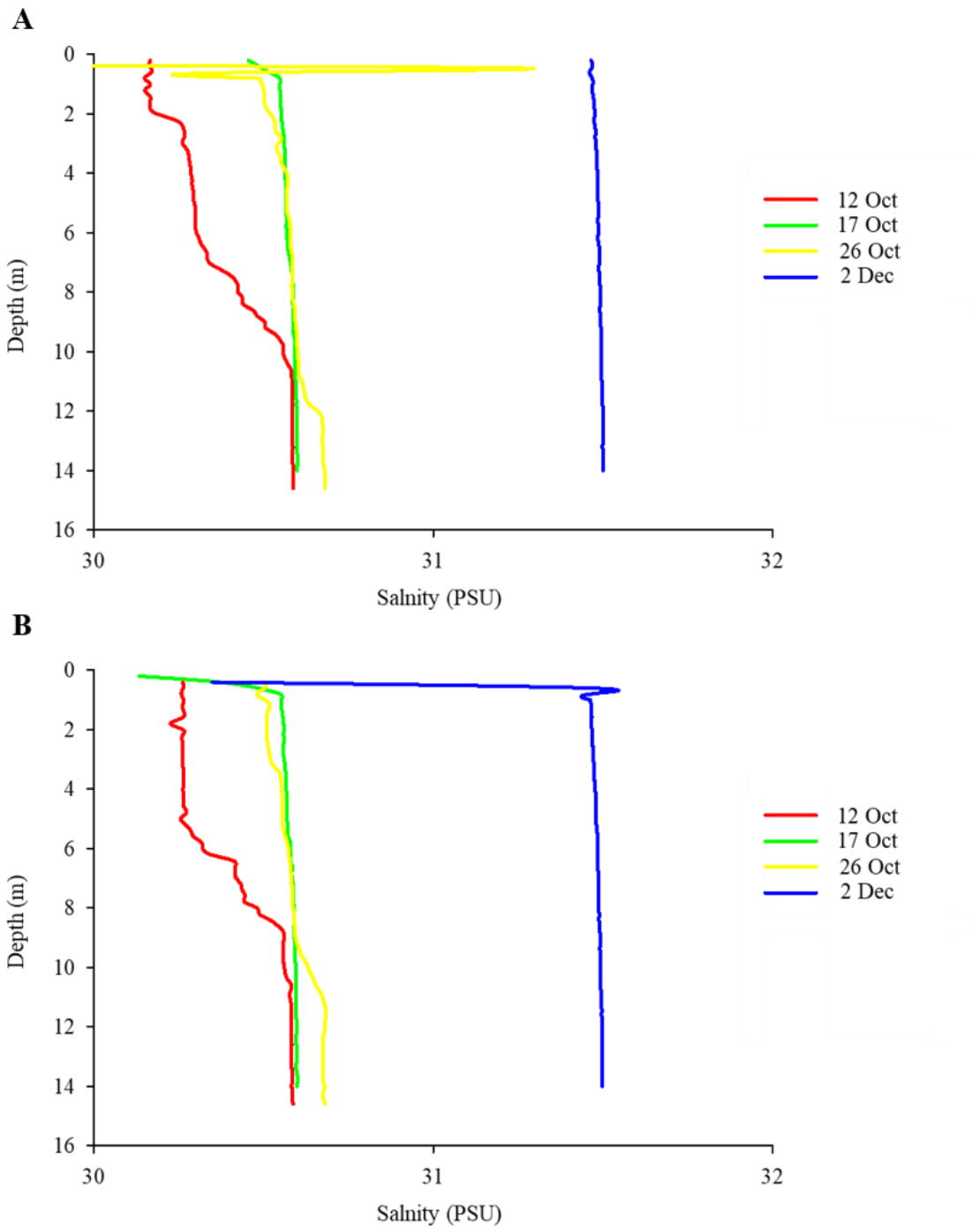

Figure B.8. Salinity between the sea surface and rhodolith bed at 15 m depth at our (A) South site and (B) North site through October and beginning of December 2017.

Table B.1. Final temperature (°C), fluorescence (mg/m^3), and salinity (psu) readings within the first 3 m above the rhodolith bed from out CTD cast progressions (see Figures B.1-8) leading up to each data collection in April, July, and December 2017 of the South and North sites through October and beginning of December 2017.

		Temperature	**Fluorescence**	**Salinity**
Site	**Collection Date**	°C (±SE)	(mg/m^3) (±SE)	psu (±SE)
South	April 2017	0.31 (0)	0.4 (0)	31.4 (0)
	July 2017	7.9 (0.5)	0.1(0)	31.2 (0.1)
	December 2017	4.4 (0)	0 (0)	31.5 (0)
North	April 2017	0.3 (0)	0.4 (0)	31.4 (0)
	July 2017	6.2 (0.2)	0.1 (0)	31.4 (0)
	December 2017	0 (0)	0 (0)	31.5 (0)

progression of each collection at the rhodolith bed. Only fluorescence data within 3 m above the bed were used in determining the timing of the bloom. This layer of water was deemed sufficiently narrow to capture benthic-pelagic trophic interactions relevant to the present study.

Inspection of the fluorescence data from March and April, 2017 indicated that the spring phytoplankton bloom began in the last few days of March and was still ongoing on 23 and 26 April, 2017 (Figure B.1). Fluorescence above 12 m was more variable than below, with benthic levels gradually increasing throughout March and stabilizing in late April. Phytoplankton concentration on 23 April (when we sampled the rhodolith community and collected rhodoliths for food web analyses) was three to four times that on 8 March. Sea temperature varied more within the first 12 m than below, although the largest difference between coldest (14 March, 2017) and warmest (26 April, 2017) water across the entire water column did not exceed ~1.3°C (Figure B.3). Salinity varied by less than ~0.4 PSU across the entire water column from 1 to 20 March, 2017, but exhibited marked changes, up to 2 PSU, within the first 5 m in the week that preceded the formation, and day that followed the retreat, of surface ice (Figure B.6). Salinity below 12 m remained comparatively much more stable, with no obvious influence of sea ice and a faster return to pre-ice salinities.

Inspection of the fluorescence data from May through July, 2017 indicated that the spring phytoplankton bloom was dwindling from late May through early July (Figure B.2). Fluorescence above 12 m was lower than below, indicating low photosynthesis rate at the surface. Benthic levels gradually decreased throughout June. Phytoplankton concentration on 10 July (when we sampled the rhodolith community) was about three times less than on 10 June. Sea temperature increased steadily from ~3°C on 30 May to ~11°C on 10 July, but with steep thermoclines on 06 and 10 July (Figure B.4). The bottom temperature at the final collection was over two times warmer than at

the beginning of the cast series. Salinity varied by less than ~0.8 PSU across the entire water column from 30 May to 10 July, 2017, Salinity below 12 m was comparatively less stable than above (Figure B.7).

Inspection of the fluorescence data from 02 December, 2017 (when we sampled the rhodolith community) indicated that the fall phytoplankton bloom was over in December. Fluorescence above and below 12 m was ~0 mg m^{-3}. Sea temperature was four times lower on 02 December (~3°C) than on 12 October (~12°C) (Figure B.5). Salinity was ~1 psu higher on 02 December than on 12 October (Figure B.8).

Appendix C

Lipid extraction and characterization

We used thin-layer chromatography and flame ionization detection (TLC-FID) to characterize lipid classes. Samples were spotted individually onto one of 10 rods in each of two racks with a 25-µL Hamilton syringe (Hamilton Co.). Samples were spotted as close as possible to the origin of each rod for consistency and accuracy of results. The present appendix shows one of the racks with rods (Figure C.1).

Figure C.1. Rack with 10 silicic acid-coated quartz rods (Chromarods, Type SV; Iatron Laboratories Inc.) used to characterize lipid classes by thin-layer chromatography and flame ionization detection (TLC-FID). Each rod's origin is marked by a line (circled in red) on each side of the rack. Samples, marked by a stain on each rod, were spotted as close as possible to the origin line.

Appendix D

Fatty acid similarity profiles

We used a one-way SIMPER analysis to identify potential food sources and the main fatty acids contributing to the lipid composition of each component (Grall et al., 2006; Gabara, 2014). To limit extraneous data variability while focusing on the most significant fatty acids, only fatty acids contributing to over 70% of the similarities were included in the SIMPER analysis (Table D.1).

Table D.1. Relative contribution to observed similarity and mean proportion of fatty acids (FA) among samples for the six animal species, two macroalgal species, and two environmental components (see Table 2.2 for species list) sampled inside (I) or outside (O) of the South site (see Figure 1.1). Only fatty acids contributing to at least 70% similarity were included in the similarity percentage analysis (SIMPER).

***Asterias rubens* (I)**

FA	Similarity (%)	Proportion (%)
20:5ω3 (EPA)	41.3	31.6
20:4ω6 (ARA)	21.2	19.8
18:0	7.3	5.9
17:1	6.9	9.2

***Hiatella arctica* (I)**

FA	Similarity (%)	Proportion (%)
20:5ω3	19.9	19.3
16:0	18.5	16.5
16:1ω7	14.2	12.7
22:6ω3 (DHA)	9.6	8.9
18:1ω7	7.1	7.0
14:0	4.1	4.3

Table D.1 (continued)

***Nereis* spp. (I)**

FA	Similarity (%)	Proportion (%)
20:5ω3	32.0	29.3
16:0	13.0	11.1
18:1ω7	7.3	6.3
18:1ω11	6.3	5.3
22:5ω3	4.9	4.8
18:0	4.7	4.1
22:4ω6	4.2	4.8

***Ophiopholis aculeata* (I)**

FA	Similarity (%)	Proportion (%)
20:5ω3	30.7	26.8
16:0	9.6	15.5
18:1ω7	8.0	6.6
14:0	7.5	6.5
16:1ω7	7.0	5.9
20:1ω11	6.1	5.2
18:4ω3	5.1	5.1

***Strongylocentrotus droebachiensis* (I)**

FA	Similarity (%)	Proportion (%)
20:5ω3	29.6	24.8
20:4ω6	16.3	14.5
16:0	10.8	8.8
18:1ω7	4.3	3.5
18:4ω3	3.9	3.8
16:1ω7	3.9	4.1
20:2ω6	3.7	3.1

Table D.1 (continued)

***Tonicella* spp. (I)**

FA	Similarity (%)	Proportion (%)
20:5ω3	25.5	21.8
16:0	12.3	10.9
18:1ω9	9.7	9.0
16:1ω7	9.3	8.1
18:1ω7	7.8	6.8
22:5ω3	5.3	4.7
14:0	3.9	3.6

***Laminaria digitata* (O)**

FA	Similarity (%)	Proportion (%)
16:0	20.7	17.5
20:4ω3	16.1	13.5
18:1ω9	16.0	13.0
18:2ω6	11.2	9.1
18:4ω3	9.6	8.0

***Lithothamnion glaciale* (I)**

FA	Similarity (%)	Proportion (%)
N/A	N/A	N/A

Seawater (O)

FA	Similarity (%)	Proportion (%)
18:1ω9	35.0	32.9
16:0	27.8	21.7
18:0	23.3	18.2

Table D.1 (continued)

Sediment (I)

FA	Similarity (%)	Proportion (%)
16:1ω7	24.1	20.6
16:0	17.2	14.6
18:1ω7	10.4	9.0
20:5ω3	8.7	7.8
18:1ω9	5.3	5.3
20:4ω6	4.2	3.7
16:3ω4	2.8	2.5

Appendix E

Grouping of food web components based on C and N isotope ratios

We carried out a cluster analysis on $\delta^{13}C$ and $\delta^{15}N$ isotope ratios simultaneously, and complementary SIMPROF test, to group and map, in the form of a dendrogram, statistically different components of the food web into trophic groups (Grall et al., 2006; Gabara, 2014). The four following trophic groups emerged: Group 1 (seston [seawater]), Group 2 (*A. rubens*, *O. aculeata*, *Tonicella* spp., and *S. droebachiensis*), Group 3 (infauna [sediment], *L. glaciale* [rhodoliths], and *H. arctica*), and Group 4 (*L. digitata* [kelp]) (Figure E.1). We also used simple linear regression analysis to examine relationships between individual fatty acid (FA) concentrations and bulk carbon ($\delta^{13}C$) stable isotope ratios. These relationships are provided as a largely exploratory tool, providing some basic information about potential fatty acid sources (Table E.1).

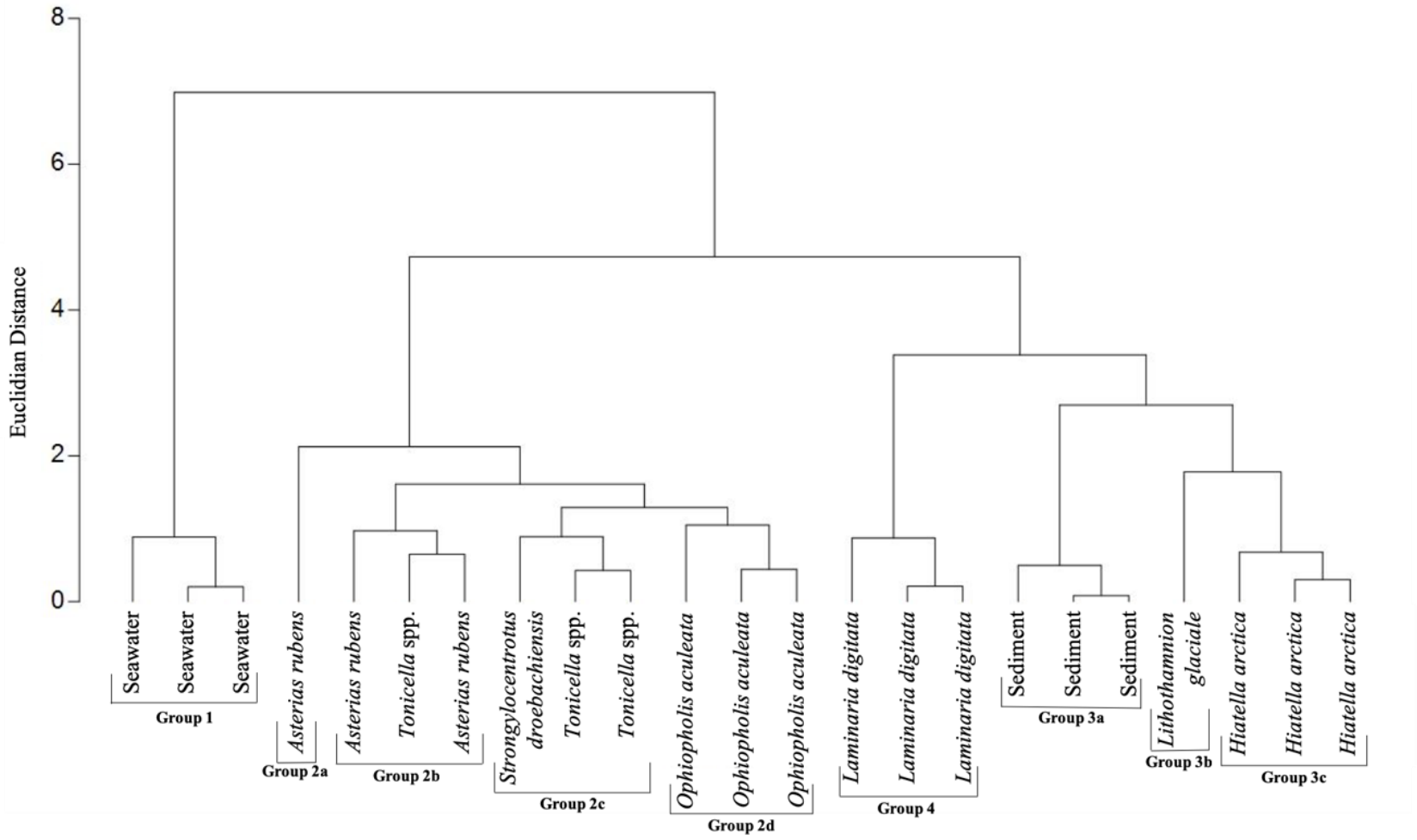
Euclidian Distance
8
6
4
2
0
Seawater
Seawater
Seawater
Group 1
Asterias rubens
Group 2a
Asterias rubens
Tonicella spp.
Asterias rubens
Group 2b
Strongylocentrotus droebachiensis
Tonicella spp.
Tonicella spp.
Group 2c
Ophiopholis aculeata
Ophiopholis aculeata
Ophiopholis aculeata
Group 2d
Laminaria digitata
Laminaria digitata
Laminaria digitata
Group 4
Sediment
Sediment
Sediment
Group 3a
Lithothamnion glaciale
Group 3b
Hiatella arctica
Hiatella arctica
Hiatella arctica
Group 3c

Figure E.1. Agglomerative hierarchical clustering (based on Euclidian distance) of bulk stable carbon ($\delta^{15}N$) and nitrogen ($\delta^{15}N$) isotope ratios in the six animal species, two macroalgal species, and two environmental components (see Table 2.2 for species list) sampled in the South site (see Figure 1.1). *Nereis* spp. was not included because of insufficient tissues for quantification in the N analysis.

Table E.1. Summary of simple linear regression analysis (applied to raw data) examining the relationship between individual fatty acids (FA) and bulk nitrogen ($\delta^{13}C$) stable isotope ratio. The six animal species, two macroalgal species, and two environmental components (see Table 2.2 for species list) sampled in the South site were included in the analysis (see Figure 1.1). Only FA with a statistically significant correlation coefficient (r) are shown.

FA	r	p-value
*i*15:0	0.2	0.014
*ai*15:0	0.3	0.004
*i*16:0	0.6	<0.001
*ai*16:0	0.6	<0.001
16:0	-0.3	<0.001
16:1ω11	0.5	<0.001
16:1ω9	0.6	<0.001
16:1ω5	0.4	<0.001
*i*17:0	0.4	<0.001
*ai*17:0	0.6	<0.001
16:2ω4	0.5	<0.001
17:0	0.2	0.028
16:3ω4	0.6	<0.001
17:1	0.6	<0.001
16:4ω3	0.5	<0.001
16:4ω1	0.5	<0.001
18:0	-0.6	<0.001
18:1ω11	0.5	<0.001
18:1ω9	-0.4	<0.001
18:2ω4	0.5	<0.001
18:3ω6 (GLA)	0.6	<0.001
18:3ω3 (ALA)	0.6	<0.001
18:4ω3 (OTA)	0.4	<0.001
19:3	0.5	<0.001
20:0	0.6	<0.001
20:1ω11	0.6	<0.001
20:1ω9	0.7	<0.001
20:1ω7	0.6	<0.001
20:2ω6	0.6	<0.001
20:4ω6 (ARA)	0.5	<0.001
20:3ω3	0.6	<0.001
20:4ω3	0.4	<0.001
20:5ω3 (EPA)	0.4	<0.001
21:5ω3	0.5	<0.001
22:4ω6	0.6	<0.001
22:5ω3 (DPA)	0.4	<0.001

Appendix F

Seawater lipids based on volume sampled

We made additional calculations of our seawater total lipids using volume sampled (3 L), rather than wet weight of filtered seawater on GF/C filters, to make appropriate unit comparisons between our seawater lipid data and those in literature (Parrish et al., 1995).

Table F.1 Sample size (N) and mean total lipid (µg L^{-1} ww) of seawater sampled outside of the South and North sites (see Figure 1.1). Each sample contained 3 L of seawater. The lowest and highest values are bolded. Each variable's lowest and highest values are bolded.

			Total Lipid
Site	**Collection Month**	**N**	µg L^{-1} ww (±SD)
South	April	3	**57.4 (31.9)**
	July	3	42.3 (13.4)
	December	3	27.3 (8.3)
North	April	3	38.0 (6.7)
	July	3	25.2 (2.1)
	December	2	**18.6 (12.7)**
Mean		17	35.8 (4.5)

Appendix G

Trophic positions excluding April *Laminaria digitata* samples

In section 3.5.4, we suggested the exclusion of our April *L. digitata* samples from our food web due to their abnormal values compared to literature, possibly due to an extended sea ice event, compromised samples, or human error. April samples were both lower than any published range of carbon ($\delta^{13}C$) and nitrogen ($\delta^{15}N$) signatures. We suggest a resampling of *L. digitata* in April to confirm this exclusion.

Table G.1. Sample size (N) and relative trophic position (TP) in the six animal species, two macroalgal species, and two environmental components (see Table 2.2 for species list) sampled in April, July, and December 2017 inside (I) or outside (O) of the South and North sites (see Figure 1.1). Trophic position is based on an isotopic model with a $\delta^{15}N$ fractionation factor of 3.4‰ (see section 2.3.8). Each component group (animal, macroalgal, environmental) variable's lowest and highest values are bolded.

Component	Site	Collection Month	N	TP
Animal				
A. rubens	South	April	3	2.61
		July	3	2.73
		December	3	2.71
	North	April	3	2.69
		July	3	**2.75**
		December	3	2.73
Mean			18	2.70
H. arctica	South	April	3	**1.24**
		July	3	1.47
		December	3	1.42
	North	April	2	1.48
		July	3	1.31
		December	3	1.49
Mean			17	1.40
Nereis spp.	South	April	N/A	N/A
		July	3	2.00
		December	2	2.34
	North	April	N/A	N/A
		July	3	2.01
		December	3	2.13
Mean			11	2.12

Table G.1. (continued):

Component	Site	Collection Month	N	TP
O. aculeata	South	April	3	2.01
		July	3	1.81
		December	3	1.88
	North	April	3	2.21
		July	3	1.93
		December	3	2.05
Mean			18	1.98
S. droebachiensis	South	April	2	2.32
		July	3	2.14
		December	3	2.17
	North	April	3	2.32
		July	3	2.06
		December	3	2.14
Mean			17	2.19
Tonicella spp.	South	April	3	2.23
		July	3	2.16
		December	3	2.18
	North	April	2	2.29
		July	3	2.16
		December	3	1.99
Mean			17	2.17

Table G.1. (continued):

Component	Site	Collection Month	N	TP
Vegetal				
L. digitata	South	April	N/A	N/A
		July	3	1.45
		December	3	**1.29**
	North	April	N/A	N/A
		July	N/A	N/A
		December	N/A	N/A
Mean			6	1.37
L. glaciale	South	April	3	1.53
		July	3	1.46
		December	3	1.54
	North	April	3	1.49
		July	3	1.57
		December	3	**1.62**
Mean			18	1.53

Table G.1. (continued):

Component	Site	Collection Month	N	TP
Environmental				
Seawater	South	April	3	1.44
		July	3	1.37
		December	3	1.68
	North	April	3	1.65
		July	3	1.74
		December	3	**1.76**
Mean			18	1.61
Sediment	South	April	3	1.23
		July	3	**1.00**
		December	3	1.24
	North	April	3	1.12
		July	3	1.28
		December	3	1.17
Mean			18	1.18